Reactivity Ratio Estimation Aspects in Multicomponent Polymerizations at Low and High Conversion Levels

by

Niousha Kazemi

A thesis
presented to the University of Waterloo
in fulfillment of the
thesis requirement for the degree of
Master of Applied Science
in
Chemical Engineering

Waterloo, Ontario, Canada, 2010

AUTHOR'S DECLARATION

I hereby declare that I am the sole author of this thesis. This is a true copy of the thesis, including any required final revisions, as accepted by my examiners.

I understand that my thesis may be made electronically available to the public.

Abstract

Estimation of reactivity ratios from cumulative copolymerization models eliminates the difficulties associated with stopping reactions at low conversion, while one gains to study the full polymerization trajectory. The parameter estimation technique used in this research is the error-in-variables-model (EVM) method, which has been shown to be the most appropriate one for parameter estimation. Two cumulative model forms, the analytical integration of the differential composition equation or Meyer-Lowry model and the one resulting from the direct numerical integration of the differential composition equation, are employed. Our results show that using the cumulative models enhance reactivity ratio estimation results in copolymerizations. In particular, it is illustrated that the latter approach is a novel and more direct method of estimating the reactivity ratios through a step-by-step integration of the copolymerization composition ordinary differential equation.

Due to the fact that multicomponent polymerizations have become increasingly important and having a good knowledge of polymerization parameters, among which reactivity ratios are the most important ones, would be very helpful, our research also looked at potential enhancements in reactivity ratio estimation for ternary systems by applying the estimation directly on terpolymerization experimental data (instead of dealing with three (often non-representative) binary copolymerizations). Conclusions from several case studies and experimental data sets illustrate that using the ternary system data is superior to previous practice.

Another related issue in multicomponent polymerizations is the existence of an azeotropic point. The feed composition of such a point would result in polymer products with homogeneous composition. Predicting the existence and also calculating the composition of the azeotropic point can reduce the effort of running costly experiments, in that computational results can be used to narrow the experimental search space. Although many attempts have been made to clarify the issue of the existence of azeotropic points in multicomponent polymerization systems, this question is still open. We propose a general numerical approach that reliably finds any and all azeotropic compositions in multicomponent systems.

Acknowledgements

First and foremost I offer my sincerest gratitude to Professor Alexander Penlidis, who has supported me throughout my thesis with patience and knowledge. I attribute the level of my Masters degree to his encouragement and effort and without him this thesis, too, would not have been completed or written. One simply could not wish for a better or friendlier supervisor.

My special thanks go to Professor Thomas Duever for his help and guidance from beginning of my research to its end. I would like to extend my thanks to the reader of my thesis, Professor Costas Tzoganakis. Also, I thank IPR members for their help and support.

My parents have been an inspiration throughout my life. They have always supported my dreams and of course I could not survive without the love I got from my younger sister. I'd like to thank my family for all they are, and all they have done for me.

And last but not least to my dearest friends in Waterloo, whose presence and support have filled my hearth with warmth and hope all the time, and I cannot imagine my life here without every one of them.

Contents

List of Figures

List of Tables

Chapter 1. Objectives and Thesis Outline

1.1 Thesis Objectives

Multicomponent polymerizations are of great scientific and practical importance for academia and industry. One of the main advantages is that they can be used for optimization of certain types of polymers properties. They also allow the gathering of information about the reactivity of certain classes of monomers not otherwise available. Modeling studies of multicomponent polymerization are of utmost importance due to the need of predicting, designing, and properly controlling polymeric material properties. Therefore, having a good knowledge of polymerization parameters, among which reactivity ratios are the most important ones, would be very helpful. A considerable number of studies on estimation of copolymerization reactivity ratios have been reported in literature while for the polymerization systems containing more than two components, there have been very few cases of parameter estimation published.

One of our intentions in this research is to develop a general parameter estimation scheme in order to obtain the parameters of a multicomponent polymerization model more directly than previous practice. In order to do this, we build on the thesis by Hauch (2005). The Mayo-Lewis model has been the basic copolymerization model which has been used for reactivity ratio estimation. Linear regression methods were the initial approach to estimate reactivity ratios. However, from a statistical point of view, using these methods for nonlinear models can provide inaccurate results. Amongst nonlinear regression methods, the error-in-variables-model (EVM) method is the statistically correct approach for estimation of reactivity ratios, as it takes into account the error for every variable (both dependent and independent) used by the model. Strange as it may sound, articles published recently still use the linear parameter estimation techniques and report unreliable results for monomer reactivity ratios.

In parallel, many multicomponent polymerizations are evaluated over the full conversion range. However, a lot of useful data of high conversion polymerizations are not utilized when

estimating monomer reactivity ratios based on instantaneous copolymer composition models, since most techniques deal with low conversion data only. In this work, implementing the EVM method on cumulative copolymer composition models has been proven successful in obtaining reactivity ratios, which eliminates the need to stop the reaction at very low conversion along with experimental difficulties associated with this practice.

Given several experimental and computational difficulties within multicomponent systems, there are few studies on polymerizations with three or more than three components. The basic mechanism of terpolymerization is not different from that of copolymerization; therefore, terpolymerization can be modeled in an analogous way. Alfrey and Goldfinger (1944) were the first who reported a composition equation for the three component system. This equation can be used directly in the parameter estimation of monomer reactivity ratios. However, in the case of ternary systems, parameters obtained from binary systems are often used, regardless of the fact that in a ternary system the values of some of these parameters may change considerably from the individual binary pairs. Our research concentrates on potential enhancements in reactivity ratio estimation by applying the EVM method directly on terpolymerization experimental data in place of corresponding copolymerization data sets. The conclusions drawn from this work illustrate that using the ternary system data might be superior to considering the more numerous binary polymerization pairs.

Furthermore, the production of polymers with homogenous composition at azeotropic conditions has been investigated due to its practical and theoretical importance. The question of the existence of azeotropes has been discussed thoroughly for binary systems and azeotropic compositions in copolymerization systems have been calculated experimentally and mathematically. However, for systems containing three and more components, this question has not yet been resolved in a direct manner, while it is obviously essential to obtain these azeotropic compositions or to verify that they do not exist. In our work, we explain a numerical approach that reliably finds any and all azeotrope compositions in multicomponent systems.

Finally, a paper by Shaikh et al. (2004) is revisited as a special case study, in which binary reactivity ratios can be obtained from a single copolymerization experiment monitored *in situ* by FTIR. This on-line technique offers the advantage of analyzing a large number of data points, which

can basically increase the quality of parameter estimation results. In our work, we illustrate the superior EVM performance once more and show the potential for online uses for reactivity ratio estimation.

1.2 Thesis Outline

Chapter 2 presents literature background on multicomponent polymerization kinetics, starting with copolymerization systems. Terpolymerization and tetrapolymerization systems are included and finally a general form of multicomponent polymerization model is presented.

Chapter 3 describes parameter estimation techniques appropriate for multicomponent models in order to estimate reactivity ratios. Details of mathematical implementations and related function derivatives are included as well.

Chapter 4 studies the issue of parameter estimation with using cumulative copolymer compositions based on high conversion range data. Successful estimation of the reactivity ratios using high conversion levels was the target of this chapter.

Chapter 5 is about reactivity ratio estimation in ternary systems using the EVM method. Several case studies have been included to highlight the potential improvements of estimating reactivity ratios directly from terpolymerization experimental data instead of utilizing binary reactivity ratio pairs obtained from copolymerization experimental data.

Chapter 6 discusses the issue of azeotropy in multicomponent polymerization followed by further investigation on azeotropic composition calculation in ternary systems. A general numerical approach which is capable of calculating the azeotropic composition in ternary systems is presented and several case studies demonstrate the performance of this numerical technique.

Chapter 7 is a case study presenting the application of EVM method for estimating on-line reactivity ratios from copolymerization reactions, based on the data by Shaikh et al. (2004).

Finally, Chapter 8 presents concluding remarks and future recommended steps with respect to this thesis objectives.

Chapter 2. Literature Background: Multicomponent Polymerizations

2.1 Copolymerization Models

2.1.1 Introduction

Copolymerization is a polymerization between two monomers units. As a result, the propagation step includes both homopropagation as well as cross-propagation reactions. The process can be simplistically depicted as:

$M_1 + M_2 \rightarrow \sim M_1M_2M_2M_1M_1M_2M_1M_2M_2M_1 \sim \ldots$

M_1 and M_2 denote monomer one and monomer two, respectively.

The copolymer structure depends on the relative monomer concentrations in the feed and their rate of incorporation in the copolymer chains. In this research, free radical (chain growth) polymerizations will be considered.

2.1.2 Copolymerization Models

For the objectives of this research, only the propagation stage is studied and the monomer consumption in other stages is assumed to be negligible. In the model that is mainly used to determine copolymerization composition, the propagation step depends only on the identity of the monomer unit at the growing end and is independent of the chain composition preceding the last monomer unit. This is referred to as the terminal model in copolymerization.

In the copolymerization of M_1 and M_2, based on the terminal model, four propagation reactions are possible:

$$M_1 + R^*_{r,1} \xrightarrow{k_{11}} R^*_{r+1,1}$$
$$M_2 + R^*_{r,1} \xrightarrow{k_{21}} R^*_{r+1,1}$$
$$M_1 + R^*_{r,2} \xrightarrow{k_{12}} R^*_{r+1,2} \quad (2.1)$$
$$M_2 + R^*_{r,2} \xrightarrow{k_{22}} R^*_{r+1,2}$$

$R_{r,i}{}^*$ denotes the radical of monomer *i*. Monomer reactivity ratios can be defined as the following ratios of the individual propagation rate constants:

$$r_1 = \frac{k_{11}}{k_{12}}, \; r_2 = \frac{k_{21}}{k_{22}} \quad (2.2)$$

2.1.2.1 Instantaneous composition model

The most widely used copolymerization model is the Mayo-Lewis model (Mayo and Lewis, 1944), or terminal model, which describes the instantaneous copolymer composition. Writing the rates of monomer incorporation into the copolymer chains and forming their ratios yields eq. (2.3):

$$\frac{d[M_1]}{d[M_2]} = \frac{k_{11}[M_1][R^*_{r,1}] + k_{21}[M_1][R^*_{r,2}]}{k_{12}[M_1][R^*_{r,1}] + k_{22}[M_2][R^*_{r,2}]} \quad (2.3)$$

where $[M_1]$ and $[M_2]$ are the concentrations of M_1 and M_2 in the polymerizing mixture. Applying the steady-state approximation for radicals, and substituting expressions for r_1 and r_2, the final equation is given by:

$$\frac{d[M_1]}{d[M_2]} = \frac{[M_1](r_1[M_1] + [M_2])}{[M_2]([M_1] + r_2[M_2])} \quad (2.4)$$

Eq. (2.4) is referred to as the instantaneous copolymer composition (ICC) equation. It relates the instantaneous copolymer composition with the instantaneous feed composition via the reactivity ratios of the monomers. The copolymerization equation can also be expressed in terms of mole fractions instead of concentrations. If f_1 is the mole fraction of unreacted M_1, and F_1 is its mole fraction incorporated in the copolymer, then eq. (2.4) can be rewritten as follows:

$$F_1 = \frac{r_1 f_1^2 + f_1 f_2}{r_1 f_1^2 + 2 f_1 f_2 + r_2 f_2^2} \tag{2.5}$$

where

$$F_1 = \frac{d[M_1]}{d[M_1] + d[M_2]} \text{ and } f_1 = \frac{[M_1]}{[M_1] + [M_2]} \tag{2.6}$$

Eq. (2.5) is another, very popular, alternative form of the instantaneous copolymer composition equation which is also referred to as the Mayo-Lewis equation.

2.1.2.2 Instantaneous triad fraction model

Measuring triad fractions is another common method to characterize polymer chain microstructure with respect to monomer unit sequence length. The typical triad fraction model is described by the following equations (Koenig, 1980):

$$A_{211+112} = \frac{2 r_1 f_1 f_2}{r_1^2 f_1^2 + 2 r_1 f_1 f_2 + f_2^2} \tag{2.7}$$

$$A_{212} = \frac{f_2^2}{r_1^2 f_1^2 + 2 r_1 f_1 f_2 + f_2^2} \tag{2.8}$$

$$A_{111} = \frac{r_1^2 f_1^2}{r_1^2 f_1^2 + 2 r_1 f_1 f_2 + f_2^2} \tag{2.9}$$

A_{ijk} above denotes triad fractions of monomers i, j and k, centered in monomer j. The formulas representing the expressions for M_2-centered triads can be found by switching

subscripts 1 and 2 in the above equations. Triad fractions are dependent on monomer feed compositions and reactivity ratios in a way analogous to composition data. It is also important to note here that since the ^{13}C-NMR peaks for both A_{211} and A_{112} overlap, it is common to combine the equations for these two fractions and present an equation for $A_{211+112}$ as shown above. Of course, the sum of all triads centered in monomer j is equal to unity, since we are dealing with mole fractions.

2.1.2.3 Cumulative copolymer composition

Most commercial copolymerizations go to high conversion; therefore, the effect of conversion on copolymer composition is of considerable interest. It is also important to know the polymer compositions at any time during the polymerization.

A limitation with the Mayo-Lewis equation is that this model assumes that all variables are measured instantaneously, which is rarely the case. However, the model can be used if one can analyze the copolymer over very short time intervals from time zero, in which case the cumulative composition (from H-NMR or other techniques) should equal the instantaneous copolymer composition. Another alternative would be to have very frequent cumulative composition data points, discretize them over very short intervals, and take successive differences in order to obtain instantaneous data (i.e., take derivatives of the cumulative distribution). However, one has the latter luxury only rarely. Therefore, the instantaneous model requires the polymerization process to be run at low conversion levels, often less than 5%. Since one cannot in general assume that composition would remain constant at higher conversion levels (due to composition drift), a model is required that would account for the feed composition at the end of the reaction. There are two commonly used models forms that give the copolymer composition at high conversion levels (or over the entire conversion trajectory).

I. The integrated model

The Meyer-Lowry equation, eq. (2.10), is the analytical solution for integrating the instantaneous Mayo-Lewis equation from f_{10} to f_1, corresponding to conversion X_n. This

equation should be employed at low to moderate conversions. Typically, the experiment should be run to conversions of approximately 25-30% to ensure that the reaction stays within the chemical control regime. Otherwise, basic assumptions used in order to carry out the analytical integration of the Mayo-Lewis model are violated (further discussion of these assumptions is given below).

$$X_n = 1 - \left[\frac{f_1}{f_{10}}\right]^{\alpha}\left[\frac{f_2}{f_{20}}\right]^{\beta}\left[\frac{f_{10}-\delta}{f_1-\delta}\right]^{\gamma} \tag{2.10}$$

where,

$$\alpha = \frac{r_2}{(1-r_2)};\ \beta = \frac{r_1}{(1-r_1)};\ \gamma = \frac{1-r_1 r_2}{(1-r_1)(1-r_2)};\ \delta = \frac{(1-r_2)}{(2-r_1-r_2)};$$

f_{10} and f_{20} are the initial mole fractions of M_1 and M_2 in the feed, and f_1 and f_2 are the mole fractions of unreacted M_1 and M_2 in the polymerizing mixture, corresponding to time t and/or conversion X_n. Molar conversion is defined as:

$$X_n = 1 - \frac{N_1+N_2}{N_{10}+N_{20}} \tag{2.11}$$

where N_{io} and N_i are the number of moles for monomer *i* initially and at time t, respectively.

It has been observed that conversion is often expressed in terms of monomer molar concentrations $[M_{10}]$ and $[M_1]$. This is subject to the assumption that the volume of the polymerizing mixture remains constant, and thus the direct substitution for the number of moles with their corresponding concentrations may not always be acceptable.

As shown in eq. (2.10), the Meyer-Lowry equation relates conversion to the mole fraction of M_1 at time t and thus one needs to measure both f_{10} and f_1 in an experiment. However, variables that are actually measured in an experiment are the initial mole fraction of M_1 in the feed and the mole fraction of M_1 in the copolymer, $\overline{F_1}$, corresponding to time t or conversion

X_n. To obtain $\bar{F}_1$, the cumulative mole fraction of monomer 1 bound (incorporated) in the copolymer, one can use a mole balance for M_1 which is as follows:

$$\underset{\text{Moles of free } M_1 \text{ (unbound) initially (t=0, } X_n=0)}{[M_0]f_{10}} - \underset{\text{Moles of free (unbound) } M_1 \text{ at } X_n\text{, unreacted}}{[M_0]f_1(1-X_n)} = \underset{\text{Moles of monomer } M_1 \text{ (bound) in copolymer at } X_n}{[M_0]X_n\bar{F}_1} \quad (2.12)$$

From eq. (2.12), the mole fraction of unreacted M_1, f_1, is obtained as:

$$f_1 = \frac{f_{10}-\bar{F}_1 X_n}{1-X_n} \quad (2.13)$$

Eq. (2.13) has been referred to as the Skeist equation as well. Moreover, $\bar{F}_1$, the cumulative mole fraction of M_1 incorporated in the copolymer, can be expressed as a function of number of moles of monomer as:

$$\bar{F}_1 = \frac{N_{10}-N_1}{N_{10}+N_{20}-N_1-N_2} \quad (2.14)$$

So, the Meyer-Lowry equation can be also written as eq. (2.15):

$$1-X_n = \left[\frac{f_{10}-\bar{F}_1 X_n}{f_{10}(1-X_n)}\right]^{\alpha}\left[\frac{1-X_n-f_{10}-\bar{F}_1 X_n}{(1-f_{10})(1-X_n)}\right]^{\beta}\left[\frac{(\delta-f_{10})(1-X_n)}{\delta-\delta X_n-f_{10}+\bar{F}_1 X_n}\right]^{\gamma} \quad (2.15)$$

The typically measured quantities in an experiment are the initial feed concentration or mole fraction, f_{10}, the mole fraction of M_1 incorporated in the copolymer, $\bar{F}_1$, and mass conversion. So, it would be preferable to have the Meyer-Lowry equation in terms of these quantities. According to the definition of the mass conversion, the relationship between molar conversion, X_n, and the usually measured mass conversion, X_w, is given by eq. (2.16).

$$X_n = X_w \frac{Mw_1 f_{10} + (1 - f_{10}) Mw_2}{Mw_1 \bar{F}_1 + (1 - \bar{F}_1) Mw_2} \tag{2.16}$$

M_{W1} and M_{W2} are the molecular weights of monomers 1 and 2. Substituting eq. (2.16) into the Meyer-Lowry equation results in the mass conversion form of the Meyer-Lowry model.

It must be mentioned that there are certain restrictive and simplifying assumptions associated with the derivation of the analytical Meyer-Lowry equation:

1. The polymerizing mixture has a constant temperature meaning that the reaction runs under isothermal conditions.
2. The volume of the polymerizing mixture does not change/shrink considerably.
3. Reactivity ratios remain constant during the course of polymerization.

The first and second assumptions are minor problems, as reactivity ratios are weak functions of the reaction temperature and in most cases (not all), the volume of the polymerizing mixture does not shrink considerably. However, the third assumption can become seriously problematic, as in order to obtain the analytical integration of the differential composition equation, the values of reactivity ratios must be independent of the conversion to be considered as constants. This scenario is not true, though, because reactivity ratios may change at high conversions due to diffusion effects on propagation rate constants.

In addition to the issues arising from these assumptions, difficulties may arise from the fact that at certain r_1 and r_2 values, the Meyer-Lowry equation is not defined. This occurs when $r_1 = r_2 = 1$. In the immediate vicinity of these values, application of equation (2.10) is limited by the numerical accuracy of the computer. Another potential problem with the Meyer-Lowry model can occur when the values of f_1 and f_{10} force the last quotient of the model to be negative. Although these values are not physically possible, they may occur in an iterative estimation scheme.

II. Numerically integrated model

The Meyer-Lowry model assumptions might be true at low to moderate conversion, but certainly do not hold for the entire polymerization. Dealing with these assumptions can create difficulties and become a source of error. In order to avoid such issues, one can use the numerical integration of the copolymer composition equation, which is a direct approach and does not involve any of the restrictive assumptions. The numerical integration is based on the Skeist equation that relates cumulative copolymer composition ($\overline{F_1}$) to the mole fraction of unreacted monomer (f_1) in the polymerizing mixture and molar conversion, X_n, by:

$$\overline{F_1} = \frac{f_{10} - f_1(1 - X_n)}{X_n} \tag{2.17}$$

The mole fraction of unbound monomer, f_1, is given by the numerical solution of the differential equation eq. (2.18).

$$\frac{df_1}{dX_n} = \frac{f_1 - F_1}{1 - X_n} \tag{2.18}$$

This relation is derived based on a material balance performed for the moles of monomer 1,

$$\frac{dN}{N} = \frac{df_1}{F_1 - f_1} \tag{2.18a}$$

where N is the total number of moles of unreacted monomer (monomer 1 plus 2), and also the relationship between conversion and total number of moles of monomer (1 plus 2):

$$\frac{dN}{N} = \frac{dX_n}{X_n - 1} \tag{2.18b}$$

The value of F_1 is given by the Mayo-Lewis equation, eq. (2.5).

2.1.2.4 Cumulative sequence length model

The cumulative triad fraction expression is shown in eq. (2.19). This equation relates instantaneous triad fraction, molar conversion, and the cumulative triads fractions.

$$\frac{d(x_n\overline{A_{ijk}})}{dx_n} = A_{ijk} \tag{2.19}$$

As an example, for the monomer-1-centered triads we have:

$$\frac{d(x_n\bar{A}_{211+112})}{dx_n} = A_{211+112} = \frac{2r_1f_1f_2}{r_1^2f_1^2+2r_1f_1f_2+f_2^2} \tag{2.20}$$

$$\frac{d(x_n\bar{A}_{212})}{dx_n} = A_{212} = \frac{f_2^2}{r_1^2f_1^2+2r_1f_1f_2+f_2^2} \tag{2.21}$$

The (symmetric) relations for monomer-2 centered triads can be obtained similarly.

2.2 Terpolymerization Models

2.2.1 Introduction

The process in which three monomers are polymerized simultaneously is called terpolymerization or ternary polymerization. The main approach for terpolymerization analysis problems is through the application of the concepts and techniques already developed for a two-component system.

2.2.2 Terpolymerization Models

Alfrey and Goldfinger (1944) derived the first composition equations for ternary systems. In their approach, three active growing radicals in terpolymerization of three monomers M_1, M_2, and M_3 were considered. This led to nine different chain propagation reactions, based on the terminal model, as shown by eq. (2.22):

$$
\begin{aligned}
&-R_{r,1}{}^{*} + M_1 \xrightarrow{k_{11}} R_{r+1,1}{}^{*} \\
&-R_{r,1}{}^{*} + M_2 \xrightarrow{k_{12}} R_{r+1,2}{}^{*} \\
&-R_{r,1}{}^{*} + M_3 \xrightarrow{k_{13}} R_{r+1,3}{}^{*} \\
&-R_{r,2}{}^{*} + M_1 \xrightarrow{k_{21}} R_{r+1,1}{}^{*} \\
&-R_{r,2}{}^{*} + M_2 \xrightarrow{k_{22}} R_{r+1,2}{}^{*} \\
&-R_{r,2}{}^{*} + M_3 \xrightarrow{k_{23}} R_{r+1,3}{}^{*} \\
&-R_{r,3}{}^{*} + M_1 \xrightarrow{k_{31}} R_{r+1,1}{}^{*} \\
&-R_{r,3}{}^{*} + M_2 \xrightarrow{k_{32}} R_{r+1,2}{}^{*} \\
&-R_{r,3}{}^{*} + M_3 \xrightarrow{k_{33}} R_{r+1,3}{}^{*}
\end{aligned}
\tag{2.22}
$$

where k_{ij} is the rate constant of the reaction between radical i and monomer j, $R_{r,i}{}^{*}$ denotes the radical of monomer *i*, and M_i denotes monomer *i*.

The rate of disappearance for each monomer can be written in the following form:

$$\frac{-d[M_1]}{dt} = k_{11}\left[R_{r,1}{}^{*}\right][M_1] + k_{21}\left[R_{r,2}{}^{*}\right][M_1] + k_{31}\left[R_{r,3}{}^{*}\right][M_1] \tag{2.23}$$

$$\frac{-d[M_2]}{dt} = k_{12}\left[R_{r,1}{}^{*}\right][M_2] + k_{22}\left[R_{r,2}{}^{*}\right][M_2] + k_{32}\left[R_{r,3}{}^{*}\right][M_2] \tag{2.24}$$

$$\frac{-d[M_3]}{dt} = k_{13}\left[R_{r,1}{}^{*}\right][M_3] + k_{23}\left[R_{r,2}{}^{*}\right][M_3] + k_{33}\left[R_{r,3}{}^{*}\right][M_3] \tag{2.25}$$

where *d[M$_i$]* is the concentration of monomer *i* in the polymer and *[M$_i$]* is the concentration of unbound monomer *i*, in the polymerizing mixture. According to the steady state assumption, the number of growing chains of type $R_{r,1}{}^{*}$,$R_{r,2}{}^{*}$and $R_{r,3}{}^{*}$ disappearing in unit time is equal to the number of $R_{r+1,1}{}^{*}$, $R_{r+1,2}{}^{*}$, and $R_{r+1,3}{}^{*}$ that appear per unit time. This relationship requires the following algebraic equations:

$$k_{12}\left[R_{r,1}{}^{*}\right][M_2] + k_{13}\left[R_{r,1}{}^{*}\right][M_3] = k_{21}\left[R_{r,2}{}^{*}\right][M_1] + k_{31}\left[R_{r,3}{}^{*}\right][M_1] \tag{2.26}$$

$$k_{21}\left[R_{r,2}{}^{*}\right][M_1] + k_{23}\left[R_{r,2}{}^{*}\right][M_3] = k_{12}\left[R_{r,1}{}^{*}\right][M_2] + k_{32}\left[R_{r,3}{}^{*}\right][M_2] \tag{2.27}$$

$$k_{31}\left[R_{r,3}{}^{*}\right][M_1] + k_{32}\left[R_{r,3}{}^{*}\right][M_2] = k_{13}\left[R_{r,1}{}^{*}\right][M_3] + k_{23}\left[R_{r,2}{}^{*}\right][M_3] \quad (2.28)$$

Combining eqs. (2.26) - (2.28) along with the rate expressions of eqs. (2.23) - (2.25), and also substituting for the concentration of monomer *i* with its mole fraction, results in the following set of differential equations:

$$\frac{df_1}{df_2} = \frac{f_1\left(\frac{f_1}{r_{21}r_{31}}+\frac{f_2}{r_{21}r_{32}}+\frac{f_3}{r_{31}r_{23}}\right)\left(f_1+\frac{f_2}{r_{12}}+\frac{f_3}{r_{13}}\right)}{f_2\left(\frac{f_1}{r_{12}r_{31}}+\frac{f_2}{r_{21}r_{32}}+\frac{f_3}{r_{13}r_{32}}\right)\left(f_2+\frac{f_1}{r_{21}}+\frac{f_3}{r_{23}}\right)} \quad (2.29)$$

$$\frac{df_1}{df_3} = \frac{f_1\left(\frac{f_1}{r_{21}r_{31}}+\frac{f_2}{r_{21}r_{32}}+\frac{f_3}{r_{31}r_{23}}\right)\left(f_1+\frac{f_2}{r_{12}}+\frac{f_3}{r_{13}}\right)}{f_3\left(\frac{f_1}{r_{13}r_{21}}+\frac{f_2}{r_{23}r_{12}}+\frac{f_3}{r_{13}r_{23}}\right)\left(f_3+\frac{f_1}{r_{31}}+\frac{f_2}{r_{32}}\right)} \quad (2.30)$$

where f_i is the mole fraction of unbound monomer i in the polymerizing mixture and df_i is the mole fraction of monomer i (bound) incorporated into the polymer chains. Reactivity ratios are analogously defined as:

$$r_{12} = \frac{k_{11}}{k_{12}}, r_{13} = \frac{k_{11}}{k_{13}}, r_{21} = \frac{k_{22}}{k_{21}}, r_{23} = \frac{k_{22}}{k_{23}}, r_{31} = \frac{k_{33}}{k_{31}}, r_{32} = \frac{k_{33}}{k_{32}} \quad (2.31)$$

In order to find the composition of a terpolymer by using the terpolymerization composition equations, eq. (2.29) and eq. (2.30), knowledge of six reactivity ratios is required. Meanwhile, none of these reactivity ratio values can be infinite or equal to zero.

Eq. (2.29) and eq. (2.30) are of the differential type, but if we assume that polymerization does not proceed to high conversions and stays in the low conversion region, df_i can be replaced by F_i, which is the instantaneous mole fraction of monomer *i* in the resulting polymer.

Over the years, several specific forms have been used, for which the general Alfrey and Goldfinger composition equations has been modified. These cases are presented below:

a) When one of the three components cannot homopolymerize (i.e., $k_{33}=0$), the composition equation is given by:

$$\frac{df_1}{df_2} = \frac{f_1\left(\frac{Rf_1}{r_{21}}+\frac{f_2}{r_{21}}+\frac{Rf_3}{r_{23}}\right)\left(f_1+\frac{f_2}{r_{12}}+\frac{f_3}{r_{13}}\right)}{f_2\left(\frac{Rf_1}{r_{12}}+\frac{f_2}{r_{12}}+\frac{f_3}{r_{13}}\right)\left(f_2+\frac{f_1}{r_{21}}+\frac{f_3}{r_{23}}\right)} \tag{2.32}$$

$$\frac{df_1}{df_3} = \frac{f_1\left(\frac{Rf_1}{r_{21}}+\frac{f_2}{r_{21}}+\frac{Rf_3}{r_{23}}\right)\left(f_1+\frac{f_2}{r_{12}}+\frac{f_3}{r_{13}}\right)}{f_3\left(\frac{f_1}{r_{13}r_{21}}+\frac{f_2}{r_{23}r_{12}}+\frac{f_3}{r_{13}r_{23}}\right)\left(f_2+Rf_3\right)} \tag{2.33}$$

where $R=k_{31}/k_{32}$. One can estimate R from a single experiment, in principle.

b) When two of the three components cannot homopolymerize (i.e., $k_{22}=k_{33}=0$), but they can add to each other, the composition equation is given by:

$$\frac{df_1}{df_2} = \frac{f_1(R_2R_3f_1+R_2f_2+R_2f_3)\left(f_1+\frac{f_2}{r_{12}}+\frac{f_3}{r_{13}}\right)}{f_2\left(\frac{R_3f_1}{r_{12}}+\frac{f_2}{r_{12}}+\frac{f_3}{r_{13}}\right)\left(R_2f_1+f_3\right)} \tag{2.34}$$

$$\frac{df_2}{df_3} = \frac{f_2\left(\frac{R_2f_1}{r_{12}}+\frac{f_2}{r_{12}}+\frac{f_3}{r_{13}}\right)\left(f_1+\frac{f_2}{r_{12}}+\frac{f_3}{r_{13}}\right)}{f_3\left(\frac{R_2f_1}{r_{13}}+\frac{f_2}{r_{12}}+\frac{f_3}{r_{13}}\right)\left(f_3+R_3f_1+f_2\right)} \tag{2.35}$$

where $R_2=k_{21}/k_{23}$ and $R_3=k_{31}/k_{32}$. Values of R_2 and R_3 must be estimated by means of terpolymerization experiments.

c) When two of the three components cannot add to themselves or to each other (i.e. $k_{33}=k_{22}=0$, and $k_{23}=k_{32}=0$), the composition equation is simplified to:

$$\frac{df_1}{df_2} = 1+\frac{r_{12}f_1}{f_2}+\frac{r_{12}f_3}{r_{13}f_2} \tag{2.36}$$

$$\frac{df_1}{df_3} = 1+\frac{r_{13}f_1}{f_3}+\frac{r_{13}f_2}{r_{12}f_3} \tag{2.37}$$

2.3 Extension to Multicomponent Polymerization Models

2.3.1 Introduction

To derive the kinetic equations related to an n-component polymerization, a propagation reaction can be written as:

$$R^*_{r,i} + M_j \xrightarrow{k_{ij}} R^*_{r+1,j} \tag{2.38}$$

where M_j denotes monomer *j*, and $R^*_{r,i}$ denotes radical ending in monomer *i*; the reactivity ratios are defined as $r_{ij} = k_{ii}/k_{ij}$. Given that monomers are consumed solely in the propagation reactions, the rate of polymerization for each of the monomers can be expressed as:

$$-\frac{d[M_i]}{dt} = [M_i]\sum k_{ij}[R^*_{r,i}] \tag{2.39}$$

$d[M_i]$ is the (instantaneous, infinitesimal) concentration of monomer *i* in the polymer and $[M_i]$ is the concentration of monomer *i* in the polymerizing mixture. According to the steady-state assumption, we have:

$$[M_i]\sum k_{ij}\left[R^*_{r,i}\right] = \left[R^*_{r,j}\right]\sum k_{ij}[M_j] \tag{2.40}$$

Substituting eq. (2.40) into eq. (2.39), the multicomponent polymer composition can be represented by eq. (2.41):

$$\frac{d[M_i]}{d[M_j]} = \frac{D_{ii}\sum_{k=1}^{n}\frac{[M_k]}{r_{ik}}}{D_{jj}\sum_{k=1}^{n}\frac{[M_k]}{r_{jk}}} \qquad n\ is\ the\ number\ of\ components \tag{2.41}$$

where D_{ii} (or D_{jj}) is the determinant D (see equation (2.42)), when the i line and i column have been omitted.

$$D=\begin{vmatrix} \left([M_1]-\sum\frac{[M_k]}{r_{1k}}\right) & \frac{[M_1]}{r_{21}} & \cdots & \frac{[M_1]}{r_{n1}} \\ \frac{[M_2]}{r_{12}} & \left([M_2]-\sum\frac{[M_k]}{r_{2k}}\right) & & \frac{[M_2]}{r_{n2}} \\ \vdots & \vdots & \ddots & \vdots \\ \frac{[M_n]}{r_{1n}} & \frac{[M_n]}{r_{2n}} & & \left([M_n]-\sum\frac{[M_k]}{r_{nk}}\right) \end{vmatrix} \quad (2.42)$$

Eq. (2.41), proposed for the first time by Walling and Briggs (1945), allows us to calculate the composition of a polymer formed by 'n' monomers provided that values of reactivity ratios are known.

In addition to this model, Roland and Cheng (1991) proposed an alternative for monomer mole fractions for an n-component polymerization in the form of a single equation by using reaction probability terms and the Boolean function "NOT". The use of this function is possible in computer applications. The general expression is:

$$\begin{aligned} F_n \propto \textstyle\sum_{i=1}^{N} P_{ai} \sum_{j=1}^{N} P_{bj} \ldots \sum_{k=1}^{N} P_{zk}\, [NOT(i=a)].[NOT(j=b)] \ldots [NOT(k=z)]. \\ .[NOT(i.j=b.a)].[NOT(i.k=c.a)].etc.(all\ 2-term\ combinations). \\ [NOT(i.j.k=b.c.a)].etc.(all\ 3-term\ combinations). \\ etc.(up\ to\ all(N-1)-term\ combinations) \end{aligned} \quad (2.43)$$

Details for eq. (2.43) and Boolean function characteristics are included in Appendix A.

2.3.2 Tetrapolymerization

The tetrapolymerization composition equation can be obtained using the Walling and Briggs approach (Walling and Briggs, 1945) for an n-component system, reduced to a four-component polymerization, as shown in eq. (2.44):

$$d[M_1]:d[M_2]:d[M_3]:d[M_4] = \left(D_{11}\left([M_1]+\frac{[M_2]}{r_{12}}+\frac{[M_3]}{r_{13}}+\frac{[M_4]}{r_{14}}\right)\right.$$
$$:\left(D_{22}\left(\frac{[M_1]}{r_{21}}+[M_2]+\frac{[M_3]}{r_{23}}+\frac{[M_4]}{r_{24}}\right)\right.$$
$$:\left(D_{33}\left(\frac{[M_1]}{r_{31}}+\frac{[M_2]}{r_{32}}+[M_3]+\frac{[M_4]}{r_{34}}\right)\right.$$
$$:\left(D_{44}\left(\frac{[M_1]}{r_{41}}+\frac{[M_2]}{r_{42}}+\frac{[M_3]}{r_{43}}+[M_4]\right)\right. \quad (2.44)$$

where D_{11}, D_{22}, D_{33}, and D_{44} are calculated using eq. (2.42). As an example, D_{11} (following eq. (2.42)) is shown in eq. (2.45a),

$$D_{11}=\begin{vmatrix} [M_2]-\left(\frac{[M_1]}{r_{21}}+[M_2]+\frac{[M_3]}{r_{23}}+\frac{[M_4]}{r_{24}}\right) & \frac{[M_2]}{r_{32}} & \frac{[M_2]}{r_{42}} \\ \frac{[M_3]}{r_{23}} & [M_3]-\left(\frac{[M_1]}{r_{31}}+\frac{[M_2]}{r_{32}}+[M_3]+\frac{[M_4]}{r_{34}}\right) & \frac{[M_3]}{r_{43}} \\ \frac{[M_4]}{r_{24}} & \frac{[M_4]}{r_{34}} & [M_4]-\left(\frac{[M_1]}{r_{41}}+\frac{[M_2]}{r_{42}}+\frac{[M_3]}{r_{43}}+[M_4]\right) \end{vmatrix} \quad (2.45a)$$

and the final result for this determinant is given by eq. (2.45b). The other determinants can be obtained similarly.

$$D_{11}=\begin{vmatrix} -\left(\frac{[M_1]}{r_{21}}+\frac{[M_3]}{r_{23}}+\frac{[M_4]}{r_{24}}\right) & \frac{[M_2]}{r_{32}} & \frac{[M_2]}{r_{42}} \\ \frac{[M_3]}{r_{23}} & -\left(\frac{[M_1]}{r_{31}}+\frac{[M_2]}{r_{32}}+\frac{[M_4]}{r_{34}}\right) & \frac{[M_3]}{r_{43}} \\ \frac{[M_4]}{r_{24}} & \frac{[M_4]}{r_{34}} & -\left(\frac{[M_1]}{r_{41}}+\frac{[M_2]}{r_{42}}+\frac{[M_3]}{r_{43}}\right) \end{vmatrix} \quad (2.45b)$$

An alternative approach is from Roland and Cheng (1991), also capable of calculating the composition of a four-component polymerization (as can be seen in eq. (2.43), their approach was also expanded to n-component polymerizations). More recently, Chen et al. (2001) proposed yet another alternative for a four-component polymerization composition equation. In what follows, the Roland and Cheng (1991) approach and the Chen et al. (2001) approach are explained, respectively.

The Roland and Cheng (1991) approach consists of using reaction probabilities. The reaction probability, P_{ij}, is defined as:

$$P_{ij} = \frac{k_{ij}[M_j]}{\sum_{j'=1}^{N} k_{ij'}[M_{j'}]} \tag{2.46}$$

where k_{ij} denotes the rate constant for the addition of monomer j to a propagating chain terminating in a monomer unit of type i, and $[M_i]$ denotes the molar concentration of monomer i. An example for P_{14} is given by:

$$P_{14} = \frac{k_{14}[M_4]}{k_{11}[M_1]+k_{12}[M_2]+k_{13}[M_3]+k_{14}[M_4]} = \frac{[M_4]/r_{14}}{[M_1]+[M_2]/r_{12}+[M_3]/r_{13}+[M_4]/r_{14}} \tag{2.47}$$

Subsequently, material balance equations for each component, using eq. (2.39), are produced and after implementing the steady-state, a set of equations is obtained, as shown in eq. (2.48). This equation set consists of four equations and four unknowns (F_1, F_2, F_3, and F_4).

$$\begin{aligned}
&F_1(k_{12}[M_2] + k_{13}[M_3] + k_{14}[M_4]) - F_2(k_{21}[M_1]) - F_3(k_{31}[M_1]) - F_4(k_{41}[M_1]) = 0\\
&F_1(k_{12}[M_2]) - F_2(k_{21}[M_1]+k_{23}[M_3] + k_{24}[M_4]) + F_3(k_{32}[M_2]) + F_4(k_{42}[M_2]) = 0\\
&F_1(k_{13}[M_3]) + F_2(k_{23}[M_3]) - F_3(k_{31}[M_1]) + k_{32}[M_2] + k_{34}[M_4]) + F_4(k_{43}[M_3]) = 0\\
&F_1(k_{14}[M_4]) + F_2(k_{24}[M_4]) + F_3(k_{34}[M_4]) - F_4(k_{41}[M_2]) + k_{43}[M_3] + k_{41}[M_1]) = 0
\end{aligned} \tag{2.48}$$

In addition, there is another related equation that can be used, i.e., $\sum_{i=1}^{4} F_i = 1$. This equation can be used in place of any one of the equations in the equation set, eq. (2.48). So, by carrying out the remaining algebraic manipulations, using the reaction probability definition P_{ij}, eq. (2.46), and substituting the variables as defined, a final expression for a tetrapolymerization composition equation can be obtained, as eq.(2.49).

$$
\begin{aligned}
F_1 \propto\ & P_{21}P_{31}P_{41} + P_{21}P_{31}P_{42} + P_{21}P_{31}P_{43} + P_{21}P_{32}P_{41} + \\
& P_{21}P_{32}P_{42} + P_{21}P_{32}P_{43} + P_{21}P_{34}P_{41} + P_{21}P_{34}P_{42} + \\
& P_{23}P_{31}P_{41} + P_{23}P_{31}P_{42} + P_{23}P_{31}P_{43} + P_{23}P_{34}P_{41} + \\
& P_{24}P_{31}P_{41} + P_{24}P_{31}P_{43} + P_{24}P_{32}P_{41} + P_{24}P_{34}P_{41} \\
F_2 \propto\ & P_{12}P_{32}P_{42} + P_{12}P_{32}P_{41} + P_{12}P_{32}P_{43} + P_{12}P_{31}P_{42} + \\
& P_{12}P_{31}P_{41} + P_{12}P_{31}P_{43} + P_{12}P_{34}P_{42} + P_{12}P_{34}P_{41} + \\
& P_{13}P_{32}P_{42} + P_{13}P_{32}P_{41} + P_{13}P_{32}P_{43} + P_{13}P_{34}P_{42} + \\
& P_{14}P_{32}P_{42} + P_{14}P_{32}P_{43} + P_{14}P_{31}P_{42} + P_{14}P_{34}P_{42} \\
F_3 \propto\ & P_{23}P_{13}P_{43} + P_{23}P_{13}P_{42} + P_{23}P_{13}P_{41} + P_{23}P_{12}P_{43} + \\
& P_{23}P_{12}P_{42} + P_{23}P_{12}P_{41} + P_{23}P_{14}P_{43} + P_{23}P_{14}P_{42} + \\
& P_{21}P_{13}P_{43} + P_{21}P_{13}P_{42} + P_{21}P_{13}P_{41} + P_{21}P_{14}P_{43} + \\
& P_{24}P_{13}P_{43} + P_{24}P_{13}P_{41} + P_{24}P_{12}P_{43} + P_{24}P_{14}P_{43} \\
F_4 \propto\ & P_{24}P_{34}P_{14} + P_{24}P_{34}P_{12} + P_{24}P_{34}P_{13} + P_{24}P_{32}P_{14} + \\
& P_{24}P_{32}P_{12} + P_{24}P_{32}P_{13} + P_{24}P_{31}P_{14} + P_{24}P_{31}P_{12} + \\
& P_{23}P_{34}P_{14} + P_{23}P_{34}P_{12} + P_{23}P_{34}P_{13} + P_{23}P_{31}P_{14} + \\
& P_{21}P_{34}P_{14} + P_{21}P_{34}P_{13} + P_{21}P_{32}P_{14} + P_{21}P_{31}P_{14}
\end{aligned}
\tag{2.49}
$$

The Chen et al. (2001) approach has the same theoretical basis as the Roland and Cheng (1991) approach. Therefore, the rates of monomer disappearance R_{ij} (see below) are the same and after applying the steady-state approximation, expressed as,

$$
\begin{cases}
R_{12}+R_{13}+R_{14}=R_{21}+R_{31}+R_{41} \\
R_{21}+R_{23}+R_{24}=R_{12}+R_{32}+R_{42} \\
R_{31}+R_{32}+R_{34}=R_{13}+R_{23}+R_{43} \\
R_{41}+R_{42}+R_{43}=R_{14}+R_{24}+R_{34}
\end{cases}
\tag{2.50}
$$

the tetrapolymerization composition equation is given by eq. (2.51).

$$
\begin{aligned}
& d[M_1]: d[M_2]: d[M_3]: d[M_4] = \\
& \{[M_1](\alpha k_{11} + \beta k_{21} + \delta k_{31} + k_{41})\} \\
& :\{[M_2](\alpha k_{12} + \beta k_{22} + \delta k_{32} + k_{42})\} \\
& :\{[M_3](\alpha k_{13} + \beta k_{23} + \delta k_{33} + k_{43})\} \\
& :\{[M_4](\alpha k_{14} + \beta k_{24} + \delta k_{34} + k_{44})\}
\end{aligned}
\tag{2.51}
$$

In eq. (2.51), α, β, and δ are defined below:

$$\alpha = \frac{k_{44}}{k_{11}}\left(\frac{\frac{-1}{r_{21}r_{43}r_{32}} - \frac{1}{r_{23}r_{41}r_{32}} - \frac{1}{r_{42}r_{23}r_{31}} - \frac{B}{r_{43}r_{31}} - \frac{C}{r_{21}r_{42}} - \frac{BC}{r_{41}}}{\frac{1}{r_{12}r_{23}r_{31}} + \frac{1}{r_{21}r_{13}r_{32}} + \frac{A}{r_{23}r_{32}} + \frac{B}{r_{13}r_{31}} + \frac{C}{r_{12}r_{21}} - ABC}\right) \quad (2.52a)$$

$$\beta = \frac{k_{44}}{k_{22}}\left(\frac{\frac{1}{r_{13}r_{31}r_{42}} - \frac{1}{r_{13}r_{41}r_{32}} - \frac{1}{r_{12}r_{43}r_{31}} - \frac{A}{r_{43}r_{32}} - \frac{C}{r_{12}r_{41}} - \frac{AC}{r_{42}}}{\frac{1}{r_{12}r_{23}r_{31}} + \frac{1}{r_{21}r_{13}r_{32}} + \frac{A}{r_{23}r_{32}} + \frac{B}{r_{13}r_{31}} + \frac{C}{r_{12}r_{21}} - ABC}\right) \quad (2.52b)$$

$$\delta = \frac{k_{44}}{k_{33}}\left(\frac{\frac{-1}{r_{13}r_{21}r_{42}} - \frac{1}{r_{23}r_{41}r_{12}} + \frac{1}{r_{12}r_{43}r_{21}} - \frac{A}{r_{23}r_{42}} - \frac{B}{r_{13}r_{41}} - \frac{BC}{r_{43}}}{\frac{1}{r_{12}r_{23}r_{31}} + \frac{1}{r_{21}r_{13}r_{32}} + \frac{A}{r_{23}r_{32}} + \frac{B}{r_{13}r_{31}} + \frac{C}{r_{12}r_{21}} - ABC}\right) \quad (2.52c)$$

whereas A, B, and C are given by:

$$A = \frac{1}{[M_1]}\left(\frac{1}{r_{12}}[M_2] + \frac{1}{r_{13}}[M_3] + \frac{1}{r_{14}}[M_4]\right) \quad (2.52d)$$

$$B = \frac{1}{[M_2]}\left(\frac{1}{r_{21}}[M_1] + \frac{1}{r_{23}}[M_3] + \frac{1}{r_{24}}[M_4]\right) \quad (2.52e)$$

$$C = \frac{1}{[M_3]}\left(\frac{1}{r_{31}}[M_1] + \frac{1}{r_{32}}[M_2] + \frac{1}{r_{34}}[M_4]\right) \quad (2.52f)$$

The Walling and Briggs (1954) and Roland and Cheng (1991) composition equations have been tested for the tetrapolymerization of styrene (Sty)/methyl methacrylate (MMA)/acrylonitrile (AN)/vinylidene chloride (VDC) with actual data reported by Koenig (1980). Values for reactivity ratios (Table 2.1) for the respective binary pairs of monomers were taken from Koenig (1980). Monomer and tetrapolymer compositions are compared in Table 2.2.

Table 2-1. Reactivity ratios for styrene/methyl methacrylate/acrylonitrile/vinyl chloride monomer pairs

M_i	M_j	r_{ij}	r_{ji}
Sty	MMA	0.5	0.50
Sty	VDC	2.0	0.14
MMA	VDC	2.53	0.24
MMA	AN	1.20	0.15
AN	VDC	0.91	0.37
Sty	AN	0.41	0.05

Table 2-2. Monomer and polymer compositions for tetrapolymerization of styrene/methyl methacrylate/acrylonitrile/vinyl chloride

Components	Monomer composition	Tetrapolymer composition (exp.)	Tetrapolymer composition (calc.) (Walling and Briggs, 1954)	Tetrapolymer composition (calc.) (Roland and Cheng, 1991)
Sty	25.21	40.7	41.0	41.0
MMA	25.48	25.5	27.4	27.4
AN	25.40	25.8	24.5	24.4
VDC	23.9	8.0	6.9	6.9

As can be seen in Table 2.2, there seems to be perfect agreement between the calculated polymer compositions with the two models, and close agreement between models and experimental data, indicating that these models are capable of predicting the polymer composition correctly.

Chapter 3. Literature Background: Reactivity Ratio Estimation from Instantaneous Copolymerization Data

3.1 Introduction

In copolymerization studies, the estimation of reactivity ratios is of a great significance. For this reason, many different approaches have been used to estimate these parameters. Many of the reactivity ratios reported in the literature are not accurate due to problems with the estimation procedures, inappropriate kinetic models, and experimental and analytical difficulties. Some of the uncertainties in the estimates result from the use of too few data points or data collected under poorly designed or undersigned conditions. The quality of experimental data is important in establishing the degree of confidence that can be associated with these reactivity ratios.

One of the first approaches was linear regression. Although the linear regression approach results in many inaccuracies in the estimated values, it has been widely used by scientists due to its simplicity. Amongst the existing linear techniques, Fineman-Ross, Kelen-Tudos, and extended Kelen-Tudos are the most readily used. The inaccuracies arise from the fact that these linear approaches are based on linearization of the Mayo-Lewis model, an inherently nonlinear model involving these reactivity ratios. A linearization procedure and the related model transformation lead to a model structure which violates basic assumptions of linear regression. These methods have been repeatedly shown to be invalid (Rossignoli and Duever (1995), Polic et al. (1998) and Hauch et al. (2008)) and will not be considered further. Since the reactivity ratio estimation problem is a nonlinear-in-the-parameters problem, an appropriate estimation approach should be based on nonlinear least squares

(NLLS) or other more advanced, but still nonlinear, variants. One of the important assumptions in conventional NLLS is that the error in the independent variables must be negligible. In a copolymerization process, however, the independent variable is the comonomer feed composition, which is set by the experimenter and, unlike other independent variables in process engineering, it is usually associated with noticeable error. Statistically correct results can only be obtained by a method that takes into account both the nonlinearity of the model and the errors involved in the values of all variables (both dependent and independent). The error-in-variables-model (EVM) method can satisfy these conditions.

In this chapter, brief descriptions of the methods used for estimating reactivity ratios are presented, starting with NLLS and continuing with the EVM approach. We again start from the point that the terminal model (Mayo-Lewis equation) adequately describes instantaneous copolymer composition.

3.2 Nonlinear Parameter Estimation Techniques

The nonlinear regression techniques that are applied to the Mayo-Lewis equation are the nonlinear least squares (NLLS) method and the error-in-variables-model (EVM) method. In what follows, brief descriptions of these methods are included for comparison purposes. Later on in this section, a discussion of the error structure is presented and is followed by the application of both NLLS and EVM for reactivity ratio estimation using the instantaneous copolymer composition equation. Finally, a comparison between NLLS and EVM is made (based on Rossignoli and Duever, 1995), justifying the reasons for considering the EVM method to be the most appropriate parameter estimation technique for this research.

3.2.1 Nonlinear Least Squares Method

Nonlinear least squares (NLLS) is the commonly used technique for solving single-response nonlinear regression problems. The method is based on eq. (3.1):

$$y_i = g(\underline{x}_i, \underline{\theta}) + \varepsilon_i \tag{3.1}$$

where y_i is the experimental measurement of the ith trial, $g(x_i, \theta)$ is the mathematical model giving the predicted value of the measurement, x_i is the value of the independent variable, θ represents parameter values, and ε_i is the random error. The error structure is discussed in section 3.4. The objective of the NLLS method is to minimize the sum of the squared residuals (differences between the measured and predicted values) given by the following equation.

$$S(\underline{\theta}) = \sum_i \left(y_i - g(\underline{x}_i, \underline{\theta})\right)^2 \tag{3.2}$$

The values of $\underline{\theta}$ that minimize $S(\underline{\theta})$ are known as the least squares parameter estimates, $\underline{\hat{\theta}}$. The underlined characters indicate vectors or matrices.

Note that while in theory minimization of the objective function should always be possible, in practice for a variety of reasons considerable difficulties may arise in finding the global minimum. A number of different optimization techniques can be used with the simplest being the Gauss-Newton algorithm. For more complicated optimization problems, methods such as the Marquardt-Levenberg algorithm, the simplex method or simulated annealing may be used, to mention a few alternatives. In principle, any method of optimization can be applied to eq. (3.2). An initial guess of the parameter values must be supplied and different initial guesses may lead to different local optima, depending on the $S(\underline{\theta})$ surface. There are three assumptions for using the NLLS method:

1. The model perfectly describes the system.
2. The errors in the independent variables are negligible (the errors are negligible compared with the error in the dependent variable).
3. The errors associated with the dependent variable are identically and independently distributed.

3.2.2 Error-in-variables-model (EVM)

The EVM model is a general regression framework for solving linear and nonlinear, single and multi-response, parameter estimation problems. Here is a brief description of this method according to Reilly and Patino-Leal (1981); further explanations can be found in the reference.

The EVM model consists of two statements. First, the vector of measurements x_i is equated to the vector of true values ξ_i, plus an error term, ε_i, where *i* is the trial number.

$$\underline{x}_i = \underline{\xi}_i + \underline{\varepsilon}_i \qquad where\ i = 1,2,\dots,n \tag{3.3}$$

Underline characters in eq. (3.3) and from now on denote vectors or matrices. The error vector is assumed to be normally distributed with a mean vector of 0, and a covariance matrix $\underline{V}$, which is non-singular and may be known or unknown (Keeler and Reilly, 1991).

The second statement relates the true (yet unknown) values of the parameters, $\underline{\theta}^*$, and variables, $\underline{\xi}_i$, via the mathematical model represented by:

$$\underline{g}(\underline{\xi}_i, \underline{\theta}^*) = 0 \qquad where\ i = 1,2,\dots,n \tag{3.4}$$

The vector function, $\underline{g}$, may be linear or nonlinear in the elements of $\underline{\xi}_i$ and $\underline{\theta}$. Using a Bayesian approach, the point estimate, $\underline{\hat{\theta}}$, can be found by minimizing

$$\phi = \frac{1}{2}\sum_{i=1}^{n} r_i \left(\underline{\bar{x}}_i - \underline{\hat{\xi}}_i\right)' \underline{V}^{-1} \left(\underline{\bar{x}}_i - \underline{\hat{\xi}}_i\right) \tag{3.5}$$

where r_i is the number of replicates at the ith trial, $\underline{\bar{x}}_i$ is the average of the r_i measurements $\underline{x}_i$, and $\underline{\hat{\xi}}_i$ denotes true values of the variables $\underline{\xi}_i$.

The EVM approach used in this research is based on the algorithm published by Reilly et al. (1993), which uses a Newton's method similar to Fisher's method of scoring to minimize ϕ based on a nested-iterative scheme. The algorithm starts by using the initial parameter estimates, $\underline{\theta}^{(o)}$. The initial variable values, $\underline{\xi}^{(o)}$, are being set equal to the measured variables $\underline{x_i}$. First, the inner iteration searches for the true values of the variables $\underline{\xi_i}$, keeping the parameter values constant. Next, the outer iteration searches for the true values of the parameters $\underline{\theta}$, while the values of the variables remain constant.

The inner iteration uses the following equation to update the estimates of $\underline{\xi}^{(k)}$, where k denotes the iteration step, for finding the true values of $\underline{\xi_i}$:

$$\underline{\xi_i}^{(k+1)} = \underline{\bar{x}_i} - \underline{VB_i'}\left(\underline{B_i}\underline{VB_i'}\right)^{-1}\left[\underline{g}\left(\underline{\xi}^{(k)}, \underline{\theta}\right) + \underline{B_i}\left(\underline{\bar{x}_i} - \underline{\xi}^{(k)}\right)\right] \tag{3.6}$$

where $\underline{V}$ is the error covariance matrix for the measurements and $\underline{B_i}$ is the vector of partial derivatives of the function, $\underline{g}\left(\underline{\xi_i}, \underline{\theta}\right)$, with respect to the variables,

$$\underline{B_i} = \left[\frac{\partial g\left(\underline{\xi_i}, \underline{\theta}\right)}{\partial\left(\underline{\xi_i}\right)_t}\right]_{\underline{\xi_i}=\underline{\xi_i}^{(k)}} \quad for\ the\ t^{th}\ element \tag{3.7}$$

Then, the outer iteration, using eq. (3.8), updates the parameter estimate values. In this equation, u denotes the iteration step, $\underline{G}$ is the expected information matrix (given by eq. (3.9)), and $\underline{q}$ is a gradient vector (to be defined later in eq. (3.12)).

$$\underline{\theta}^{(u+1)} = \underline{\theta}^{(u)} - \underline{G}^{-1}\underline{q} \tag{3.8}$$

$$\underline{G} = E\left[\frac{d^2\phi}{d\theta_i d\theta_j}\right] \qquad i,j\ elements \tag{3.9}$$

Since ϕ is given by eq. (3.5), $\underline{G}$ can be rewritten as:

$$\underline{G} = \sum_{i=1}^{n} r_i \underline{Z}_i^{'} (\underline{B}_i \underline{V} \underline{B}_i^{'})^{-1} \underline{Z}_i \tag{3.10}$$

and $\underline{Z}$ is the vector of partial derivatives with respect to the parameters given by:

$$\underline{Z}_i = \left[\frac{\partial g(\underline{\xi}_i, \underline{\theta})}{\partial \theta_m}\right] \qquad m^{th}\ element \tag{3.11}$$

The gradient vector, q, is defined as:

$$\underline{q} = \left[\frac{d\phi}{d\theta_m}\right] \qquad m^{th}\ element \tag{3.12}$$

which, upon substitution, becomes

$$\underline{q} = \sum_{i=1}^{n} r_i \underline{Z}_i^{'} \left(\underline{B}_i \underline{V} \underline{B}_i^{'}\right)^{-1} \underline{B}_i \, (\underline{\bar{x}}_i - \underline{\hat{\xi}}_i) \tag{3.13}$$

If the error distribution is normally distributed, $N(0, \sigma^2)$, a maximum likelihood estimate can be used and inferences can be made including the construction of confidence intervals or regions. It should be pointed out that even under the assumption of normality, the inferences made about the parameters are only approximate. Precision of the estimates can be given by presenting joint confidence regions or contours, such that values of the parameters inside or on the contour represent plausible values of the parameters at the specified confidence level.

Considering the variance to be known and the distribution of the errors to follow a normal distribution, the confidence intervals or regions can be constructed using the formula for elliptical joint confidence regions (JCR), given by (Keeler, 1989):

$$(\underline{\theta} - \underline{\hat{\theta}})^{'} \underline{G} (\underline{\theta} - \underline{\hat{\theta}}) \leq \chi^2_{(p, 1-\alpha)} \tag{3.14}$$

where χ^2 represents the value of the chi-squared distribution, p is the number of parameters $\underline{\theta}$ (and hence the degree of freedom of χ^2), $(1-\alpha)$ is the chosen confidence level, and " $\wedge$ " indicates again estimates of the parameters.

For a very nonlinear model, it may be better to construct the joint confidence contour having exact shape and approximate probability content (Bates and Watts, 1988). The joint confidence contour having the exact/correct shape but approximate probability is given by (Keeler, 1989):

$$\phi(\underline{\theta}) = \phi(\hat{\underline{\theta}}) + \frac{1}{2}\chi^2_{(p,1-\alpha)} \tag{3.15}$$

$\phi(\hat{\underline{\theta}})$ is defined by eq. (3.5) and values of $\hat{\underline{\theta}}$ are found by eq. (3.8). It is important to note that both the shape and probability of contours obtained from eq. (3.14) are approximate, whereas the shape of contours obtained from eq. (3.15) is correct while the probability content is approximate (Polic et al., 2004).

A major advantage of the EVM model is that it provides not only parameter estimates but also true values of the variables. The assumptions required for EVM are that the model is correct and that successive measurement vectors are independent of one another. In addition, since the EVM algorithm is a Newton-type search method, initial guesses are of great importance, as poor initial guesses may result in convergence problems or faulty parameter estimates.

3.3 Error Structure

In parameter estimation the error structure and magnitude are very important and should be considered prior to applying any parameter estimation techniques. In applying EVM, this is particularly important since the error structure/magnitude must be stated explicitly. "Error structure", in general, refers to the size of the error associated with each measured variable, the distribution of the error, how the error is related to the variable, and, in a multiresponse estimation problem, whether or not the measurements are correlated or independent. To

determine the magnitude of the error, the measurement error variance or standard deviation should be obtained from replicate experiments. In the absence of replicate experiments, expert opinion or past experience can be used to determine the measurement covariance matrix V. In NLLS applications, error magnitude is very important, as the variable with the largest amount of error is considered to be the dependent variable while the others are designated to be the independent variables. The distribution of the error must also be considered, something that is often unknown in copolymerization processes. Very few articles contain information about the error magnitude and, even fewer, for the error distribution. Often it is assumed that errors are normally distributed and are expressed in terms of a percentage of the measured value (e.g., error in feed composition is ±5% of the measured f_{10} or f_1 (see section 3.4)). In general, errors are related to the variables by either being additive or multiplicative, which is discussed in the following subsections.

3.3.1 Additive error

Consider a measurement x that has an additive error following a uniform distribution as:

$$x = x^* + k\varepsilon \tag{3.16}$$

where x^* is the true value of the measured quantity, k is a constant multiplier, and ε is a random variable, which, for illustration purposes, has a uniform distribution in the interval from -1 to 1. Therefore, the error is plus or minus k units, where the units are those used to measure x.

The following equation gives the variance of x, $V(x)$:

$$V(x) = V(x^* + k\varepsilon) = k^2 V(\varepsilon) \tag{3.17}$$

Using standard distribution theory, the variance of the uniformly distributed error is calculated as:

$$V(\varepsilon) = E(\varepsilon^2) - [E(\varepsilon)]^2 = \int_{-1}^{1} \frac{\varepsilon^2}{2} d\varepsilon = 1/3 \quad (3.18)$$

So the variance of x is:

$$V(x) = k^2/3 \quad (3.19)$$

3.3.2 Multiplicative error

The multiplicative error structure is expressed as follows:

$$x = x^*(1 + k\varepsilon) \quad (3.20)$$

Taking logarithms of both sides of eq. (3.20):

$$\ln x = \ln x^* + \ln(1 + k\varepsilon) \quad (3.21)$$

In this equation, $\ln(1 + k\varepsilon)$ can be replaced by $k\varepsilon$, provided that the magnitude of the error does not exceed 10% ($k < 0.1$). So, the variance of $\ln x$ eventually becomes $k^2/3$. Comparing eqs. (3.19) and (3.21), it can thus be seen that the variances for both multiplicative and additive error structure become identical.

3.4 Application of NLLS

In this section we describe the application of NLLS to the estimation of reactivity ratios from copolymer composition data. Starting from the Mayo-Lewis model, eq. (2.5), one can rewrite it in the following form:

$$F_1 = \frac{r_1 f_1^2 + f_1(1-f_1)}{r_1 f_1^2 + 2f_1(1-f_1) + r_2(1-f_1)^2} + \varepsilon$$

A commonly employed way of estimating r_1 and r_2 is based on data (measurements) of the mole fraction of monomer 1 in the feed and in the copolymer. The error structure and levels in measuring f_1 and F_1 have been shown (based on experimental observations over many years, see for instance Dube et al. (1991)) to be multiplicative at the levels of 0.5% to 1% for f_1 and up to 4% or 5% for F_1. The model therefore is given as:

$$\ln(F_1) = \ln\left(\frac{r_1 f_1^2 + f_1(1-f_1)}{r_1 f_1^2 + 2f_1(1-f_1) + r_2(1-f_1)^2}\right) + \ln(1+\varepsilon) \tag{3.22}$$

where $\ln(1+\varepsilon)$ is approximated by ε, as the error is less than 10%. The partial derivatives are given by:

$$Z = \left[\frac{\partial \ln(g(\underline{x_i}, \underline{\theta}))}{\partial \theta_j}\right] = \left[\frac{1}{g(x_i, \underline{\theta})} \frac{\partial g(\underline{x_i}, \underline{\theta})}{\partial \theta_j}\right] \tag{3.23}$$

$\underline{\theta}$ is the vector of parameters (r_1, r_2). So, the required derivatives are:

$$\frac{\partial \ln(F_1)}{\partial r_1} = \frac{f_{1i}(r_2 - 2r_2 f_{1i} + r_2 f_{1i}^2 + f_{1i}(1-f_{1i})}{(r_1 f_{1i} + 1 - f_{1i})(r_1 f_{1i}^2 + r_2 - 2r_2 f_{1i}(1-f_{1i}) + 2f_{1i} - 2{f_{1i}}^2)} \tag{3.24}$$

$$\frac{\partial \ln(F_1)}{\partial r_2} = \frac{(f_{1i}-1)^2}{r_1 f_{1i}^2 + r_2 - 2r_2 f_{1i}(1-f_{1i}) + 2f_{1i} - 2{f_{1i}}^2} \tag{3.25}$$

As previously mentioned, to quantify the uncertainty of the estimates, joint confidence regions can be constructed. In general, to determine the quality of parameter estimates, confidence regions need to be generated. The joint confidence region (JCR) is a p dimensional space, where p is equal to the number of parameters to be estimated. Since it is not possible to view this space if p is greater than 3, JCR's of two parameters are usually

obtained for easy visualization. One should keep in mind that these regions are conditional confidence regions at fixed values of other parameters, and that they will change with the values of the other parameters. In general, eq. (3.14) will result in a contour having the correct shape but only approximate probability, as discussed earlier. If the JCR is open or the area is very large, then this is an indication of very poor parameter estimates. Many times the JCR looks like an open "band" encompassing the point estimates; this is an indication that one has a good parameter estimate for θ_i but a poor estimate for θ_j. The poor estimate of θj may be a reflection of the low level of information provided by the response(s) used in the specific estimation scenario, i.e., in such a case the gradients given by eq. (3.24) or (3.25) would be rather small for the response(s) considered, an indication of low information content or, equivalently, that a large number of trials would be required to obtain a better parameter estimate.

3.5 Application of EVM

Again, for the same estimation problem as in section 3.4, the EVM model needs to have two statements. With a multiplicative error, the first statement relates the measured values to the true (yet unknown) values of the variables and errors, as follows:

$$\begin{cases} f_{1j} = f_{1j}^{*}(1 + \varepsilon_{f_1}) \\ F_{1j} = F_{1j}^{*}(1 + \varepsilon_{F_1}) \end{cases} \tag{3.26}$$

where f^* and F^* denote true values of the measurements f and F. Taking logarithms and approximating ln(1+ε), as in section 3.4, yields:

$$\begin{cases} \ln\left(f_{1j}\right) = \ln\left(f_{1j}^{*}\right) + \varepsilon_{f_1} \\ \ln\left(F_{1j}\right) = \ln\left(F_{1j}^{*}\right) + \varepsilon_{F_1} \end{cases} \tag{3.27}$$

In the EVM formulation, the Mayo-Lewis model must be re-written as:

$$g_i(\xi_i^*, \theta^*) = F_1^* - \frac{r_1^* f_{1i}^{*2} + f_{1i}^*(1-f_{1i}{}^*)}{r_1{}^* f_{1i}^{*2} + 2f_{1i}{}^*(1-f_{1i}{}^*) + r_2{}^*(1-f_{1i}{}^*)^2} \tag{3.28}$$

The EVM model needs derivatives with respect to the parameters and derivatives with respect to the true values of the variables. These derivatives are given by:

$$\frac{\partial g(\underline{\xi}, \underline{\theta})}{\partial r_1} = \frac{f_1^2(f_1^2 - f_1 - r_2 f_1^2 + 2r_2 f_1 - r_2)}{(r_2 - 2r_2 f_1 + r_2 f_1^2 + 2f_1 - 2f_1^2 + r_1 f_1^2)^2} \tag{3.29}$$

$$\frac{\partial g(\underline{\xi}, \underline{\theta})}{\partial r_2} = \frac{f_1(r_1 f_1 + 1 - f_1)(1-f_1)^2}{(r_2 - 2r_2 f_1 + r_2 f_1^2 + 2f_1 - 2f_1^2 + r_1 f_1^2)^2} \tag{3.30}$$

The EVM variable is actually the logarithm of the measured variable. Hence, for the partial derivatives of the function with respect to the variables, the variables are ln ($\underline{\xi_i}$) and not $\underline{\xi_i}$. This transformation is given by:

$$\frac{\partial g(\xi_i, \theta)}{\partial \ln(\xi_i)} = \frac{\partial g(\xi_i, \theta)}{\partial \xi_i} \cdot \frac{\partial \xi_i}{\partial \ln(\xi_i)} = \xi_i \cdot \frac{\partial g(\xi_i, \theta)}{\partial \xi_i} \tag{3.31}$$

Hence, for the Mayo-Lewis equation, we have the following derivatives:

$$\frac{\partial g(\underline{\xi}, \underline{\theta})}{\partial \ln(f_1)} = f_1 \cdot \frac{f_1^2(2r_1 r_2 - r_1 - r_2) + 2r_2 f_1 - 2r_1 r_2 f_1 - r_2)}{(r_2 - 2r_2 f_1 + r_2 f_1^2 + 2f_1 - 2f_1^2 + r_1 f_1^2)^2} \tag{3.32}$$

$$\frac{\partial g(\underline{\xi}, \underline{\theta})}{\partial \ln(F_1)} = F_1 \tag{3.33}$$

Finally, for the covariance matrix for copolymer composition data with no correlation between feed and copolymer composition (as per section 3.3), we have:

$$\underline{V} = \begin{bmatrix} \frac{k_{f_1}^2}{3} & 0 \\ 0 & \frac{k_{F_1}^2}{3} \end{bmatrix} \tag{3.34}$$

where the errors of the mole fraction of monomer *i* in the feed and terpolymer are $\pm k_{f_i}$ and $\pm k_{F_i}$ units, respectively.

3.6 A Quick Comparison between NLLS and EVM

As was outlined in Rossignoli and Duever (1995), a question often arises whether EVM is in general a better approach for parameter estimation in copolymerization studies than NLLS.

On the one hand, EVM is a better method as it takes into account the presence of error in all variables (both independent and dependent). Also, the fact that error structure information has to be considered in the algorithm and be quantified shows, if nothing else, that EVM forces one to think about the errors involved (and, hence, in turn, about the process variables), which is very important. Moreover, as mentioned earlier, EVM provides true values of the variables as well as of the parameter estimates. Additionally, the appropriateness of EVM is significant for multi-response experiments in which, say, combinations of copolymer triad fractions, composition and rate are used to estimate reactivity ratios. On the other hand, execution of the EVM algorithm requires more complicated computational tools. It is also not readily available in standard statistical software packages. The last reasons could have been perceived as drawbacks maybe 20-30 years ago, but they are (and should) not be of any issue nowadays.

3.7 Program Development

The EVM program refined further in this thesis was developed in the Matlab programming environment. Estimation of reactivity ratios can be achieved by using the

instantaneous copolymer composition equation, provided that the polymerization is run at low conversion. Preliminary work carried out by Dalvi (2003) converted the EVM program described in Reilly et al. (1994) from FORTRAN to Matlab. In addition, Hauch (2005) investigated several copolymerization systems with respect to reactivity ratio estimation using this program. Hauch (2005) included both composition and triad fraction data in her research and showed with her benchmarking cases that the program was successful in giving reliable reactivity ratio estimates.

The covariance matrix plays an important role in the EVM analysis. Recalling the types of error structure one usually deals with, the covariance matrix for additive errors and multiplicative errors is found to be the same. According to Hauch (2005), for copolymer composition data, the error structure is assumed to be multiplicative. So, assuming that there is no correlation between comonomer feed and copolymer composition measurements, the covariance matrix in the EVM program is given by eq. (3.34).

To demonstrate the performance of the EVM program, a case study was chosen with experimental data from a recent thesis (see Haque (2010)). The reactivity ratio estimation was conducted based on available instantaneous composition data, and the results are being compared with reported reactivity ratios in the literature in section 3.7.1.

3.7.1 Case Study: Acrylamide/Acrylic acid

The data come from the copolymerization of acrylamide (AAm, M_1)/acrylic acid (AA, M_2) in aqueous media (Haque, 2010). Reactivity ratios for this copolymerization have been determined previously in the literature. However, different studies have shown a wide range of values for the monomer reactivity ratios. Thus, the objective in this case study was to determine values of the reactivity ratios with respect to different initiators under study and also to compare them with the published values in the literature. Meanwhile, since the analysis was done by the error-in-variables-model (EVM) technique, the performance of this technique would be demonstrated in this case as well.

As mentioned earlier, for this case study, the effect of different initiators was investigated. The copolymerization reactions were carried out at 40°C using two different

initiators: 4,4′-azo-bis-(4-cyano valeric acid) (ACVA) and potassium persulphate (KPS). Tables 3.1-3.2 show copolymerization composition data with these two initiators. This copolymerization system was previously investigated by Rintoul and Wandrey (2005), who also performed free radical copolymerizations of AAm/AA with KPS as initiator. The monomer reactivity ratios were subsequently estimated using the Kelen-Tudos linear parameter estimation technique. These results are included in Table 3.3.

In order to use the EVM method for estimating the reactivity ratios, the reported reactivity ratios by Rintoul and Wandrey (2005) were used as the initial estimates. The error values for monomer feed and copolymer compositions were assumed to be 1% and 5% ($k_{f_1} = 0.01 \; and \; k_{F_1} = 0.05$, as introduced in section 3.5). Therefore, the covariance matrix (following eq. (3.34)) is given by:

$$V = \begin{bmatrix} \frac{0.01^2}{3} & 0 \\ 0 & \frac{0.05^2}{3} \end{bmatrix} \tag{3.35}$$

Table 3-1. Experimental data for AAm (M_1)/AA (M_2) copolymerization (low conversion) with ACVA initiator

Feed composition	Copolymer composition
f_{AM}	F_{AM}
0.58667	0.68831
0.58667	0.71541
0.58667	0.72123
0.17472	0.362168
0.17472	0.386959
0.17472	0.388711
0.44263	0.604341
0.44263	0.627048
0.44263	0.648347
0.49878	0.642779
0.49878	0.616691
0.49878	0.624412
0.13753	0.303973
0.13753	0.304759
0.13522	0.314079
0.13522	0.306983

Table 3-2. Experimental data for AAm (M_1)/AA (M_2) copolymerization (low conversion) with KPS initiator

Feed composition	Copolymer composition
f_{AM}	F_{AM}
0.4902	0.696
0.4902	0.688
0.4902	0.678
0.4902	0.694
0.4902	0.622
0.4902	0.680
0.1664	0.349
0.1664	0.333
0.1664	0.330
0.4423	0.644
0.4423	0.649
0.44223	0.657

The reactivity ratio estimates by EVM for both initiators are included in Table 3.3. It can be seen that reactivity ratios reported in Rintoul and Wandrey (2005) are close to our point estimates obtained from KPS initiator data, whereas for ACVA initiator, our reactivity ratio estimates have changed considerably and these values are no longer in agreement with Rintoul and Wandrey (2005). According to Table 3.3, one can easily observe that the values of reactivity ratios of this copolymerization system show considerable shift when using different initiators, confirming the effect of initiator on these values.

Table 3-3. Reactivity ratio estimates for AAm (M_1)/AA (M_2) copolymerization (low conversion) with different initiators

Initiator	Reference	r_1	r_2
KPS	Rintoul and Wandrey (2005)	2.5	0.39
ACVA	Current work	1.36	0.29
KPS	Current work	2.0066	0.3424

The joint confidence regions (in this case, we calculate and present JCRs of approximate shape and probability, as per eq. (3.14)) for the point estimates obtained from copolymerization data from different initiators (Tables 3.1 and 3.2) were generated next and

are plotted in Figures 3.1 and 3.2. In each figure, the open circle denotes the EVM point estimates from current work and the star represents the reported reactivity ratios from Rintoul and Wandrey (2005).

For ACVA initiator (Figure 3.1), it can be seen that the Rintoul and Wandrey (2005) results are not located close to our point estimates (also noted for Table 3.3) and they are not contained in the corresponding JCR. These results were expected, as the initiators for these copolymerization data sets are different and the AAm/AA polymerization is notorious for being affected by the reaction environment (initiator and solvent type, pH drift, ionic strength, etc.). For KPS initiator (Figure 3.2), the Rintoul and Wandrey (2005) reactivity ratios are located inside our calculated JCR, indicating that our results are in acceptable agreement. However, the Rintoul and Wandrey (2005) estimate is indeed located at the outer fringes of the ellipse, indicating a tendency to differ from the EVM point estimates, which can be related to the different parameter estimation techniques used (Kelen-Tudos, a linear parameter estimation technique, versus EVM).

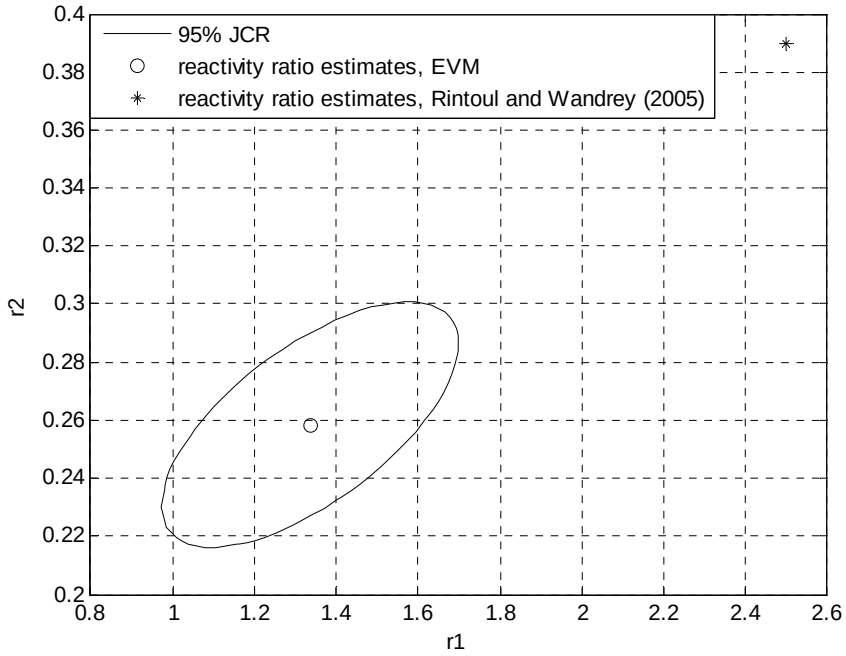

Figure 3-1. JCR for reactivity ratio estimates for copolymerization of AAm (M_1)/AA (M_2) with ACVA initiator

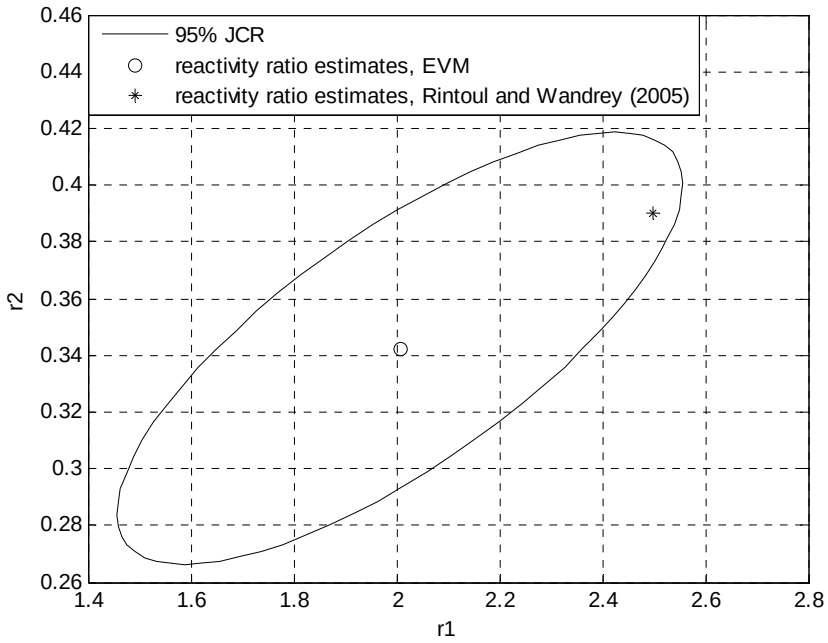

Figure 3-2. JCR for reactivity ratio estimates for copolymerization of AAm (M_1)/AA (M_2) with KPS initiator

Chapter 4. Reactivity Ratio Estimation from Cumulative Copolymer Composition Data

4.1 Introduction

As discussed previously, there are two general models for estimation of copolymerization reactivity ratios: instantaneous models and cumulative models. Monomer reactivity ratios are generally determined at low conversion levels using the instantaneous copolymer composition (ICC) model, otherwise referred to as the Mayo-Lewis equation, owing to the assumption that the composition drift in the monomer feed (and, hence, in the copolymer chains) is negligible at low conversion levels. However, most copolymerization reactions will inevitably show compositional drift as the degree of conversion increases (the exception being certain specific, not frequently encountered, cases). Also, the requirement of stopping a reaction at low conversion results often in experimental difficulties which could be considered as significant sources of errors in most of the cases. Therefore, it is reasonable to suggest that cumulative copolymer composition (CCC) models, i.e., the integrated form of instantaneous copolymerization models that can be applied over the whole conversion trajectory, and therefore to high conversion levels, should be preferred over the use of instantaneous models. In addition, considering reactivity ratio estimation using high conversion copolymerizations, a great advantage could potentially come from the fact that a single copolymerization can provide numerous data points and, hence, a wealth of information from a statistical estimation viewpoint.

Utilizing high conversion range experimental data with cumulative copolymer composition models has received little attention in the literature with respect to reactivity ratio estimation. In addition, the fact that reliable experimental data for copolymerization reactions at high conversion levels are very limited has compounded the issue even further. Therefore, the objectives of this chapter are to: (1) employ integrated models in order to

estimate monomer reactivity ratios from high conversion data, and (2) determine which one of the available models can provide better estimates of the reactivity ratios and offer comparative comments.

4.2 Cumulative Copolymer Composition (CCC) Models

As mentioned in Chapter 2, there are two types of models for integrated copolymer composition, and these are discussed in the following subsections.

4.2.1 Analytical Integration

The so-called Meyer-Lowry model is the result of the analytical integration of the differential copolymerization equation (instantaneous or Mayo-Lewis equation). The Meyer-Lowry model can be used in order to estimate reactivity ratios from the reaction at low to moderate levels of conversion (i.e., say, up to 30%-50% conversion, with the range of up to 25-30% conversion being safer). The derivation of this model was discussed in Chapter 2 in more detail. One must note that there were certain simplifying and restrictive assumptions involved in the derivation of this model. For instance, the polymerization should be isothermal, hence no temperature-varying scenarios can be accommodated. This assumption could be considered a minor problem, since reactivity ratios are weak functions of temperature (for many systems but not all), unless of course temperature levels change by more than 30 degrees Celcius. Another (relatively minor) assumption is that the volume of the polymerizing mixture does not shrink considerably. This would again be true at low to moderate conversion levels, but not throughout the entire reaction. The major assumption that has to be satisfied for the integration to take place and the analytical solution to be obtained is that reactivity ratios should remain constant during the course of polymerization, meaning that changes in the reactivity ratio values are assumed to be independent of

conversion. However, it is well known that at high conversion levels, even propagation reactions can become diffusion-controlled (and hence, a function of conversion), as long as the polymerization temperature is below the glass transition temperature of the polymerizing mixture. Since it is likely that these assumptions might be violated during a typical copolymerization, utilizing this model for kinetic investigations (especially above a conversion level of 25-50%, always depending on the specific copolymer system) can be a source of error.

Typically there are two popular forms of the Meyer-Lowry model encountered in the literature. One form is a logarithmic model which has been used in the publications of German and Heikens (1971), Van der Meer et al. (1978), and Patino-Leal et al. (1980). This form of the Meyer-Lowry model is given by eq. (4.1).

$$\log\left(\frac{[M_2]}{[M_{20}]}\right) = \frac{r_2}{1-r_2} log\left(\frac{[M_{20}][M_1]}{[M_{10}][M_2]}\right) - \frac{1-r_1 r_2}{(1-r_1)(1-r_2)} log\left(\frac{(r_1-1)\frac{[M_1]}{[M_2]}-r_2+1}{(r_1-1)\frac{[M_{10}]}{[M_{20}]}-r_2+1}\right) \tag{4.1}$$

In this equation, $[M_1]$ and $[M_2]$ denote the monomer concentrations at some time t corresponding to a certain conversion level X_n, whereas $[M_{10}]$ and $[M_{20}]$ denote initial monomer (feed) concentrations. This form of the Meyer-Lowry model, based only on the conversion of monomer 2 (see the left-hand side of eq. (4.1)), has led to misinterpretations with respect to measurements choices (i.e., one may choose to monitor only the conversion of monomer 2 due to the form of eq. (4.1)). Thus, for cases when the difference between the reactivity ratios is significant, using this model may not be appropriate. The other form of the model uses the overall monomer (total) conversion as a response. This is the general form of the Meyer-Lowry model and is given by eq. (4.2):

$$X_n = 1 - \left(\frac{f_1}{f_{10}}\right)^{\alpha}\left(\frac{f_2}{f_{20}}\right)^{\beta}\left(\frac{f_{10}-\delta}{f_1-\delta}\right)^{\gamma} \tag{4.2}$$

where

$$\alpha = \frac{r_2}{(1-r_2)}; \quad \beta = \frac{r_1}{(1-r_1)}; \quad \gamma = \frac{1-r_1 r_2}{(1-r_1)(1-r_2)}; \quad \delta = \frac{(1-r_2)}{(2-r_1-r_2)}$$

f_1 and f_2 are the free (unreacted, unbound) monomer mole fractions at time, t, whereas f_{10} and f_{20} are the initial monomer (feed) mole fractions. X_n is molar conversion, defined by eq. (4.3), assuming that the polymerizing mixture has a constant volume.

$$X_n = 1 - \frac{[M_1]+[M_2]}{[M_{10}]+[M_{20}]} \tag{4.3}$$

One must note that typical measurements in an experiment are the initial monomer mole fractions and final monomer mole fractions. Therefore, the molar conversion cannot be obtained as described in eq. (4.3). To avoid this problem, and using the expression for the cumulative mole fraction of monomer 1 bound in the copolymer at conversion X_n, given by eq. (4.4), the molar conversion can be obtained by the so-called Skeist equation, as shown in eq. (4.5).

$$\bar{F}_1 = \frac{[M_{10}]-[M_1]}{[M_{10}]+[M_{20}]-[M_1]-[M_2]} \tag{4.4}$$

$$X_n = \frac{f_1-f_{10}}{f_1-\bar{F}_1} \tag{4.5}$$

Subsequently, the Meyer-Lowry model can be rewritten as eq. (4.6), for which all participating variables can be measured directly in a typical experiment.

$$g(f_1, f_{10}, \bar{F}_1) = \frac{f_1-f_{10}}{f_1-\bar{F}_1} - 1 + \left(\frac{f_1}{f_{10}}\right)^{\alpha} \left(\frac{f_2}{f_{20}}\right)^{\beta} \left(\frac{f_{10}-\delta}{f_1-\delta}\right)^{\gamma} \tag{4.6}$$

Eq. (4.6) is referred to as the **molar conversion form** of the Meyer-Lowry model.

An alternative form for the Meyer-Lowry model could also be developed to yield a relationship between the initial monomer (feed) mole fraction, f_{10}, final copolymer mole

fraction, $\bar{F}_1$, and conversion on a weight basis, X_w (further explanations were included in Chapter 2). This relation is:

$$g(X_n, f_{10}, \bar{F}_1) = X_n - 1 + \left(\frac{f_{10}-\bar{F}_1 X_n}{f_{10}(1-X_n)}\right)^{\alpha} \left(\frac{1-X_n-f_{10}-\bar{F}_1 X_n}{(1-f_{10})(1-X_n)}\right)^{\beta} \left(\frac{(\delta-f_{10})(1-X_n)}{\delta-\delta X_n-f_{10}+\bar{F}_1 X_n}\right)^{\gamma} \quad (4.7)$$

X_n in eq. (4.7) can be replaced by mass conversion using eq. (4.8). Eq. (4.7) is usually referred to as the **mass conversion form** of the Meyer-Lowry model and this is the form that will be used in the remainder of this chapter, for parameter estimation purposes.

$$X_n = X_w \frac{Mw_1 f_{10}+(1-f_{10})Mw_2}{Mw_1 \bar{F}_1+(1-\bar{F}_1)Mw_2} \quad (4.8)$$

where Mw_1 and Mw_2 are the molecular weights of monomer 1 and 2.

As pointed out in the literature (Hautus et al., 1985), there are some potential problems in dealing with the Meyer-Lowry model. In some cases, certain values of f_{10} and f_1 may result in the last quotient of eq. (4.6) to be negative. These values, although not feasible, may arise internally during iterative estimation schemes. In addition, in the neighborhood of r_1=1 or r_2=1, eq. (4.6) is numerically unstable. To avoid having these problems, Hautus et al. (1985) proposed certain transformation techniques, which are not discussed here for the sake of brevity (more details can be found in the original paper). However, applying mathematical transformations on the Meyer-Lowry model (as with many other models) might subsequently change the error structure involved; as a result, certain assumptions related to the estimation methodology (least squares) are violated, and hence the estimation results are not reliable.

4.2.2 Numerical Integration

Using the direct numerical integration of the differential copolymer composition equation is an alternative approach for estimating reactivity ratios of monomers. Compared with the

analytical form of the Meyer-Lowry model, numerically solving a differential equation with simultaneous parameter estimation may be computationally more intensive but it has the great advantages of employing a direct approach and avoiding transformations that tend to distort the error structure (in addition to avoiding simplifying or other restrictive assumptions).

The basis of the numerical integration, as mentioned in Chapter 2, is the model that relates cumulative copolymer composition ($\overline{F_1}$) to the mole fraction of unreacted monomer (f_1) in the polymerizing mixture and molar conversion, X_n. As mentioned earlier, this relation, called the Skeist equation, is given by eq. (4.5), and can be re-expressed as follows:

$$\overline{F_1} = \frac{f_{10} - f_1(1 - X_n)}{X_n} \tag{4.9}$$

As the reaction proceeds with time, X_n changes, and f_1, the mole fraction of unreacted monomer in the polymerizing mixture, is evaluated by the numerical solution of the differential equation, given by eq. (4.10).

$$\frac{df_1}{dx_n} = \frac{f_1 - F_1}{1 - X_n} \tag{4.10}$$

Meanwhile, the value of F_1 is given by the Mayo-Lewis equation, repeated below for quick reference:

$$F_1 = \frac{r_1 f_1^2 + f_1 f_2}{r_1 f_1^2 + 2 f_1 f_2 + r_2 f_2^2} \tag{2.5}$$

In order to solve (i.e., numerically integrate) the ordinary differential eq. (4.10), the initial condition $f_1 = f_{10}$ when $X_n = 0$ is required.

4.3 Reactivity Ratio Estimation Approach

4.3.1 Parameter Estimation with Error-in-Variables-Model

Both cumulative composition models are nonlinear and thus in order to estimate their parameters we need to use nonlinear parameter estimation techniques. Implementation of linear parameter estimation methods combined with model transformations is statistically unsound, as has repeatedly been discussed in the literature and earlier in this thesis (see Chapter 3). As discussed in Chapter 3, the nonlinear least squares (NLLS) method and the error-in-variables-model (EVM) method are commonly used. The NLLS method is not appropriate for parameter estimation with the cumulative copolymer composition models because, regardless of whether F_1 or f_1 is selected as the independent variable, the associated amount of error would not be negligible. Therefore, EVM is the preferable estimation technique. The great improvement provided by the EVM method comes from simply accounting correctly for the major sources of errors in all variables. A detailed description of the EVM method was included in Chapter 3, and a brief development follows below as a quick reminder.

The EVM procedure consists of two statements. First, the vector of measurements x_i is equated to the vector of true (yet unknown) values of these measurements, ξ_i, plus an error term ε_i.

$$x_i = \xi_i + \varepsilon_i \qquad where\ i = 1,2,\dots,n \tag{4.11}$$

In the above, n denotes the number of available experiments (trials). The second statement relates the true (yet unknown) values of the parameters, θ^*, with the true values of variables, ξ_i, via a model represented by:

$$g(\xi_i, \theta^*) = 0 \qquad where\ i = 1,2,\dots,n \tag{4.12}$$

The vector function g ( ) in eq. (4.12) may be linear or nonlinear in the elements of ξ_i and θ.

A point estimate of $\hat{\theta}$ can be found by minimizing

$$\phi = \frac{1}{2}\sum_{i=1}^{n} r_i\left(x_i - \widehat{\xi_i}\right)' V^{-1}\left(x_i - \widehat{\xi_i}\right) \tag{4.13}$$

where r_i is the number of replicates at the i[th] trial and V denotes the error covariance matrix for the measurements (see Chapter 3, subsection 3.3, for more information about the error covariance matrix).

The EVM program was developed in the Matlab programming environment. Details about the objective functions employed in EVM for both the Meyer-Lowry model and the direct numerical integration are discussed in the following subsections. Lastly, it should be mentioned that the error structure and levels for the possible measurements, namely, the mass conversion X_w, the initial feed composition, f_{10}, and the final copolymer composition, $\bar{F}_1$, were multiplicative at the levels of ±1%, ±1%, and ±5%, respectively (i.e., error on $\bar{F}_1 = 5\%$ of $\bar{F}_1$ value as measured). These structure and levels have also been repeatedly shown to reflect real experimental situations (for instance, see Dube et al. (1991), Dube and Penlidis (1996), and McManus and Penlidis (1996)).

4.3.2 Application of EVM with the Meyer-Lowry Model

To illustrate the steps of the EVM method, the mass conversion form of the Meyer-Lowry model, and combining eqs. (4.5) and (4.6), is written in the following form:

$$g(f_{10}, X_w, \bar{F}_1) = 1 - X_n - \left(\frac{f_1}{f_{10}}\right)^{\alpha}\left(\frac{1-f_1}{1-f_{10}}\right)^{\beta}\left(\frac{f_{10}-\delta}{f_1-\delta}\right)^{\gamma} = 0 \tag{4.14}$$

where $\alpha = \frac{r_2}{(1-r_2)}$, $\beta = \frac{r_1}{(1-r_1)}$, $\gamma = \frac{1-r_1 r_2}{(1-r_1)(1-r_2)}$, $\delta = \frac{(1-r_2)}{(2-r_1-r_2)}$

and $f_1 = \frac{f_{10} - \bar{F}_1 X_n}{1 - X_n}$, $X_n = X_w \frac{Mw_1 f_{10} + (1 - f_{10}) Mw_2}{Mw_1 \bar{F}_1 + (1 - \bar{F}_1) Mw_2}$

The EVM variables are f_{10}, X_w, and $\bar{F}_1$. According to Chapter 3, which gives more details on the EVM algorithm implementation, and the brief development of section 4.3.1, the first EVM statement relates the measured values of the variables with the true (yet unknown) values of the measurements and the associated errors (given below for quick reference):

$$f_{10j} = f_{10j}^{*}\left(1 + \varepsilon_{f_1}\right)$$
$$X_{wj} = X_{wj}^{*}\left(1 + \varepsilon_{X_w}\right) \tag{4.15}$$
$$\bar{F}_{1j} = \bar{F}_{1j}^{*}\left(1 + \varepsilon_{\bar{F}_1}\right)$$

where an asterisk denotes true values and ε is the error term associated with these three variables. Since the error is multiplicative, taking the natural logarithm of both sides of eq. (4.15) and approximating $\ln(1+\varepsilon)$ with ε, yields:

$$\ln(f_{10j}) = \ln\left(f_{10j}^{*}\right) + \varepsilon_{f_{10}}$$
$$\ln(X_{wj}) = \ln\left(X_{wj}^{*}\right) + \varepsilon_{X_w} \tag{4.16}$$
$$\ln(\bar{F}_{1j}) = \ln(\bar{F}_{1j}^{*}) + \varepsilon_{\bar{F}_1}$$

Briefly, EVM performs two iteration routines. First, an inner loop is performed, which searches for the true values of the variables, followed by an outer loop, searching for the true values of the parameters (more details were given in Chapter 3).

4.3.3 Application of EVM with the Direct Numerical Integration Model

The direct numerical integration approach begins with the Skeist equation, eq. (4.9), relating the cumulative copolymer composition to conversion and the initial feed composition. Therefore, the objective function used in EVM is then:

$$g(\bar{F}_1) = \bar{F}_1 - \frac{f_{10} - f_1(1 - X_n)}{X_n} \tag{4.17}$$

X_n is related to the measured variable X_w by equation (4.8). Unlike what has been done during the execution of the EVM method on the Meyer-Lowry model, in this case, the only EVM variable is the cumulative copolymer composition, $\bar{F}_1$; f_{10} and X_w have already been used in the solution of the ordinary differential equation, eq. (4.10), and thus cannot be considered as independent variables. So, $\bar{F}_1$, as the only EVM variable, is defined in exactly the same way as shown earlier in eqs. (4.15) and (4.16):

$$\bar{F}_{1j} = \bar{F}_{1j}^{*}(1 + \varepsilon_{\bar{F}_1}) \tag{4.18}$$

For multiplicative error, and by taking the natural logarithm of both sides of eq. (4.18), we have:

$$\ln(\bar{F}_{1j}) = \ln(\bar{F}_{1j}^{*}) + \varepsilon_{\bar{F}_1} \tag{4.19}$$

The rest of the implementation steps of EVM in this case are analogous to explanations given earlier in section 4.3.2 and will not be repeated here for the sake of brevity.

4.4 Evaluation of Estimation Performance: Case Studies

4.4.1 Evaluation Approach

Estimation of reactivity ratios from cumulative copolymerization models eliminates the difficulties associated with stopping reactions at low conversion, while one gains to study the full polymerization trajectory. The estimation of reactivity ratios from high conversion level data can be made either by using the Meyer-Lowry model or by the direct numerical integration approach. It must be noted that considering cumulative models for estimating reactivity ratios, not only are the model equations different from those used for low conversion data analysis (Mayo-Lewis model), but also the way of obtaining the data is different in that a single copolymerization can provide numerous data points, and, hence, a lot of information for the statistical analysis. Due to the fact that determining monomer reactivity ratios with the highest possible precision is vital, our goal is to offer comparisons and indicate some of the limitations of existing estimation approaches, while presenting a novel method of estimation of monomer reactivity ratios at moderate/high conversion levels. The evaluation approach basically considers the following factors: (1) The method/model should give unbiased estimates of the parameters, (2) The method/model should take into account (nearly) all information available in the data with regard to the parameters to be estimated, thus providing precise point estimates, as well as uncertainty (error) bounds for these estimates (something that other approaches in the literature do not do), and (3) The method should be reasonably easy to use.

A number of copolymerization systems were studied using cumulative composition data to estimate the reactivity ratios using the EVM method. In general, it was intended to (a) demonstrate the agreement between the point estimates obtained from cumulative models and those obtained from the instantaneous model using low conversion data, and (b) emphasize the advantages of using the cumulative copolymerization composition (CCC) models for moderate to high conversion levels, where the compositional drift may be significant. An important point that one should bear in mind is that due to the difficulties

involved with collecting experimental data at high conversion for some systems, not all literature data sets can be considered as adequately representative data sets for our investigations.

As part of the evaluation process, and for the subsequent judgment call whether the calculated/published reactivity ratios are reliable to use, the magnitude of the 95% joint confidence regions (JCR) can be considered as an appropriate criterion. The 95% JCR, expressing the degree of uncertainty associated with the point estimates of the monomer reactivity ratios, is a reflection of the choice of initial monomer concentrations (i.e., design of experiments), the number of collected data points (and hence the corresponding information content), and the error in the experimental data.

4.4.2 Case Study 1: Styrene/Methyl Methacrylate

The first copolymerization system under study is the copolymerization of styrene (Sty, M_1) and methyl methacrylate (MMA, M_2). This (almost "model") system has been studied extensively in the literature at both low and high conversion levels. The low conversion Sty/MMA copolymerization data were selected from Kinsinger et al. (1962). The Sty/MMA copolymerizations were performed in bulk at 60 °C and the reactions were kept at very low conversion levels. Table 4.1 shows the low conversion experimental data. The reactivity ratios of Sty and MMA were estimated using linear parameter estimation techniques such as Finemann-Ross and Kelen-Tudos. O' Driscoll et al. (1984) studied the Sty/MMA system at moderate to high conversion levels in bulk at 60 °C and provided the experimental data cited in Table 4.2. In this reference, monomer reactivity ratios were also estimated using the EVM method. The published reactivity ratios from both references are included in Table 4.3.

The aim of this case study is to illustrate the performance of reactivity ratio estimation when the EVM method is applied on instantaneous versus cumulative copolymerization models based on low conversion levels. In addition, it is intended to find out whether utilizing the cumulative copolymer composition models when dealing with moderate to high

conversion range data can improve the reactivity ratio estimation. Lastly, it is important to know which approach, between the Meyer-Lowry and the direct numerical integration one, can provide more accurate reactivity ratio estimates.

Table 4-1. Low conversion experimental data for Sty/MMA copolymerization

Feed composition	Conversion (wt%)	Copolymer composition
f_{sty}	X_w	F_{sty}
0.761	1.68	0.674
0.655	4.81	0.595
0.393	4.05	0.498
0.321	4.43	0.351
0.196	3.85	0.286

Table 4-2. High conversion experimental data for Sty/MMA copolymerization

Feed composition	Conversion (wt%)	Copolymer composition
$(f_o)_{Sty}$	X_w	$\overline{F}_{sty}$
0.6	4.5	0.5413
0.6	4.7	0.5644
0.6	26.1	0.5523
0.6	27.3	0.5805
0.6	49.6	0.5855
0.6	55.6	0.5734
0.6	70	0.5865
0.35	4.6	0.3946
0.35	24.1	0.4115
0.35	69.6	0.3966

Table 4-3. Reactivity ratio estimates for Sty/MMA copolymerization (low and high conversion) based on different copolymerization models for parameter estimation

	Copolymerization model	Conversion level	r_1	r_2
Kinsinger et al. (1963)	Mayo-Lewis	Low	0.43	0.41
Current work	Mayo-Lewis	Low	0.4244	0.4278
Current work	Meyer-Lowry	Low	0.4616	0.4315
Current work	Direct Numerical	Low	0.4662	0.4390
O' Driscoll et al. (1984)	Meyer-Lowry	Moderately high	0.4317	0.4215
Current work	Meyer-Lowry	Moderately high	0.4281	0.4183
Current work	Direct Numerical Integration	Moderately high	0.4402	0.4385

First of all, the low conversion composition data (using the data set from Table 4.1) were considered and the monomer reactivity ratios were estimated using three models: the Mayo-Lewis model, the Meyer-Lowry model, and the direct numerical integration. The reactivity ratio estimates are shown in Table 4.3. Subsequently, the 95% joint confidence regions (JCRs) were calculated for all three models and are presented in Figure 4.1 together. In this figure o, ∆ , and □ correspond to the point estimates obtained from the Mayo-Lewis model, the Meyer-Lowry model, and the direct numerical integration, respectively.

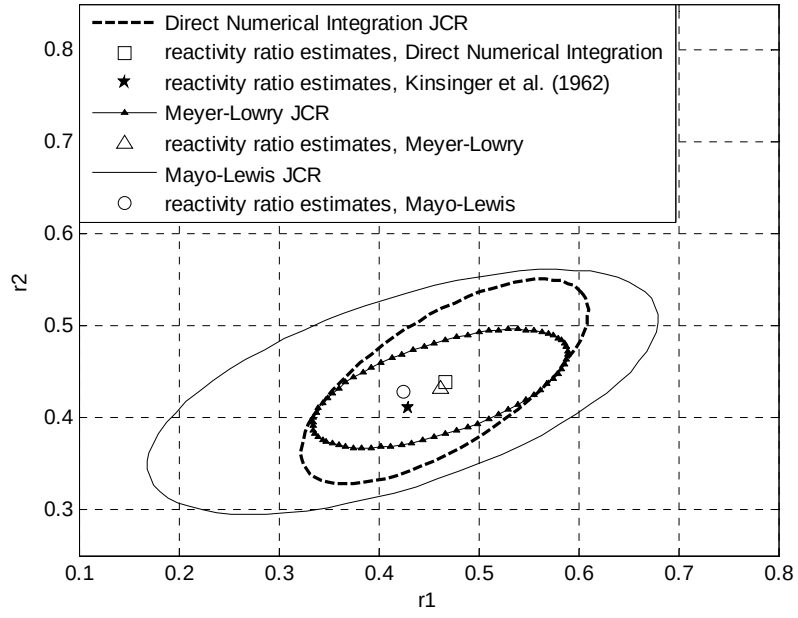

Figure 4-1. JCRs for the Mayo-Lewis model, the Meyer-Lowry model, and direct numerical integration using low conversion data for Sty/MMA copolymerization

It can be seen in Figure 4.1 that the point estimates obtained from the three models are in relatively good agreement; more specifically, there is excellent agreement between the Meyer-Lowry model and the direct numerical integration point estimates. In addition, the reactivity ratios reported in Kinsinger et al. (1962) are contained in all JCRs, demonstrating that these literature values are in agreement with current work. Considering Figure 4.1, it can be seen that the JCRs from the cumulative models (the Meyer-Lowry and the direct numerical integration model) are completely contained within the instantaneous model JCR (the Mayo-Lewis model), thus indicating that the cumulative models are capable of providing reliable results even based on low conversion range data.

As mentioned earlier, the precision of the parameter estimation results is reflected in the size of the corresponding JCRs, hence comparisons can be made on that basis. That is, the smaller the area of the JCR, the higher the reliability of the point estimates. It is evident from Figure 4.1 that the size of the Mayo-Lewis JCR is considerably larger than the other cumulative models, and thus it can be said that even using low conversion range data, the cumulative models provide more precise point estimates. This result was expected as the cumulative models involve more information in the parameter estimation procedure and thus the addition of more information contributes to higher confidence (smaller JCRs) for the point estimates. Meanwhile, considering the cumulative model JCRs, it can be seen that although the point estimates are almost identical, the size of the Meyer-Lowry JCR is smaller and completely included within the direct numerical integration JCR. This result shows that in this case of dealing with low conversion data the Meyer-Lowry model provided more reliable point estimates; this can be explained based on the fact that the implementation of EVM on the Meyer-Lowry model involves three variables (f_{10}, X_w, $\bar{F}_1$), whereas for the direct numerical integration the only variable is $\bar{F}_1$. As a result, these three variables have provided more information for the Meyer-Lowry model analysis, thus leading to higher precision of the results. This result is not only expected from a propagation of information point of view, as discussed above, but is also valid from a mathematical functional analysis point of view; if a direct analytical solution exists and is valid in the region of interest, it will be superior to any numerical solution (or approximation).

The next step is to compare the results from parameter estimation between low conversion and high conversion levels. The low conversion data were analyzed using the Mayo-Lewis model (as per usual practice), whereas the high conversion data were analyzed using both the Meyer-Lowry model and the direct numerical integration. The point estimates obtained based on the high conversion level data are shown in Table 4.3 as well. Figure 4.2 illustrates JCRs obtained by the three models (in a way similar to the low conversion data). In this figure, the reactivity ratios published in both reference papers (low and high conversion levels) were also included.

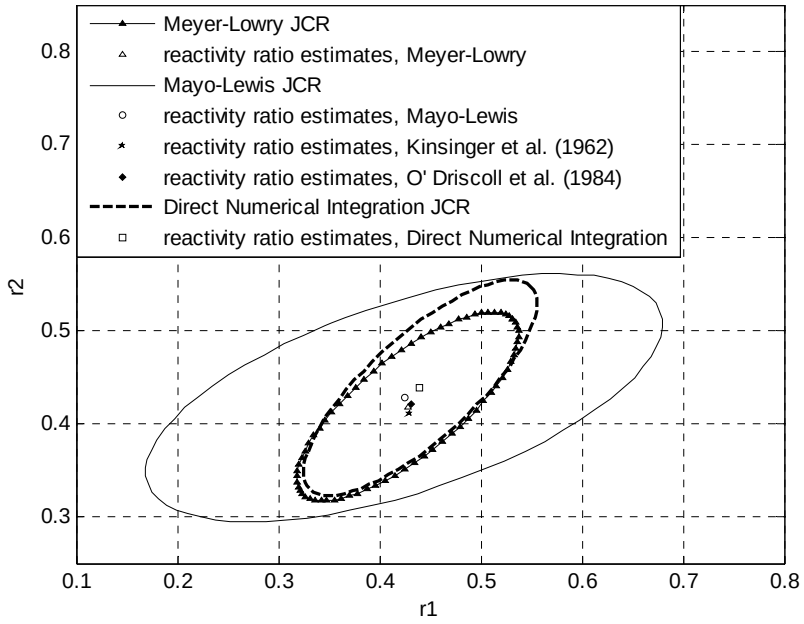

Figure 4-2. JCRs for the Meyer-Lowry model and direct numerical integration (high conversion data) and the Mayo-Lewis model (low conversion data) for Sty/MMA copolymerization

Considering Figure 4.2, once again it can be seen that the literature point estimates (from both low and high conversion level data) and the current work results are in good agreement. Also, it is evident that the Mayo-Lewis model JCR is significantly larger than the Meyer-Lowry model and direct numerical integration JCRs, meaning that the cumulative models offer higher precision (higher confidence) in the point estimates. These results confirm that properly accounting for the effect of compositional drift during the reactivity ratio estimation procedure does increase the level of certainty in the results.

Also, as can be seen in Figure 4.2, there is almost a complete overlap between the Meyer-Lowry JCR and the direct numerical integration JCR. This indicates excellent agreements between the results of these two approaches. This would be expected as both models are using the same experimental data. However, one can argue that the direct numerical integration makes it possible to avoid the limitations of the Meyer-Lowry model (as mentioned in section 4.2.1) and therefore it can be considered as a more general and direct approach.

4.4.3 Case Study 2: Di-n-Butyl Itaconate/Methyl Methacrylate

The free radical copolymerization of di-n-butyl itaconate (DBI, M_1) and methyl methacrylate (MMA, M_2) was carried out in a benzene solution at 50°C by Madruga and Fernandez-Garcia (1994) at low conversion levels. Later, the same authors studied the same copolymerization system in benzene solution and 50°C up to high conversion levels at several feed monomer compositions (Madruga and Fernandez-Garcia (1995)). The experimental data at low and high conversions are included in Tables 4.4 and 4.5, respectively. Reactivity ratio estimation studies were subsequently performed by the authors using the extended Kelen-Tudos parameter estimation method. Their published point estimates are shown in Table 4.6.

The goal in this case study is to, first, estimate the reactivity ratios based on high conversion experimental data using the cumulative models (the Meyer-Lowry model and the direct numerical integration) and, subsequently, to compare the reliability of the high conversion results with the conventional point estimates obtained from the low conversion range data.

Table 4-4. Low conversion experimental data for DBI/MMA copolymerization, Madruga and Fernandez-Garcia (1994)

Feed composition	Conversion (wt%)	Copolymer composition
$(f_o)_{DBI}$	X_w	$\overline{F}_{DBI}$
0.3	6.46	0.025
0.3	6.04	0.043
0.3	8.05	0.056
0.3	5.34	0.165
0.3	5.09	0.246
0.3	5.97	0.259
0.3	3.61	0.377
0.3	8.77	0.382
0.3	3.86	0.411
0.3	4.18	0.459
0.3	3.17	0.512
0.3	4.47	0.623
0.3	4.64	0.732
0.5	4.82	0.272
0.5	4.05	0.416
0.5	4.75	0.628

Table 4-5. High conversion experimental data for DBI/MMA copolymerization, Madruga and Fernandez-Garcia (1995)

Feed composition	Conversion (wt%)	Copolymer composition
$(f_o)_{DBI}$	X_w	$\overline{F}_{DBI}$
0.3	22.2	0.237
0.3	43.8	0.273
0.3	48.8	0.268
0.3	47.4	0.272
0.3	54.8	0.265
0.3	58.9	0.270
0.3	55.4	0.269
0.3	65.3	0.286
0.3	70.6	0.269
0.3	86.6	0.324
0.5	8.1	0.405
0.5	12.0	0.401
0.5	37.0	0.439
0.5	42.2	0.448
0.5	47.3	0.448
0.5	54.5	0.454
0.5	56.8	0.466
0.5	58.7	0464
0.5	65.8	0.487
0.5	79.6	0.427
0.7	16.3	0.645
0.7	23.1	0.634
0.7	26.7	0.634
0.7	31.0	0.631
0.7	34.1	0.632
0.7	40.9	0.661
0.7	42.5	0.684
0.7	44.0	0.645
0.7	49.1	0.649
0.7	52.7	0.675
0.7	54.5	0.666
0.7	64.3	0.675
0.7	71.8	0.690

Similar to the previous case study, the reactivity ratios of the low conversion range data were estimated using the Mayo-Lewis model. Also, at higher conversions, both the Meyer-Lowry model and the direct numerical integration were utilized to estimate the reactivity ratios. The obtained point estimates are shown in Table 4.6 as well. The values of the reactivity ratios obtained based on different models at different conversion levels are all very similar; our results are in good agreement with the published ones with this data set. Also, the results show that at high conversion levels, the choice of the model to be used for reactivity ratio estimation does not have a strong effect on the point estimates (of course, if the implicit assumption is satisfied that the copolymerization data are reliable and have been collected with the utmost care, i.e., they contain reasonably low experimental error).

To be able to actually decide which model and for what level of conversion the calculated reactivity ratio estimates are more reliable, the performance of the proposed approaches were compared based on their calculated JCR areas; as explained earlier, JCRs indicate the level of uncertainty in the point estimates. In the first step of the evaluation of the results for this copolymerization, we wanted to compare the performance of the instantaneous model based on low conversion data versus the cumulative models based on high conversion range data. Figure 4.3 shows the Mayo-Lewis JCR and the Meyer-Lowry JCR together. In this figure, the open circle and square are the point estimates calculated by the Mayo-Lewis model and the Meyer-Lowry model, respectively. Also, the star corresponds to the point estimates reported in the reference paper based on the high conversion range data.

Table 4-6. Reactivity ratio estimates for DBI/MMA copolymerization (low and high conversion) based on different copolymerization models for parameter estimation

	Copolymerization model	Conversion level	r_1	r_2
Madruga and Fernandez-Garcia (1994)	Mayo-Lewis	Low	0.717	1.329
Current work	Mayo-Lewis	Low	0.7098	1.313
Current work	Meyer-Lowry	High	0.6794	1.229
Current work	Direct Numerical Integration	High	0.6798	1.238

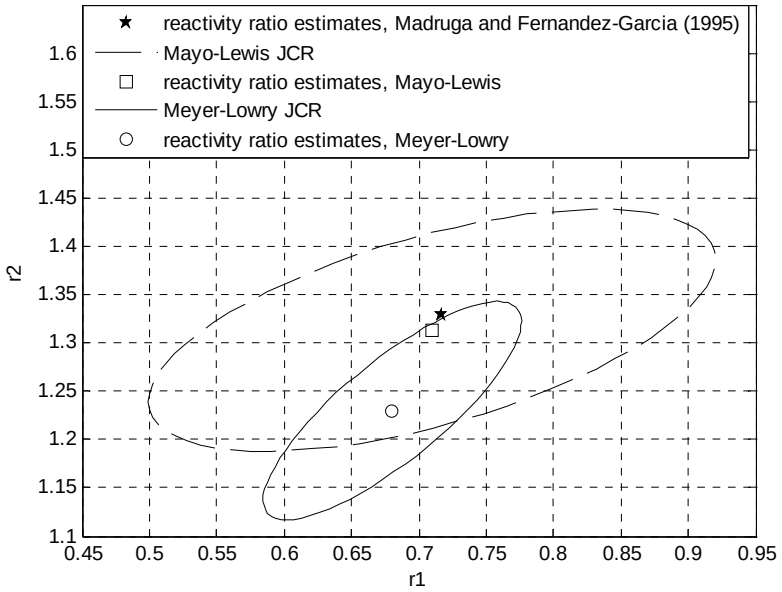

Figure 4-3. JCRs for the Meyer-Lowry model (using high conversion data) and the Mayo-Lewis model (low conversion data) for DBI/MMA copolymerization

According to Figure 4.3, the results of low conversion analysis are in relatively good agreement with the high conversion analysis due to the considerable overlap between the corresponding JCRs. However, one can note that the Meyer-Lowry model is not completely contained in the Mayo-Lewis JCR. Moreover, the point estimates reported by Madruga and Fernandez-Garcia (1995) based on the high conversion data fall only at the borderline of (but outside) the Meyer-Lowry JCR, whereas they show a better agreement with the results from the low conversion instantaneous analysis (which exhibits a much larger JCR area, anyway). Therefore, it can be said that, although all point estimates are satisfactorily close, the published reactivity ratios and our results based on high conversion data could be in acceptable agreement only if the experimental error were higher that 5% (since 5% is the error level used to construct the Meyer-Lowry JCR in Figure 4.3). Another observation from Figures 4.3 is that the size of the Meyer-Lowry JCR is considerably smaller that the Mayo-Lewis JCR, indicating that the level of certainty for the reactivity ratios obtained from the Meyer-Lowry model is considerably higher; using the high conversion data set has improved the performance of parameter estimation in this copolymerization system.

Once again, similar to the first case study, we compared the performance of the Meyer-Lowry model and the direct numerical integration on reactivity ratio estimation using high conversion data. The point estimates obtained for the DBI/MMA system, which are very similar regardless of the different cumulative model used, are also included in Table 4.6. JCRs obtained from implementations of these models on the high conversion range data are shown together in Figure 4.4. The open circle and square correspond to the point estimates obtained by the Meyer-Lowry model and the direct numerical integration, respectively. Again, the star represents literature reactivity ratios, as shown earlier in Figure 4.3.

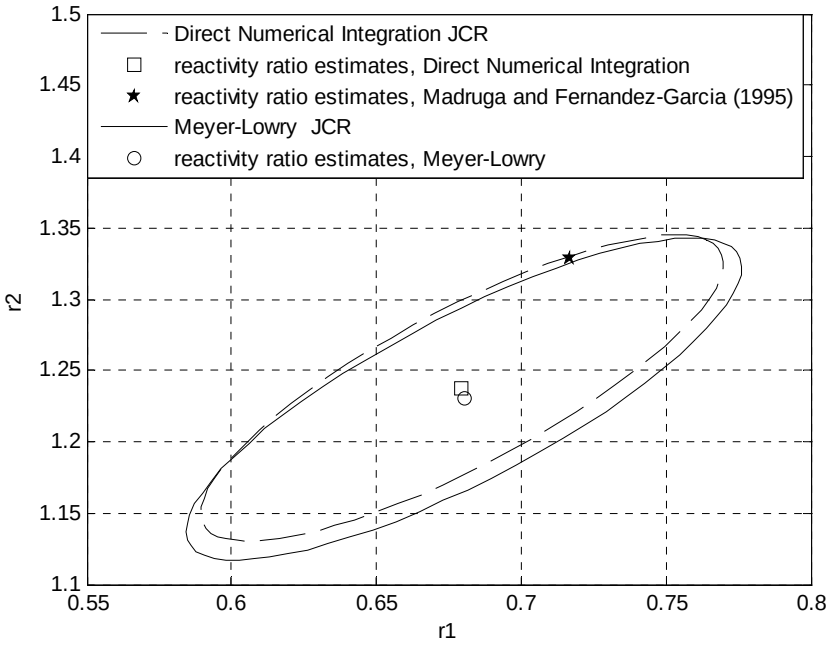

Figure 4-4. JCRs for the Meyer-Lowry model and direct numerical integration using high conversion data for DBI/MMA copolymerization

It can be seen from Figure 4.4 that there is a great overlap between the JCRs from the two cumulative models (and that point estimates are very similar as well). These results are very similar to the previous case study and thus confirm the point that the analysis of high conversion level data provides comparable results independent of the choice of the model used. Careful observation of Figure 4.4 shows that the Meyer-Lowry JCR is slightly larger

than the direct numerical integration JCR, meaning that the confidence on the results obtained from the direct numerical integration is slightly higher. This observation points to the benefit of using the direct numerical integration in that it improves the reactivity ratio estimation results while it avoids dealing with the difficulties and uncertainties that one might encounter when working with the Meyer-Lowry model.

4.4.4 Case Study 3: Acrylamide/Acrylic Acid

The copolymerization of acrylamide (AAm, M_1) and acrylic acid (AA, M_2) is studied in this case study. Homopolymers and copolymers of AAm/AA are an important class of water soluble polymers, generally made by free radical polymerization. Hauch (2005) estimated monomer reactivity ratios for this copolymerization system using low and high conversion range data published in Bourdais (1955) and Shawki and Hamielec (1979), respectively. In these reference papers, polymerizations were carried out in aqueous media at 40°C. The experimental data sets from Bourdais (1955) and Shawki and Hamielec (1979) are presented in Tables 4.7 and 4.8, respectively. A reactivity ratio estimation study was conducted in Bourdais (1955) based on low conversion experimental data using linear parameter estimation techniques. These point estimates are included in Table 4.9. Reactivity ratio estimates in Shawki and Hamielec (1979) were obtained using nonlinear least squares and integrating the instantaneous model over conversion. Their reactivity ratio estimates are shown in Table 4.9, as well.

In this case study, we re-visited the work by Hauch (2005) and our objectives were to: (1) estimate the reactivity ratios from available experimental data at high and low conversion levels and, (2) evaluate the performance of different applicable models with respect to improving the estimation of the reactivity ratios, similar to what we have done in previous case studies. First, reactivity ratios at low conversion levels using the Mayo-Lewis model, the Meyer-Lowry model, and the direct numerical integration were estimated in order to contrast the results of cumulative models versus the instantaneous model. Moreover, the Meyer-

Lowery model as well as the direct numerical integration were applied on the high conversion data from Shawki and Hamielec (1979) and the reactivity ratios re-estimated, so that the effect of using high conversion data could be investigated. That way, an extra comparison could also be made between two different cumulative models.

Table 4-7. Low conversion experimental data from Bourdais (1955) for AAm/AA copolymerization

Feed composition	Copolymer composition	Conversion (wt%)
f_{AAm}	F_{AAm}	X_w
0.125	0.183	7
0.25	0.327	10
0.375	0.466	6
0.50	0.607	6
0.625	0.712	5
0.75	0.817	2
0.875	0.901	3

Table 4-8. High conversion experimental data from Shawki and Hamielec (1979) for AAm/AA copolymerization

Feed composition	Conversion (wt%)	Copolymer composition
$(f_o)_{AAm}$	X_w	$\overline{F}_{AAm}$
0.08	16.4	0.128
0.08	24.1	0.115
0.08	38	0.117
0.08	50.9	0.111
0.08	58.3	0.103
0.08	68.9	0.096
0.15	23.4	0.217
0.15	31.8	0.204
0.15	47.2	0.21
0.15	52.1	0.194
0.15	60.2	0.186
0.15	71.1	0.18
0.2	19.7	0.288
0.2	27.6	0.273
0.2	38.1	0.264
0.2	49	0.266
0.2	58.3	0.256
0.2	62.1	0.239
0.25	22.8	0.335
0.25	34	0.334
0.25	44.9	0.323
0.25	51.2	0.313
0.25	63.8	0.309
0.25	66.1	0.297

As mentioned earlier, results from the estimations based on the low conversion data of Table 4.7 are shown in Table 4.9. These values seem to be similar and thus to further investigate the validity of these point estimates, the JCRs obtained from these three different models were plotted together in Figure 4.5. In this figure o, ∆, and □ correspond to the reactivity ratio estimates from the Mayo-Lewis model, the Meyer-Lowry model, and the direct numerical integration. As can be seen, these points are located close to each other. Also, the Mayo-Lewis JCR completely includes the Meyer-Lowry and direct numerical integration JCRs, showing that the results are in agreement. Another important observation is

that in this case the sizes of the JCRs from the cumulative models are almost the same, whereas the Mayo-Lewis JCR is considerably larger. Therefore, similar to previous case studies, it seems that using cumulative composition models which take into account more information for the analysis (conversion values) results in higher precision for the reactivity ratio estimates. Finally, it must be mentioned that the reported reactivity ratios in Bourdais (1955) are contained in the three JCRs of Figure 4.5, indicating that our results, regardless of the choice of the composition model, are in good agreement with the literature.

Table 4-9. Reactivity ratio estimates for AAm (M_1)/AA (M_2) copolymerization (low and high conversion) with different copolymerization models for parameter estimation

	Copolymerization model	Conversion level	r_1	r_2
Bourdais (1955)	Mayo-Lewis	Low	1.43	0.60
Current work	Mayo-Lewis	Low	1.410	0.6388
Current work	Meyer-Lowry	Low	1.417	0.6227
Current work	Direct Numerical Integration	Low	1.426	0.6241
Shawki and Hamielec (1979)	Meyer-Lowry	Moderately high	1.45	0.57
Current work	Meyer-Lowry	Moderately high	1.4608	0.5720
Current work	Direct Numerical Integration	Moderately high	1.4734	0.5720

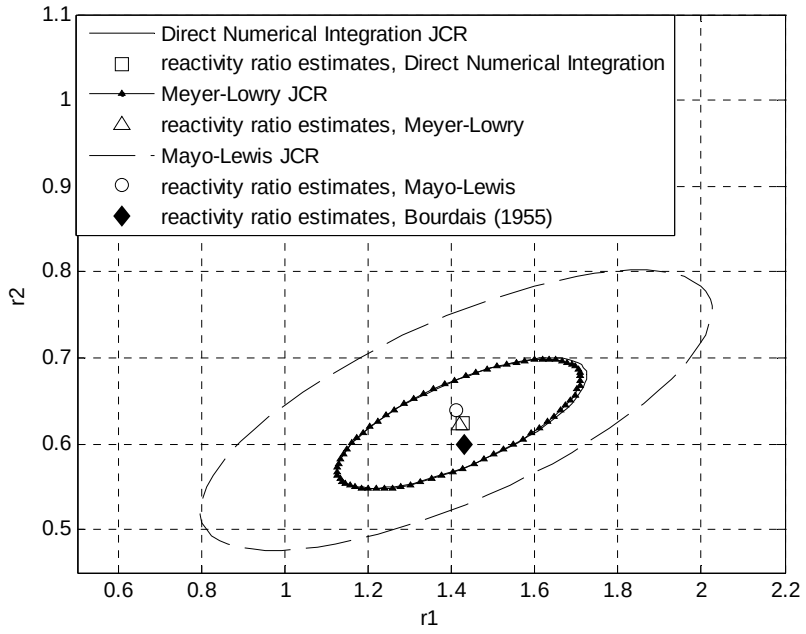

Figure 4-5. JCRs for the Mayo-Lewis model, the Meyer-Lowry model, and direct numerical integration with low conversion data for AAm/AA copolymerization

In the second step of the analysis for this system, the high conversion range data (Table 4.8) were used to estimate the reactivity ratios. The point estimates obtained from the Meyer-Lowry model and the direct numerical integration are also included in Table 4.9. The corresponding JCRs for the Meyer-Lowry model and the direct numerical integration, obtained from high conversion data, are shown in Figure 4.6 along with the Mayo-Lewis JCR, obtained from low conversion data. Also, the reactivity ratio values reported in Bourdais (1955) and Shawki and Hamielec (1979) are included in Figure 4.6. It can be clearly seen from this figure that the cumulative model JCRs are considerably smaller than the Mayo-Lewis JCR and almost completely contained in it, showing that the results obtained from high conversion data are more reliable than (and still in good agreement with) the low conversion data analysis. Moreover, the sizes of the Meyer-Lowry JCR and the direct numerical integration JCR are exactly the same, indicating that these two cumulative models provided comparable and identical precision for the point estimates. Lastly, it can be seen in Figure 4.6 that the point estimates provided by Shawki and Hamielec (1979) are not included in the cumulative model JCRs, while the reactivity ratios reported in Bourdais (1955) also

fall outside of these JCRs (and are away from the Shawki and Hamielec (1979) point estimates). These results are not surprising as we expected (based also on results obtained from previous case studies) that analyzing high conversion data with cumulative copolymerization models affects the position of the point estimates.

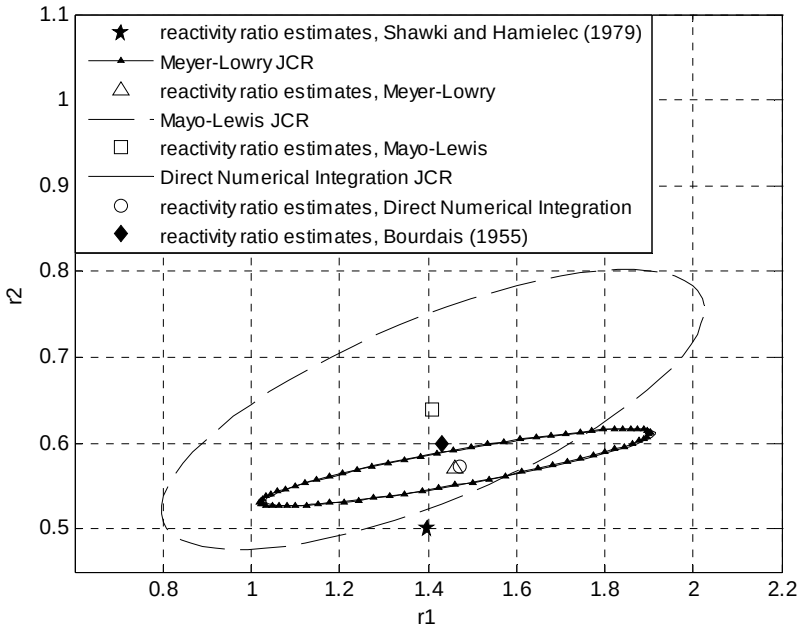

Figure 4-6. JCRs for the Meyer-Lowry model and direct numerical integration (using high conversion data) and the Mayo-Lewis model (low conversion data) for AAm/AA copolymerization

Overall, this case study presents supporting results for our points throughout this chapter. It demonstrates that our approach in implementing the cumulative models for reactivity ratio estimation is capable of increasing the accuracy of the results, compared with the low conversion analysis. It also emphasizes that considering high conversion range data with the cumulative models does affect the reactivity ratio point estimates. And lastly, it shows that the performance of the Meyer-Lowry model and the direct numerical integration approach is similar, which again points to the benefits of using the direct numerical approach, as it is more straightforward and general than the Meyer-Lowry model.

4.4.5 Case Study 4: Acrylamide/Acrylic Acid; A Counter-example

Reactivity ratio estimation studies for the copolymerization of acrylamide (AAm, M_1) and acrylic acid (AA, M_2) were discussed in the previous case study, case study 3. In addition to the literature sources discussed earlier about this system, this copolymerization was recently investigated by Haque (2010) in order to study the kinetics of this copolymerization in aqueous media in more detail. Copolymerizations were performed at 25°C for both low and high conversion ranges. The experimental data sets from Haque (2010) for low and high conversions are presented in Tables 4.10 and 4.11, respectively.

The goal of presenting this case study is to re-estimate reactivity ratios from these more recent available experimental data at both low and high conversion levels. Since these data sets are from a new source, it is interesting to compare the precision obtained from different applicable models with respect to reactivity ratio estimation results. This way, effect of errors associated with the experimental data at high conversion can also be investigated. Once more, we estimated the reactivity ratios at low conversion levels using the Mayo-Lewis model, the Meyer-Lowry model, and the direct numerical integration, in order to contrast cumulative models versus the instantaneous model. The reactivity ratio estimates are summarized in Table 4.12.

Table 4-10. Low conversion experimental data from Haque (2010) for AAm/AA copolymerization

Feed composition	Copolymer composition	Conversion (wt%)
f_{AAm}	F_{AAm}	X_w
0.4988	0.643	7.6
0.4988	0.617	6.1
0.4988	0.624	9.1
0.1747	0.356	4.9
0.1747	0.355	5.8
0.1747	0.369	3.6
0.4426	0.604	5.9
0.4426	0.627	6.9
0.4426	0.648	6.3
0.1375	0.304	3.4
0.1375	0.305	4.9
0.1352	0.314	15.5
0.1352	0.307	16.8
0.1352	0.315	15.4

Table 4-11. High conversion experimental data from Haque (2010) for AAm/AA copolymerization

Feed composition	Conversion (wt%)	Copolymer composition
$(f_o)_{AAm}$	X_w	$\overline{F}_{AAm}$
0.500286	0.0889	0.64871
0.500286	0.0921	0.63755
0.500286	0.1124	0.63183
0.500286	0.1693	0.65908
0.500286	0.2412	0.65349
0.500286	0.2973	0.62539
0.500286	0.3075	0.63043
0.500286	0.3179	0.64740
0.500286	0.3258	0.63625
0.500286	0.4633	0.63654
0.500286	0.4944	0.63036
0.500286	0.5608	0.63048
0.500286	0.7828	0.57110
0.500286	0.9713	0.56068

From the entries of Table 4.12, the point estimates obtained at low conversion seem close. So, similar to the previous cases, the JCRs for the corresponding models were plotted together, as shown in Figure 4.7. In this figure o, Δ, and □ correspond to the reactivity ratio estimates from the Mayo-Lewis model, the Meyer-Lowry model, and the direct numerical integration, respectively. It is evident that point estimates are located close to each other and also their JCRs lie close to each other, showing that the results are in agreement. Another important observation is that in this case the sizes of the JCRs are almost the same for the three models, due to the nature of the data points employed in the estimation scheme (i.e., the errors involved). One can observe that, due to the nature of the copolymer system in question (fast polymerizing system), the supposedly low conversion data of Table 4.10 can go to almost 15-20%, thus making the use of the Mayo-Lewis model and the Meyer-Lowry model almost equivalent.

Table 4-12. Reactivity ratio estimates for AAm (M_1)/AA (M_2) copolymerization (low and high conversion) with different copolymerization models for parameter estimation

	Copolymerization model	Conversion level	r_1	r_2
Current work	Mayo-Lewis	Low	1.3373	0.2691
Current work	Meyer-Lowry	Low	1.2932	0.2410
Current work	Direct Numerical Integration	Low	1.3157	0.2475
Current work	Meyer-Lowry	high	2.3167	0.6573

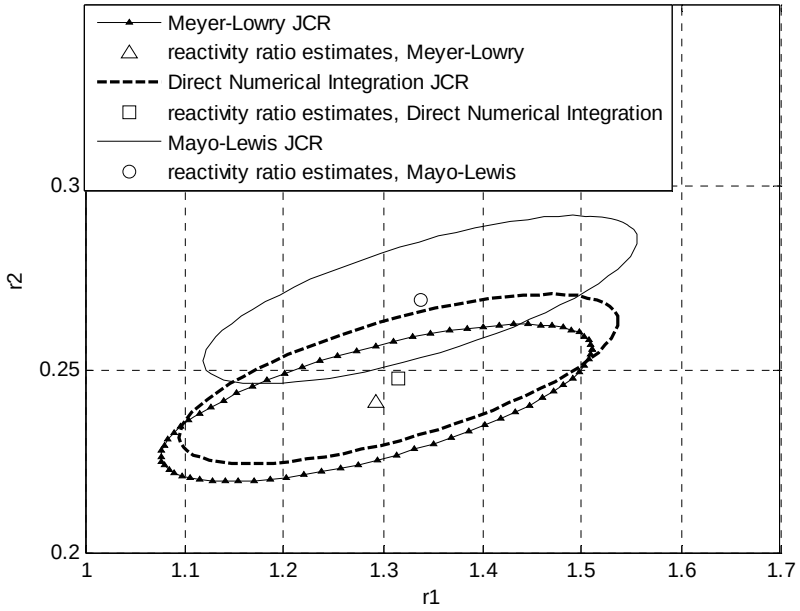

Figure 4-7. JCRs for the Mayo-Lewis model, the Meyer-Lowry model, and direct numerical integration with low conversion data for AAm/AA copolymerization

The next step was to use the high conversion range data (Table 4.11) to estimate the reactivity ratios. The point estimates obtained from the Meyer-Lowry model are also included in Table 4.12. In order to compare the accuracy of the obtained results from high conversion and low conversion data, like in earlier cases, the Meyer-Lowry JCR obtained from high conversion data along with the Meyer-Lowry JCR obtained from low conversion data are plotted together in Figure 4.8. It can be clearly seen from this plot that for high conversion data, the JCR does not close and extends to negative (infeasible) values, which is an indication of great uncertainty in the results of parameter estimation (and in the data set). The low conversion JCR is completely contained within the high conversion JCR (showing that there is a relatively acceptable agreement between these data sets). However, the sizes of the two JCRs are not even comparable, and the point estimates are not close to each other at all. Therefore, it is reasonable to suggest that the reported high conversion range data points in Haque (2010) contain more error (uncertainty) than normally expected, thus confirming typical problems encountered with this (fast reacting and high molecular weight producing) copolymer system. An additional corroboration of this was the fact that the direct numerical integration approach had severe difficulties with convergence, hence this gave another

indication that the magnitude of the error dominated and completely masked the actual signals (actual polymerization information). In other words, with this data set, the error in composition seems considerable (and overwhelming) for parameter estimation purposes.

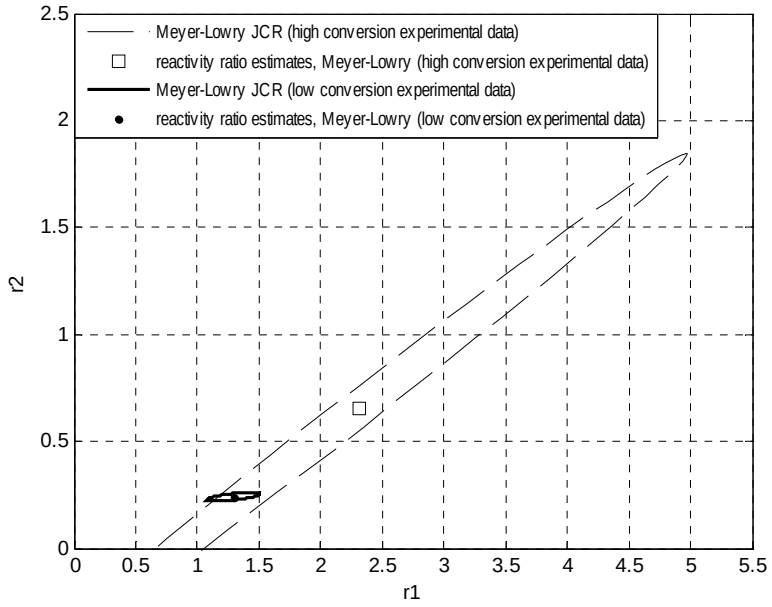

Figure 4-8. JCRs for the Meyer-Lowry model with low and high conversion data for AAm/AA copolymerization

This case study and its results comprise a significant counter-example. Based on our observations so far, it must be emphasized that, while our approach in utilizing high conversion data and cumulative models has proven to be superior to the conventional studies based on low conversion data, a statistical technique, no matter how novel or sophisticated it might be, cannot compensate for low (or complete lack of) information content in the data. In other words, as shown in this counter-example, it is highly crucial to have reliable experimental data at high conversion levels with reasonable amount of error associated with the measurements, in order to be able to obtain high quality monomer reactivity ratios for copolymerization. Otherwise, the estimation results and analysis are not to be trusted and no valid conclusions can be drawn based on an ill-conditioned data set (which may arise either from badly designed experiments or from experimental analysis with significant error).

4.4.6 Case Study 5: Styrene/Ethyl Acrylate

An experimental study of the bulk free radical copolymerization of styrene (Sty, M_1)/ethyl acrylate (EA, M_2) initiated by 2,2'-azobisisobutyronitrile at 50°C was conducted by McManus and Penlidis (1996). In this study, copolymerizations were carried out for reactivity ratio determination at low conversion level (conversion below 2%). In addition, full conversion range copolymerizations were planned with three different initial feed points (including the azeotropic feed composition for this system) and the cumulative copolymer compositions were obtained. Experimental conversion data for full, mid- and low range are shown in Tables 4.13 to 4.15. It is important to note that the first initial feed in Table 4.13 is the Sty/EA copolymerization azeotropic point, $(f_o)_{Sty}$=0.762, the third point is the composition with the largest compositional drift, $(f_o)_{Sty}$=0.152, and the second feed mole fraction corresponds to somewhere in between, $(f_o)_{Sty}$=0.458. Table 4.16 contains experimental results for a combined data set (low conversion of Table 4.15 and only the azeotropic data of Table 4.13), which will be discussed at the end of this subsection. McManus and Penlidis (1996) calculated the reactivity ratios based on the instantaneous copolymer composition using the low conversion range data of Table 4.15. The EVM method was used as the parameter estimation technique and their point estimates are presented in Table 4.17, along with estimates from other cases in our study.

Our goal in this case study is to estimate the reactivity ratios based on full conversion data using the cumulative models so that we can compare them with the values obtained from low conversion data and investigate the effect of considering higher conversion level data for reactivity ratio estimation studies. Further investigations can also be made into comparing the performance of the direct numerical integration and the Meyer-Lowry model, similar to previous case studies. As mentioned earlier in this chapter, the Meyer-Lowry model is suitable for data at relatively moderate conversion levels (i.e., below 30-40 %). Therefore, interesting points to be checked in this case study are the effect of using full conversion range data versus moderate level (mid-range) conversion data with the Meyer-Lowry model and also to compare the results with the direct numerical integration approach. In order to do this,

the data points with conversion values, $X_{w,}$ greater than 30% were left out of Table 4.13, and the new data set for the moderate level conversion range, as shown in Table 4.14, was used in the analysis. Reactivity ratio estimates from all these different combinations of models and data ranges are cited in Table 4.17

Table 4-13. Full conversion range experimental data from McManus and Penlidis (1996) for Sty/EA copolymerization at 50°C

Feed composition	Conversion (wt%)	Copolymer composition	Feed composition	Conversion (wt%)	Copolymer composition	Feed composition	Conversion (wt%)	Copolymer composition
$(f_o)_{Sty}$	X_w	$\overline{F}_{Sty}$	$(f_o)_{Sty}$	X_w	$\overline{F}_{Sty}$	$(f_o)_{Sty}$	X_w	$\overline{F}_{Sty}$
0.762	5.91745	0.756531	0.458	5.83151	0.6058	0.152	4.22755	0.35515
0.762	11.0093	0.798299	0.458	11.7823	0.627342	0.152	8.0379	0.38248
0.762	16.5733	0.763259	0.458	16.2626	0.605036	0.152	12.1788	0.36768
0.762	21.6025	0.735561	0.458	20.9505	0.621176	0.152	15.9654	0.36205
0.762	26.5056	0.768199	0.458	26.5336	0.631756	0.152	19.5886	0.38023
0.762	36.9661	0.758484	0.458	31.0206	0.618607	0.152	22.4555	0.35082
0.762	38.2197	0.747447	0.458	36.7533	0.587051	0.152	27.1326	0.32867
0.762	39.4881	0.752862	0.458	44.6665	0.586471	0.152	30.0431	0.35970
0.762	46.7575	0.807308	0.458	52.7688	0.598698	0.152	34.3593	0.33756
0.762	55.2128	0.775765	0.458	63.0109	0.585127	0.152	38.682	0.32459
0.762	61.8961	0.780883	0.458	70.3714	0.566273	0.152	45.711	0.30968
0.762	69.2998	0.784133	0.458	78.2768	0.554705	0.152	62.6608	0.28525
0.762	78.154	0.794617	0.458	91.7165	0.485955	0.152	73.8426	0.27202
0.762	98.1528	0.753301	0.458	98.5876	0.536734	0.152	96.1546	0.17413

Table 4-14. Mid-range conversion level experimental data from McManus and Penlidis (1996) for Sty/EA copolymerization at 50°C

Feed composition	Conversion (wt%)	Copolymer composition
$(f_o)_{Sty}$	X_w	$\overline{F}_{Sty}$
0.762	5.91745	0.756531
0.762	11.0093	0.798299
0.762	16.5733	0.763259
0.762	21.6025	0.735561
0.762	26.5056	0.768199
0.458	5.83151	0.6058
0.458	11.7823	0.627342
0.458	16.2626	0.605036
0.458	20.9505	0.621176
0.458	26.5336	0.631756
0.152	4.22755	0.355157
0.152	8.0379	0.382489
0.152	12.1788	0.367686
0.152	15.9654	0.362053
0.152	19.5886	0.380235
0.152	22.4555	0.350826
0.152	27.1326	0.328676

Table 4-15. Low conversion range experimental data from McManus and Penlidis (1996) for Sty/EA copolymerization at 50°C

Feed composition	Copolymer composition	Conversion (wt%)
f_{Sty}	F_{Sty}	X_w
0.0788	0.296	1.2
0.0788	0.308	1.27
0.0788	0.303	1.16
0.0788	0.286	1.04
0.7193	0.716	1.49
0.7193	0.736	1.48
0.7193	0.736	1.40
0.7193	0.732	1.46

Table 4-16. Combined data set from low conversion and high conversion at azeotropic point for Sty/EA copolymerization

Feed composition	Copolymer composition	Conversion (wt%)
f_{Sty}	F_{Sty}	X_w
0.0788	0.296	1.2
0.0788	0.308	1.27
0.0788	0.303	1.16
0.0788	0.286	1.04
0.7193	0.716	1.49
0.7193	0.736	1.48
0.7193	0.736	1.40
0.7193	0.732	1.46
0.762	0.756531	5.91745
0.762	0.798299	11.0093
0.762	0.763259	16.5733
0.762	0.735561	21.6025
0.762	0.768199	26.5056
0.762	0.758484	36.9661
0.762	0.747447	38.2197
0.762	0.752862	39.4881
0.762	0.807308	46.7575
0.762	0.775765	55.2128
0.762	0.780883	61.8961
0.762	0.784133	69.2998
0.762	0.794617	78.154
0.762	0.753301	98.1528

Table 4-17. Reactivity ratio estimates for Sty (M_1)/EA (M_2) copolymerization (low and high conversion) with different models and data ranges for parameter estimation at 50°C

	Copolymerization model	Conversion level	r_1	r_2
McManus and Penlidis (1996)	Mayo-Lewis	Low	0.717	0.128
Current work	Mayo-Lewis	Low	0.717	0.1282
Current work	Meyer-Lowry	Low	0.7166	0.1257
Current work	Direct Numerical Integration	Low	0.7127	0.1256
Current work	Meyer-Lowry	Moderate	0.9687	0.1496
Current work	Direct Numerical Integration	Moderate	0.9794	0.1542
Current work	Meyer-Lowry	High	---	---
Current work	Direct Numerical Integration	High	0.9318	0.1403
Current work	Mayo-Lewis	Combined data set (low and high conversion at azeotropic point)	0.7576	0.1290

As can be seen in Table 4.17, the point estimates obtained at low conversion from either the instantaneous model or cumulative models are almost identical and in complete agreement with the published values in the reference paper. However, it is noticeable that the point estimates obtained from moderate level conversion data have shifted, indicating again that the conversion level does affect the reactivity ratio values. Also, as seen in previous case studies with low conversion level data, the Meyer-Lowry model and the direct numerical integration point estimates are very close.

Another interesting observation from Table 4.17 and its full conversion range data is that the direct numerical integration has resulted in point estimates that are not close to the moderate level point estimates. These results further emphasize the effect high conversion data can have on the output of parameter estimation analysis. It must be noted that the parameter estimation with the Meyer-Lowry model did not converge to any reactivity ratio values when using the full conversion range data (denoted as 'high' in Table 4.17). One

potential reason, indicated earlier in subsection 4.2.1, is related to certain assumptions involved in the derivation of the Meyer-Lowry model that are likely to be violated during a typical copolymerization, namely the assumption that reactivity ratios should remain constant during the course of polymerization. Moreover, the non-convergence can also be attributed to the level of uncertainty (error) associated with data at higher conversion levels, as an ill-conditioned situation can definitely affect the performance of the Meyer-Lowry model in estimating reactivity ratios. Which reason may be at work here causing problems with the Meyer-Lowry model is left for a future investigation.

In order to further explore the performance of different models used for reactivity ratio estimation, the 95% joint confidence regions (JCR) for the corresponding point estimates of Table 4.17 were produced. In the first step, the JCRs for the Mayo-Lewis model, the Meyer-Lowry model, and the direct numerical integration from analyzing the low conversion level data of Table 4.15, were plotted together in Figure 4.9. It can be seen that the point estimates are in very good in agreement, as observed in Table 4.17, and the sizes of JCRs for all three models are almost the same. Recalling from previous results in case studies 1 and 2, it was expected that the cumulative models provide higher quality parameter estimates (smaller JCRs) due to the fact that they incorporate more information in the parameter estimation procedure (values of conversion that are not considered when working with the Mayo-Lewis model). The fact that all JCRs in Figure 4.9 are the same can be explained based on the nature of the collected experimental data, shown in Table 4.15: the (low) conversion data points are almost the same! Since changes in the values of conversion are minimal, the X_w data of Table 4.15 do not offer any additional information to the cumulative models, i.e., they do not increase the information content of the cumulative models more than what the instantaneous model knows! Hence, it makes sense that all models give almost the same JCRs with the data of Table 4.15. If for some points of Table 4.15 the conversion level X_w had been allowed to go to slightly higher levels, say, 2-4 % (still below 5 %), then the cumulative models would have yielded higher precision reactivity ratio point estimates (i.e., smaller JCRs) compared with the Mayo-Lewis model.

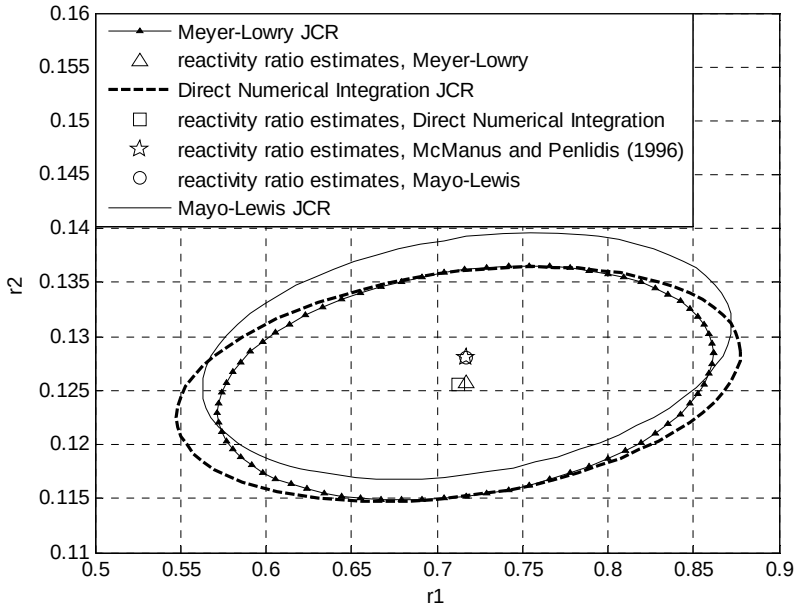

Figure 4-9. JCRs for the Mayo-Lewis model, Meyer-Lowry model, and direct numerical integration with low conversion data for Sty/EA copolymerization

Figure 4.10 shows the cumulative model JCRs based on the moderate level (mid-range) conversion data (Table 4.14) along with the Mayo-Lewis JCR obtained from low conversion data (Table 4.15). Considering this figure, one can appreciate (1) the effect of utilizing higher conversion experimental data on the parameter estimation results instead of instantaneous, low conversion, data, and (2) the performance of the Meyer-Lowry model and the direct numerical integration with respect to the quality of the point estimates. It can clearly be seen from this figure that the point estimates have shifted considerably for the cumulative model results and their corresponding JCRs do not overlap with the instantaneous model, the Mayo-Lewis model. Also, it can be seen that the Meyer-Lowry model and the direct numerical integration results are in excellent agreement (JCR contours overlap significantly and of course the point estimates are very close). The final observation from this figure is that the point estimates published in McManus and Penlidis (1996) do not fall inside neither of the cumulative model JCRs, as expected, since they had been obtained based on low conversion experimental data.

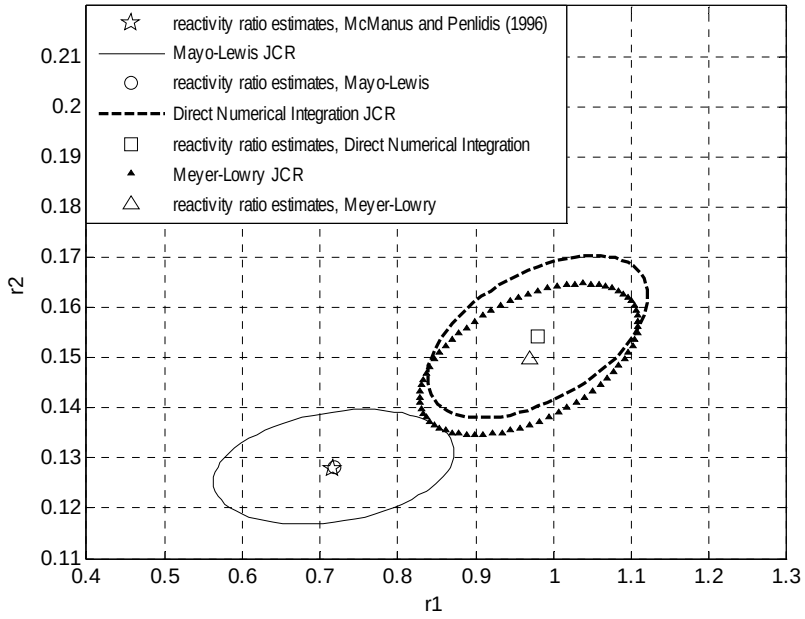

Figure 4-10. JCRs for the Mayo-Lewis model with low conversion data and the Meyer-Lowry model and direct numerical integration with moderate conversion data for Sty/EA copolymerization

Considering Table 4.17, which summarizes the calculated point estimates from different approaches, it is noticeable that the point estimates obtained from low, moderate, and full conversion levels using the direct numerical integration are different. Subsequently, one can see the effect of adding higher conversion data on the output of the parameter estimation analysis with respect to their precision (as can be realized based on the size of the corresponding JCRs). Figure 4.11 presents the direct numerical integration JCRs based on low, moderate, and full conversion range data. It is evident from this figure that the point estimates obtained from the full range (high) conversion data have the smallest JCR and hence highest precision. The comparison between moderate conversion and low conversion range results shows that although the reactivity ratio values have considerably shifted, the sizes of their JCRs are almost the same (potential reasons were pointed out earlier in this case study). These observations underline that considering full conversion range data can increase the precision of the parameter estimation results compared to moderate and low conversion range data, which could be attributed to the higher information content that is gained due to the inclusion of all the data points. Another thing to note is that the JCR based on the full

conversion range data is located in between (and overlaps with both) the low and moderate JCRs, thus representing a trade-off and compromise that can describe the whole data set.

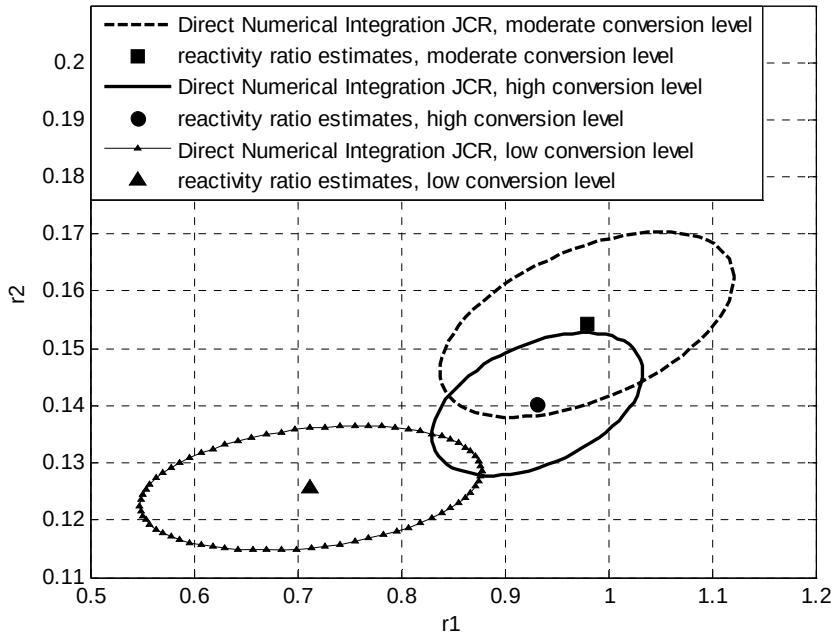

Figure 4-11. JCRs for the direct numerical integration based on low, moderate, and high conversion range data for Sty/EA copolymerization

In the full conversion range experiments conducted by McManus and Penlidis (1996) for Sty/EA copolymerization, the azeotropic composition ($(f_o)_{Sty}$=0.762) was one of the initial feed points. According to the definition of the azeotropic point, the cumulative copolymer composition remains constant and equal to the feed composition during the course of polymerization. In other words, since the cumulative copolymer composition remains constant with conversion, then the cumulative copolymer composition is equal to the instantaneous copolymer composition at any point throughout the reaction. This would then mean that the Mayo-Lewis equation (instantaneous composition equation) could be applicable over the full conversion range data that were obtained with initial feed composition of $(f_o)_{Sty}$=0.762 at the azeotropic condition. As mentioned earlier, Table 4.16 presented a combined data set from azeotropic high conversion data points from Table 4.13 and low conversion data points from Table 4.15. So, our intention was to estimate reactivity

ratios using the Mayo-Lewis model for this combined data set from Table 4.16 and compare with reactivity ratio estimates from other data ranges.

The point estimates obtained from this analysis are shown in the last row of Table 4.17. Also, Figure 4.12 shows the Mayo-Lewis JCR based on the combined data set of Table 4.16, along with the Mayo-Lewis JCR from the low conversion data of Table 4.15. It can be seen in this figure that the point estimates from the combined data set are in good agreement with point estimates from low conversion data and also the reported values in McManus and Penlidis (1996). The most important observation from this figure is that the JCR from the combined data set is greatly overlapping with (in fact, completely included within) the JCR based on low conversion data. In addition, the JCR from the combined set is much smaller than the low conversion one. This first-ever observation is a great demonstration of the fact that combining high conversion information at azeotropic conditions with low conversion data is much preferable, as it will increase the reliability/quality of the reactivity ratio estimates. Needless to say, the results of Figure 4.12 confirm once more that combined and enhanced information content will improve the parameter estimates, as long as the combination of different pieces of information is the appropriate one!

In summary, this case study highlighted the effects of considering data points at higher conversion levels in the parameter estimation analysis and showed how logically the new information adds to the quality of the parameter estimates, when combined appropriately with other data ranges.

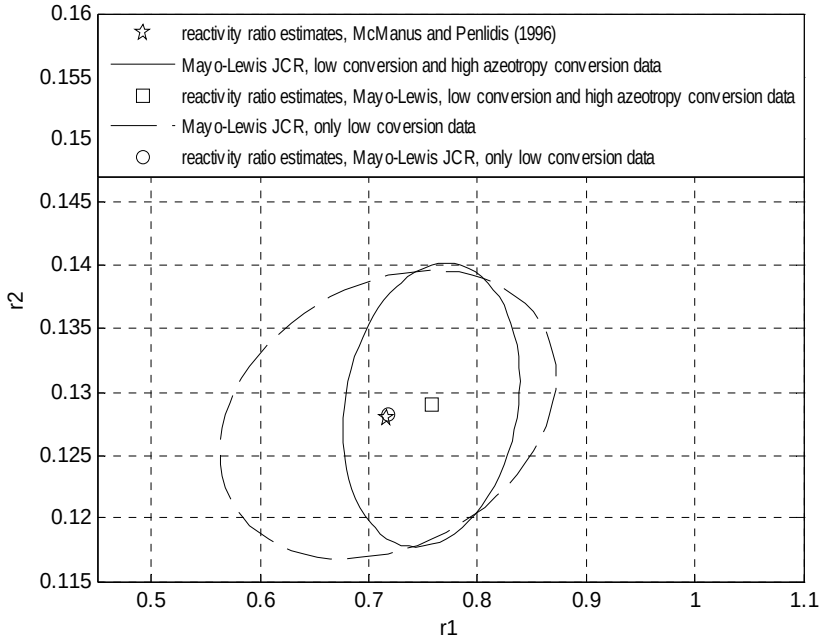

Figure 4-12. JCRs for the Mayo-Lewis model with low conversion data and combined data set from low conversion and azeotropy high conversion data for Sty/EA copolymerization

4.5 Concluding Remarks

Due to outlined practical and theoretical deficiencies in using instantaneous models for copolymerization reactivity ratio estimation, Chapter 4 has suggested that monomer reactivity ratios should be estimated based on cumulative copolymer composition models. The parameter estimation technique used in this chapter is the EVM method, which has been shown to be the most appropriate one for parameter estimation. Two cumulative model forms were discussed in particular, namely, the analytical integration of the differential composition equation or Meyer-Lowry model, and the one resulting from the direct numerical integration of the differential composition equation. Our objective was to show that the latter approach is a novel and more direct method of estimating the reactivity ratios through a step-by-step integration of the copolymerization composition ordinary differential equations.

The following general overall conclusions can be drawn based on the results of the case studies.

- The performance of instantaneous and cumulative models is very similar at low conversions (less than 5-10%). If the appropriate information content is available, then one would expect the cumulative models to yield reactivity ratio estimates of higher quality (more precise, hence with smaller JCRs).
- At higher conversion levels, (i.e., moderate range, say, between 10-50%), it has been shown that both the Meyer-Lowry model and the direct numerical integration approach are capable of providing consistent reactivity ratio estimates that are comparable and in acceptable agreement with literature values. Moreover, the performances of the Meyer-Lowry model (analytical approach) and the direct numerical approach were proven to be indistinguishable.
- In general, if one considers the full conversion range, the reactivity ratio estimation results illustrate that at both low and high conversion levels, the direct numerical integration is straightforward, easy, and a more reliable approach, since it avoids the difficulties associated with the use of the Meyer-Lowry model.
- With the appropriate information content, all models and data ranges should be giving consistent results (reactivity ratio estimates).

Chapter 5. Estimation of Reactivity Ratios in Ternary Systems

5.1 Introduction

Despite the importance of terpolymerization, studies on terpolymerization and especially on estimation aspects with terpolymerization data are very scarce. In fact, reliable terpolymerization data per se are scarce. Based on the analogy between terpolymerization and copolymerization mechanisms, reactivity ratios obtained for binary pairs from copolymerization experiments have commonly been used in models dealing with terpolymerization reactions. However, inaccuracies in binary reactivity ratios can be a source of error propagation in the terpolymerization composition equations. The solution to this problem would be using the experimental data directly from terpolymerization to obtain reactivity ratios. A potential benefit of this approach would be to exploit the terpolymerization composition equation since it provides the opportunity to compare results eventually with data from binary copolymerizations. Given the fact that compared to a binary system, the new types of calculations are more complicated, the question is how significantly one can improve the estimation of the reactivity ratios for a ternary system, using terpolymerization data. Therefore, our objective in this chapter is to investigate aspects of reactivity ratio estimation from low conversion terpolymerization data using instantaneous models, essentially expanding the ideas from copolymerization instantaneous models using the error-in-variables-model (EVM) technique. In doing this, we will potentially/hopefully point out advantages of using data from ternary polymerization experiments rather than from separate sets of data obtained from the three corresponding binary pairs.

5.2 Instantaneous Terpolymerization Composition Model

As mentioned in Chapter 2, according to Alfrey and Goldfinger (1944), in ternary systems, the instantaneous composition of the monomer and polymer phase can be described by the following equations, referred to as AG equations from now on:

$$\frac{df_1}{df_2} = \frac{f_1\left(\frac{f_1}{r_{21}r_{31}}+\frac{f_2}{r_{21}r_{32}}+\frac{f_3}{r_{31}r_{23}}\right)\left(f_1+\frac{f_2}{r_{12}}+\frac{f_3}{r_{13}}\right)}{f_2\left(\frac{f_1}{r_{12}r_{31}}+\frac{f_2}{r_{21}r_{32}}+\frac{f_3}{r_{13}r_{32}}\right)\left(f_2+\frac{f_1}{r_{21}}+\frac{f_3}{r_{23}}\right)} \tag{5.1}$$

$$\frac{df_3}{df_2} = \frac{f_3\left(\frac{f_1}{r_{13}r_{21}}+\frac{f_2}{r_{23}r_{12}}+\frac{f_3}{r_{13}r_{23}}\right)\left(f_3+\frac{f_1}{r_{31}}+\frac{f_2}{r_{32}}\right)}{f_2\left(\frac{f_1}{r_{12}r_{31}}+\frac{f_2}{r_{21}r_{32}}+\frac{f_3}{r_{13}r_{32}}\right)\left(f_2+\frac{f_1}{r_{21}}+\frac{f_3}{r_{23}}\right)} \tag{5.2}$$

where f_i is the mole fraction of (free, unbound) monomer *i* in the mixture, df_i is the mole fraction of monomer *i* incorporated into the terpolymer, and r_{ij} are the monomer reactivity ratios. The AG equations are of the differential type, but if the polymerization is considered over a very small time interval (infinitesimal time slice), then df_i can be replaced by F_i, which is the instantaneous mole fraction of monomer *i* incorporated in the resulting terpolymer. In such a case, and if the conversion level is kept low (say, below 3-5%), then the measured cumulative polymer composition can be equated to the instantaneous copolymer composition, F_i, from a data collection point of view.

Based on the analogy of copolymerization and terpolymerization mechanisms, the definitions of the reactivity ratios are identical to those of binary copolymerizations:

$$r_{12} = \frac{k_{11}}{k_{12}},\ r_{13} = \frac{k_{11}}{k_{13}},\ r_{21} = \frac{k_{22}}{k_{21}},\ r_{23} = \frac{k_{22}}{k_{23}},\ r_{31} = \frac{k_{33}}{k_{31}},\ r_{32} = \frac{k_{33}}{k_{32}} \tag{5.3}$$

As a result, in the literature, ternary system reactivity ratios are commonly considered from the corresponding binary pairs. However, terpolymerization experimental data can be used directly in order to estimate reactivity ratios. Since applications of EVM have been

shown by Duever et al. (1983) with more complicated models, it would be interesting to see the potential with terpolymerization data.

5.3 Program Development

Computer code was developed in the Matlab programming environment to implement the EVM method on terpolymerization experimental data based on the AG equations. Only highlights of the technique as well as the most important modifications will be pointed out here, since the basics have been shown in Chapter 3, section 3.2.2. The regular EVM routine consists of two iterative loops. The inner loop obtains the point estimates of the parameters. The outer loop, then, converges to the true value of the measured variables. It was observed that implementation of EVM on the terpolymerization composition equations needed further adaptation due to convergence problems of the regular EVM routine and thus a more robust optimization routine was required to implement the EVM procedure.

So, the objective function of the EVM routine, which is included here as a quick reference from Chapter 3, was minimized using an optimization function developed in the Matlab programming environment.

$$\Phi = \sum r_i(\underline{\bar{x}}_i - \underline{\hat{\xi}})'\underline{V}(\underline{\bar{x}}_i - \underline{\hat{\xi}}) \tag{3.7}$$

As a reminder from Chapter 3, r_i is the number of replicates at the ith trial, $\underline{\bar{x}}_i$ is the average of the r_i measurements $\underline{x}_i$, and $\underline{\hat{\xi}}_i$ denotes the best estimates of the variables $\underline{\xi}_i$. Underline characters denote vectors and matrices.

It must be noted that minimizing a nonlinear objective function is an iterative problem. The optimization algorithm starts with an initial guess of the values of the model parameters and then generates a sequence of improved estimates until a minimum is found. Among the unconstrained optimization functions existing in Matlab, “fminsearch” and “fminunc” are

suitable for minimization of the objective function above. The algorithm "fminsearch" uses the Nedler-Mixed Simplex method (Lagrasias et al., 1998), whereas "fminunc" uses the Broyden-Fletcher-Goldfarb-Shanno (BFGS) Quasi-Newton method with a mixed quadratic and cubic line search procedure. Therefore, "fminsearch" converges very slowly compared to "fminunc". However, the disadvantage of "fminunc" is that it requires more function evaluations to perform the line search and it cannot handle discontinuities. For this reason, "fminunc" was chosen as the optimization solver, and this has resulted in reliable convergence for all case studies with terpolymerization data.

5.3.1 Application of EVM

To apply the EVM method, the definitions of the vector of variables and the vector of parameters used in this problem are as follows (following Duever et al., 1983):

$$\xi' = (\xi_1 \ \xi_2 \ \xi_3 \ \xi_4 \ \xi_5 \ \xi_6) = (f_1 \ f_2 \ f_3 \ F_1 \ F_2 \ F_3) \tag{5.5}$$

$$\theta' = (\theta_1 \ \theta_2 \ \theta_3 \ \theta_4 \ \theta_5 \ \theta_6) = (r_{12} \ r_{13} \ r_{21} \ r_{23} \ r_{31} \ r_{32}) \tag{5.6}$$

where prime denotes transposition.

To carry out the EVM mathematical implementation, it is convenient to define the AG equations in the following forms:

$$\frac{F_1}{F_2} = \frac{f_1 G_1 H_1}{f_2 G_2 H_2} \qquad \text{and} \qquad \frac{F_1}{F_3} = \frac{f_1 G_1 H_1}{f_3 G_3 H_3} \tag{5.7}$$

where, G_1, G_2, G_3, H_1, H_2, and H_3 (according to eqs. (5.1) and (5.2)) are given by:

$$G_1 = f_1 r_{23} r_{32} + f_2 r_{31} r_{23} + f_3 r_{32} r_{21} \tag{5.8}$$

$$G_2 = f_1 r_{32} r_{13} + f_2 r_{13} r_{31} + f_3 r_{12} r_{31} \tag{5.9}$$

$$G_3 = f_1 r_{12} r_{23} + f_2 r_{13} r_{21} + f_3 r_{12} r_{21} \tag{5.10}$$

$$H_1 = f_1 r_{12} r_{13} + f_2 r_{13} + f_3 r_{12} \quad (5.11)$$

$$H_2 = f_2 r_{21} r_{23} + f_1 r_{23} + f_3 r_{21} \quad (5.12)$$

$$H_3 = f_3 r_{31} r_{32} + f_1 r_{32} + f_2 r_{31} \quad (5.13)$$

Then the mathematical model, written as $P\left(\underline{\xi}, \underline{\theta}\right) = 0$ becomes:

$$P_1 = F_2 f_1 G_1 H_1 - F_1 f_2 G_2 H_2 = 0 \quad (5.13)$$

$$P_2 = F_2 f_3 G_3 H_3 - F_3 f_2 G_2 H_2 = 0 \quad (5.14)$$

$$P_3 = f_1 + f_2 + f_3 - 1 = 0 \quad (5.15)$$

$$P_4 = F_1 + F_2 + F_3 - 1 = 0 \quad (5.16)$$

Eqs. (5.13) and (5.14) are equivalent to the AG equations (eqs. (5.1) and (5.2)), whereas eqs. (5.15) and (5.16) are based on the fact that the mole fractions of the components sum up to unity.

According to the implementation steps of the EVM method, shown in Chapter 3, section 3.2.2, the derivatives of eqs. (5.13)-(5.16) with respect to variables and parameters are needed. The derivatives with respect to the elements of $\underline{\xi}$ are given by:

$$\underline{B} = \left[\frac{\partial P_i}{\partial \xi_j}\right] \qquad (i, j\ element) \quad (5.17)$$

and with respect to the parameters $\underline{\theta}$ are given by:

$$\underline{Z} = \left[\frac{\partial P_i}{\partial \theta_j}\right] \qquad (i, j\ element) \quad (5.18)$$

For the terpolymerization composition model (as shown in eqs. (5.13)-(5.16)), both $\underline{B}$ and $\underline{Z}$ are 4×6 matrices (4 equations and 6 variables).

One of the statistical approaches to quantify the uncertainty in the parameter estimates is the 95% joint probability contour, which is one of the outputs of our EVM program (details are given in section 3.3.2). The interpretation of a joint confidence contour is that values of the parameters within the contour indicate plausible values of the parameters at the particular confidence level. These contours can be loosely referred to as 95% joint confidence regions (JCR) as well. In the analysis of a ternary system, the 95% JCRs are studied for three respective monomer pairs (i.e., r_{ij} vs. r_{ji}). In the remainder of this chapter, the calculated JCRs are approximate JCRs, as per the discussion in section 3.2.2.

5.3.2 Error Structure

As mentioned in section 3.4, the covariance matrices used in the EVM program for both additive and multiplicative error structures are identical, provided that the errors do not exceed $\pm$10%. Therefore, the covariance matrix for terpolymer composition data with no correlation between feed and copolymer compositions (as per section 3.3) is given by:

$$\underline{V} = \begin{bmatrix} \frac{k_{f_1}^2}{3} & 0 & 0 & 0 & 0 & 0 \\ 0 & \frac{k_{f_2}^2}{3} & 0 & 0 & 0 & 0 \\ 0 & 0 & \frac{k_{f_3}^2}{3} & 0 & 0 & 0 \\ 0 & 0 & 0 & \frac{k_{F_1}^2}{3} & 0 & 0 \\ 0 & 0 & 0 & 0 & \frac{k_{F_2}^2}{3} & 0 \\ 0 & 0 & 0 & 0 & 0 & \frac{k_{F_3}^2}{3} \end{bmatrix} \tag{5.19}$$

where the errors for the mole fraction of monomer *i* in the feed and terpolymer are $\pm k_{f_i}$ and $\pm k_{F_i}$units, respectively. For the following case studies, as explained in Chapters 3 and 4, error structure and levels for the feed compositions, f_i, and the terpolymer composition. F_i, were assumed to be multiplicative at the levels of ±1% and ±5%, respectively (i.e., error on

F_i =5% of F_i value as measured). As a result, for terpolymer composition, the covariance matrix is given by:

$$\underline{V} = \begin{bmatrix} \frac{0.01^2}{3} & 0 & 0 & 0 & 0 & 0 \\ 0 & \frac{0.01^2}{3} & 0 & 0 & 0 & 0 \\ 0 & 0 & \frac{0.01^2}{3} & 0 & 0 & 0 \\ 0 & 0 & 0 & \frac{0.05^2}{3} & 0 & 0 \\ 0 & 0 & 0 & 0 & \frac{0.05^2}{3} & 0 \\ 0 & 0 & 0 & 0 & 0 & \frac{0.05^2}{3} \end{bmatrix} \tag{5.20}$$

5.4 Case Studies in Terpolymerization

In the following case studies, terpolymerization monomer reactivity ratios were estimated based directly on terpolymerization experimental data and results were compared to binary reactivity ratios that have been obtained from the corresponding binary copolymerizations, which is certainly a much more tedious procedure in every respect. Our main objective here was to determine the potential improvements in reactivity ratio estimates that can be realized by utilizing terpolymerization experimental data.

5.4.1 Case study 1: Acrylonitrile/Styrene/Methyl Methacrylate

The bulk terpolymerization of acrylonitrile (AN, M_1)/styrene (Sty, M_2)/methyl methacrylate (MMA, M_3) has often been discussed in the literature, including Shukla and Sirvastrava (1994), Hocking and Klimchuk (1996), and Brar and Hekmatyar (1999), but reactivity ratio studies were only conducted in Brar and Hekmatyar (1999). In addition, the terpolymerization experimental data sets provided by Shukla and Sirvastrava (1994) and

Hocking and Klimchuk (1996) consist of only a few points and for this reason these data sets cannot be used for estimation of monomer reactivity ratios. The Brar and Hekmatyar (1999) experimental data are shown in Table 5.1. The authors used values of reactivity ratios from the respective binary copolymerization systems of AN-Sty, Sty-MMA, and AN-MMA as the reactivity ratios of the AN/Sty/MMA ternary system. These binary reactivity ratios, included in Table 5.2, were estimated using a variant of the EVM method by Brar et al. (1998).

Hauch (2005) conducted a preliminary investigation on the reactivity ratio estimation of this system using EVM, based on the terpolymerization experimental data from Brar and Hekmatyar (1999). The objective of this case study was then to re-estimate the reactivity ratios by implementing EVM on the same terpolymerization data set, provided in Brar and Hekmatyar (1999). The binary reactivity ratios reported by Brar and Hekmatyar (1999) were used as the initial guesses in this work. The results are presented in Table 5.2 as well. Moreover, 95% joint confidence regions (JCR) for the reactivity ratios of the respective copolymer pairs were generated next and are plotted in Figures 5.1a to 5.1c, alongside the reported reactivity ratios from Brar and Hekmatyar (1999). In each figure, the open circle denotes the EVM point estimate from current work and the star denotes the reported reactivity ratio pair in Brar and Hekmatyar (1999).

Table 5-1. Experimental terpolymerization data for terpolymerization of AN (M_1)/ Sty(M_2)/MMA (M_3)

Feed composition			Experimental terpolymer composition			Calculated terpolymer composition, Brar and Hekmatyar (1999)			Calculated terpolymer composition, Current work		
AN	Sty	MMA	AN	Sty	MMA	AN	Sty	MMA	AN	Sty	MMA
0.63	0.22	0.15	0.46	0.40	0.14	0.44	0.41	0.15	0.437	0.4342	0.1280
0.42	0.36	0.22	0.37	0.46	0.17	0.35	0.46	0.19	0.3502	0.4743	0.1761
0.23	0.53	0.24	0.27	0.53	0.20	0.25	0.53	0.22	0.2508	0.5358	0.2134
0.41	0.16	0.43	0.32	0.29	0.39	0.31	0.29	0.40	0.2975	0.3104	0.3921
0.29	0.08	0.63	0.22	0.15	0.63	0.22	0.16	0.62	0.2048	0.1717	0.6235
0.29	0.44	0.27	0.30	0.48	0.22	0.28	0.48	0.24	0.2782	0.4951	0.2267

Table 5-2. Monomer reactivity ratios for terpolymerization of AN (M_1)/Sty (M_2)/MMA (M_3)

Reference	r_{12}	r_{21}	r_{13}	r_{31}	r_{23}	r_{32}
Brar and Hekmatyar (1999)	0.04	0.31	0.17	1.45	0.47	0.52
Current work	0.0718	0.2942	0.2023	1.3243	0.5729	0.5455

It is evident in Figures 5.1a to 5.1c that the reactivity ratios used by Brar and Hekmatyar (1999) do not fall within the JCRs from the current work, indicating a potential significant disagreement. Our results are similar to the results mentioned in Hauch (2005) as well. There are two potential reasons for this disagreement. The type of data used for evaluation of the reactivity ratios, copolymerization data versus terpolymerization data, and the parameter estimation method applied on the data for the analysis. Since Brar and Hekmatyar (1999) claimed that they implemented a variant of EVM, then the parameter estimation method is unlikely to be the reason for this disagreement, and thus, it is reasonable to suggest that only the fact that we directly used the terpolymerization experimental data for reactivity ratio estimation rather than the corresponding copolymerization experimental data has caused this noticeable difference in the results. Subsequently, it is evident that the addition of the third monomer to a binary copolymerization affects the values of monomer reactivity ratios, and hence it makes sense to use terpolymer data directly in order to include all the available process information in the parameter estimation scheme.

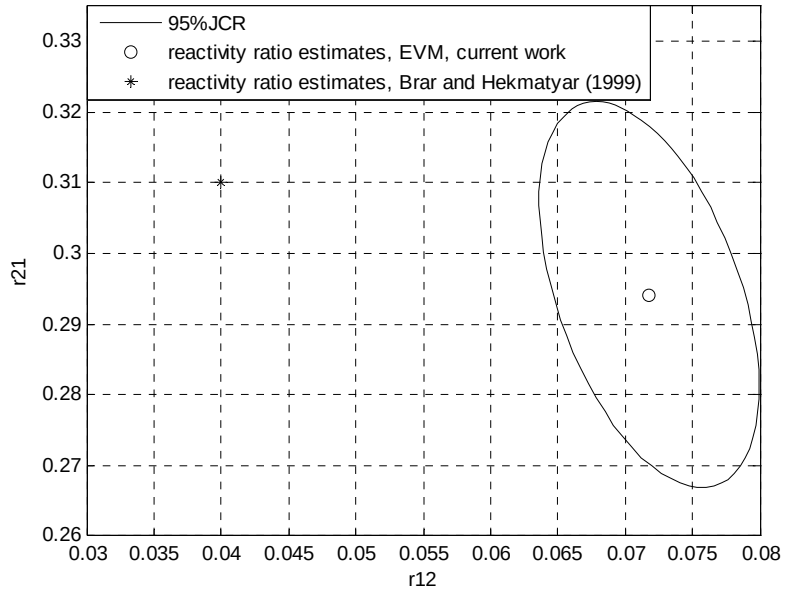

Figure 5-1a. r_{12} and r_{21} estimates, terpolymerization of AN(M_1)/Sty(M_2)/MMA(M_3)

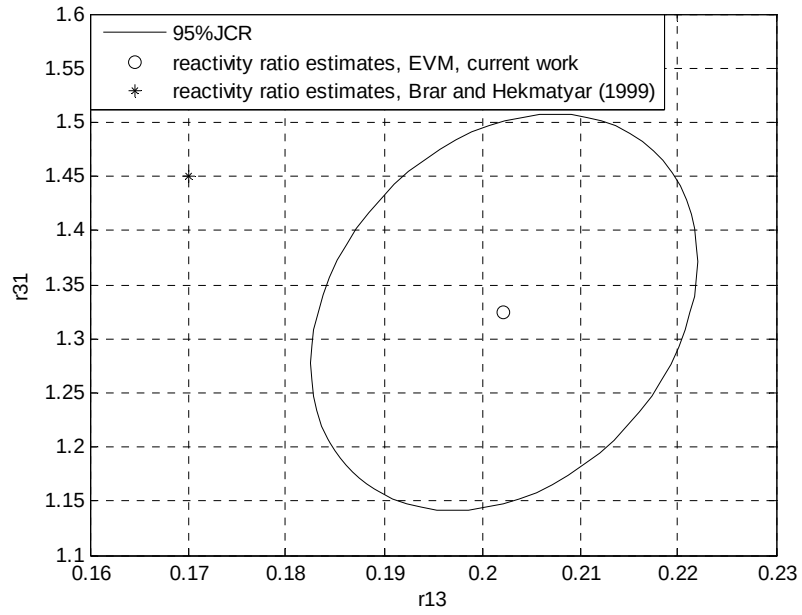

Figure 5-1b. r_{13} and r_{31} estimates, terpolymerization of AN(M_1)/Sty(M_2)/MMA(M_3)

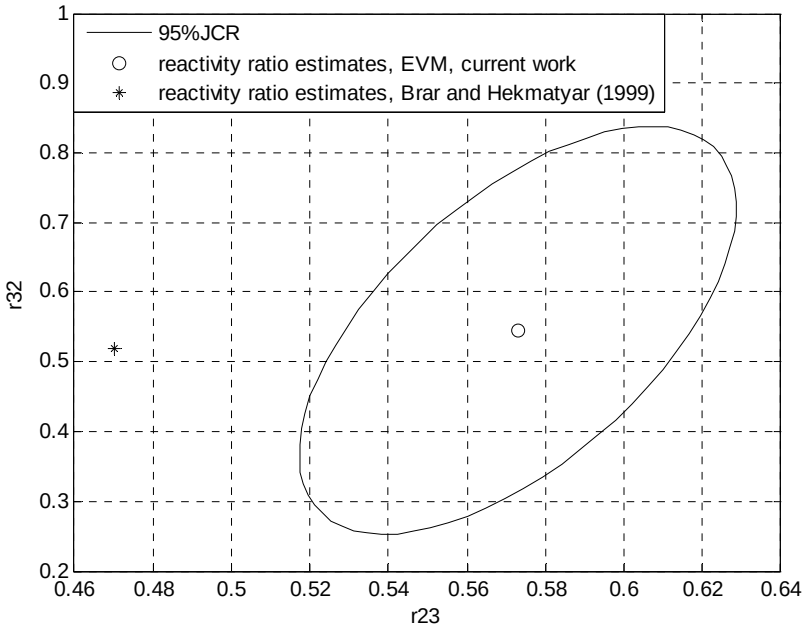

Figure 5-1c. r_{23} and r_{32} estimates, terpolymerization of AN(M_1)/Sty(M_2)/MMA(M_3)

Brar and Hekmatyar (1999) pointed out that the reliability of the reactivity ratio values may be judged subjectively by the agreement between the experimental and calculated terpolymer compositions and thus they included the calculated terpolymer compositions (which were obtained based on the AG equations using the binary reactivity ratios). These calculated compositions are shown in Table 5.1. We, similarly, calculated the terpolymer compositions using the ternary reactivity ratios that were estimated in the current work, and these composition values are also included in Table 5.1. It was anticipated that the agreement between experimental and calculated terpolymer compositions might be better with the "ternary" reactivity ratios. However, as shown in Table 5.1, there is no clear difference between predictions made using reactivity ratios estimated from binary data versus those estimated from ternary data. Thus, one cannot draw any reliable conclusion based on these comparisons, especially since the experimental compositions are themselves subject to uncertainty.

Figure 5.2 presents all the JCRs together along with the reported reactivity ratios by Brar and Hekmatyar (1999). In this figure, "r_{ij}, r_{ji}, current work" stands for the EVM point estimates from the current work, and "r_{ij}, r_{ji}, Brar and Hekmatyar (1999)" stands for the

reported reactivity ratio values of the corresponding binary system in the reference paper. It can be seen that the variation in the size of JCRs is considerable, which reflects varying amounts of uncertainty in the parameter estimates. The smaller the size of the region, the more precise the parameter estimates are. The amount of uncertainty in a parameter estimate is determined by a number of factors including the amount of data available, the uncertainty in making the measurements and the design of the experiment. The data set presented by Brar and Hekmatyar (1999) consists of only 6 data points which is the minimum number of data points necessary to estimate the six parameters in the terpolymerization model. However, the same number of data points are available for the estimation of each of the parameters, therefore, this cannot explain the differences in the quality of the parameter estimates obtained. Another possible reason for the differences in the precision of the parameter estimates could be related to the design of the experiments (i.e., the distribution of the data points along the experimental operating region). However, no information in this regard was given in Brar and Hekmatyar (1999).

To further investigate this aspect, Figure 5.3 shows three plots for the mole fraction of monomers 1, 2, and 3 in the polymerizing mixture (feed) and the terpolymer. The solid line in each plot is obtained using the Mayo-Lewis copolymer composition equation, and the corresponding reactivity ratios estimated from the "ternary" data. The stars are the terpolymerization experimental data as reported in Brar and Hekmatyar (1999). The only difference that is obvious is that the data in the first plot (Monomer 1) span a somewhat narrower range of F_1, the copolymer composition measured, compared with plots 2 and 3. However there is no indication of a trend in these plots that can explain the trends in the JCRs, observed in Figure 5.2. Another possible contribution to the differences between the JCRs is the form and possibly the nonlinearity of the model. For further investigation, the use of Monte Carlo techniques is required, which is beyond the scope of this thesis.

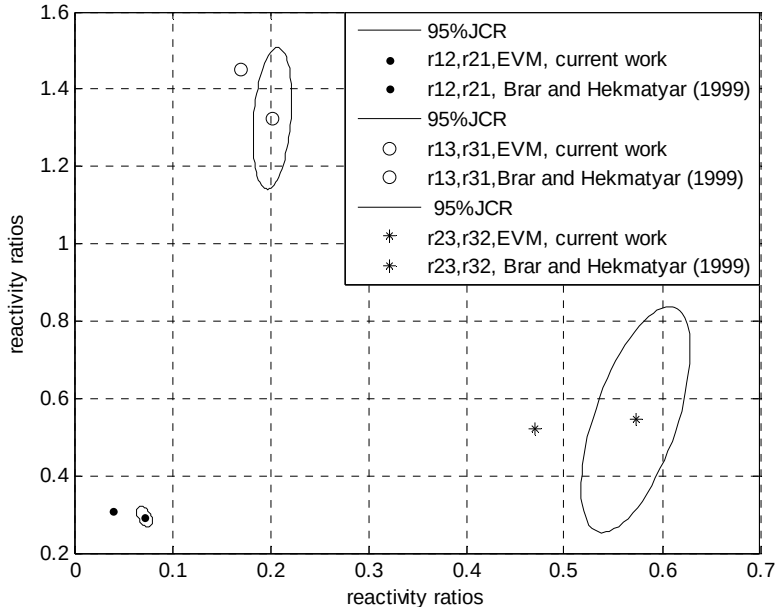

Figure 5-2. JCRs of reactivity ratios for terpolymerization of AN(M_1)/Sty(M_2)/MMA(M_3)

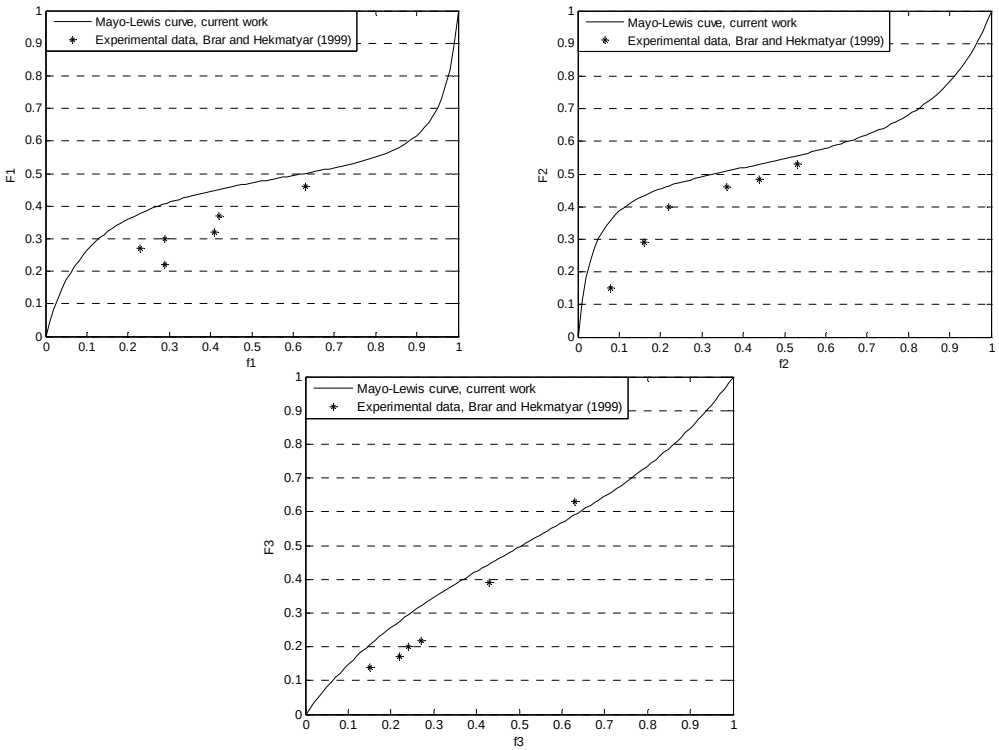

Figure 5-3. Feed and terpolymer composition for the three components of the AN(M_1)/Sty(M_2)/MMA(M_3) terpolymerization

As mentioned earlier, in order to conduct the analysis by EVM, the feed data points were assumed to have a measurement error of 1%, while the terpolymer data were assumed to have a 5% measurement error. In order to ensure that the assumed level of error in the terpolymer composition measurements is not a potential reason for the disagreement between our point estimates and published values, the reactivity ratios were re-estimated using an error level of 10% for the terpolymer composition. These point estimates were exactly the same as the ones calculated with our usual error levels. Figure 5.4 summarizes the three new JCRs for the respective reactivity ratio pairs along with the reported binary reactivity ratios from Brar and Hekmatyar (1999). Comparing Figures 5.2 and 5.4, it can be seen that as expected, the sizes of the JCRs increased because of the increased error level. However, the reported values of r_{12} and r_{21} based on the binary data are still not contained inside the corresponding JCR and the other two reactivity ratio pairs are located very close to the borderline of the JCRs. So, it seems that the effect of the assumed error level in our analysis is not the source of disagreement in the results. However, if we had assumed an error of 15%, probably all point estimates would be within the JCRs, thus indicating (only in a speculative way) that the literature data might have contained considerable error.

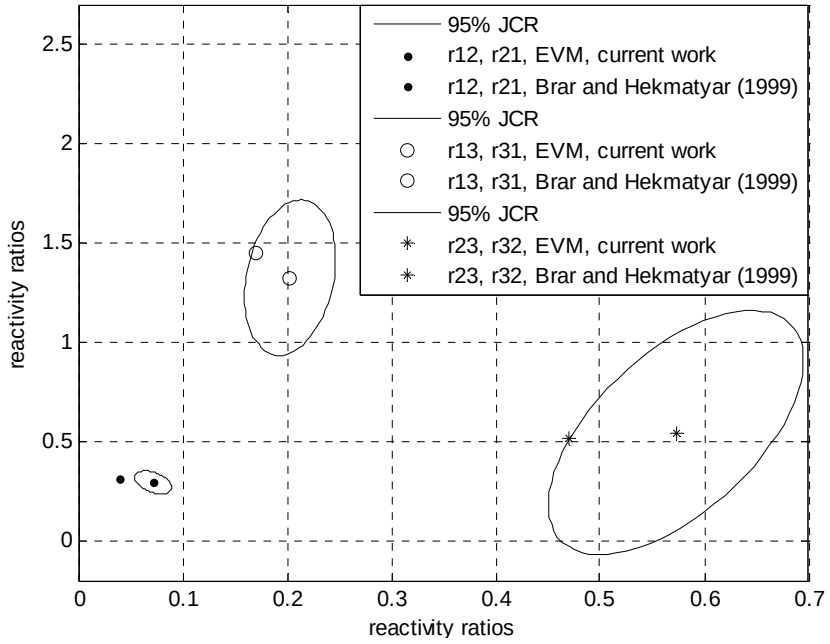

Figure 5-4. JCRs of reactivity ratios for terpolymerization of AN(M_1)/Sty(M_2)/MMA(M_3), 10% error for the terpolymerization composition

Further inspection of the terpolymerization experimental data reported in Brar and Hekmatyar (1999) shows that three experimentally measured monomer mole fractions in the polymerizing mixture (f_1, f_2, f_3) and the terpolymer (F_1, F_2, F_3) always add up to one, for all the data samples. There is no explanation offered in the paper to indicate whether all three components were individually measured or if the values for two components were measured and then the third one was calculated by subtracting the other two from 1. Therefore, we modified the estimation procedure to reflect the assumption that there might only be two independent mole fractions measured in both the feed and the terpolymer.

To test this hypothesis, the EVM method was modified by changing the model such that the mole fraction of the third monomer was calculated from the measured mole fractions of the other two monomers. That is, instead of considering six variables (three monomer mole fractions in the feed (f_1, f_2, f_3) and three mole fractions in the terpolymer (F_1, F_2, F_3)), only four measured values were used, namely, f_1, f_2 and F_1, F_2. The mathematical formula (as per eqs. (5.1) and (5.2)) were adjusted by using $f_3 = 1-f_1-f_2$ and $F_3 = 1-F_1-F_2$. Subsequently, the reactivity ratios were re-estimated. Figure 5.5 shows the three JCRs for the new reactivity

ratio pairs along with the reported binary reactivity ratios reported by Brar and Hekmatyar (1999). The new reactivity ratios are slightly different from the ones estimated using the original approach with 6 variables (Table 5.2). Also, the sizes of the JCRs, especially for the r_{23} and r_{32} pair, have changed; yet the reported binary reactivity ratios are still outside of their corresponding JCRs, indicating that even by implementing this constraint, the results of parameter estimation still do not agree with the reported binary reactivity ratios.

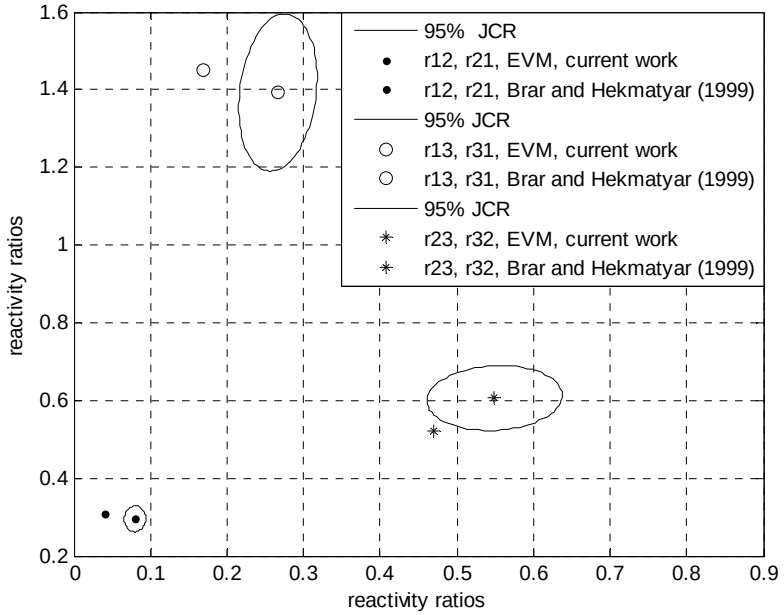

Figure 5-5. JCRs of reactivity ratios estimates for terpolymerization of AN(M_1)/Sty(M_2)/MMA(M_3), using only f_1, f_2 and F_1, F_2 as model variables

5.4.2 Case study 2: Leucine-N-carboxyanhydride/β-benzyl asparatate-N-carboxyanhydride/Valine-N-carboxyanhydride

Wamsley et al. (2004) provided experimental data for the free radical terpolymerization of leucine-N-carboxyanhydride (L-NCA, M_1)/β-benzyl asparatate-N-carboxyanhydride (D-NCA, M_2)/valine-N-carboxyanhydride (V-NCA, M_3), presented in Table 5.3. The purpose of their study was to synthesize random poly (α-amino acids) which function as drug delivery

carriers. They pointed out that the term ‘random’ means that the probability of the monomer appearing in the polymer chain for all monomers is constant and independent of position. Also, the degree of randomness for copolymerization can be measured with respect to the product of the respective monomer reactivity ratios, as the highest degree of randomness is for the case where $r_i r_j=1$. To determine if random, blocky or alternating polymers can be produced, binary copolymers were synthesized first. Subsequently, the reactivity ratio study was performed on copolymerization experimental results using three parameter estimation methods: Fineman-Ross, Kelen-Tudos, and nonlinear least squares. The point estimates are summarized in Table 5.4. Since the respective binary reactivity ratio product values were close to one, especially when nonlinear least squares was applied, Wamsley et al. (2004) concluded that these copolymerization reactions are of the random type. Also, the terpolymer compositions were calculated by the authors using the binary reactivity ratios. Similar to the previous case study, Wamsley et al. (2004) also mentioned that the agreement between the experimental and calculated terpolymer compositions indicates that the reactivity ratios from binary systems are capable of describing the terpolymerization perfectly.

The aim of this work was to re-analyze the terpolymerization data using the EVM parameter estimation method to determine whether the point estimates were in good agreement with the reported ones from copolymerization data. The nonlinear least squares point estimates were used as initial estimates for EVM. The results are also shown in Table 5.4. In addition, similar to the first case study, JCRs for the reactivity ratios of the respective copolymer pairs are plotted in Figures 5.6a to 5.6c, alongside the point estimates from the other parameter estimation methods, reported by Wamsley et al. (2004). In these figures, the FR, KT, and NLS abbreviations stand for Fineman-Ross, Kelen-Tudos, and nonlinear least squares techniques.

Table 5-3. Experimental data for the terpolymerization of L-NCA (M_1)/D-NCA (M_2)/V-NCA (M_3)

Feed composition			Experimental terpolymer composition			Calculated terpolymer composition, Wamsley et al. (2004)			Calculated terpolymer composition, Current work		
M_1	M_2	M_3	M_1	M_2	M_3	M_1	M_2	M_3	M_1	M_2	M_3
0.10	0.10	0.80	0.12	0.24	0.64	0.13	0.21	0.66	0.1200	0.2134	0.6666
0.10	0.80	0.10	0.05	0.92	0.03	0.06	0.90	0.04	0.0667	0.8962	0.0371
0.20	0.20	0.60	0.19	0.38	0.43	0.21	0.36	0.43	0.2069	0.3708	0.4223
0.20	0.40	0.40	0.23	0.55	0.22	0.17	0.60	0.23	0.1736	0.6981	0.2183
0.20	0.60	0.20	0.19	0.72	0.09	0.14	0.77	0.09	0.1477	0.7643	0.0880
0.33	0.33	0.33	0.29	0.46	0.25	0.28	0.52	0.20	0.2872	0.5200	0.1927
0.40	0.20	0.40	0.35	0.35	0.30	0.38	0.35	0.27	0.3757	0.3516	0.2728
0.40	0.40	0.20	0.31	0.54	0.15	0.31	0.58	0.11	0.3172	0.5768	0.1060
0.60	0.20	0.20	0.52	0.39	0.09	0.54	0.34	0.12	0.5244	0.3409	0.1347
0.80	0.10	0.10	0.72	0.20	0.08	0.75	0.18	0.07	0.7311	0.1901	0.0788

Table 5-4. Reactivity ratio values for the terpolymerization of L-NCA (M_1)/D-NCA (M_2)/V-NCA (M_3)

Reference	Method of estimation	r_{12}	r_{21}	r_{13}	r_{31}	r_{23}	r_{32}
Wamsley et al. (2004)	Fineman-Ross	0.46	1.62	1.20	0.48	2.07	0.20
Wamsley et al. (2004)	Kelen-Tudos, graphical linear fitting	0.40	1.46	1.37	0.55	2.34	0.34
Wamsley et al. (2004)	Nonlinear least squares	0.52	1.99	1.40	0.59	2.78	0.43
Current work	EVM	0.4462	1.6466	1.0263	0.7215	3.1194	0.4087

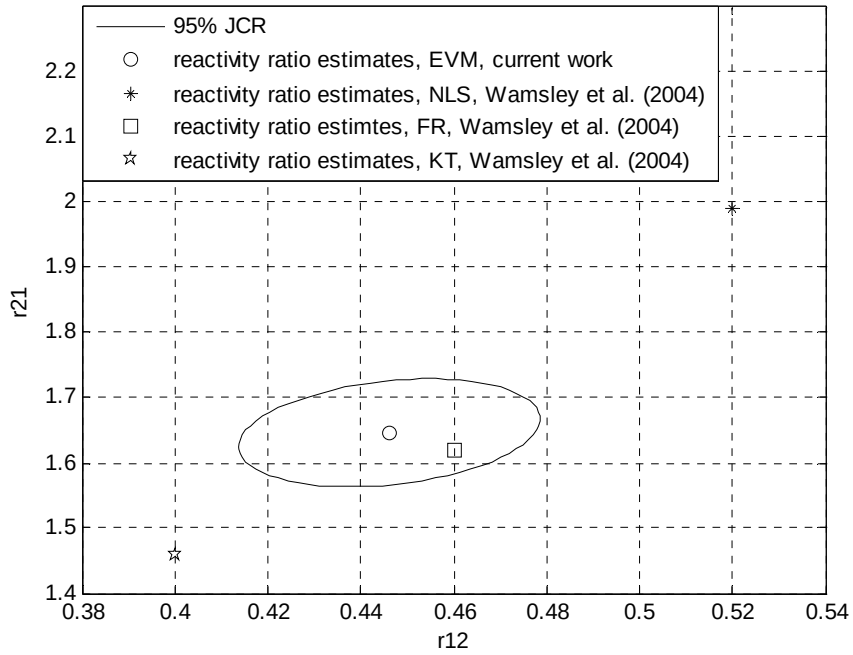

Figure 5-6a. r_{12} and r_{21} estimates, terpolymerization of L-NCA (M_1)/D-NCA (M_2)/V-NCA (M_3)

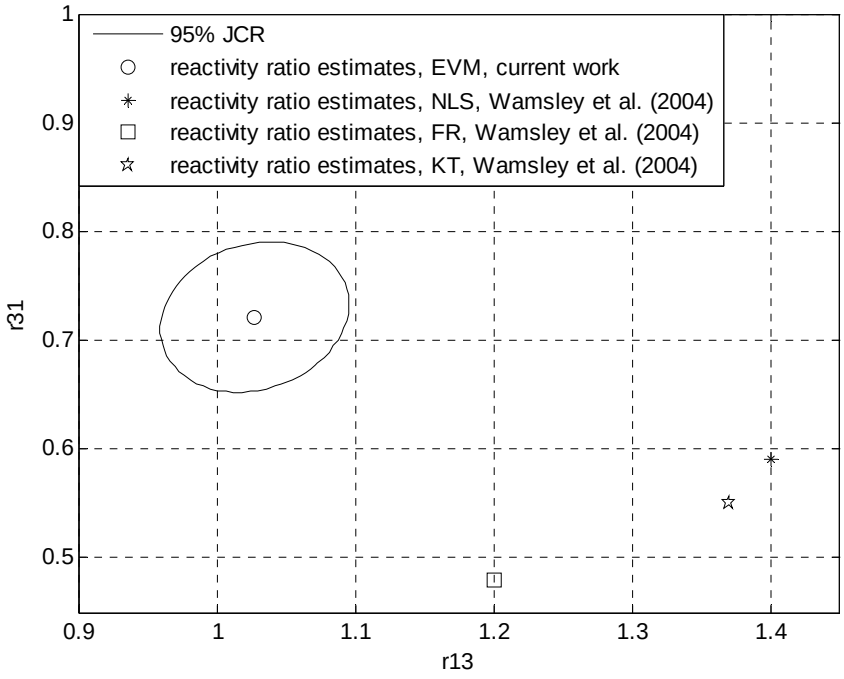

Figure 5-6b. r_{13} and r_{31} estimates, terpolymerization of L-NCA (M_1)/D-NCA (M_2)/V-NCA (M_3)

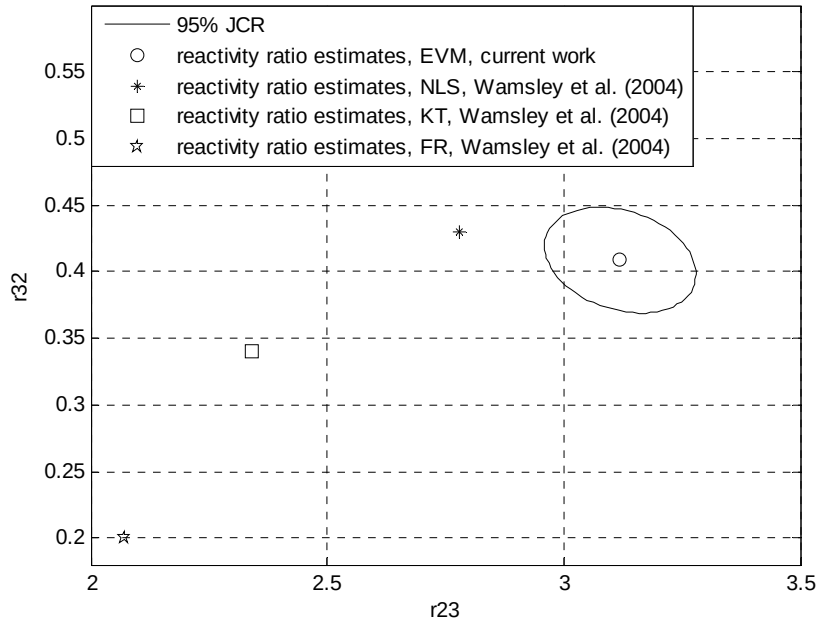

Figure 5-6c. r_{23} and r_{32} estimates, terpolymerization of L-NCA (M_1)/D-NCA (M_2)/V-NCA (M_3)

As shown in Figures 5.6a to 5.6c, the EVM point estimates are considerably different from the reported reactivity ratios by Wamsley et al. (2004); all, but one, of the reported binary reactivity ratio pairs fall outside of the corresponding JCRs. Once again, it was observed that using the terpolymerization experimental data directly for parameter estimation can affect the point estimates noticeably. Moreover, Wamsley et al. (2004) used linear parameter estimation techniques such as Fineman-Ross and graphical Kelen-Tudos for the Mayo-Lewis copolymer composition equation, which is a nonlinear model. As extensively discussed in the literature, applying linear parameter estimation techniques to nonlinear polymerization kinetic models can result in defective parameter estimates, and thus their reported values of reactivity ratios are erroneous from the outset. The reported reactivity ratios from nonlinear least squares are the most reliable in this regard, nevertheless, as mentioned in Chapter 3, section 3.6, the EVM method is a superior parameter estimation technique for the reactivity ratio estimation problem. Thus, the disagreement between our point estimates and the literature results can be partly explained by the use of inappropriate estimation techniques and partly based on the improved way that EVM handles measurement error information (which is essentially ignored in the other techniques).

In the next step of the analysis, all three JCRs for the EVM reactivity ratio estimates along with the reported values by Wamsley et al. (2004) are presented together in Figure 5.7. In this figure, "r_{ij}, r_{ji}, current work" stands for the EVM point estimates from the current work and "r_{ij}, r_{ji}, Wamsley et al. (2004)" denote the reported values for the corresponding reactivity ratios by Wamsley et al. (2004) using the NLS method. From this plot, it is evident that the JCRs are almost of the same size, illustrating that the amount of information provided by the experimental data for our parameter estimation procedure is the same for all point estimates (the information provided by the experimental data in this case study can be considered as the "appropriate information" for the case in point).

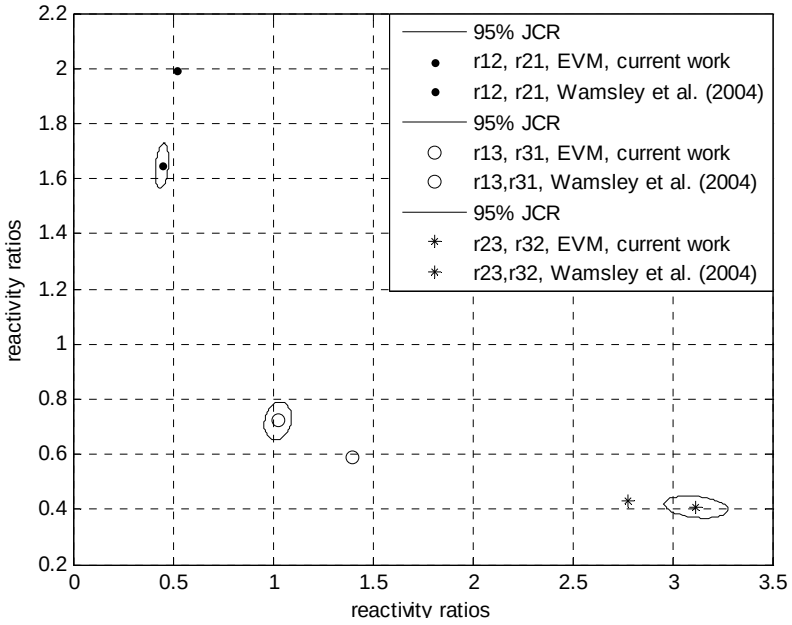

Figure 5-7. JCRs for terpolymerization of L-NCA (M_1)/D-NCA (M_2)/V-NCA (M_3)

As mentioned earlier, Wamsley et al. (2004) calculated the terpolymerization composition values using the binary reactivity ratios and stated that since these calculated values are in acceptable agreement with the experimental ones, it can be concluded that this ternary system is well described using binary reactivity ratios. In this study, the instantaneous terpolymer compositions for the reported feed compositions were calculated using the AG equations and the reactivity ratio estimates by EVM. As can be seen in Table 5.3, the

calculated instantaneous terpolymer compositions in our study show better agreement with the terpolymer experimental data than those calculated by Wamsley et al. (2004). Therefore, it seems that both binary reactivity ratios and ternary reactivity ratios can predict the terpolymer composition generally well, and thus this comparison does not provide enough support for the conclusion about which set of reactivity ratios can truly describe this ternary system, especially since no error estimates were reported for the experimental data presented in Wamsley et al. (2004).

5.4.3 Case study 3: Acrylonitrile/ Styrene/ 2,3-Dibromopropyl Acrylate

The experimental data at low conversion for acrylonitrile (AN, M_1)/ styrene (Sty, M_2)/ 2,3-dibromopropyl acrylate (DBPA, M_3) terpolymerization were collected by Saric et al. (1983) in emulsion and dimethyl formamide (DMF) solution; data sets for both systems are shown in Tables 5.5 and 5.6. Saric et al. (1983) determined the reactivity ratios from copolymerization experimental data of the corresponding comonomer pairs using linear parameter estimation techniques. These reactivity ratio estimates for both systems are presented in Table 5.7, rows one and three.

The aim of this work was to re-analyze the data using the EVM parameter estimation technique to compare the reactivity ratios obtained directly from terpolymerization data with the reactivity ratios of the corresponding binary pairs. The EVM point estimates from this work for emulsion and DMF solution are also included in Table 5.7. Figures 5.8a to 5.8f show the related JCRs for the reactivity ratio estimates along with the corresponding reported reactivity ratio estimates from Saric et al. (1983).

Table 5-5. Experimental data for terpolymerization of AN(M_1)/Sty(M_2)/DBPA(M_3) in emulsion

Feed composition			Experimental terpolymer composition			Calculated terpolymer composition, Saric et al. (1983)			Calculated terpolymer composition, Current work		
M_1	M_2	M_3	M_1	M_2	M_3	M_1	M_2	M_3	M_1	M_2	M_3
0.300	0.600	0.100	0.294	0.605	0.101	0.297	0.604	0.099	0.3012	0.5943	0.1045
0.650	0.200	0.150	0.496	0.405	0.126	0.470	0.420	0.110	0.4550	0.4178	0.1271
0.220	0.370	0.410	0.167	0.505	0.328	0.175	0.503	0.322	0.1944	0.4745	0.3312
0.220	0.530	0.260	0.208	0.560	0.232	0.203	0.568	0.229	0.2095	0.5492	0.2414
0.362	0.313	0.325	0.276	0.456	0.267	0.279	0.472	0.249	0.2912	0.4515	0.2573
0.520	0.270	0.210	0.399	0.428	0.173	0.389	0.453	0.158	0.3855	0.4443	0.1702
0.205	0.360	0.435	0.174	0.469	0.357	0.166	0.488	0.364	0.1824	0.4692	0.3484
0.108	0.310	0.582	0.118	0.423	0.459	0.091	0.429	0.480	0.1030	0.4450	0.4520
0.400	0.400	0.200	0.310	0.527	0.163	0.319	0.522	0.159	0.3279	0.5016	0.1705
0.100	0.700	0.200	0.126	0.649	0.225	0.166	0.654	0.230	0.1214	0.6416	0.2370
0.150	0.750	0.100	0.213	0.808	0.147	0.188	0.687	0.125	0.1923	0.6779	0.1298

Table 5-6. Experimental data for terpolymerization of AN(M1)/Sty(M2)/DBPA(M3) in DMF solution

Feed composition			Experimental terpolymer composition			Calculated terpolymer composition, Saric et al. (1983)			Calculated terpolymer composition, Current work		
M_1	M_2	M_3	M_1	M_2	M_3	M_1	M_2	M_3	M_1	M_2	M_3
0.395	0.505	0.100	0.388	0.539	0.073	0.395	0.527	0.078	0.4119	0.5184	0.0697
0.8435	0.0361	0.1204	0.740	0.155	0.105	0.753	0.136	0.111	0.7383	0.1550	0.1067
0.234	0.566	0.200	0.262	0.581	0.157	0.270	0.556	0.174	0.2886	0.5499	0.1616
0.300	0.500	0.200	0.347	0.500	0.153	0.314	0.525	0.161	0.3296	0.5234	0.1471
0.263	0.400	0.337	0.285	0.478	0.235	0.263	0.478	0.259	0.2678	0.4925	0.2397
0.173	0.300	0.527	0.154	0.462	0.384	0.173	0.419	0.408	0.1664	0.4561	0.3775
0.0385	0.5615	0.400	0.062	0.567	0.371	0.050	0.561	0.389	0.0562	0.5666	0.3772

As shown in Figures 5.8a to 5.8f, for the emulsion terpolymerization and DMF solution terpolymerization, respectively, all of the reported reactivity ratios from the binary data sets fall outside their related JCRs, indicating that once again our results from terpolymerization

experimental data are not in an acceptable agreement with those reported from binary copolymerizations by Saric et al. (1983).

Table 5-7 . Monomer reactivity ratios for terpolymerization of AN (M_1)/Sty (M_2)/DBPA (M_3)

Reference	r_{12}	r_{21}	r_{13}	r_{31}	r_{23}	r_{32}
Emulsion, Saric et al. (1983)	0.1	0.44	0.90	0.86	0.43	0.14
Emulsion, current work	0.0753	0.4180	0.3863	0.4607	0.4104	0.1895
DMF, Saric et al. (1983)	0.16	0.30	0.87	0.75	0.41	0.22
DMF, current work	0.1870	0.2343	0.9818	1.9839	0.3883	0.1615

The disagreement between the reported reactivity ratios and our point estimates can be attributed to the two main reasons pointed out from the first case study. Firstly, the parameter estimation techniques used by Saric et al. (1983) are very approximate and this can be a major reason for the disagreement. Secondly, making use of terpolymerization experimental data versus binary copolymerization data, once more, has affected the values of reactivity ratios significantly. Also, Saric et al. (1983) calculated terpolymer compositions using reactivity ratios obtained from binary copolymerizations and the AG equations (Tables 5.5 and 5.6). They pointed out that the calculated and experimental terpolymer compositions are in very good agreement, proving that this ternary system is well described with binary reactivity ratios. However, in this work, we also calculated the terpolymer compositions using the estimated ternary reactivity ratios and the AG equations. It has been observed that the agreement between the experimental data and the calculated compositions is also acceptable (Tables 5.5 and 5.6 show these values as well). Therefore, regardless of whether the prediction of polymer compositions are based on binary reactivity ratios or "ternary" reactivity ratios, the calculated compositions are still in satisfactory agreement with the experimental compositions, and thus this cannot be relied on to distinguish between these two sets of reactivity ratios.

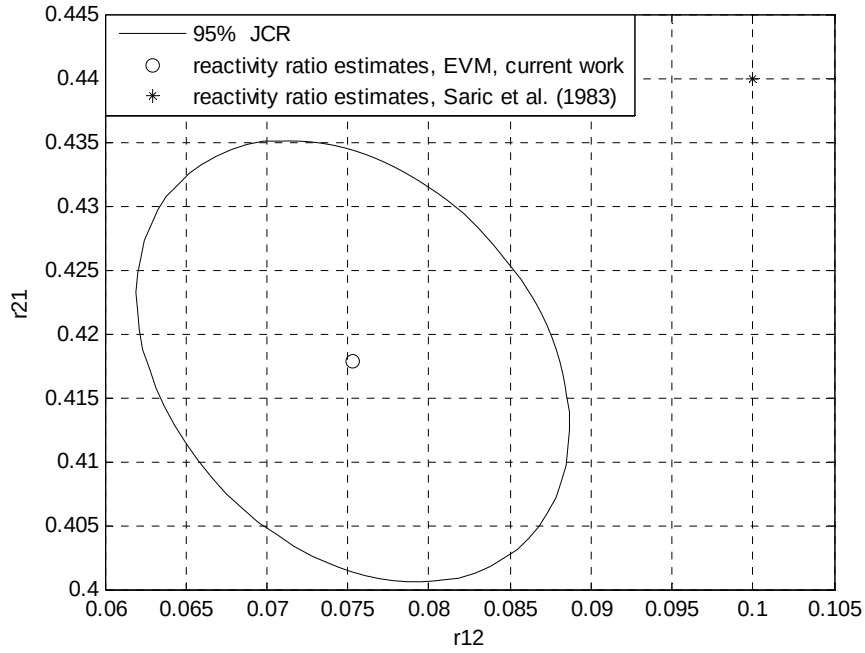

Figure 5-8a. r_{12} and r_{21} estimates, terpolymerization of AN(M_1)/Sty(M_2)/DBPA(M_3) in emulsion

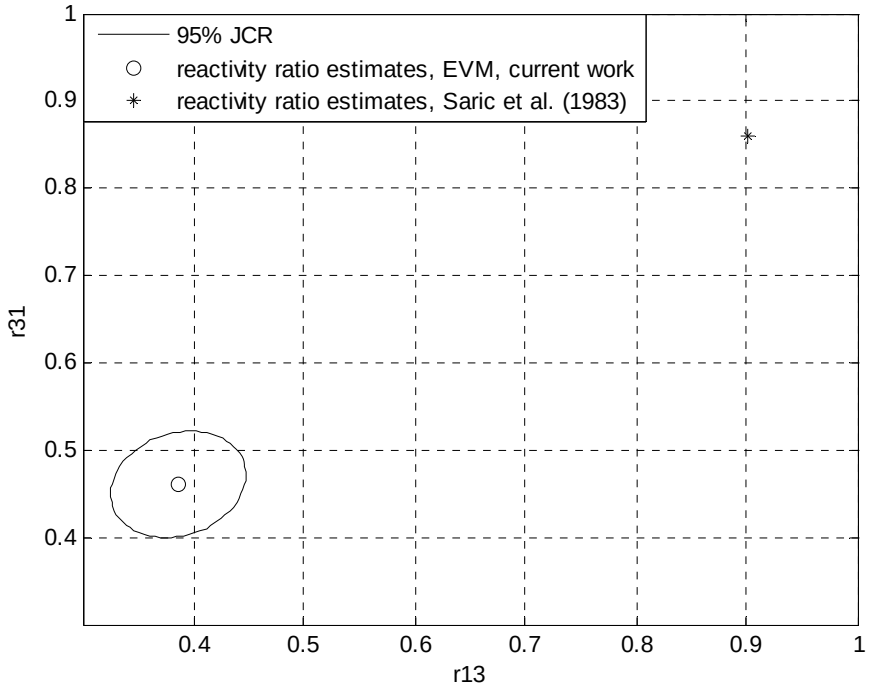

Figure 5-8b. r_{13} and r_{31} estimates, terpolymerization of AN(M_1)/Sty(M_2)/DBPA(M_3) in emulsion

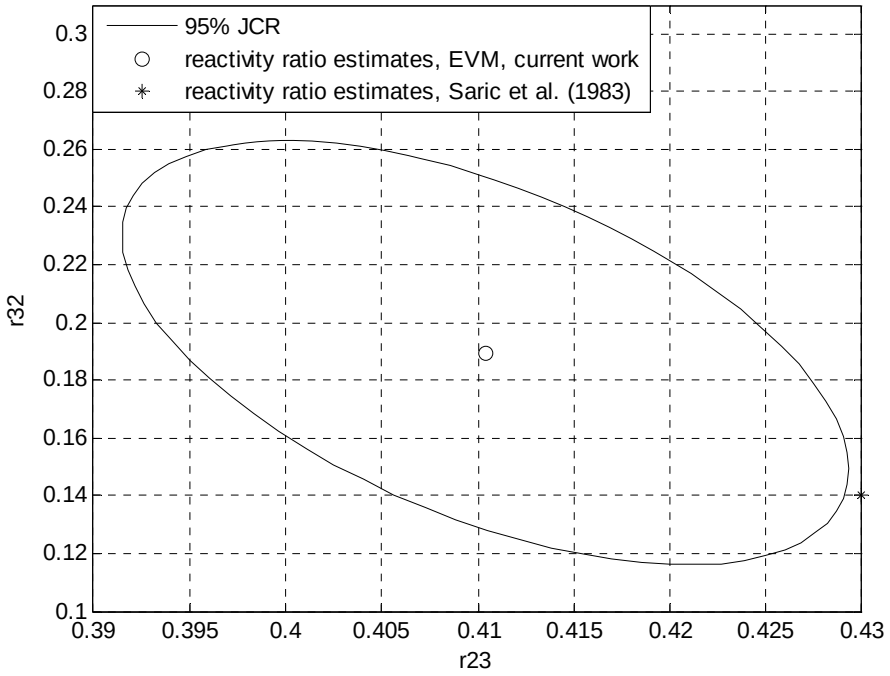

Figure 5-8c. r_{23} and r_{32} estimates, terpolymerization of AN(M_1)/Sty(M_2)/DBPA(M_3) in emulsion

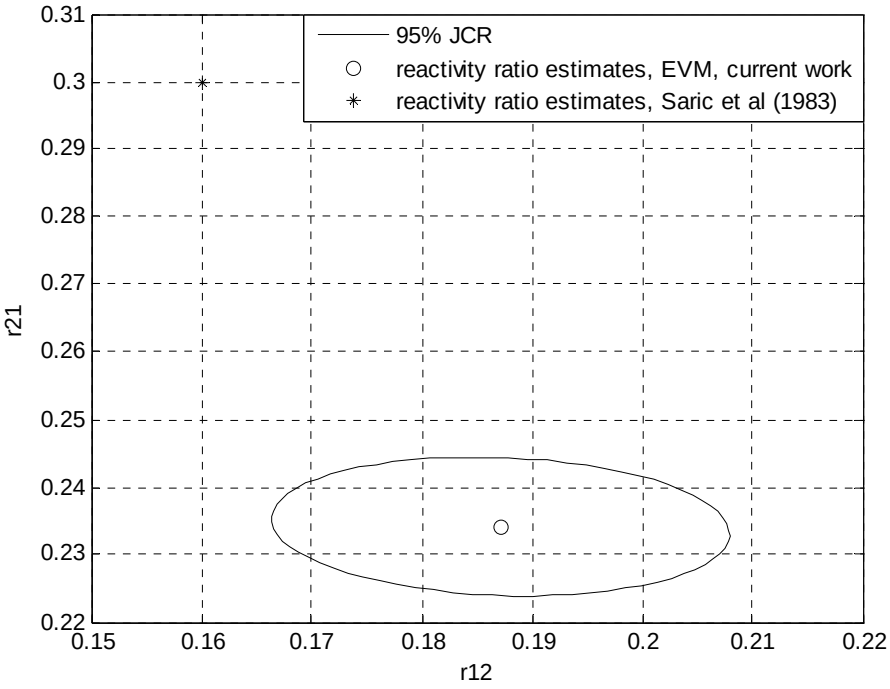

Figure 5-8d. r_{12} and r_{21} estimates, terpolymerization of AN(M_1)/Sty(M_2)/DBPA(M_3) in DMF

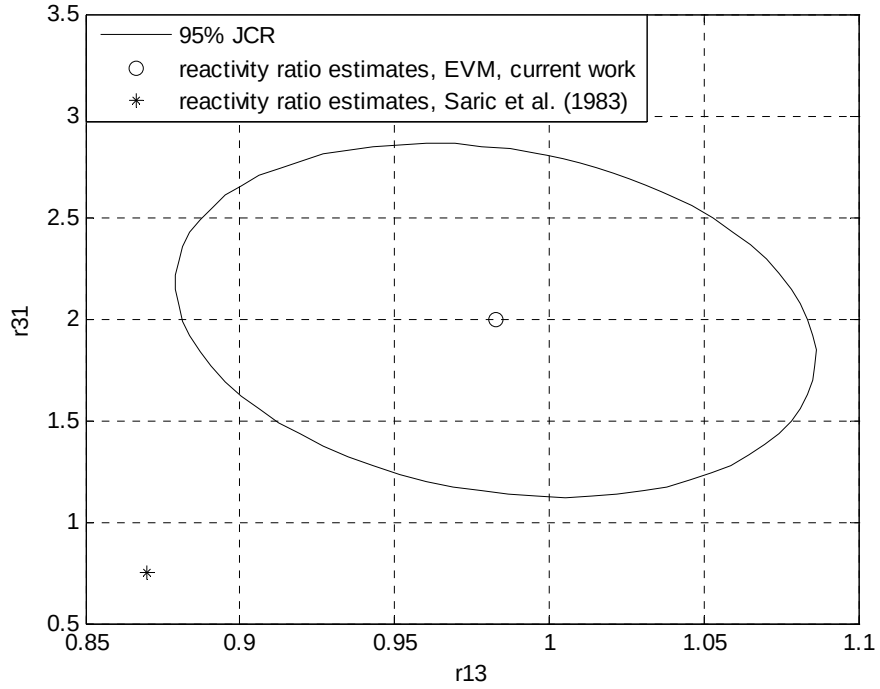

Figure 5-8e. r_{13} and r_{31} estimates, terpolymerization of AN(M_1)/Sty(M_2)/DBPA(M_3) in DMF

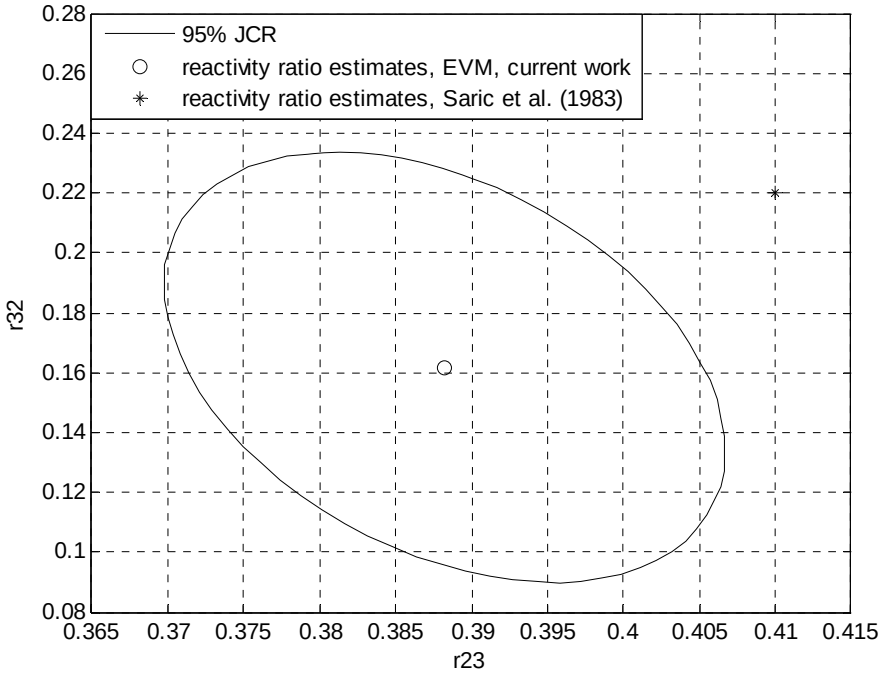

Figure 5-8f. r_{23} and r_{32} estimates, terpolymerization of AN(M_1)/Sty(M_2)/DBPA(M_3) in DMF

Similar to the previous case studies, Figures 5.9a and 5.9b show the JCRs of all reactivity ratio estimates from the current work along with the reported values of reactivity ratios by Saric et al. (1983), for terpolymerization in emulsion and DMF solution, respectively. In these figures, similar to previous case studies, "r_{ij}, r_{ji}, current work" denotes the EVM point estimates by the current work, and "r_{ij}, r_{ji}, Saric et al. (1983)" denotes the reported values for the corresponding reactivity ratios. As shown in Figure 5.9a, for the emulsion system, the size of the JCR for r_{13} and r_{31} is slightly larger than the other two JCRs. Once again, this variation in the sizes of JCRs can be related to several factors in the experimental data (i.e., design, associated errors with experimental points). For the DMF solution, it can be seen in Figure 5.4b that the size of JCR for the r_{13} and r_{31} pair is again significantly larger than the other two JCRs, possibly for the same reasons as in Figure 5.9a, due to some additional uncertainty when M_3 is involved.

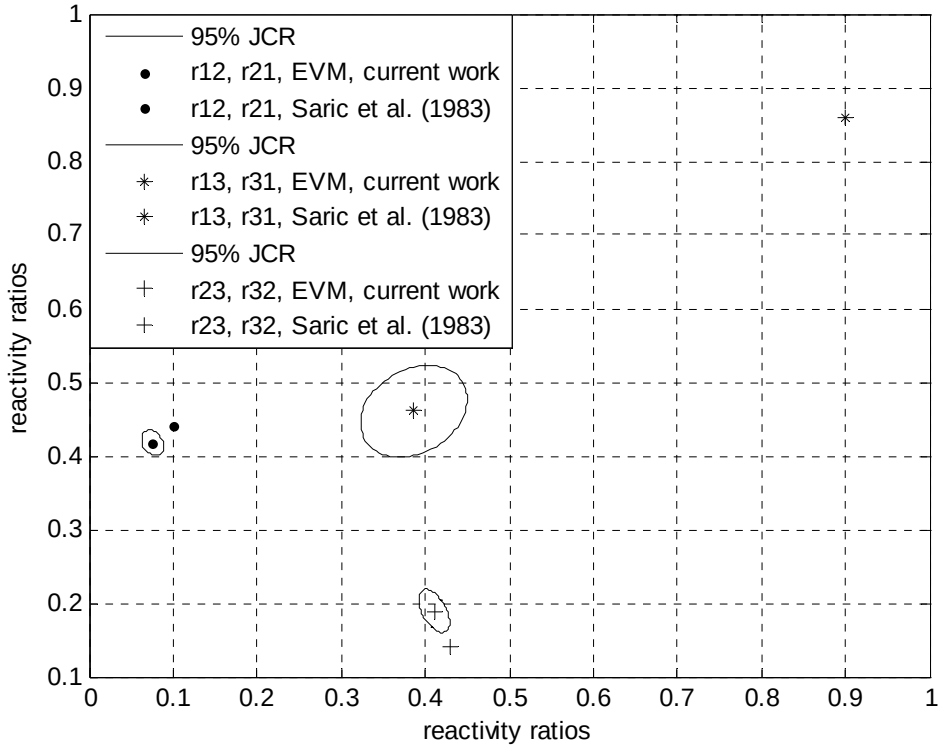

Figure 5-9a. JCRs for terpolymerization of AN(M_1)/Sty(M_2)/DBPA(M_3) in emulsion

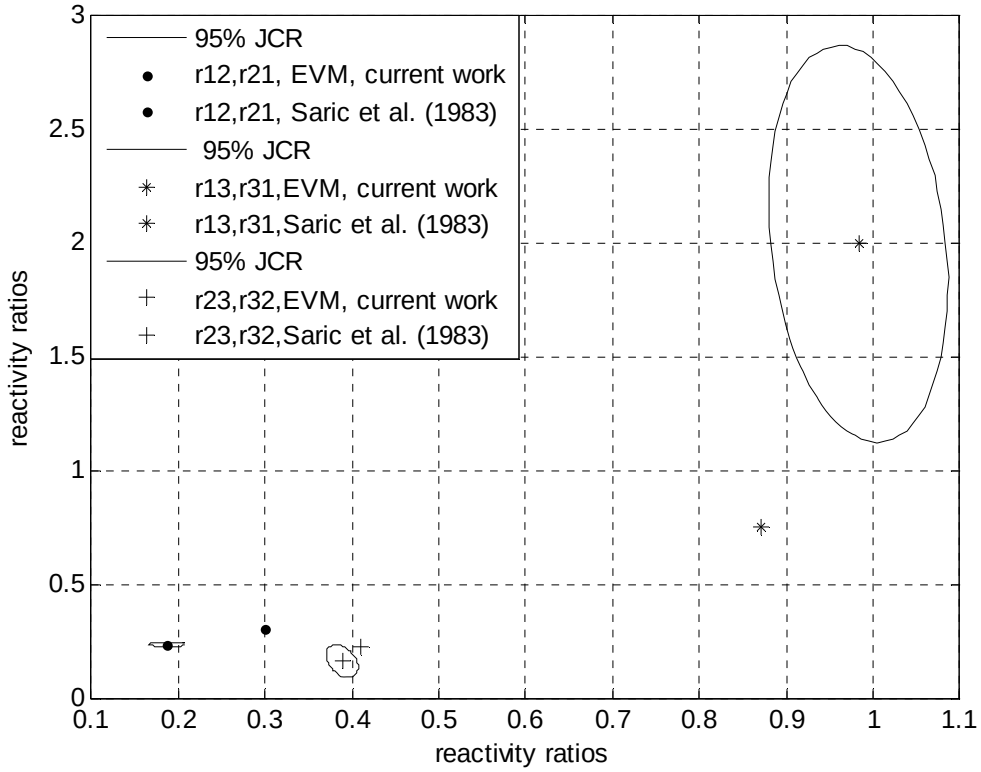

Figure 5-9b. JCRs for terpolymerization of AN(M_1)/Sty(M_2)/DBPA(M_3) in DMF

5.4.4 Case study 4: Ethylene/Methyl methacrylate/Vinyl acetate

Luft et al. (1993) studied the terpolymerization of ethylene (E, M_1)/methyl methacrylate (MMA, M_2)/vinyl acetate (VAc, M_3) under high pressure and presented extensive experimental data. To assess the effect of pressure and temperature on the reaction, the polymerization reactions were carried out at two different pressures of 1900 and 1100 bar and at two different temperatures of 180 and 230℃. The data set can be seen in Tables 5.8-5.10. The authors mentioned that the kinetics of terpolymerization was described by the AG equations, and estimation of the monomer reactivity ratios for the terpolymerization system was based on NLLS as described in Rudin et al. (1973).

As mentioned in Chapter 2, NLLS minimizes the sum of squared differences between observed and fitted ratios of monomer mole fractions in the terpolymer (F_1/F_2 and F_1/F_3). The

reported reactivity ratios in Luft et al. (1993) can be seen in Tables 5.11-5.13. The aim of this work was to re-analyze the data using the EVM parameter estimation technique and compare the results with those reported in Luft et al. (1993). The initial estimates for the EVM method were the reactivity ratios obtained by Luft et al. (1993) and the results of the parameter estimation are presented in Tables 5.11-5.13. According to these tables, it can be seen that our point estimates and the reported reactivity ratios are very similar for each data set. In Figures 5.10a to 5.10i, the JCRs of these reactivity ratio estimates are plotted alongside the corresponding point estimates by Luft et al. (1993).

Table 5-8. Experimental terpolymerization data for E(M_1)/MMA(M_2)/VAc(M_3) at 1900 bar and 180 °C

Feed composition			Terpolymer composition		
E	**MMA**	**VA**	**E**	**MMA**	**VA**
0.854	0.053	0.094	0.5823	0.3612	0.0565
0941	0.021	0.038	0.7417	0.2288	0.0295
0.841	0.022	0.138	0.6767	0.2206	0.1027
0.852	0.055	0.094	0.5913	0.3534	0.0553
0.773	0.024	0.203	0.6426	0.2050	0.1524
0.663	0.154	0.183	0.4013	0.5075	0.0912
0.723	0.159	0.117	0.4438	0.5044	0.0518
0.876	0.026	0.098	0.6533	0.2757	0.0710
0.708	0.051	0.241	0.5219	0.3278	0.1503
0.758	0.052	0.189	0.5218	0.2583	0.1199

Table 5-9 Experimental terpolymerization data for E(M_1)/MMA(M_2)/VAc(M_3) at 1100 bar and 180 °C

Feed composition			Terpolymer composition		
E	**MMA**	**VA**	**E**	**MMA**	**VA**
0.8568	0.0518	0.0914	0.5495	0.3794	0.0711
0.8603	00478	0.0919	0.5685	0.3606	0.0709
0.9400	0.0223	0.0377	0.7147	0.2485	0.0368
0.8437	0.0214	0.1349	0.6494	0.2270	0.1236
0.7802	0.0213	0.1985	0.5904	0.2251	0.1845
0.6799	0.1319	0.1882	0.3728	0.5178	0.1085
0.8983	0.0517	0.0500	0.5868	0.3757	0.0375
0.7029	0.1806	0.1165	0.3408	0.5937	0.0655
0.9286	0.0167	0.0547	0.7402	0.2052	0.0546
0.6929	0.0765	0.2309	0.4190	0.4268	0.1542
0.8969	0.0214	0.0817	0.6874	0.2359	0.0767

Table 5-10. Experimental terpolymerization data for E(M_1)/MMA(M_2)/VAc(M_3) at 1100 bar and 230 °C

Feed composition			Terpolymer composition		
E	**MMA**	**VA**	**E**	**MMA**	**VA**
0.9691	0.0047	0.0262	0.9270	0.0468	0.0262
0.9398	0.0218	0.0384	0.8023	0.1665	0.0312
0.8386	0.0234	0.1380	0.7213	0.1709	0.1078
0.6736	0.1404	0.1860	0.4422	0.4680	0.0898
0.9120	0.0492	0.0388	0.6997	0.2750	0.0253
0.6970	0.1804	0.1226	0.4205	0.5243	0.0552
0.6970	0.1804	0.1226	0.4205	0.5243	0.0552
0.7526	0.0568	0.1906	0.5812	0.2984	0.1204

Although the values of the reactivity ratio estimates obtained by EVM are very close to the reported reactivity ratios by Luft et al. (1993), as seen in Tables 5.11-5.13, it can be seen in Figures 5.10a to 5.10i that some of the JCRs do not contain the reported reactivity ratios. For instance, the reported r_{12} and r_{21} values of all three different operating conditions do not

fall within the related JCRs, whereas for the r_{13} and r_{31} pair, we are in good agreement for all three conditions. Since in both Luft et al. (1993) and our study the estimation procedure is based on terpolymerization experimental data, the disagreement between the results can only be attributed to the choice of the parameter estimation technique (once more, EVM vs. NLLS, as contrasted earlier in section 3.6).

Table 5-11. Monomer reactivity ratios for terpolymerization of E (M_1)/MMA (M_2)/VAc (M_3) at 1900 bar and 180°C

Reference	r_{12}	r_{21}	r_{13}	r_{31}	r_{23}	r_{32}
Luft et al. (1993)	0.05	2.07	0.89	0.92	3.23	0.39
Current work	0.0498	2.4665	0.9001	0.8298	3.6419	0.3518

Table 5-12. Monomer reactivity ratios for terpolymerization of E (M_1)/MMA (M_2)/VAc (M_3) at 1100 bar and 180°C

Reference	r_{12}	r_{21}	r_{13}	r_{31}	r_{23}	r_{32}
Luft et al. (1993)	0.05	3.34	0.71	0.79	3.25	0.07
Current work	0.0503	2.6731	0.7331	0.8916	3.4728	0.0807

Table 5-13 Monomer reactivity ratios for terpolymerization of E (M_1)/MMA (M_2)/VAc (M_3) at 1100 bar and 230°C

Reference	r_{12}	r_{21}	r_{13}	r_{31}	r_{23}	r_{32}
Luft et al. (1993)	0.09	2.01	0.92	0.78	3.89	0.24
Current work	0.0923	2.4038	0.9469	0.6419	3.9576	0.1182

Luft et al. (1993) pointed out that reactivity ratios can be affected because of changes in pressure and temperature. In our analysis the values of the reactivity ratios shifted, as well, due to the changes in the reaction conditions. It was also observed that the trends of change in our calculated point estimates were similar to the trends reported in the reference paper.

Figures 5.11a to 5.11c show all JCRs for the estimated reactivity ratios together with the reported ones from Luft et al. (1993) at three different operating conditions. In these figures,

similar to previous case studies, "r_{ij}, r_{ji}, current work" stands for the EVM point estimates obtained in the current work, and "r_{ij}, r_{ji}, Luft et al (1993)" denotes the reported values for the corresponding reactivity ratios in the reference paper. It can be clearly seen that the sizes of the JCRs are not considerably different. Figure 5.11c, which is for the lowest pressure and temperature, shows the smallest variation in size of JCRs, whereas Figure 5.11a shows the largest variation in the size of JCRs. These results can be potentially related to the experimental error associated with each data set. Clearly, obtaining more accurate compositions at 180°C/1100 bar resulted in less uncertainty than at 230°C/1900 bar.

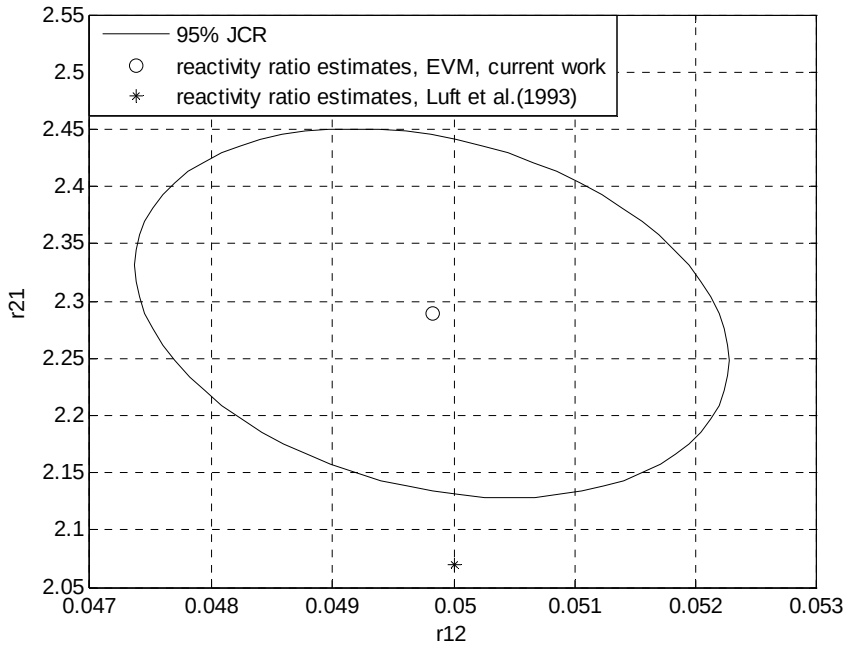

Figure 5-10a. r_{12} and r_{21} estimates, terpolymerization of E (M_1)/MMA (M_2)/VAc (M_3) at P=1900 bar and T=180°C

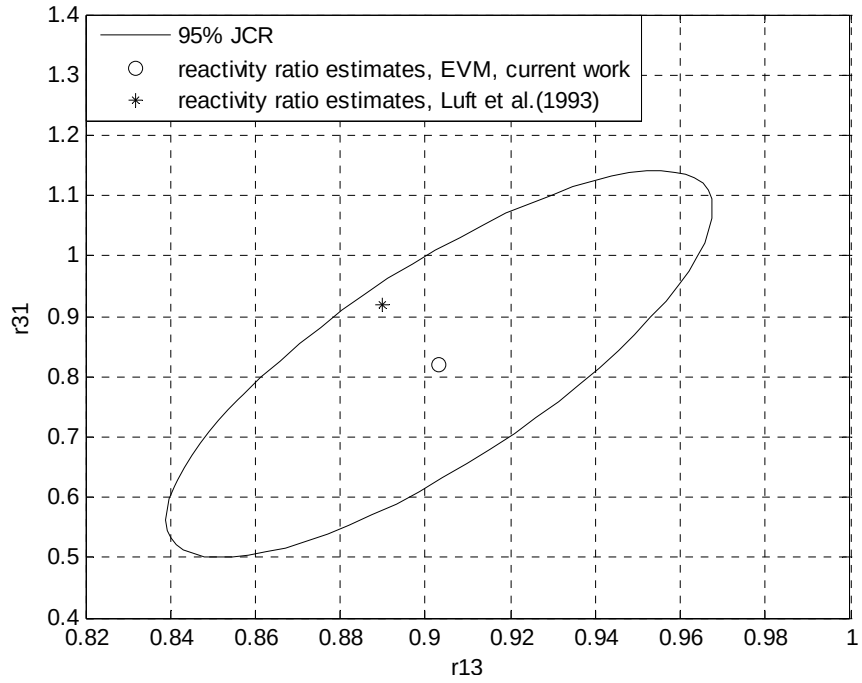

Figure 5-10b. r_{13} and r_{31} estimates, terpolymerization of E (M_1)/MMA (M_2)/VAc (M_3) at P=1900 bar and T=180°C

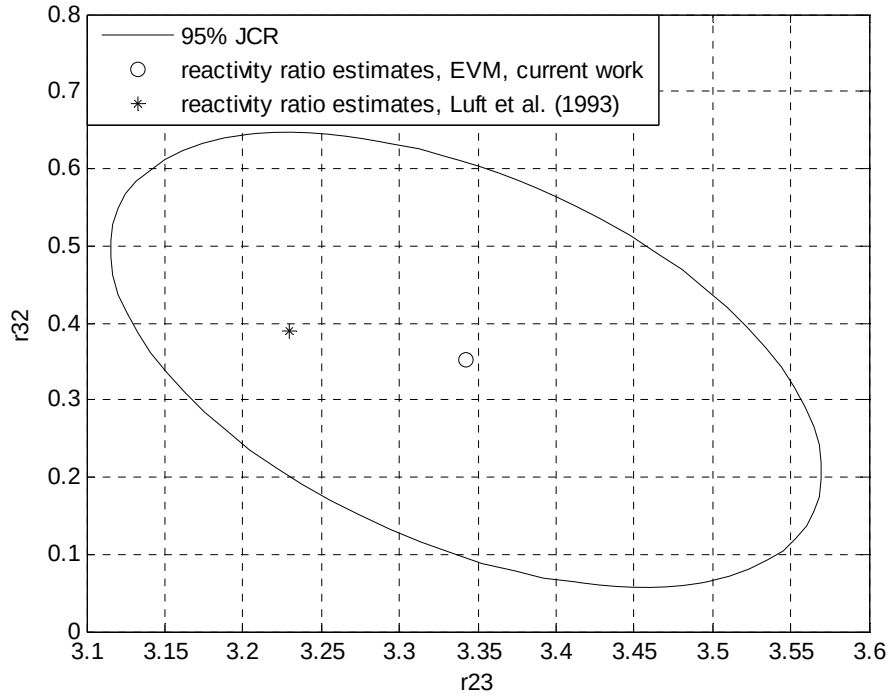

Figure 5-10c. r_{23} and r_{32} estimates, terpolymerization of E (M_1)/MMA (M_2)/VAc (M_3) at P=1900 bar and T=180°C

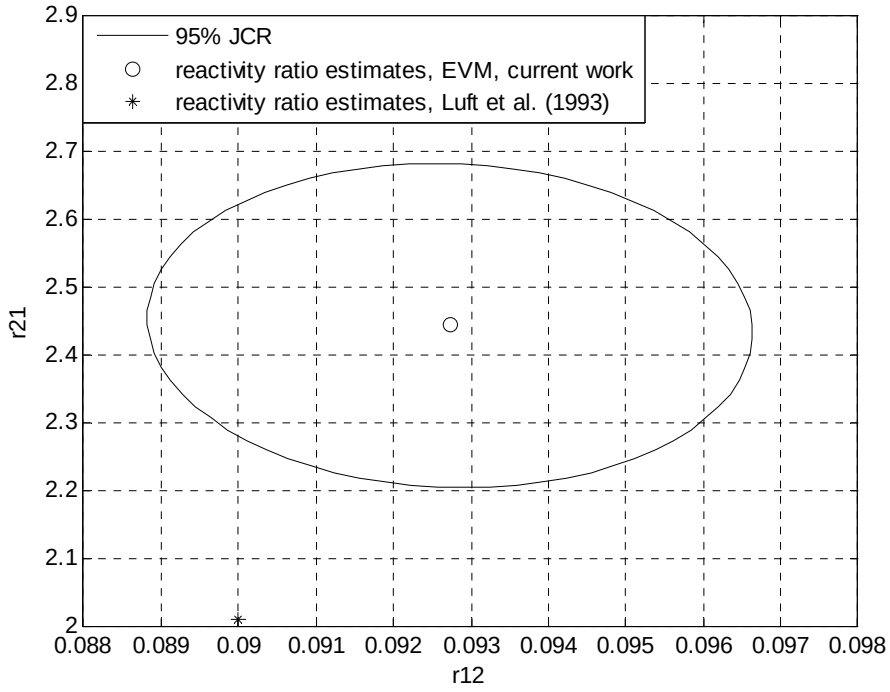

Figure 5-10d. r_{12} and r_{21} estimates, terpolymerization of E (M_1)/MMA (M_2)/VAc (M_3) at P=1100 bar and T=230°C

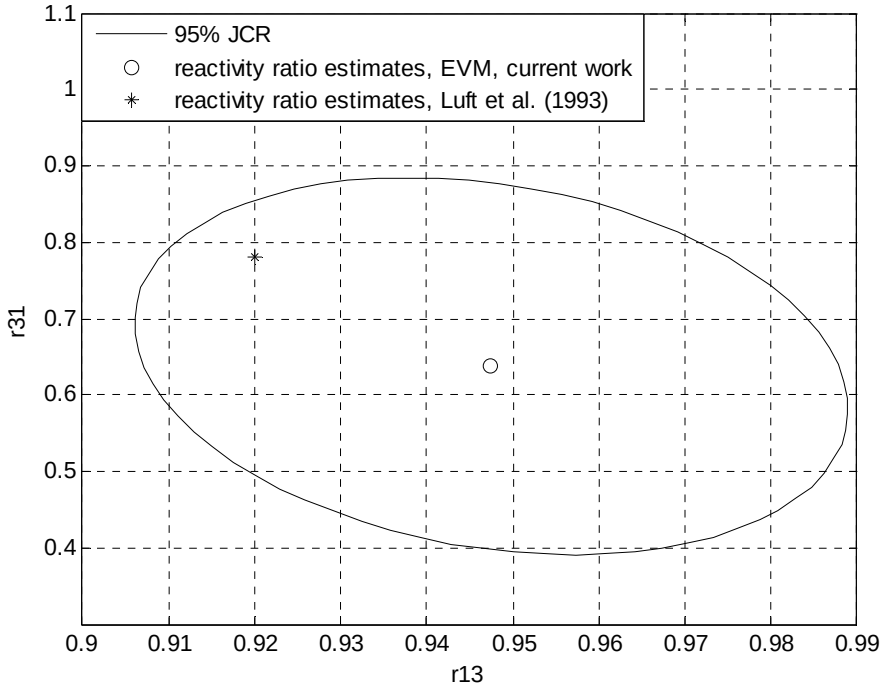

Figure 5-10e. r_{13} and r_{31} estimates, terpolymerization of E (M_1)/MMA (M_2)/VAc (M_3) at P=1100 bar and T=230°C

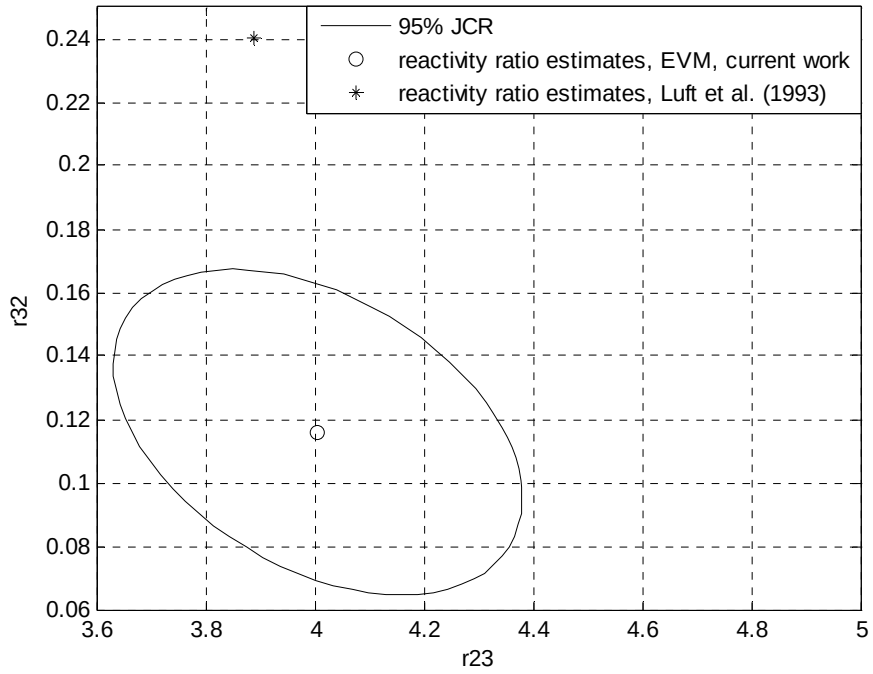

Figure 5-10f. r_{23} and r_{32} estimates, terpolymerization of E (M_1)/MMA (M_2)/VAc (M_3) at P=1100 bar and T=230°C

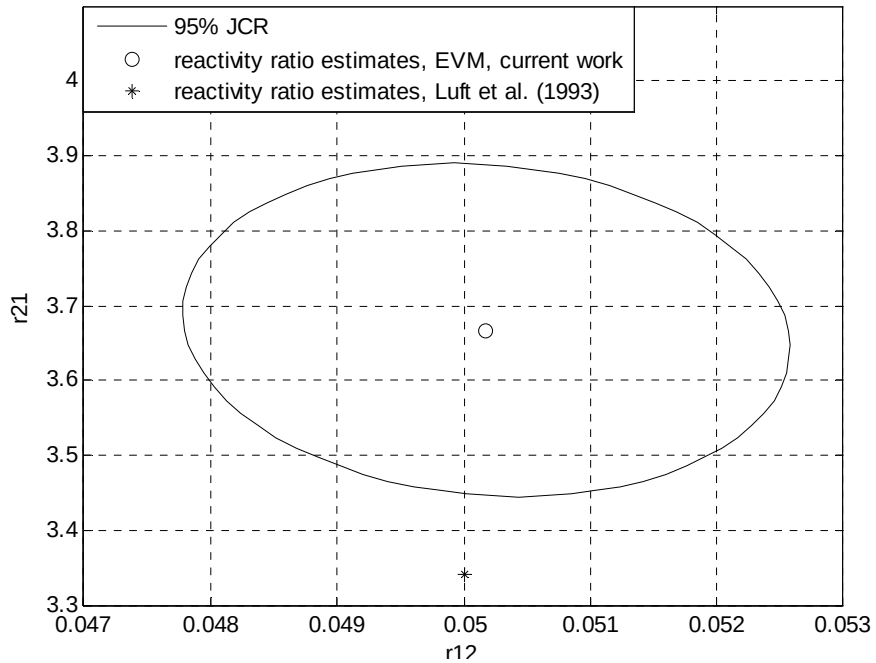

Figure 5-10g. r_{12} and r_{21} estimates, terpolymerization of E (M_1)/MMA (M_2)/VAc (M_3) at P=1100 bar and T=180°C

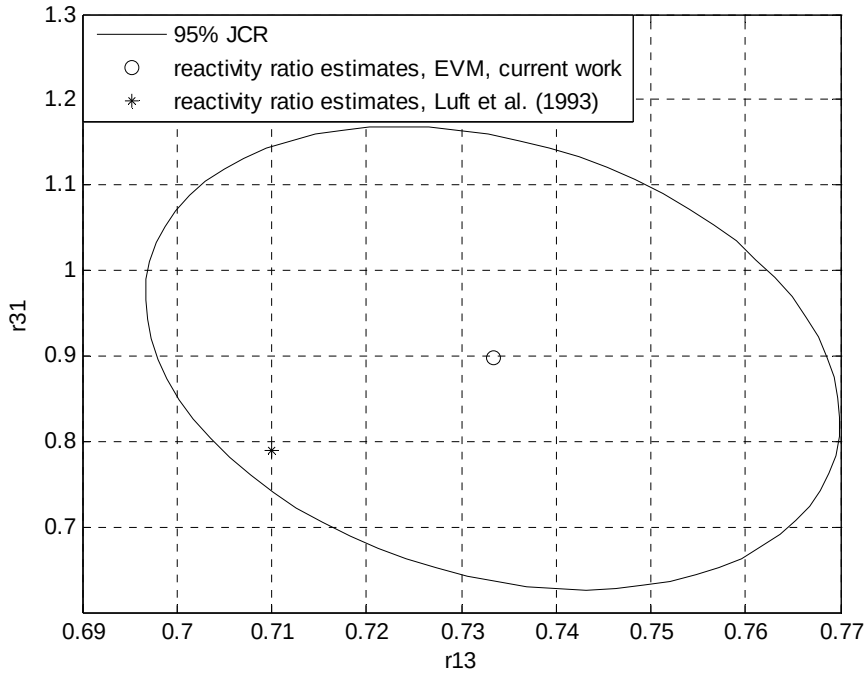

Figure 5-10h. r_{13} and r_{31} estimates, terpolymerization of E (M_1)/MMA (M_2)/VAc (M_3) at P=1100 bar and T=180°C

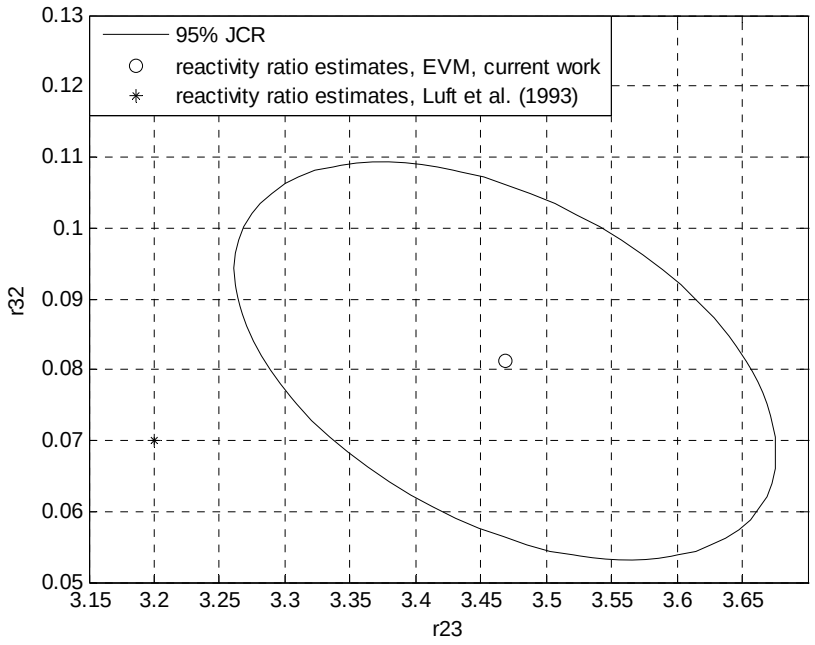

Figure 5-10i. r_{23} and r_{32} estimates, terpolymerization of E (M_1)/MMA (M_2)/VAc (M_3) at P=1100 bar and T=180°C

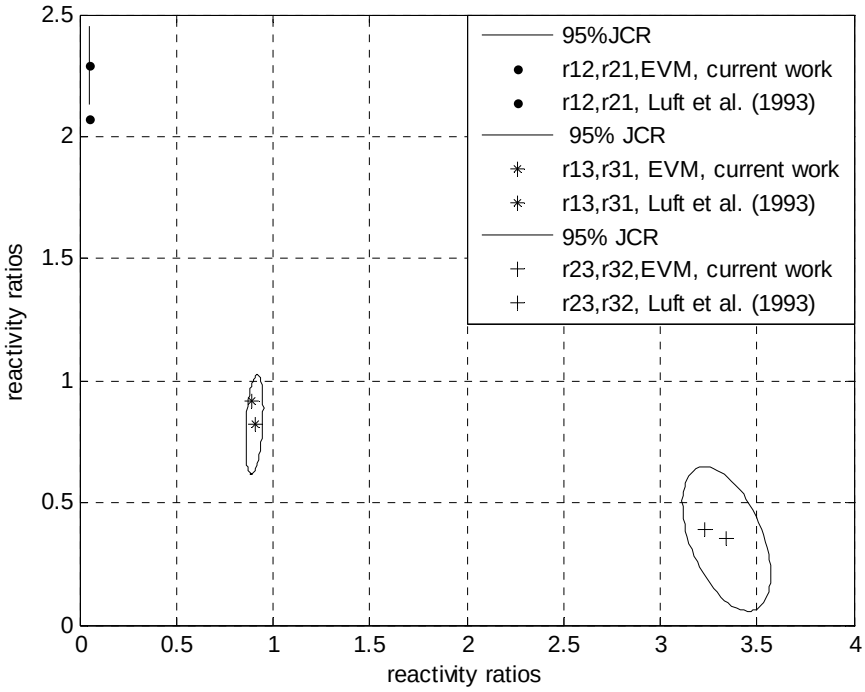

Figure 5-11a. JCRs of reactivity ratios for terpolymerization of E (M_1)/MMA (M_2)/VAc (M_3) at P=1900 bar and T=180°C

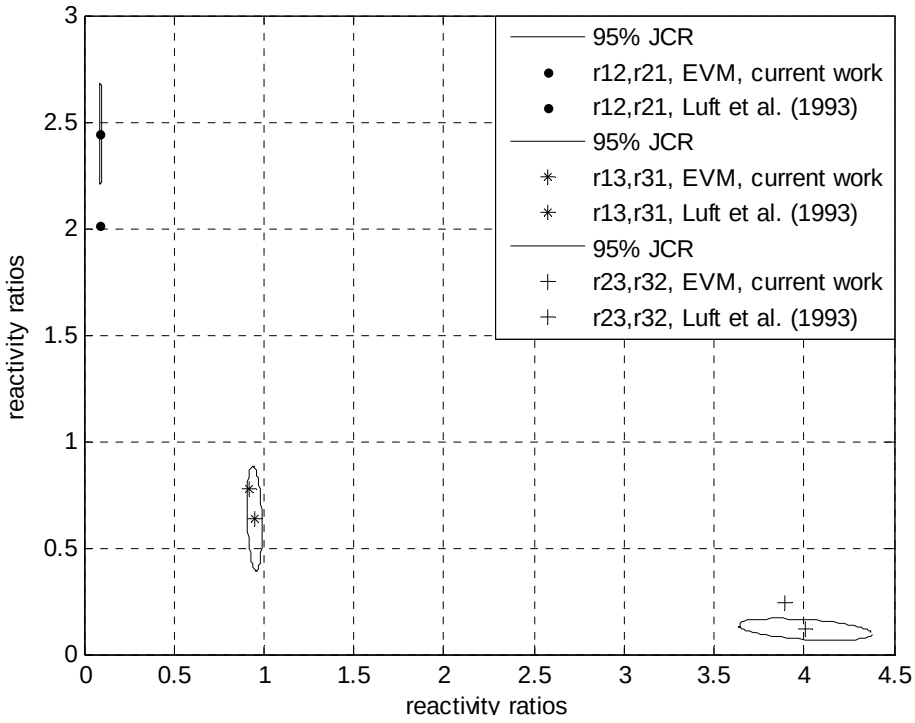

Figure 5-11b. JCRs of reactivity ratios for terpolymerization of E (M_1)/MMA (M_2)/VAc (M_3) at P=1100 bar and T=230°C

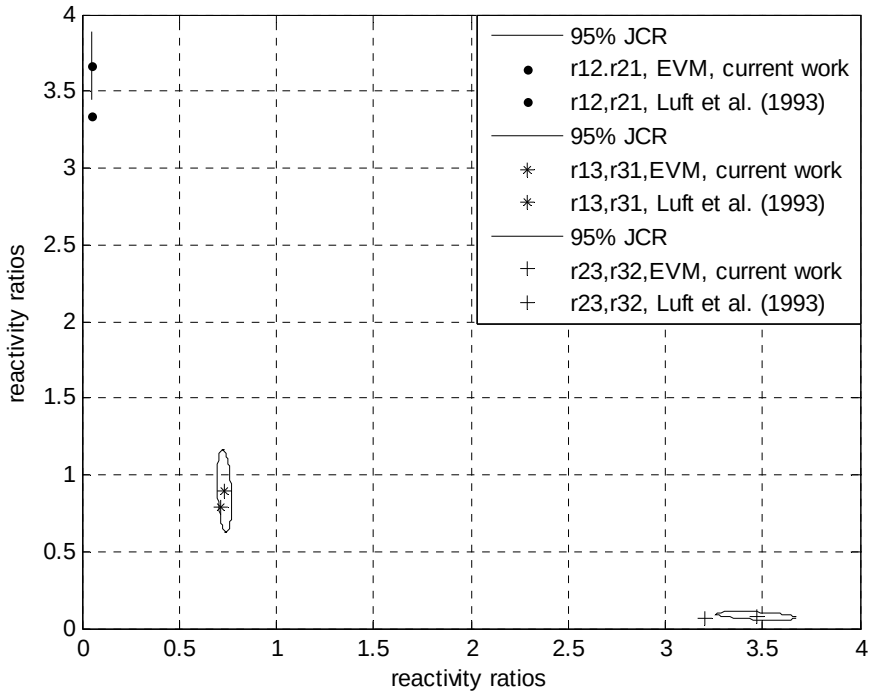

Figure 5-11c. JCRs of reactivity ratios for terpolymerization of E (M_1)/MMA (M_2)/VAc (M_3) at P=1100 bar and T=180°C

5.4.5 Case study 5: N,N-dimethylaminoethyl methacrylate/Dodecyl methacrylate/Methyl methacrylate

Two terpolymerization systems of N,N-dimethylaminoethyl methacrylate (DMAEMA, M_1) and dodecyl methacrylate (DMA, M_2), with methyl methacrylate (MMA, M_3) on the one hand and styrene (Sty, M_3) on the other, were investigated by Soljic et al. (2010). These terpolymerization reactions were carried out at low conversion isothermally at 70℃, in toluene solution. Experimental data were presented and the authors cited that experimental terpolymer compositions agreed well with calculated terpolymer compositions based on the AG equations; data sets for both systems are shown in Tables 5.14 and 5.15. To investigate these two systems, the authors referred to five binary copolymerizations (DMAEMA/MMA, DMAEMA/Sty, DMA/MMA, DDMA/Sty, and DMAEMA/DMA) from which the reactivity ratio pairs were estimated. The authors evaluated DMA/MMA, DMA/Sty, and

DMAEMA/DMA copolymerizations in Soljic et al. (2010). For DMAEMA/MMA and DMAEMA/Sty copolymerizations, they referred to previous work by Soljic et al. (2009). They used linear parameter estimation techniques, Fineman-Ross and Kelen-Tudos, and also the nonlinear parameter estimation technique described by Tidwell and Mortimer (1965). They also concluded that since different parameter estimation methods resulted in very similar reactivity ratios, these values were highly reliable and thus the average of these reactivity ratios would be accurate enough to be used for further investigation of the terpolymerization studies. These values are presented in Tables 5.16 and 5.17. Soljic et al. (2010) pointed out that for the ternary system (DMAEMA, M_1)/(MMA, M_2)/(DMA, M_3), the values of reactivity ratios show that the addition tendencies of the growing radicals towards monomers are approximately equal and thus this ternary system can be considered as an ideal system. Also, since feed compositions and terpolymer compositions were very similar (see Table 5.16), they stated that this system runs at azeotropic conditions with negligible compositional heterogeneity. On the other hand, for terpolymerization of (DMAEMA, M_1)/(Sty, M_2)/(DMA, M_3), according to the values of the reactivity ratios, the system is non-ideal. The comparison between terpolymer compositions and initial monomer mixture compositions shows significant differences (see Table 5.17); this system is richer in one monomer (Sty) than in the other two methacrylates ($r_{Sty} > 2$ and $r_{DMA} < 0.5$).

The aim of this work was to estimate reactivity ratios using the EVM parameter estimation technique to (1) compare the results from the ternary system with the point estimates reported by Soljic et al. (2009) and (2010), obtained from binary pairs, and (2) to study the behavior of both terpolymerization systems with respect to their azeotropic/non-azeotropic behavior in order to examine the conclusions pointed out by Soljic et al. (2010) in this regard. Similar to the previous case studies, reactivity ratios were estimated by EVM and the initial estimates were chosen from the average values of reactivity ratios, given by Soljic et al. (2010). The results from parameter estimation are shown in Tables 5.16 and 5.17 for both systems. Also, Figures 5.12a to 5.12f show the JCRs for reactivity ratio estimates of comonomer pairs alongside the respective point estimates from Soljic et al. (2010).

Table 5-14. Experimental data for terpolymerization of DMAEMA(M_1)/MMA(M_2)/ DMA(M_3)

Feed composition			Experimental terpolymer composition			Calculated terpolymer composition, Soljic et al. (2010)			Calculated terpolymer composition, Current work		
M_1	M_2	M_3	M_1	M_2	M_3	M_1	M_2	M_3	M_1	M_2	M_3
0.100	0.100	0.800	0.114	0.084	0.802	0.126	0.086	0.788	0.1211	0.0869	0.7920
0.100	0.400	0.500	0.125	0.381	0.494	0.128	0.377	0.495	0.1259	0.3760	0.4981
0.100	0.700	0.200	0.128	0.690	0.182	0.125	0.686	0.189	0.1256	0.6826	0.1918
0.200	0.200	0.600	0.243	0.118	0.569	0.237	0.179	0.584	0.2317	0.1801	0.5883
0.200	0.500	0.300	0.237	0.476	0.287	0.236	0.476	0.288	0.2355	0.4753	0.2892
0.400	0.100	0.500	0.422	0.090	0.488	0.424	0.089	0.487	0.4187	0.0915	0.4898
0.400	0.400	0.200	0.423	0.378	0.199	0.425	0.381	0.194	0.4239	0.3838	0.1922
0.600	0.200	0.200	0.599	0.195	0.206	0.600	0.196	0.204	0.5983	0.1996	0.2021
0.800	0.100	0.100	0.310	0.118	0.099	0.782	0.106	0.110	0.7816	0.1091	0.1093

Table 5-15. Experimental data for terpolymerization of DMAEMA(M_1)/Sty(M_2)/DMA(M_3)

Feed composition			Experimental terpolymer composition			Calculated terpolymer composition, Soljic et al. (2010)			Calculated terpolymer composition, Current work		
M_1	M_2	M_3	M_1	M_2	M_3	M_1	M_2	M_3	M_1	M_2	M_3
0.100	0.100	0.800	0.108	0.181	0.711	0.111	0.189	0.700	0.0988	0.1794	0.7218
0.100	0.400	0.500	0.095	0.579	0.326	0.083	0.581	0.336	0.0913	0.6002	0.3085
0.100	0.700	0.200	0.077	0.829	0.094	0.066	0.825	0.109	0.0763	0.8367	0.0870
0.200	0.200	0.600	0.194	0.330	0.476	0.189	0.335	0.476	0.1894	0.3354	0.4752
0.200	0.500	0.300	0.160	0.669	0.171	0.148	0.664	0.188	0.1642	0.6733	0.1625
0.400	0.100	0.500	0.367	0.172	0.461	0.383	0.177	0.440	0.3677	0.1754	0.4569
0.400	0.400	0.200	0.312	0.557	0.131	0.301	0.562	0.137	0.3215	0.5566	0.1220
0.600	0.200	0.200	0.509	0.322	0.169	0.503	0.328	0.169	0.5134	0.3244	0.1622
0.800	0.100	0.100	0.718	0.189	0.093	0.715	0.185	0.100	0.7180	0.1831	0.0989

For the first system with the three methacrylates, as can be seen in Figures 5.12a to 5.12c, we have a good agreement between the reported reactivity ratios and the re-estimated ones, except for the reported reactivity ratio for r_{12} and r_{21} that are not contained within the respective JCR. The values of reactivity ratios are very close to each other and close to unity.

Therefore, it can be concluded that this system acts as an ideal one. For the second system, containing styrene, our results are very different from the reported ones for all three comonomer pairs, as shown in Figures 5.12d to 5.12f.

Similar to the previous case studies, it has been observed that using terpolymerization experimental data changes the reactivity ratio values that are obtained from binary copolymerizations. Moreover, another important reason for the disagreement between our results and the ones reported by Soljic et al. (2010) can be attributed to using linear parameter estimation techniques, such as Fineman-Ross, that are not compatible with nonlinear polymerization models and thus provided unreliable reactivity ratio estimates. As shown in Table 5.16, for the terpolymerization of DMAEMA (M_1)/MMA (M_2)/DMA (M_3), the reactivity ratios r_{23} and r_{32} are both above one. These values were reported from copolymerization data by Soljic et al. (2010) despite the fact that the existence of such a binary system is highly questionable.

Observing this discrepancy, we used the experimental data from the corresponding binary systems, included in Soljic et al. (2009) and (2010), to re-estimate the copolymerization reactivity ratios of all the comonomer pairs. The results are summarized in Tables 5.16 and 5.17, as well. The reactivity ratios for the MMA/DMA pair were found to be r_{MMA}=1.09 and r_{DMA}=0.94. These results are more reasonable since now one of the reactivity ratios is less than unity. However, based on the results of the reactivity ratio estimation from terpolymerization data, the reactivity ratios estimates for this pair of monomers are above one. This shows once more that adding a third monomer to a copolymerization system can definitely change the values of the reactivity ratios. Also, it is reasonable to suggest that although binary systems with reactivity ratios greater than one have not been found yet, this conclusion may not necessarily extend to ternary systems as well.

Table 5-16. Monomer reactivity ratios for the terpolymerization of DMAEMA(M_1)/ MMA(M_2)/DMA(M_3)

Reference	r_{12}	r_{21}	r_{13}	r_{31}	r_{23}	r_{32}
Soljic et al. (2010)	0.85	0.86	0.79	0.75	1.12	1.19
Current work, using copolymerization data	0.81	0.80	0.95	0.85	1.09	0.95
Current work, using terpolymerization data	0.8047	0.7573	0.8102	0.7895	1.0803	1.1968

Table 5-17. Monomer reactivity ratios for the terpolymerization of DMAEMA(M_1)/ Sty(M_2)/DMA(M_3)

Reference	r_{12}	r_{21}	r_{13}	r_{31}	r_{23}	r_{32}
Soljic et al. (2010)	0.43	1.74	0.79	0.75	2.19	0.45
Current work, using copolymerization data	0.43	1.74	0.95	0.85	2.22	0.5007
Current work, using terpolymerization data	0.4285	1.5006	0.7760	1.0575	3.0699	0.5531

For the terpolymerization of DMAEMA/Sty/DMA, the reactivity ratio estimates are considerably different from the ones reported by Soljic et al. (2010). An additional reason, aside from the different parameter estimation technique and different source of experimental data (binary versus ternary system), could be the level of error associated with their experimental data for this terpolymerization, which may be higher than one would normally expect. Soljic et al. (2010) concluded that due to the closeness of the calculated terpolymer compositions and experimental data, the reactivity ratios from binary systems are able to describe these terpolymerizations. As shown in the previous case studies, using reactivity ratios from terpolymerization data also results in close values of terpolymer compositions to experimental data. So, closeness of the predicted values to experimental ones does not give sufficient support for this type of conclusion.

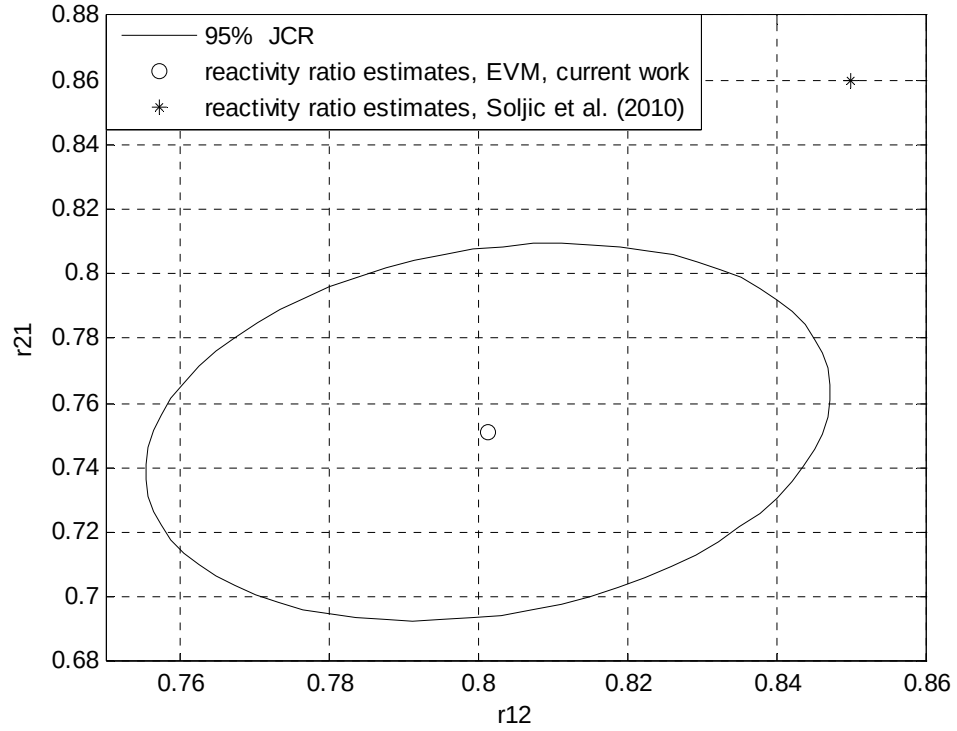

Figure 5-12a. r_{12} and r_{21} estimates, terpolymerization of DMAEMA (M_1)/MMA (M_2)/DMA (M_3)

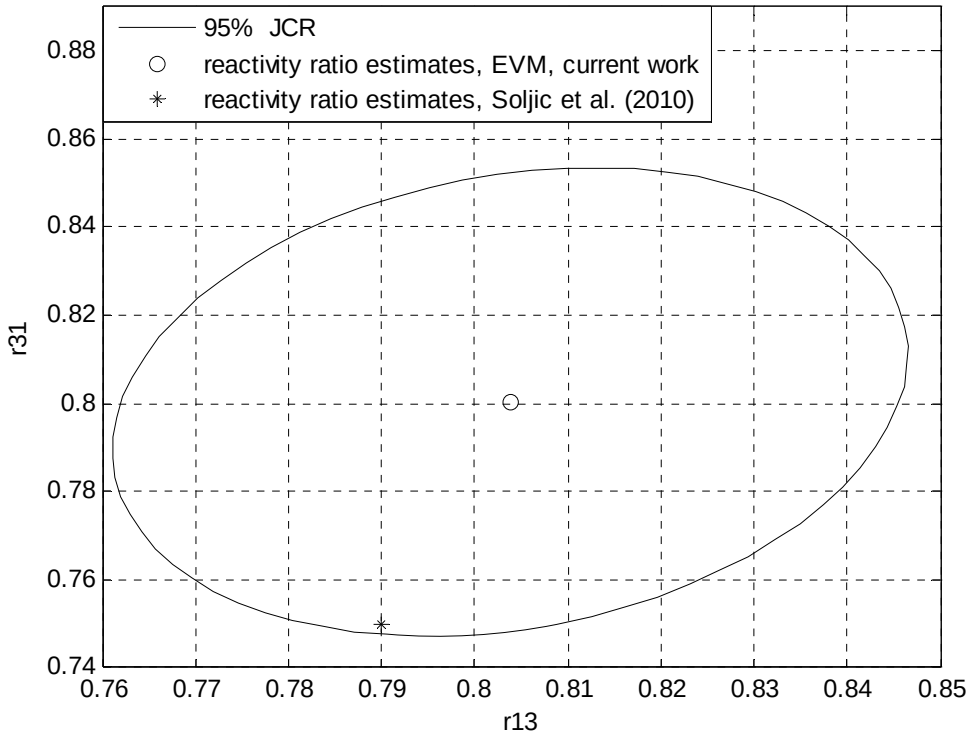

Figure 5-12b. r_{13} and r_{31} estimates, terpolymerization of DMAEMA (M_1)/MMA (M_2)/DMA (M_3)

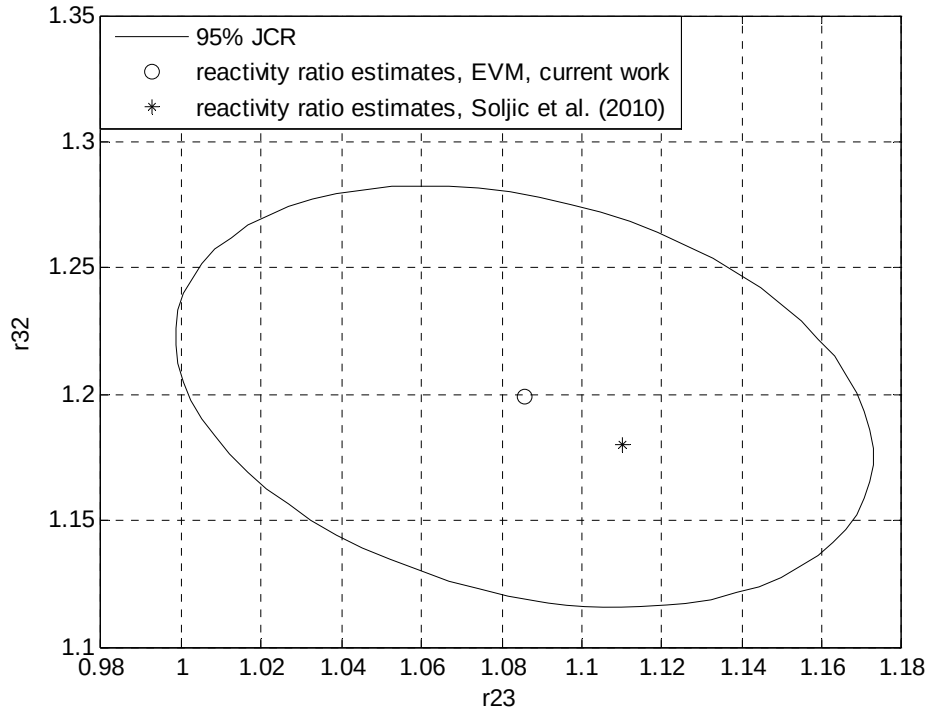

Figure 5-12c. r_{23} and r_{32} estimates, terpolymerization of DMAEMA (M_1)/MMA (M_2)/DMA (M_3)

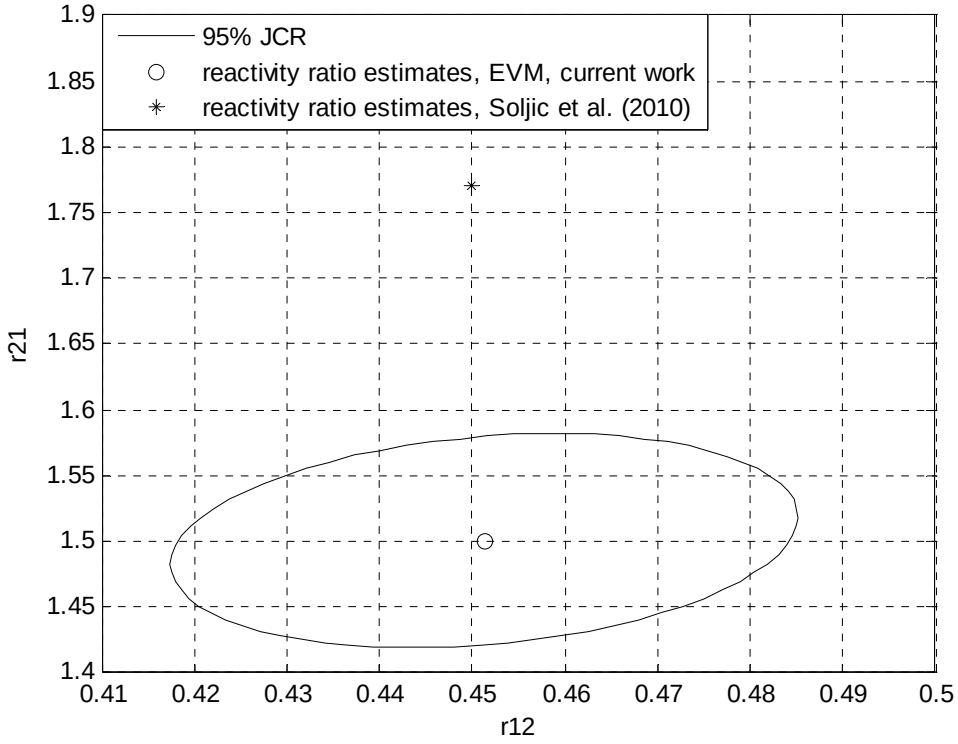

Figure 5-12d. r_{12} and r_{21} estimates, terpolymerization of DMAEMA (M_1)/Sty (M_2)/DMA (M_3)

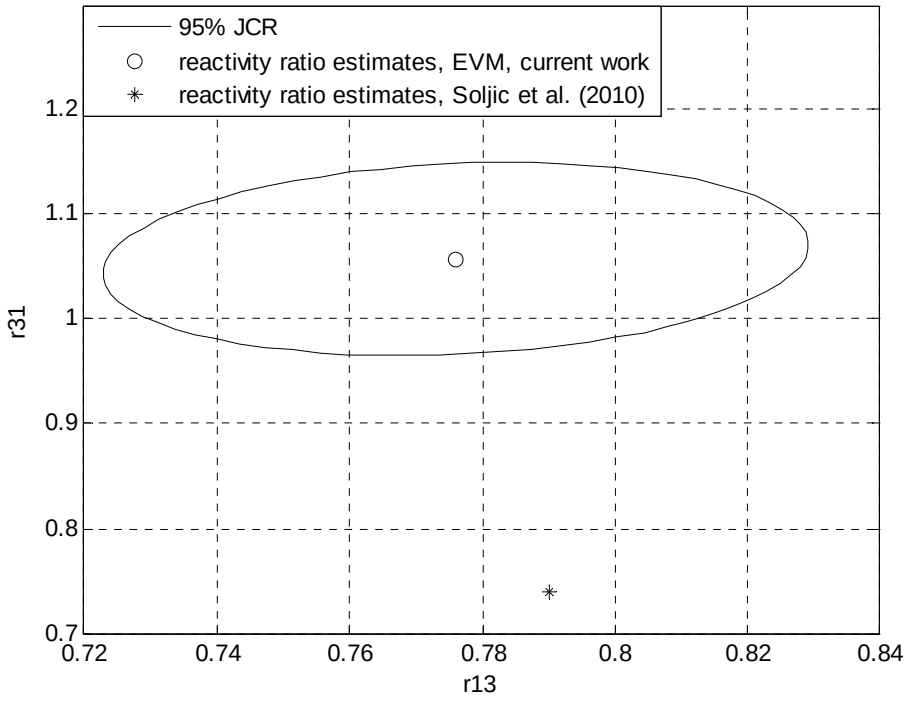

Figure 5-12e. r_{13} and r_{31} estimates, terpolymerization of DMAEMA (M_1)/Sty (M_2)/DMA (M_3)

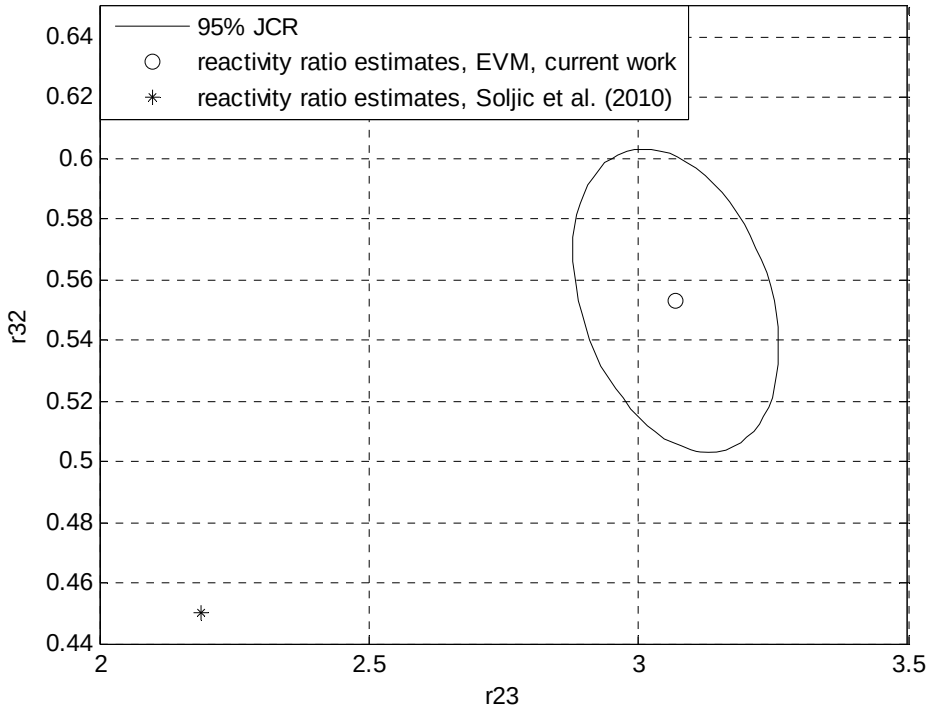

Figure 5-12f. r_{23} and r_{32} estimates, terpolymerization of DMAEMA (M_1)/Sty (M_2)/DMA (M_3)

Figures 5.13a and 5.13b show JCRs of all reactivity ratio estimates together for these two systems. In these figures the reported values of reactivity ratios by Soljic et al. (2010) and the re-estimated binary reactivity ratios in the current work are also included. "r_{ij}, r_{ji}, terpolymerization data, current work" stands for the EVM point estimates obtained from terpolymerization data in the current work, "r_{ij}, r_{ji}, copolymerization data, current work" stands for the EVM point estimates from copolymerization data in the current work, and "r_{ij}, r_{ji}, Soljic et al. (2010)" is for the reported values for the corresponding reactivity ratios in the reference paper. It can be seen in Figure 5.13a that the sizes of the JCRs for the r_{12} and r_{21} and r_{13} and r_{31} pairs are almost the same. For the r_{23} and r_{32} pair, there is a considerable increase in the size of JCR. The real reason for this observation is not clear, as mentioned in previous case studies too, and several factors, such as the experimental errors associated with composition data, have strong influence on the precision and reliability of the point estimates. In Figure 5.13b, all JCRs are almost of the same size. This is likely an indication for a more proper information content via the data which has resulted in more reliable parameter estimation results.

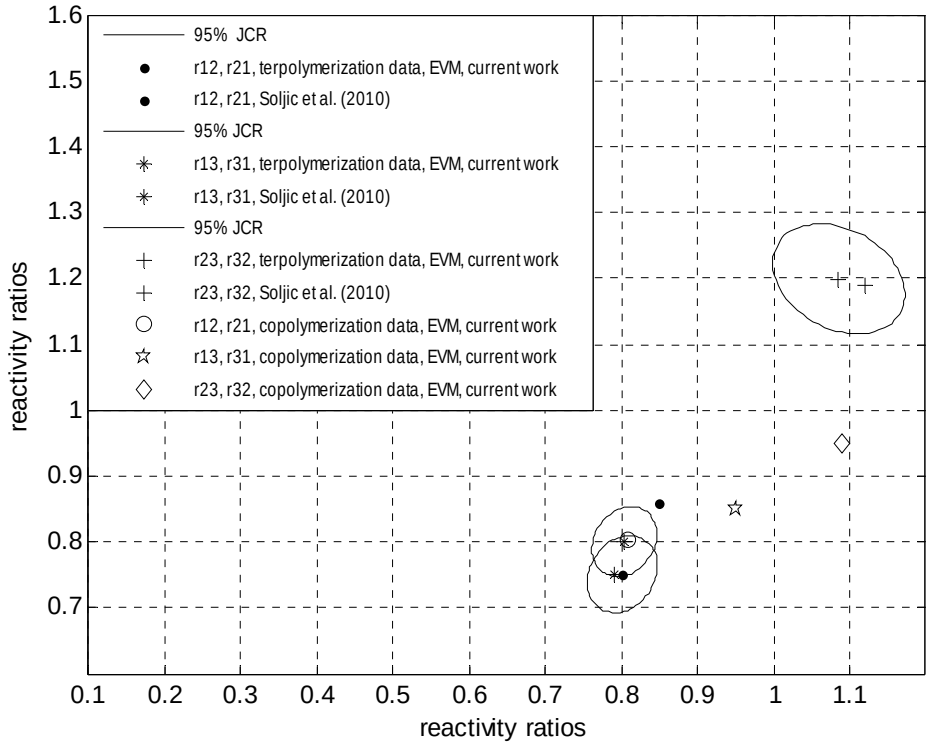

Figure 5-13a. JCRs for the terpolymerization of DMAEMA(M_1)/ MMA(M_2)/DMA(M_3)

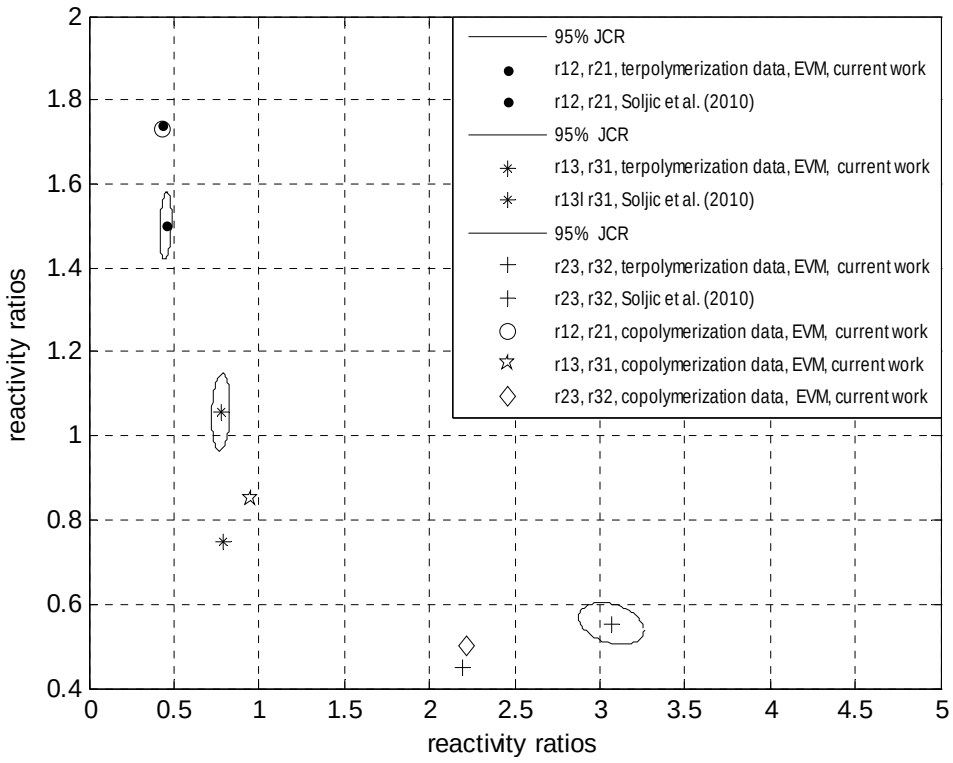

Figure 5-13b. JCRs for the terpolymerization of DMAEMA(M_1)/ Sty(M_2)/DMA(M_3)

As an aside, we also explored another interesting point by trying different combinations of the component mole fraction ratios in the AG equations. As mentioned earlier in this chapter, we used the following combination of the AG equations:

$$\frac{F_1}{F_2} = \frac{f_1\left(\frac{f_1}{r_{21}r_{31}}+\frac{f_2}{r_{21}r_{32}}+\frac{f_3}{r_{31}r_{23}}\right)\left(f_1+\frac{f_2}{r_{12}}+\frac{f_3}{r_{13}}\right)}{f_2\left(\frac{f_1}{r_{12}r_{31}}+\frac{f_2}{r_{21}r_{32}}+\frac{f_3}{r_{13}r_{32}}\right)\left(f_2+\frac{f_1}{r_{21}}+\frac{f_3}{r_{23}}\right)} \tag{5.21}$$

$$\frac{F_3}{F_2} = \frac{f_3\left(\frac{f_1}{r_{13}r_{21}}+\frac{f_2}{r_{23}r_{12}}+\frac{f_3}{r_{13}r_{23}}\right)\left(f_3+\frac{f_1}{r_{31}}+\frac{f_2}{r_{32}}\right)}{f_2\left(\frac{f_1}{r_{12}r_{31}}+\frac{f_2}{r_{21}r_{32}}+\frac{f_3}{r_{13}r_{32}}\right)\left(f_2+\frac{f_1}{r_{21}}+\frac{f_3}{r_{23}}\right)} \tag{5.22}$$

The other combinations of the AG equations are as follows:

$$\frac{F_1}{F_3} = \frac{f_1\left(\frac{f_1}{r_{21}r_{31}}+\frac{f_2}{r_{21}r_{32}}+\frac{f_3}{r_{31}r_{23}}\right)\left(f_1+\frac{f_2}{r_{12}}+\frac{f_3}{r_{13}}\right)}{f_3\left(\frac{f_1}{r_{13}r_{21}}+\frac{f_2}{r_{23}r_{12}}+\frac{f_3}{r_{13}r_{23}}\right)\left(f_3+\frac{f_1}{r_{31}}+\frac{f_2}{r_{32}}\right)} \tag{5.23}$$

$$\frac{F_2}{F_3} = \frac{f_2\left(\frac{f_1}{r_{12}r_{31}}+\frac{f_2}{r_{21}r_{32}}+\frac{f_3}{r_{13}r_{32}}\right)\left(f_2+\frac{f_1}{r_{21}}+\frac{f_3}{r_{23}}\right)}{f_3\left(\frac{f_1}{r_{13}r_{21}}+\frac{f_2}{r_{23}r_{12}}+\frac{f_3}{r_{13}r_{23}}\right)\left(f_3+\frac{f_1}{r_{31}}+\frac{f_2}{r_{32}}\right)} \tag{5.24}$$

and,

$$\frac{F_3}{F_1} = \frac{f_3\left(\frac{f_1}{r_{13}r_{21}}+\frac{f_2}{r_{23}r_{12}}+\frac{f_3}{r_{13}r_{23}}\right)\left(f_3+\frac{f_1}{r_{31}}+\frac{f_2}{r_{32}}\right)}{f_1\left(\frac{f_1}{r_{21}r_{31}}+\frac{f_2}{r_{21}r_{32}}+\frac{f_3}{r_{31}r_{23}}\right)\left(f_1+\frac{f_2}{r_{12}}+\frac{f_3}{r_{13}}\right)} \tag{5.25}$$

$$\frac{F_2}{F_1} = \frac{f_2\left(\frac{f_1}{r_{12}r_{31}}+\frac{f_2}{r_{21}r_{32}}+\frac{f_3}{r_{13}r_{32}}\right)\left(f_2+\frac{f_1}{r_{21}}+\frac{f_3}{r_{23}}\right)}{f_1\left(\frac{f_1}{r_{21}r_{31}}+\frac{f_2}{r_{21}r_{32}}+\frac{f_3}{r_{31}r_{23}}\right)\left(f_1+\frac{f_2}{r_{12}}+\frac{f_3}{r_{13}}\right)} \tag{5.26}$$

The mathematical details for EVM implementation on the original form of the AG equations that we used (eqs. (5.21) and (5.22)) are given in section 5.3. Our objective is then

to investigate whether there are any benefits in applying different combinations of the AG equations for reactivity ratio estimation. Also, it would be very interesting to determine which combination should be chosen so that an experiment would contain the maximum amount of information with respect to all reactivity ratios. Therefore, the new combinations, eq.(5.23)- eq.(5.24) and eq.(5.25)-eq.(5.26), were substituted into the Matlab program and the reactivity ratios were re-estimated. The point estimates were exactly the same as the ones obtained from the original AG equations we considered initially. Figures 5.14 and 5.15 summarize the JCRs for all three pairs, for the three model combinations for DMAEMA/MMA/DMA and DMAEMA/Sty/DMA terpolymerizations, respectively. Figures 5.14 and 5.15 are analogous to Figure 5.13.

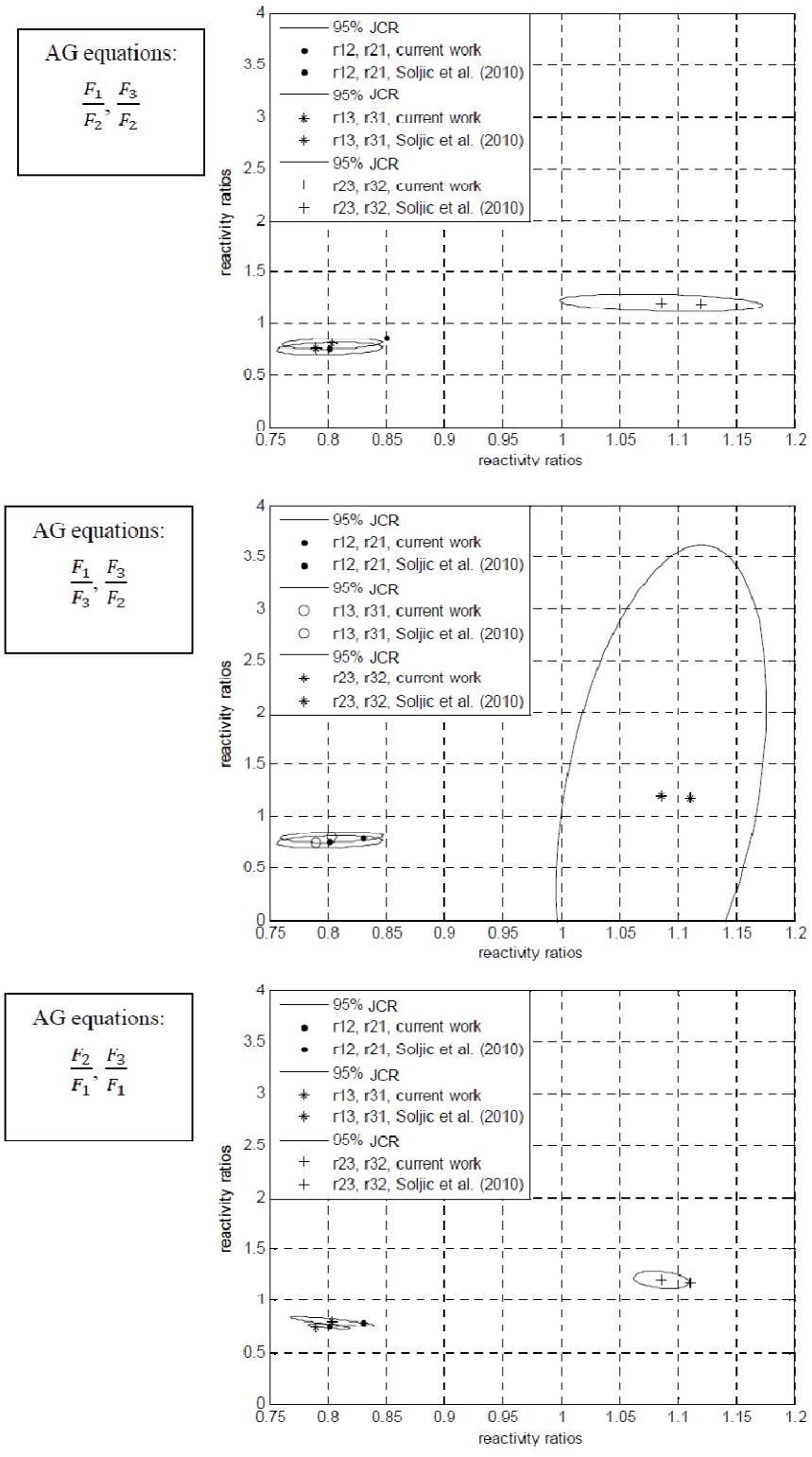

Figure 5-14. JCRs for the terpolymerization of DMAEMA(M_1)/ MMA(M_2)/DMA(M_3)

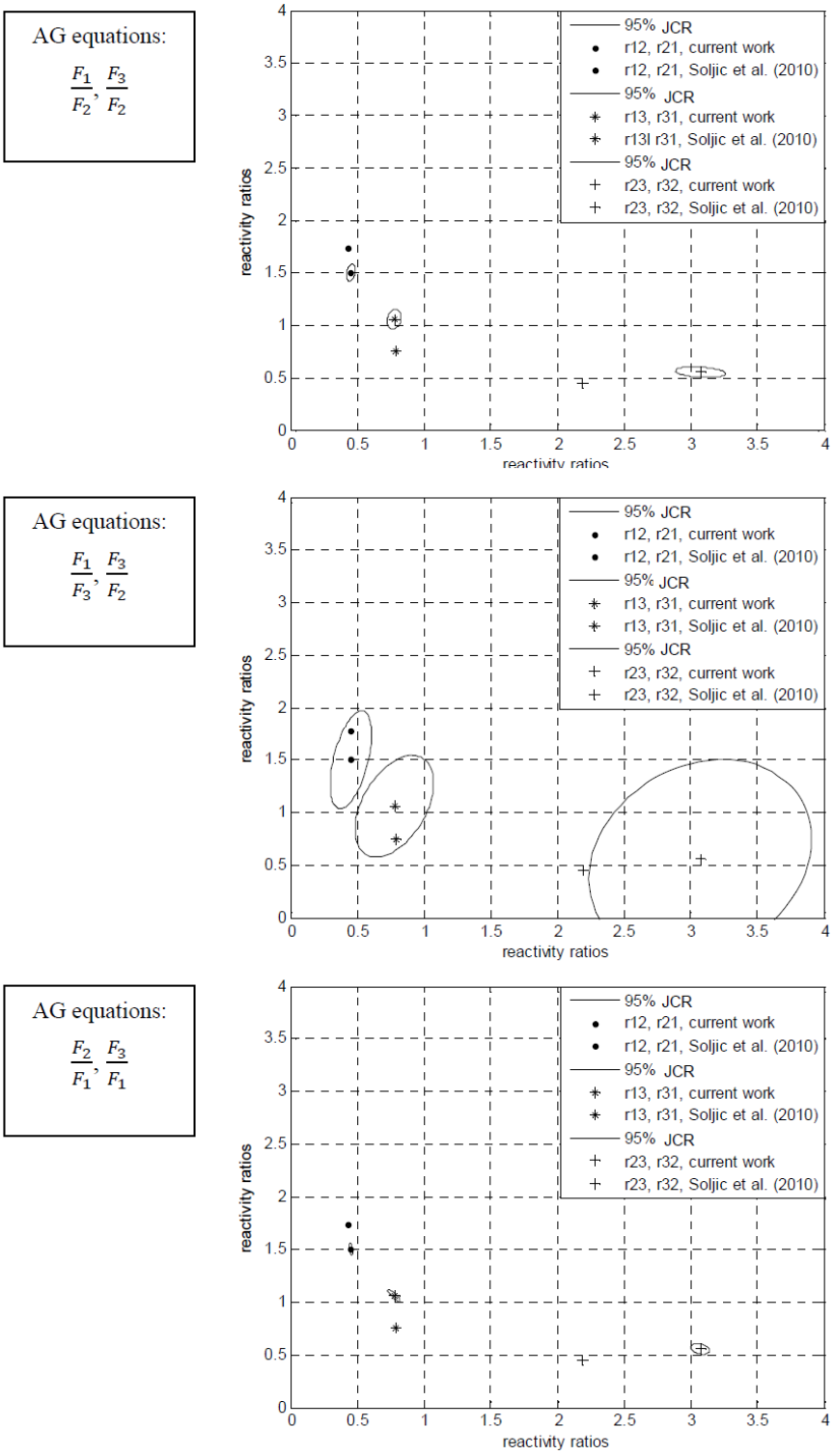

Figure 5-15. JCRs for the terpolymerization of DMAEMA(M_1)/ Sty(M_2)/DMA(M_3)

The following points can be made for Figure 5.14 for the DMAEMA/MMA/DMA terpolymerization:

1. Comparing the first and the second plot, it can be seen that changing the model combination from (F_1/F_2)-(F_3/F_2) to (F_1/F_3)-(F_2/F_3) has resulted in a significantly larger confidence region for r_{32}. The values of r_{32} have gone into the negative region, which is an indication of a large amount of uncertainty for the point estimate. The other reactivity ratios do not seem to be affected by this change. So, it can be suggested that by using the (F_1/F_3)-(F_2/F_3) model combination, the results of parameter estimation is become much more sensitive to the third component and thus the uncertainty existed in the terpolymer composition regarding the third component is reflected significantly.
2. Using the (F_2/F_1)-(F_3/F_1) model combination seems to result in the smallest areas for the JCRs, meaning that highest precision was obtained using this combination; also, the variation in the size of JCRs is very insignificant. Therefore, it can be suggested that this combination can provide the best results regarding reactivity ratio estimation for this system.

The following points are made about the plots of Figure 5.15 for the DMAEMA/Sty/DMA terpolymerization:

1. Comparing the second plot with the two others, the (F_1/F_3)-(F_2/F_3) combination resulted in the highest level of uncertainty in the reactivity ratio estimation (as seen by the large size of the JCRs as well as the considerable variation in their sizes). Once again, it can be seen that using this combination pushed r_{32} to the negative region.
2. The third plot shows the smallest JCRs, meaning that the results are the most reliable in this case. The sizes of the JCRs are almost the same, which can be considered as another indication of the reliable parameter estimation results by choosing this combination of the AG equations.

The changes in the level of uncertainty of our parameter estimation results when one combination is taken into account versus another are effected either by the choice of different combinations of the AG equations or by experimental error associated to the

data. Hence, it is recommended that the effect of different combinations of the AG equations on the parameter estimation results be investigated in a more systematic way so that all these combined effects become clearer.

5.5 Summary of Main Results

According to the results from the five case studies of this chapter, the following points can be made:

- Estimation aspects in terpolymerization have been traditionally approached through an application of concepts and techniques already developed for binary copolymerization systems. Our research concentrates on potential enhancements in reactivity ratio estimation by applying a novel and powerful estimation technique, the EVM method, directly on terpolymerization experimental data (instead of dealing with three (often non-representative) binary copolymerizations).
- Observations from several case studies and experimental data sets illustrate that using the ternary system data affects the values of the binary reactivity ratios considerably. In most cases, binary reactivity ratios obtained from the literature are not contained within joint confidence regions provided by our analysis.
- In certain cases, reactivity ratio estimation results reflect levels of uncertainty which in turn were investigated by trying several hypotheses such as considering distribution of data points, changing the number of variables used for implementing the EVM method on experimental data, and different combinations of the AG equations. However, these aspects require a much more thorough effort in order to clarify further the effect on the quality of the obtained parameter estimates.

Chapter 6. Azeotropy in Multicomponent Polymerizations

6.1 Introduction

Examination of the literature demonstrates that the study of azeotropy in multicomponent polymerization was initiated in the early 1960s with the goal of understanding the conditions under which "azeotropes" or "near-azeotropes" could be expected in multicomponent polymerization as well as obtaining the composition of this point mathematically. Predicting the existence and also calculating the composition of the azeotropic point can reduce the effort of running costly experiments, in that computational results can be used to narrow the experimental search space. Although many attempts have been made to clarify the issue of the existence of azeotropic points in multicomponent polymerization systems (systems with more than two components), the fact that the question still remains open triggered this study to revisit multicomponent azeotropy. Our objective is to present a general method that reliably finds any and all azeotropes for multicomponent polymerization systems, and also confirms the nonexistence of azeotropes if none are present.

6.2 Background: Azeotropy in Copolymerization

In copolymerization systems (binary systems), the instantaneous copolymer composition is related to the monomer (feed) composition via the instantaneous copolymer composition model, referred to as the Mayo-Lewis model, by the following equation:

$$F_1 = \frac{r_1 f_1^2 + f_1 f_2}{r_1 f_1^2 + 2 f_1 f_2 + r_2 f_2^2} \tag{6.1}$$

where F_1 is the monomer 1 mole fraction in the polymer, f_1 is the monomer 1 mole fraction in the monomer mixture, and r_1 and r_2 are the reactivity ratios.

By definition, and borrowing the idea from batch distillation, the azeotropic point is the point at which the compositions of the copolymer and the (unreacted) monomer (feed) mixture are the same. Hence, the azeotropic composition can be determined by equating the copolymer and monomer compositions, $F_1=f_1$. After applying the azeotropic condition on the Mayo-Lewis equation, we obtain the binary azeotropic composition as:

$$F_1 = f_1 = \frac{1-r_2}{2-r_1-r_2} \tag{6.2}$$

Eq. (6.2) is an analytical expression (solution) for the binary azeotropic point. One can see that in order to have a feasible non-negative azeotropic point in the binary system, both reactivity ratios must be less or greater than unity. However, free radical copolymerization systems in which both monomers have reactivity ratios greater than unity have not been observed yet. If both reactivity ratios are equal to unity, then eq. (6.2) does not yield an azeotrope. Practically speaking, if $r_1=r_2=1$, then $F_1=f_1$, and hence one obtains an azeotrope at all feed compositions. Wittmer et al. (1967) cite an extensive table with reactivity ratios for various binary systems along with their azeotropic compositions, which is a good source of information for many copolymerization systems.

The binary azeotropic composition can also be calculated numerically from the Mayo-Lewis equation, eq. (6.1), recognizing from the outset that there are two trivial solutions, for $f_1 = 0$ and $f_1 = 1$. Given values of monomer reactivity ratios r_1 and r_2, the non-trivial azeotropic composition can be obtained via an appropriate root-finding numerical technique.

Consider eq. (6.3), based on the definition of azeotropic point and by using eq. (6.1):

$$F_1 = f_1 = \frac{r_1 f_1^2 + f_1(1-f_1)}{r_1 f_1^2 + 2f_1(1-f_1) + r_2(1-f_1)^2} \tag{6.3}$$

One can now apply a Newton-Raphson numerical technique on eq. (6.3) in order to obtain the azeotropic point (solution). A brief description of the Newton-Raphson technique is included in Appendix C. For example, following McManus and Penlidis (1996) for the styrene (Sty)/ethyl acrylate (EA) binary copolymer system, with $r_1 = 0.717$ ($1 = $ Sty) and $r_2 = 0.128$ ($2 = $ EA), one obtains the analytical and numerical solutions of Table 6.1.

Table 6-1. Comparison between calculated azeotropic points (Sty/EA)

	M_1	M_2
Analytical azeotropic point	0.7550	0.245
Numerical azeotropic point	0.7550	0.245

One can see from Table 6.1 that the solutions are in perfect agreement for this copolymer system, whose azeotropic point has also been experimentally verified.

6.3 Background: Azeotropy in Terpolymerization

6.3.1 Ternary Azeotropic Point

As was mentioned in Chapter 5, section 5.1, the terpolymerization composition equations derived by Alfrey and Goldfinger (1944) (to be referred to as AG equations from now on) are as follows:

$$\frac{df_1}{df_2} = \frac{f_1\left(\frac{f_1}{r_{21}r_{31}}+\frac{f_2}{r_{21}r_{32}}+\frac{f_3}{r_{31}r_{23}}\right)\left(f_1+\frac{f_2}{r_{12}}+\frac{f_3}{r_{13}}\right)}{f_2\left(\frac{f_1}{r_{12}r_{31}}+\frac{f_2}{r_{21}r_{32}}+\frac{f_3}{r_{13}r_{32}}\right)\left(f_2+\frac{f_1}{r_{21}}+\frac{f_3}{r_{23}}\right)} \tag{6.4}$$

$$\frac{df_1}{df_3} = \frac{f_1\left(\frac{f_1}{r_{21}r_{31}}+\frac{f_2}{r_{21}r_{32}}+\frac{f_3}{r_{31}r_{23}}\right)\left(f_1+\frac{f_2}{r_{12}}+\frac{f_3}{r_{13}}\right)}{f_3\left(\frac{f_1}{r_{13}r_{21}}+\frac{f_2}{r_{23}r_{12}}+\frac{f_3}{r_{13}r_{23}}\right)\left(f_3+\frac{f_1}{r_{31}}+\frac{f_2}{r_{32}}\right)} \quad (6.5)$$

f_i is the mole fraction of monomer *i* in the feed, df_i is the mole fraction of monomer *i* incorporated into the terpolymer, and reactivity ratios are defined as :

$$r_{12} = \frac{k_{11}}{k_{12}}, \quad r_{13} = \frac{k_{11}}{k_{13}}, \quad r_{21} = \frac{k_{22}}{k_{21}}, \quad r_{23} = \frac{k_{22}}{k_{23}}, \quad r_{31} = \frac{k_{33}}{k_{31}}, \quad r_{32} = \frac{k_{33}}{k_{32}} \quad (6.6)$$

By definition, the ternary azeotropic point, similar to binary systems, is the composition at which the reaction can be performed to high conversion without compositional drift, and thus a homogenous polymer can be obtained. At the azeotropy point, the terpolymer composition is exactly the same as the monomer mixture (feed). This relation can be demonstrated as:

$F_1=f_1$, $F_2=f_2$, and $F_3=f_3$ (6.7)

The relationship between the compositions of the feed and the resulting polymer is commonly presented in the form of a triangular plot. In the triangle, a side represents the mole fraction of the monomer assigned to that side, while the corners of the triangle represent 100% concentration of each monomer. In addition, the sides describe the corresponding binary mixtures. Compositional drift in the terpolymer mixture is illustrated by arrows. The head of the arrow indicates the instantaneous composition of the resulting polymer, its tail the composition of the monomer mixture, and thus the length of the arrow is an indicator of the magnitude of the compositional drift.

In the initial attempts researchers arrived at the ternary azeotropic point graphically. That is, they observed that the composition arrows point toward the ternary azeotrope composition, and the length of the composition arrow at the azeotropic composition is reduced to a point because of no (or minimal) composition drift (e.g., Slocombe, 1957). To visualize this approach, Figure 6.1 has been chosen from the literature (Azab, 2004) for methyl methacrylate/di(tri-n-butyltin) itaconate/acrylonitrile terpolymerization. In this figure,

the region in which the composition drift arrows are more or less reduced to points is approximately delineated by the light grey area. It can clearly be seen that the other compositional drift arrows point towards this specific area, where the azeotrope lies. This is an important observation, and the basis of the proposed graphical approaches.

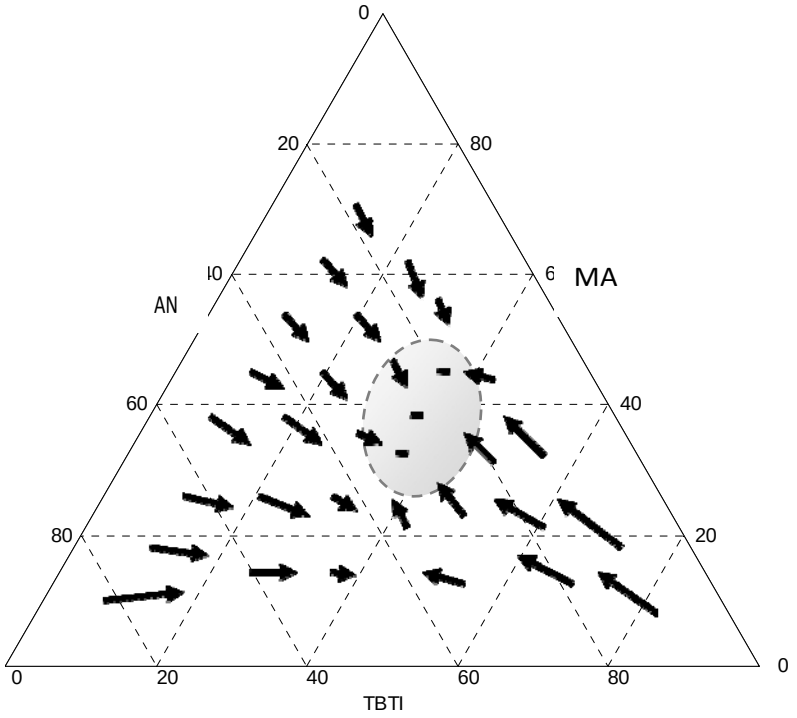

Figure 6-1. Triangular plot for the terpolymerization of methyl acrylate (MA)/di(tri-n-butyltin) itaconate (TBTI)/acrylonitrile (AN) (Azab, 2004)

The question of azeotropy in terpolymerization has been discussed in several publications through a variety of approaches. Tarasov et al. (1960) suggested a mathematical solution for the azeotropy problem, according to which the azeotropic composition can be calculated using eq. (6.8).

$$M_1 : M_2 : M_3 = R\left(\frac{Q}{r_{13}r_{32}} + \frac{S}{r_{12}r_{23}} + \frac{R}{r_{12}r_{13}}\right):$$
$$S\left(\frac{S}{r_{21}r_{23}} + \frac{Q}{r_{31}r_{23}} + \frac{R}{r_{21}r_{13}}\right):$$
$$Q\left(\frac{Q}{r_{31}r_{32}} + \frac{S}{r_{21}r_{32}} + \frac{R}{r_{12}r_{31}}\right) \qquad (6.8)$$

M_i denotes the concentration of monomer i in the feed, whereas r_{ij} denote the reactivity ratios of the monomers. A ternary azeotrope will then occur if values of S, Q, and R are non-zero and of the same sign. S, Q and R are defined by:

$$S = \left(1 - \frac{1}{r_{13}}\right)\left(\frac{1}{r_{32}} - 1\right) - \left(\frac{1}{r_{12}} - \frac{1}{r_{13}}\right)\left(\frac{1}{r_{31}} - 1\right) \tag{6.9}$$

$$Q = -\left(1 - \frac{1}{r_{23}}\right)\left(1 - \frac{1}{r_{13}}\right) + \left(\frac{1}{r_{21}} - \frac{1}{r_{23}}\right)\left(\frac{1}{r_{12}} - \frac{1}{r_{13}}\right) \tag{6.10}$$

$$R = \left(\frac{1}{r_{31}} - 1\right)\left(1 - \frac{1}{r_{23}}\right) - \left(\frac{1}{r_{21}} - \frac{1}{r_{23}}\right)\left(\frac{1}{r_{32}} - 1\right) \tag{6.11}$$

This criterion was later adopted by several other researchers, such as Wittmer et al. (1967) and Quella (1989). Wittmer et al. (1967) investigated over 700 terpolymerization systems mathematically, amongst which 37 systems seemed to have azeotropic compositions. The values of reactivity ratios for these systems were obtained from binary systems reported in the literature and no actual experimental confirmations were reported. Hence, the reliability of the reported azeotropic compositions can be discussed merely based on the accuracy of the reactivity ratio values. Wittmer et al. (1967) also suggested that a ternary azeotrope exists only when at least one binary azeotropic composition is found among the three constituent binary pairs. However, Ring (1968) contested this suggestion and claimed this not to be a prerequisite for having ternary azeotropes.

Around the same time, Ham (1964) suggested that terpolymer azeotropes may not exist. He also pointed out that the Tarasov et al. (1960) approach was based on the necessary condition that $r_{12}r_{23}r_{31} \neq r_{13}r_{32}r_{21}$, whereas extending the concept of alternation from a binary system the equality $r_{12}r_{23}r_{31} = r_{13}r_{32}r_{21}$ should hold for the azeotropic terpolymer. According to Ham (1964), an alternating terpolymer means that terpolymer sequences such as $M_1M_3M_2M_1M_2M_3\ldots M_1$ and $M_1M_2M_3M_1M_3M_2...M_1$ occur with equal probability. So, the alternation in ternary systems can be described in the following development.

$$P_{12}P_{23}P_{31} = P_{13}P_{32}P_{21} \tag{6.12}$$

P_{ij} represents the probability of monomer *j* adding to radical *i* in the presence of all three monomers. As an example, this probability can be defined in the form of eq. (6.13) for P_{12}:

$$P_{12} = \frac{k_{12}[R_{1,r}{}^*][M_2]}{k_{12}[R_{1,r}{}^*][M_2]+k_{13}[R_{1,r}{}^*][M_3]+k_{11}[R_{1,r}{}^*][M_1]} \tag{6.13}$$

$[R_{1,r}{}^*]$ is the concentration of radicals ending in monomer 1. $[M_1]$, $[M_2]$, and $[M_3]$ are the monomer concentrations. k_{11}, k_{12}, and k_{13} are the propagation rate constants. Therefore, eq. (6.13) can be rewritten in the following form:

$$P_{12} = \frac{[M_2]r_{13}}{[M_2]r_{13}+[M_3]r_{13}r_{12}+[M_1]r_{12}} \tag{6.14}$$

Deriving similar expressions for $P_{23}, P_{31}, P_{13}, P_{32}, and\ P_{21}$ and substituting into eq. (6.12) results in the following equation:

$$r_{12}r_{23}r_{31} = r_{13}r_{32}r_{21} \tag{6.15}$$

The next approach for calculating the ternary azeotropic point was proposed by Braun et al. (1975) using binary reactivity ratios (obtained from the literature). Based on the AG equations, they derived a fourth-degree polynomial for monomer concentration f_i, and solved iteratively for its zeros. Later, Rios and Guillot (1987) used the same fourth-degree equation and obtained the same azeotropic composition results, following a different solution approach. One of the first experimental evidence of a ternary azeotrope for the system acrylonitrile/butyl acrylate/vinylidene chloride was published by Tomescu (1979), and later acknowledged by Ham (1991). Overall, the early approaches to determining ternary azeotropic compositions via numerical or analytical techniques were rather circuitous and numerically unstable, and this led investigators from the 1960s to date to resort to what became traditional graphical approaches. Even nowadays, research conducted on

investigating ternary azeotropy uses approximate graphical techniques (e.g., Azab (2004), Soljic et al. (2010), etc.), and no attempts have been made to employ a general, stable, reliable and direct numerical approach for determining ternary azeotropic points (and for subsequently constructing the related useful triangular diagrams).

6.3.2 Partial Azeotropy

Aside from the more strictly defined ternary azeotropy of section 6.3.1, special cases of partial azeotropy may also be considered in terpolymerization systems. In fact, these special cases have often been considered in the literature, albeit as unreliable or unverified approximations or ways to circumvent the direct numerical solution for determining azeotropic information. Two such categories of partial azeotropy in terpolymers are the so-called "unitary" and "binary" azeotropes. These categories have been discussed as special cases in the azeotropy characteristics of terpolymers since the mid-1980s and have arguably generated rather confusing and conflicting statements in the terpolymer literature, especially due to lack of experimental verifications.

6.3.2.1 "Unitary" azeotropic curves

"Unitary" azeotropes refer to each monomer individually and are identified by the condition when the mole fraction of one of the three monomers is the same in the terpolymer and in the monomer feed. For instance, consider the unitary azeotropic composition with respect to monomer 1. For the mole fraction of monomer 1 in the feed and the terpolymer, we then have to satisfy only the following relation:

$$F_1 = f_1 \tag{6.16}$$

Under the condition described by eq. (6.16), the curve for "unitary" azeotropy (to be discussed shortly) gives the composition of a monomer mixture leading to a terpolymer that

includes the same proportion of monomer 1 as the monomer feed. Unitary azeotropic curves for monomers 2 and 3 can be defined in a similar fashion. Figure 6.2 illustrates an example for the terpolymer system, methyl methacrylate (MMA)/styrene (Sty)/4-vinylpyridine (4VP) (taken from Rios and Guillot, 1987), with a unitary azeotropy curve for styrene shown in the corresponding triangular plot. As an example of a unitary azeotropy curve, the unitary azeotropy curve for styrene is shown in this triangular plot. This curve represents the monomer (feed) compositions that lead to a terpolymer with the same proportion of styrene in the terpolymer chains as in the feed.

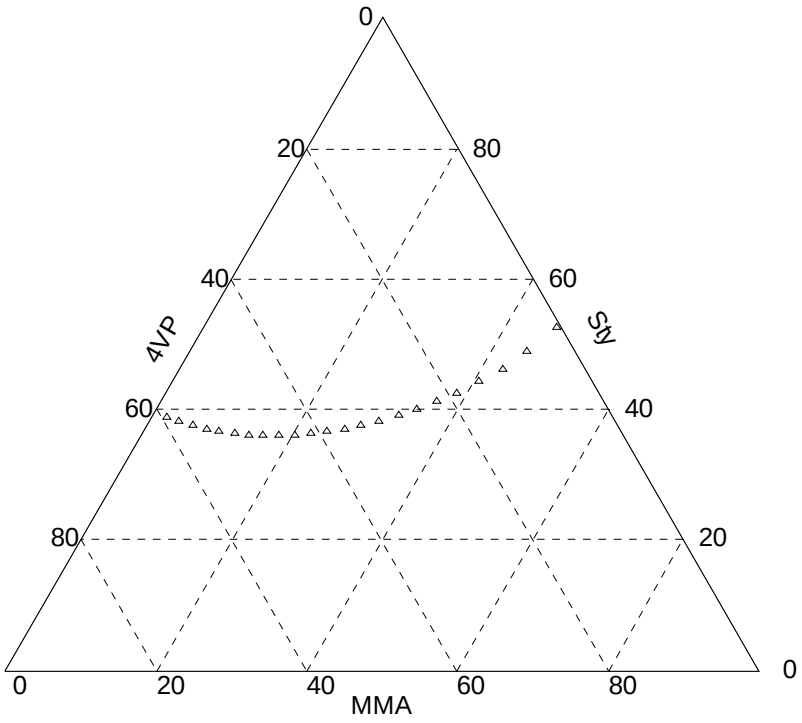

Figure 6-2. Styrene unitary azeotropic curve for terpolymerization of MMA/Sty/4VP

If, of course, a ternary azeotrope exists (as per the general strict definition of section 6.3.1), then this ternary azeotropic point can be viewed as the intersection of three "unitary azeotropic" curves. In the triangular diagram (plot) of Figure 6.3, the ternary azeotrope (black star) can be viewed as the intersection of three curves, each one essentially representing $F_i=f_i$ (i.e., a "unitary" azeotrope) for each monomer. In Figure 6.3, the

triangular points correspond to the styrene "unitary azeotropy" line, the squares correspond to the methyl methacrylate azeotropy curve, whereas the small x's are for 4-vinylpyridine.

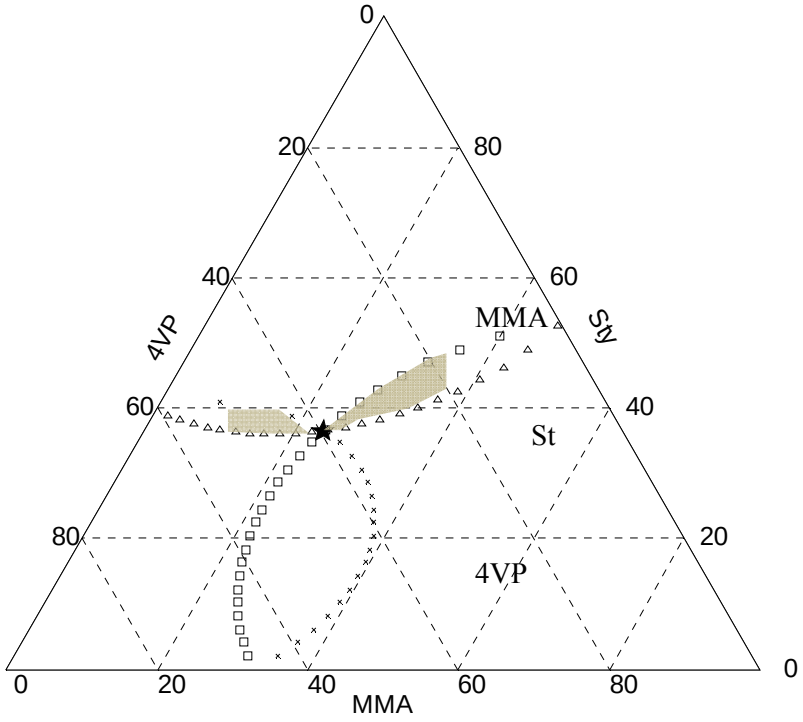

Figure 6-3. Unitary azeotropic curves for the terpolymerization of MMA/Sty/4VP

6.3.2.2 "Binary" azeotropic curves

"Binary" azeotropes are defined as follows:

$$\frac{F_1}{F_2} = \frac{f_1}{f_2} \tag{6.17}$$

In other words, in a terpolymer system of components 1, 2 and 3, a "binary" azeotrope for components 1 and 2 exists when the ratio between the mole fractions of monomers 1 and 2 in the terpolymer is the same as the ratio of the mole fractions of monomers 1 and 2 in the monomer mixture (feed). The equality of ratios is not necessarily satisfied for the other component combinations, i.e.,

$$\frac{F_1}{F_3} \neq \frac{f_1}{f_3} \qquad \frac{F_2}{F_3} \neq \frac{f_2}{f_3} \tag{6.18}$$

"Binary" azeotropes for the other monomer pairs can, of course, be defined in an analogous way.

For example, for the terpolymerization of MMA/Sty/4VP, Figure 6.4 shows a binary azeotropic line containing the compositions for which ratios of the MMA/4VP mole fractions in the feed and the terpolymer are the same.

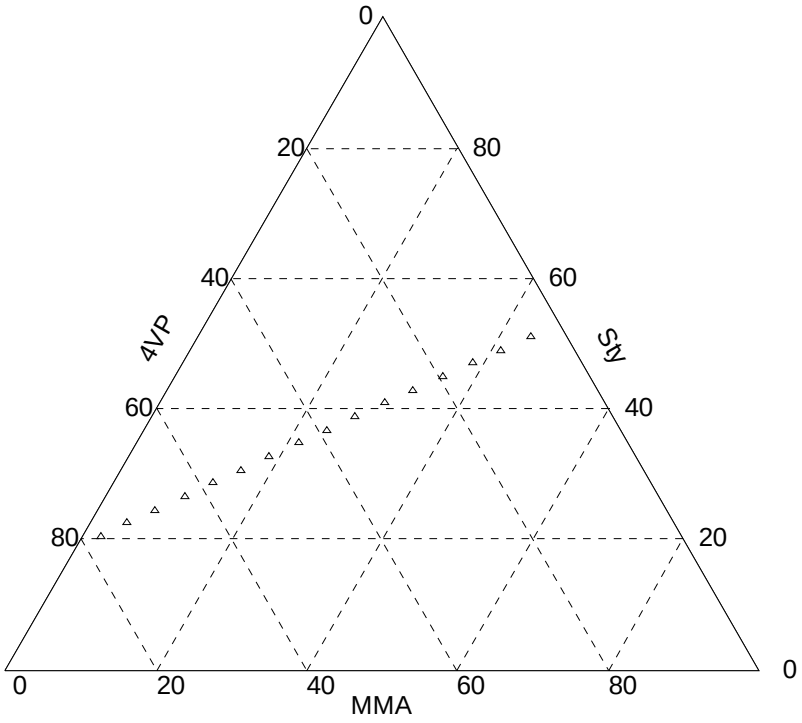

Figure 6-4. (MMA/4VP) binary azeotropic curve for terpolymerization of MMA/Sty/4VP

Again, if a ternary azeotrope exists, then it can be viewed as the intersection of three "binary azeotropic" curves, as illustrated in Figure 6.5 for the same terpolymer system of Figure 6.3 (again the case study has been reconstructed based on information from Rios and Guillot (1987)). In Figure 6.5, three curves are labeled by M_i/M_j representing the "binary

azeotropic" lines for the corresponding monomer pairs (□ is for M_1/M_2, Δ denotes M_1/M_3, and x is for M_2/M_3).

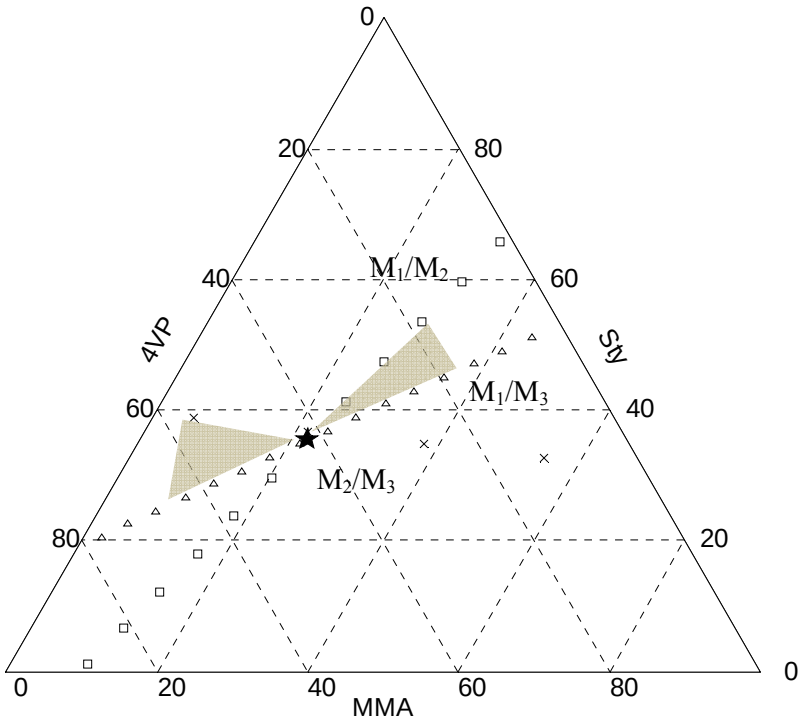

Figure 6-5 Binary azeotropic curves for the terpolymerization of (MMA, M_1)/(styrene, M_2)/(4VP, M_3)

6.3.2.3 Graphical and analytical solutions

As seen earlier, the intersection of "unitary" azeotropic curves and "binary" azeotropic curves gives graphical solutions for obtaining a ternary azeotropic point, if any. In addition to these graphical solutions, other, rather arbitrary, approximate solutions and definitions have also been discussed in the literature.

Based on the definition of the azeotropic point, a feed composition that remains constant throughout the polymerization and results in a homogenous polymer product, it is of interest to determine a composition or even a range of compositions with small compositional drifts, where there is a high probability of obtaining homogenous (or nearly homogenous) polymer product as well. Such a region can be termed as a "pseudo-azeotropic" region. Consider

again Figure 6.1 for the terpolymerization of methyl acrylate/di(tri-n-butyltin) itaconate/acrylonitrile. The area representing low composition drift and hence an almost homogenous terpolymer, given by the shaded oval area on Figure 6.1, is the "pseudo-azeotropic" domain. This region is located around the ternary azeotrope. Rios and Guillot (1987) stated that other domains along the partial azeotropy curves might also correspond to small compositional changes. These domains may be situated along "unitary" or "binary" azeotropy lines, as shown by the shaded (grey) areas inside Figures 6.3 and 6.5. However, they mentioned that this may not always be the case. Once more, determining "pseudo-azeotropic" domains can be rather subjective, and therefore not necessarily always reliable.

One may hence look for a more reliable quantification of a "compositional drift" criterion for terpolymerization or multicomponent polymerization azeotropy cases. Such a simple criterion may be the sum of the absolute values of the differences between $\bar{F}_{i_x}$ and $\bar{F}_{i_0}$. $\bar{F}_i$ represents cumulative composition of monomer (component) i (*i=1, 2,* and 3, for example, for the terpolymer case). The second subscript *x* refers to some chosen conversion level, preferably high (say, at 90%), whereas zero (as second subscript) denotes initial conditions. Thus, the criterion becomes:

$$\Delta = \sum |\bar{F}_{i_x} - \bar{F}_{i_0}| \tag{6.18}$$

Certainly, the point that meets the condition $\Delta = 0$ (or close to zero, given some acceptable pre-specified tolerance level, TOL), is the ternary azeotrope. Compositions that satisfy $\Delta \leq TOL$ are located close to the ternary azeotrope (and can thus be construed as almost "pseudo-azeotropic" domains). TOL, of course, being an acceptable tolerable magnitude of compositional drift, could exclusively depend (in practical terms) on the end-use of the polymerization products. For instance, if a terpolymer is prepared for optical applications, then composition specifications are very narrow (strict), and TOL could be 1-3%. On the other hand, if the terpolymer is some type of rubber, then TOL may be as high as 10-15%. Of course, as one can appreciate from the examples of Figures 6.1 to 6.5, that an increase in TOL will result in the enlargement of the "pseudo-azeotropic" domain.

6.4 Multicomponent Polymerization Systems

As was mentioned earlier in section 2.4, a model proposed by Walling and Briggs (1945) can describe the polymer composition in multicomponent systems with n monomers. This model is given by eq. (6.19):

$$\frac{d[m_i]}{d[m_j]} = (D_{ii} \sum \frac{[m_k]}{r_{ik}})/(D_{jj} \sum \frac{[m_k]}{r_{jk}}) \tag{6.19}$$

$d[m_i]$ is the concentration of monomer *i* in the polymer and $[m_i]$ is the concentration of monomer *i* in the feed. D_{ii} represents the determinant D, given by eq. (6.20), when the *i* row and *i* column have been omitted.

$$D = \begin{vmatrix} ([m_1] - \sum \frac{[m_k]}{r_{1k}}) & \frac{[m_1]}{r_{21}} & \cdots & \frac{[m_1]}{r_{n1}} \\ \frac{[m_2]}{r_{12}} & ([m_2] - \sum \frac{[m_k]}{r_{2k}}) & & \frac{[m_2]}{r_{n2}} \\ \vdots & \vdots & \ddots & \vdots \\ \frac{[m_n]}{r_{1n}} & \frac{[m_n]}{r_{2n}} & & ([m_n] - \sum \frac{[m_k]}{r_{nk}}) \end{vmatrix} \tag{6.20}$$

Based on eq. (6.19) of the Walling and Briggs (1945) approach, Moad et al. (1986) proposed a method for calculation of azeotropic composition in multicomponent systems (up to 10 components). They also claimed that they could define possible combinations of reactivity ratios in ternary systems that would result in an azeotropic composition for the system.

Using eq. (6.21), the multicomponent azeotropy condition, Moad et al. (1986) presented a set of equations, given in eq. (6.22), the solution of which would be the composition of the azeotropic point in the system.

$$\frac{d[m_1]}{[m_1]} dt = \frac{d[m_2]}{[m_2]} dt = \cdots \tag{6.21}$$

$$\begin{aligned}
\left(1-\frac{\Delta}{\Delta_1}\right)[m_1] \quad &+ \quad \frac{[m_2]}{r_{12}} \quad + \quad \frac{[m_3]}{r_{13}} \quad + \cdots = 0 \\
\frac{[m_1]}{r_{21}} \quad &+ \quad \left(1-\frac{\Delta}{\Delta_2}\right)[m_2] \quad + \quad \frac{[m_3]}{r_{23}} \quad + \cdots = 0 \\
\frac{[m_1]}{r_{31}} \quad &+ \quad \frac{[m_2]}{r_{32}} \quad + \quad \left(1-\frac{\Delta}{\Delta_3}\right)[m_3] \quad + \cdots = 0
\end{aligned} \tag{6.22}$$

where $\Delta, \Delta_1, \Delta_2$ ... denote determinants given by:

$$\Delta = \begin{vmatrix} 1 & \frac{1}{r_{21}} & \frac{1}{r_{31}} & \frac{1}{r_{41}} & \cdots \\ \frac{1}{r_{12}} & 1 & \frac{1}{r_{32}} & \frac{1}{r_{42}} & \cdots \\ \frac{1}{r_{13}} & \frac{1}{r_{23}} & 1 & \frac{1}{r_{43}} & \cdots \\ \vdots & \vdots & \vdots & \vdots & \ddots \end{vmatrix} \tag{6.23}$$

$$\Delta_1 = \begin{vmatrix} 1 & \frac{1}{r_{21}} & \frac{1}{r_{31}} & \frac{1}{r_{41}} & \cdots \\ 1 & 1 & \frac{1}{r_{32}} & \frac{1}{r_{42}} & \cdots \\ 1 & \frac{1}{r_{23}} & 1 & \frac{1}{r_{43}} & \cdots \\ \vdots & \vdots & \vdots & \vdots & \ddots \end{vmatrix} \tag{6.24}$$

$$\Delta_2 = \begin{vmatrix} 1 & 1 & \frac{1}{r_{31}} & \frac{1}{r_{41}} & \cdots \\ \frac{1}{r_{12}} & 1 & \frac{1}{r_{32}} & \frac{1}{r_{42}} & \cdots \\ \frac{1}{r_{13}} & 1 & 1 & \frac{1}{r_{43}} & \cdots \\ \vdots & \vdots & \vdots & \vdots & \ddots \end{vmatrix} \tag{6.25}$$

Eq. (6.22) is a set of linear algebraic equations. The solution of this set is an assignment of values to the variables [m_1], [m_2], [m_3], … and [m_n] such that each of the equations is satisfied. Eq. (6.22) is equivalent to a matrix equation of the form Ax=0, where x is the vector of unknown variables [m_i] and A is the matrix of coefficients, given by:

$$A = \begin{matrix} \left(1-\frac{\Delta}{\Delta_1}\right) & \frac{1}{r_{12}} & \frac{1}{r_{13}} & \frac{1}{r_{14}} & \cdots \\ \frac{1}{r_{21}} & \left(1-\frac{\Delta}{\Delta_2}\right) & \frac{1}{r_{23}} & \frac{1}{r_{24}} & \cdots \\ \frac{1}{r_{31}} & \frac{1}{r_{32}} & \left(1-\frac{\Delta}{\Delta_3}\right) & \frac{1}{r_{34}} & \cdots \\ \vdots & \vdots & \vdots & \vdots & \ddots \end{matrix} \tag{6.26}$$

One of the required conditions to obtain a solution for such a system is to have a nonsingular matrix of coefficients, i.e., the determinant of matrix A in eq. (6.26) should be non-zero. However, the determinant of eq. (6.26) is zero; as a result, the solution for this set of equations does not exist or is not unique. Therefore, the azeotropic composition cannot be calculated reliably using this approach.

6.5 Azeotropy in Multicomponent Polymerizations

6.5.1 Generalizing the Approach

Mainly because of experimental difficulties which increase in parallel with the number of monomers within the system, literature sources for multicomponent polymerizations are scarce and their analyses relatively insufficient, in particular with respect to azeotropic studies. Therefore, one of our research objectives is to revisit the discussion on multicomponent azeotropy and develop a computational scheme which will yield reliable

numerical solutions for the azeotropic point. When multicomponent azeotropy occurs, the composition of the polymer is exactly the same as the composition of the monomer mixture (feed). In other words, for a system of n components, we have:

$$F_1 = f_1,\ F_2 = f_2,\ \text{and}\ \ldots\ F_n = f_n \tag{6.27}$$

This condition then is applied on the composition equations of the multicomponent system. Therefore, the composition equations are transformed to a system of nonlinear algebraic equations. The variables of these equations are the mole fractions of the participating monomers (f_i, $i=1,2,\ldots,n$). The solution is a particular realization of the mole fractions of all monomers that simultaneously satisfies all the equations. This solution is the composition of the azeotropic point. Our approach consists of obtaining an azeotropy composition through appropriate root finding numerical techniques. Numerical techniques such as the Newton-Raphson method may be used. This method can reliably find the solution of a set of nonlinear algebraic equations. The basis of our calculations and program development is in the Matlab programming environment.

6.5.2 Azeotropic Composition in Ternary Systems

The instantaneous terpolymerization composition is described by the AG equations, given below:

$$\frac{F_1}{F_3} = \frac{f_1\left(\frac{f_1}{r_{21}r_{31}}+\frac{f_2}{r_{21}r_{32}}+\frac{f_3}{r_{31}r_{23}}\right)\left(f_1+\frac{f_2}{r_{12}}+\frac{f_3}{r_{13}}\right)}{f_3\left(\frac{f_1}{r_{13}r_{21}}+\frac{f_2}{r_{23}r_{12}}+\frac{f_3}{r_{13}r_{23}}\right)\left(f_3+\frac{f_1}{r_{31}}+\frac{f_2}{r_{32}}\right)}$$

$$\frac{F_1}{F_2} = \frac{f_1\left(\frac{f_1}{r_{21}r_{31}}+\frac{f_2}{r_{21}r_{32}}+\frac{f_3}{r_{31}r_{23}}\right)\left(f_1+\frac{f_2}{r_{12}}+\frac{f_3}{r_{13}}\right)}{f_2\left(\frac{f_1}{r_{12}r_{31}}+\frac{f_2}{r_{12}r_{32}}+\frac{f_3}{r_{13}r_{32}}\right)\left(f_2+\frac{f_1}{r_{21}}+\frac{f_3}{r_{23}}\right)} \tag{6.28}$$

Of course, the mole fraction in the unreacted monomer mixture and in the resulting terpolymer should satisfy:

$$\sum_{i=1,2,3} f_i = \sum_{i=1,2,3} F_i = 1 \tag{6.29}$$

The monomer and polymer compositions are the same at the azeotropic point. As mentioned before, the norm in earlier literature, due to the mathematical complexity (at the time) of the terpolymerization model, is that no general solution methodology for calculating the azeotropic point has been reported. In order to clarify this, the goal of this study is to solve eq. (6.28) at the azeotropic conditions as a set of nonlinear algebraic equations via the Newton-Raphson technique. Considerable benchmarking of the Newton-Raphson (NR) technique took place initially. Details of these benchmarking tests with complex equations are given in Appendix C. All the tests showed that the developed code could solve problems with sufficient accuracy within a reasonable number of iterations. Such root-finding methods are typically initialization-dependent, that is, they require an initial guess to begin the search. In order to avoid possible numerical artifacts due to using inappropriate initial guesses and ensure a reliable solution, it was decided to consider simulated feed compositions, containing 40 points, generated by a random number generator function in Matlab, as initial guesses. These 40 points were chosen in a way that they covered a wide range of feasible compositions for the monomer mixture (feed). Subsequently, all these starting points (initial guesses) were used in the NR technique until all solutions were found and, in fact, found to converge to the same final answer, thus ensuring that the answer (and hence azeotropic composition) was unique.

Eventually, we arrived at a general numerical scheme to solve the terpolymerization model using the NR routine to obtain the azeotropic composition. Moreover, unitary and binary azeotropic curves were established by using the Matlab computer program. Details are discussed in the case studies of section 6.6. The first case study is the system of acrylonitrile/ethyl vinyl ether/methyl methacrylate which has been used to troubleshoot and validate our azeotropic composition calculation approach. The two subsequent case studies

were used to check the validity of reported ternary azeotropic compositions and also to demonstrate the importance of using reliable values of reactivity ratios, emphasizing once more the fact that poorly estimated reactivity ratios seem to be the culprit again in the confusion around ternary (or multicomponent) azeotropic points. The next ternary system was used to check the validity of partial azeotropy curves while illustrating the impact of modern analytical and data handling techniques. Finally, a summary table including several azeotropic ternary systems is provided presenting the calculated azeotropic composition for the specific systems and indicating whether this is in agreement with the corresponding literature or not.

6.6 Case Studies: Azeotropic Ternary Systems

6.6.1 Case 1: Acrylonitrile/Ethyl vinyl ether/Methyl methacrylate

For the ternary system of acrylonitrile (AN, M_1)/ethyl vinyl ether (EVE, M_2)/methyl methacrylate (MMA, M_3), the values of the reactivity ratios, given below by eq. (6.30), are reported by Wittmer et al. (1967) and used in the Matlab program in order to calculate the azeotropic composition for this system. As mentioned earlier, Wittmer et al. (1967) used the approach by Tarasov et al. (1960) to calculate the azeotropic composition. Braun et al. (1975) also arrived at the same azeotropic composition. Our results for the azeotropic point along with the reported values in the literature, obtained by Wittmer et al. (1967) and Braun et al. (1975), are presented in Table 6.2. In principle, if the calculations are conducted correctly, all techniques should arrive at the same numerical values for the azeotropic composition. Possible fluctuations within some reasonable tolerance level are to be expected due to truncation error propagation. Hence, in this case study, the aim of the analysis was to confirm that our calculations were on target, since this ternary system had been studied extensively before.

$$r_{12} = 0.7 \qquad r_{21} = 0.03$$
$$r_{13} = 1.5 \qquad r_{31} = 0.84$$
$$r_{23} = 0.0001 \qquad r_{32} = 3.3 \tag{6.30}$$

Table 6-2. Azeotropic composition for the terpolymerization of AN(M_1)/EVE(M_2)/MMA(M_3)

Reference	M_1	M_2	M_3
Azeotropic composition, Wittmer et al. (1967)	0.540	0.090	0.320
Azeotropic composition, Braun et al. (1975)	0.600	0.100	0.350
Azeotropic composition, current work	0.590	0.087	0.321

Figure 6.6 shows the azeotropic compositions within the triangular plot. The three points are very similar in location, confirming good agreement between the values of azeotropic compositions obtained from different groups.

As further confirmation, and in order to verify that the suggested azeotropes were correct, we checked the compositional homogeneity (or equivalently, the composition drift) of the terpolymer using as feed composition the composition of the azeotrope and allowing the polymerization to proceed to almost complete conversion. At the azeotropic condition, the compositional drift is supposed to be zero or minimal. A diagnostic check was performed in order to ensure that the reaction is indeed at the azeotropic point. In order to determine the variation of the polymer composition when conversion is increasing, the AG equations were evaluated for instantaneous composition and integrated to yield the cumulative terpolymer composition versus conversion (using a Rung-Kutta-Fehlberg routine (RKF45) in Matlab). For the azeotropic compositions reported in Table 6.2, the cumulative terpolymer composition was determined at these initial conditions as well as at high conversion (90%). The difference between the initial composition and the corresponding composition at high conversion is an indication of the compositional drift. If the compositional drift is significant, it can be concluded that the azeotropic condition cannot be maintained during the course of polymerization and thus the suggested composition is not a true ternary azeotrope. In order to

quantify the compositional drift, it was decided to use the measure of eq. (6.18), expanded below as eq. (6.31):

$$\left|\left(\bar{F}_{1_x} - \bar{F}_{1_0}\right)\right| + \left|\left(\bar{F}_{2_x} - \bar{F}_{2_0}\right)\right| + \left|\left(\bar{F}_{3_x} - \bar{F}_{3_0}\right)\right| \tag{6.31}$$

i.e., the sum of absolute differences between the cumulative composition of monomer *i* in the terpolymer at a selected high conversion *x* ($\bar{F}_{i_x}$) and the corresponding one at initial conditions ($\bar{F}_{i_0}$). Figure 6.7 shows the variation of the cumulative terpolymer composition at the azeotropic point as a function of conversion. It can easily be seen that the terpolymer composition remains constant over the entire conversion range. Also, the measure of the compositional drift as per eq. (6.31) was found to be 1.16%, which is acceptably negligible, based on all sources of error in obtaining the azeotropic composition (i.e., round-off numerical error propagation).

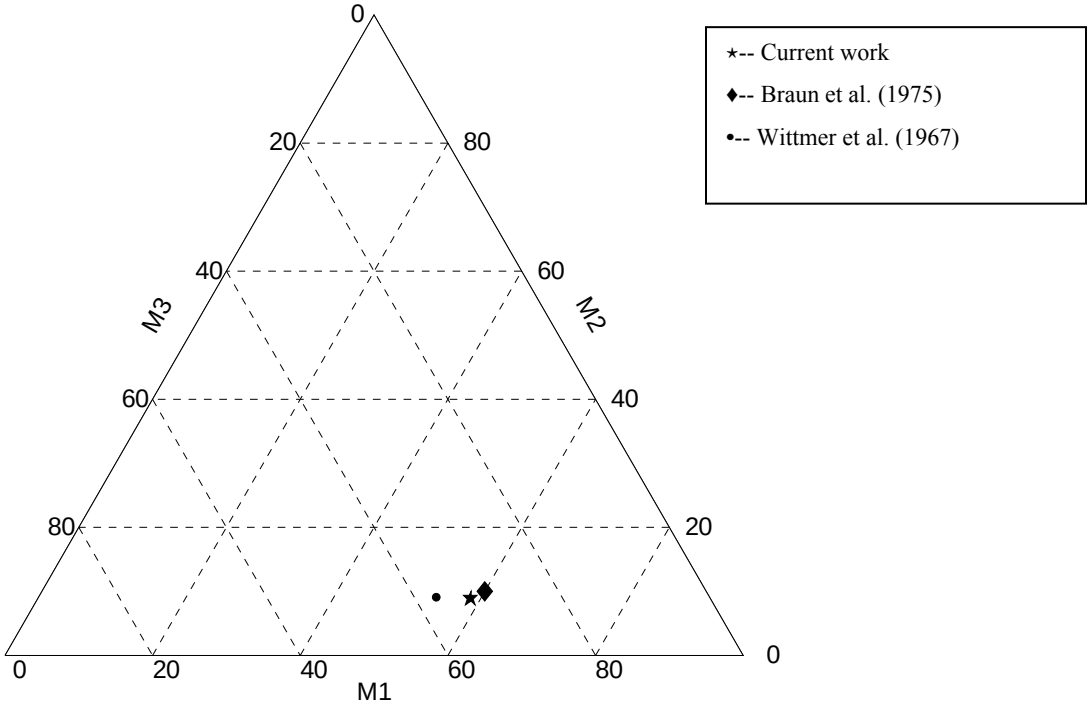

Figure 6-6. Azeotropic composition for the terpolymerization system of AN(M_1)/EVE(M_2)/MMA(M_3)

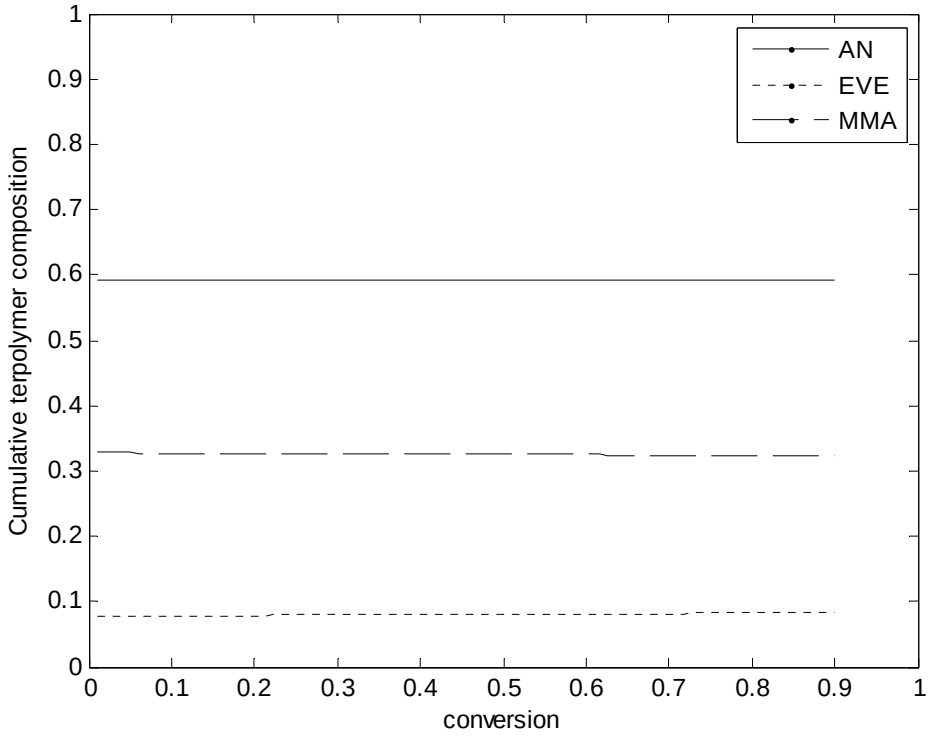

Figure 6-7. Compositional drift of AN(M_1)/EVE(M_2)/MMA(M_3) terpolymerization at the azeotropic composition

6.6.2 Case 2: Acrylonitrile/Styrene/2,3-Dibromopropylacrylate

The terpolymerization of acrylonitrile (AN, M_1) /styrene (Sty, M_2)/2,3-dibromopropylacrylate (DBPA, M_3) was investigated by Saric et al. (1983). Polymerizations were carried out at 60℃ in emulsion and in dimethyl formamide (DMF) solution. The authors mentioned that the reported experimental terpolymerization data were in agreement with calculated terpolymer compositions based on the AG equations and values of reactivity ratios from the corresponding binary copolymer pairs. These values are given in Table 6.3 for both emulsion and DMF solution.

Table 6-3. Monomer reactivity ratios for the terpolymerization of AN(M_1)/Sty(M_2)/DBPA(M_3) in emulsion and DMF solution

	r_{12}	r_{21}	r_{13}	r_{31}	r_{23}	r_{32}
Emulsion, Saric et al.	0.1	0.44	0.9	0.86	0.43	0.14
Emulsion, current work	0.077	0.419	0.390	0.460	0.411	0.191
DMF, Saric et al. (1983)	0.16	0.30	0.87	0.75	0.41	0.22
DMF, current work	0.188	0.234	0.983	2.008	0.387	0.16

Saric et al. (1983) used the concept of partial azeotropy to obtain the composition of the ternary azeotrope. As previously mentioned, partial azeotropes, unitary and binary, can be presented in forms of curves within the triangular plot and the intersection of these curves (if any) gives the composition of the ternary azeotrope. For the emulsion system, the reported azeotrope composition by Saric et al. (1983) is given in Table 6.4. For the DMF solution no azeotrope was reported. Our numerical approach, on the other hand, could not find any azeotrope for either of these systems using the reported reactivity ratios by Saric et al. (1983).

In the next step, reactivity ratios were re-estimated using the EVM parameter estimation technique described in Chapter 5, section 5.4.2, using directly the reported terpolymer composition data. The results for emulsion and DMF solution are shown in the second and fourth rows of Table 6.3, respectively. For the emulsion system, these re-estimated values were subsequently used to calculate the azeotropic composition and the results are showing in Table 6.4. For the DMF solution, again no azeotrope was detected.

Table 6-4. Reactivity ratios and azeotropic composition for the terpolymerization of AN(M_1)/Sty(M_2)/DBPA(M_3) in emulsion.

	Saric et al.	Re-estimated by current work		M_1	M_2	M_3
r_{12}	0.1	0.077	Azeotropic composition by Saric et al. (1983) using original reactivity ratio values	0.27	0.61	0.12
r_{21}	0.44	0.419				
r_{13}	0.9	0.390	Azeotropic composition, current work, using original reactivity ratio values	---	---	---
r_{31}	0.86	0.460				
r_{23}	0.43	0.411	Azeotropic composition, current work, using re-estimated reactivity ratio values	0.232	0.575	0.193
r_{32}	0.14	0.191				

Several remarks can now be made about the analysis of this terpolymer system. Firstly, there is agreement between Saric et al. (1983) and our technique with respect to solution terpolymerization in DMF; no azeotrope is detected. Secondly, with respect to emulsion terpolymerization, the azeotropic points between Saric et al. (1983) and our approach seem relatively close (as one can see from Table 6.4 and also from the triangular plot of Figure 6.8), but only after using the re-estimated values for the three pairs of reactivity ratios. Use of the Saric et al. (1983) reactivity ratio values did not yield a solution for the azeotropic point. This shows quite a sensitivity of the existence (location) of the azeotropic point solution to values (and fluctuations thereof) of the reactivity ratios, which will be revisited below for further clarification (see subsection 6.6.2.1). Certainly, graphical solutions or more time-consuming approximate solutions based on partial azeotropy curves are not as direct as general numerical techniques. However, the main culprit here appears to be again the sensitivity of the solution to reactivity ratio values. If the reactivity ratios are only approximate, then a certain set of values may lead to results different from another set, as illustrated above with this terpolymer system. Initially, no azeotropic point was calculated based on the reactivity ratio values used by Saric et al. (1983). A point was subsequently located, with re-estimated values based directly on terpolymer composition data (not on binary reactivity ratios from copolymer data). This is an important observation. As far as the location of the ternary (and even more, of a higher multicomponent) azeotropic point is concerned, the uncertainty in reactivity ratio estimates (and its propagation through model equations) becomes significant. Use of binary reactivity ratios seems to be an oversimplification, not only with respect to the values themselves but also with respect to not considering measures (and hence effects) of their uncertainty.

Next, in a way similar to the first case study of section 6.6.1, a diagnostic check was run for both azeotropic compositions reported in Table 6.4. The cumulative terpolymer composition results versus conversion are shown in Figures 6.9a for the azeotropic composition for Saric et al (1983), whereas Figure 6.9b shows the picture with our calculated azeotropic point. The magnitude of compositional drift was also calculated based on eq. (6.31). This magnitude was 2.2% for the Saric et al. (1983) azeotrope versus 0.0% for our

calculated azeotrope. Granted, the difference might be considered small (or negligible), but still points to the benefits of (a) using a direct numerical approach, and (b) employing correct reactivity ratio values. A final remark is related to section 6.3.2. A region containing low compositional drift points can be considered as a "pseudo-azeotropic" region. So, since the compositional drift for both compositions of Figure 6.8 was found to be minimal, it can be suggested that these compositions are both contained within a "pseudo-azeotropic" region.

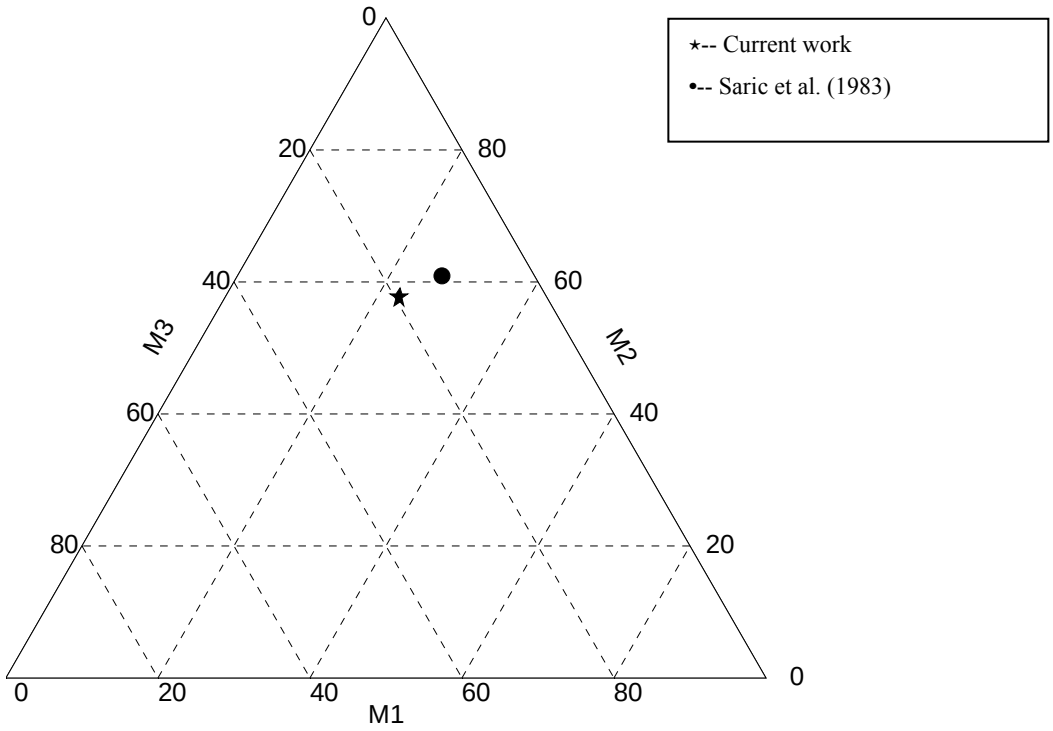

Figure 6-8 Azeotropic composition for the terpolymerization of AN(M_1)/Sty(M_2)/DBPA(M_3) in emulsion

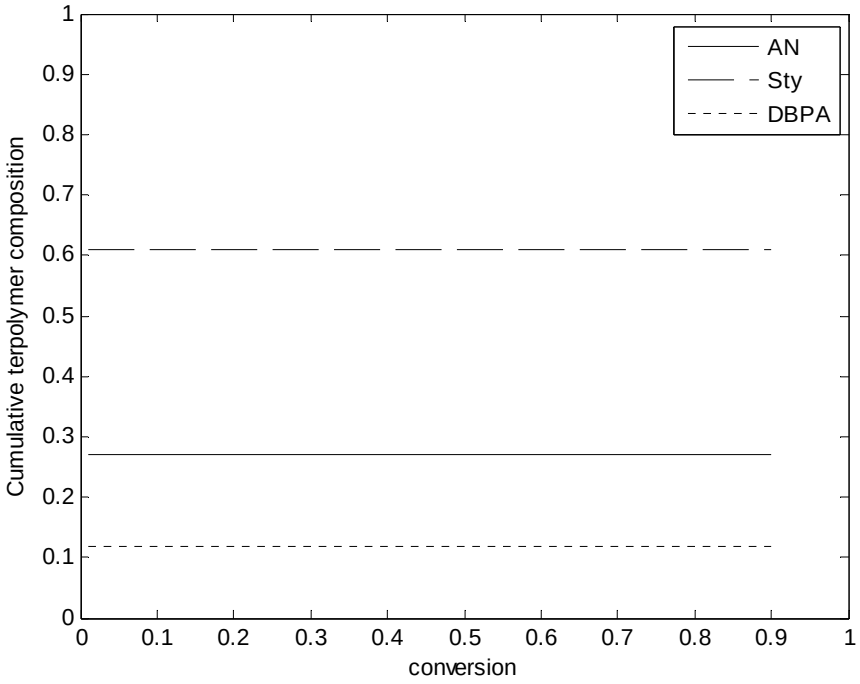

Figure 6-9 a. Cumulative terpolymer composition versus conversion in emulsion for AN(M_1)/Sty(M_2)/DBPA(M_3) (Saric et al. (1983) azeotrope)

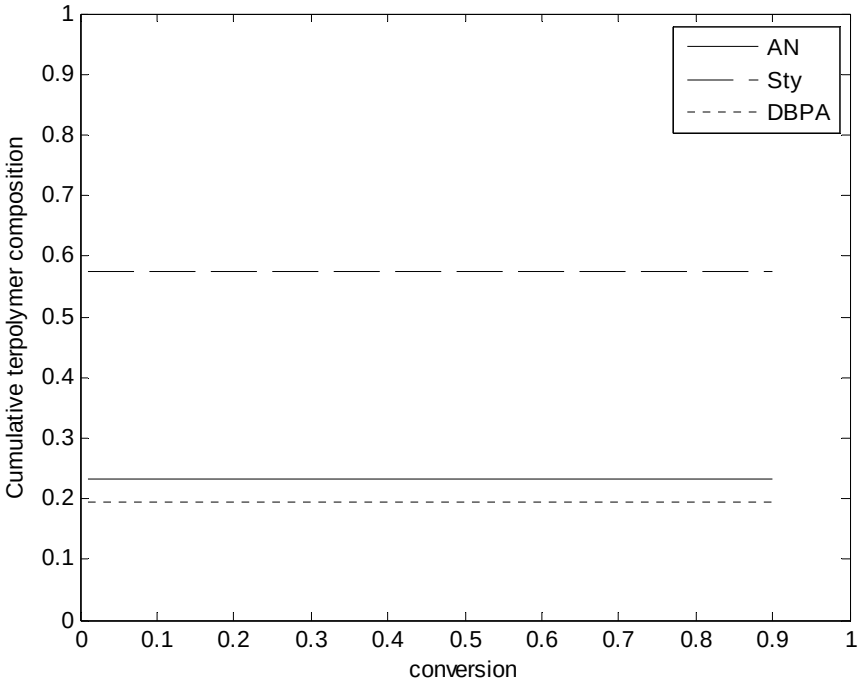

Figure 6-9 b. Cumulative terpolymer composition versus conversion in emulsion for AN(M_1)/Sty(M_2)/DBPA(M_3) (azeotrope from current work)

6.6.2.1 Sensitivity of azeotropic composition to reactivity ratio values

In order to find a ternary azeotrope, six reliable reactivity ratios are needed, as it has been observed that changes in the reactivity ratio values can influence the position of the ternary azeotrope considerably. In a system where the existence of a ternary azeotrope is confirmed, one can try different sets of reactivity ratios to calculate the azeotropic composition. While the intention is to find feed composition ranges which yield homogeneous terpolymer, the question is how to obtain viable combinations of reactivity ratios for a specific terpolymerization system. As mentioned earlier in the case study, the reactivity ratios of the system were re-estimated by applying the EVM parameter estimation technique directly on the terpolymerization experimental data reported by Saric et al. (1983). Another highly beneficial output of this analysis is the joint confidence region for these reactivity ratio estimates. These confidence regions define reliable choices of values for these reactivity ratios that can be used further for sensitivity studies. Hence, in order to have plausible sets of reactivity ratio values, several points inside these joint confidence regions were selected.

Figure 6.10 shows these confidence regions for the three pairs of reactivity ratios for the ternary system in question. It must be noted that the open circles in the center of each joint confidence region are the reactivity ratio point estimates for this system. These values were used originally to calculate the ternary azeotrope. The stars are selected values of reactivity ratios within the confidence regions. For each set, the corresponding azeotropic composition can be calculated. Figure 6.11 presents the corresponding viable azeotropic region. As such, it also represents the sensitivity of the azeotropic point to possible estimated reactivity ratio values. The calculated ternary azeotrope is marked with a star in Figure 6.11, whereas the azeotropic composition reported by Saric et al. (1983) is marked with a square. Open circles correspond to a "region" of possible azeotropic points (essentially, the "pseudo-azeotropic" domain), based on the possible combinations of reactivity ratios of Figure 6.10 (a calculation that is possible only of one has the related confidence regions from reactivity ratio estimation). One can clearly see that the azeotropic domain does contain the star (our azeotropic point), whereas the square (the Saric et al. (1983) azeotropic point) is off the

domain. Once more, reactivity ratios based on terpolymer data and use of direct numerical techniques to calculate azeotropic points yield results that are much more reliable than approximate binary reactivity ratios and circuitous partial azeotropy curves.

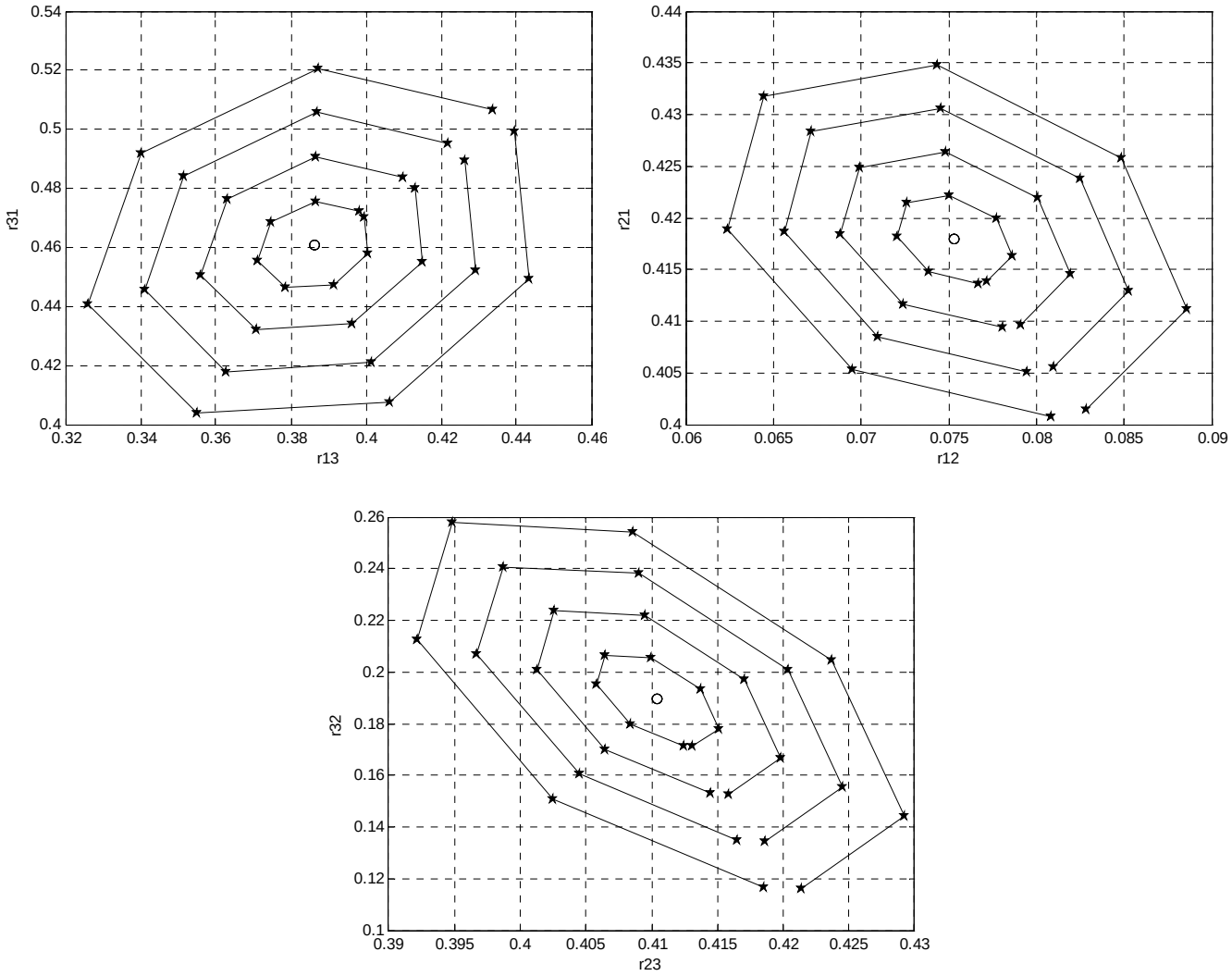

Figure 6-10. The three joint confidence regions for emulsion terpolymerization of AN(M_1)/Sty(M_2)/DBPA(M_3)

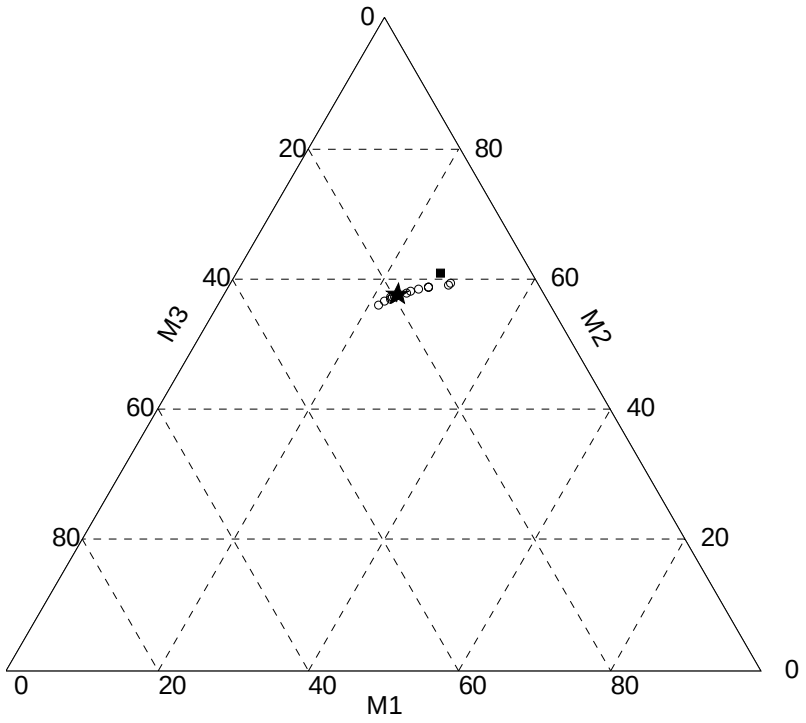

Figure 6-11. Pseudo-azeotropic domain for the emulsion terpolymerization of AN(M_1)/Sty(M_2)/DBPA(M_3)

6.6.3 Case 3: N,N-dimethylaminoethyl methacrylate/Dodecyl methacrylate/Methyl methacrylate

Soljic et al. (2010) analyzed the N,N-dimethylaminoethyl methacrylate (DMAEMA, M_1)/dodecyl methacrylate (DMA, M_2)/methyl methacrylate (MMA, M_3) terpolymerization system. Reactions were carried out isothermally at 70℃, in toluene solution. The authors stated that experimental terpolymer compositions agreed well with calculated terpolymer compositions based on the AG equations. Similar to case study 2, they calculated the ternary azeotrope using partial azeotropy curves. According to their results, the existence of the azeotropic point was established and experimentally verified. In our analysis, we first calculated the azeotropic composition using the reported reactivity ratios by Soljic et al.

(2010); their azeotropic point and ours are shown in the first two rows of Table 6.5. It can be seen that these values are in very good agreement.

Table 6-5. Reactivity ratios and azeotropic composition for the terpolymerization of DMAEMA(M_1)/DMA(M_2)/MMA(M_3)

	Soljic et al.	Re-estimated by current		M_1	M_2	M_3
r_{12}	0.83	0.8014	Azeotropic composition, Soljic et al. (2010), using original reactivity ratio values	0.56	0.41	0.03
r_{21}	0.79	0.7510				
r_{13}	0.79	0.8137	Azeotropic composition, current work, using original reactivity ratio values	0.5656	0.4078	0.0266
r_{31}	0.74	0.8002				
r_{23}	1.11	1.0856	Azeotropic composition, current work, using re-estimated reactivity ratio values	0.5817	0.2814	0.1369
r_{32}	1.18	1.1987				

Once more, it must be noted that obtaining the azeotropic point numerically is a simpler and more direct approach. In the next analysis step, we re-estimated (via EVM) the reactivity ratios based on the Soljic et al. (2010) terpolymer composition data. Then the azeotropic composition was recalculated using the new set of reactivity ratios. The new set of the reactivity ratios and the corresponding azeotropic composition are also shown in Table 6.5. Figure 6.12 shows the calculated azeotropic compositions by Soljic et al. (2010) and our technique. As it can clearly be seen in this figure, there is agreement between Soljic et al. (2010) and our approach when binary reactivity ratios are utilized in order to obtain the azeotropic composition. However, when using the re-estimated reactivity ratios (which are estimated based directly on terpolymerization experimental data), the composition of the azeotropic point changes considerably. So, similar to case study 2, the sensitivity of the azeotropic point to the values of the reactivity ratios can be considerable, and thus it must be noted again that uncertainty in the reactivity ratios from binary copolymer pairs has a significant effect on the location of the azeotropic composition.

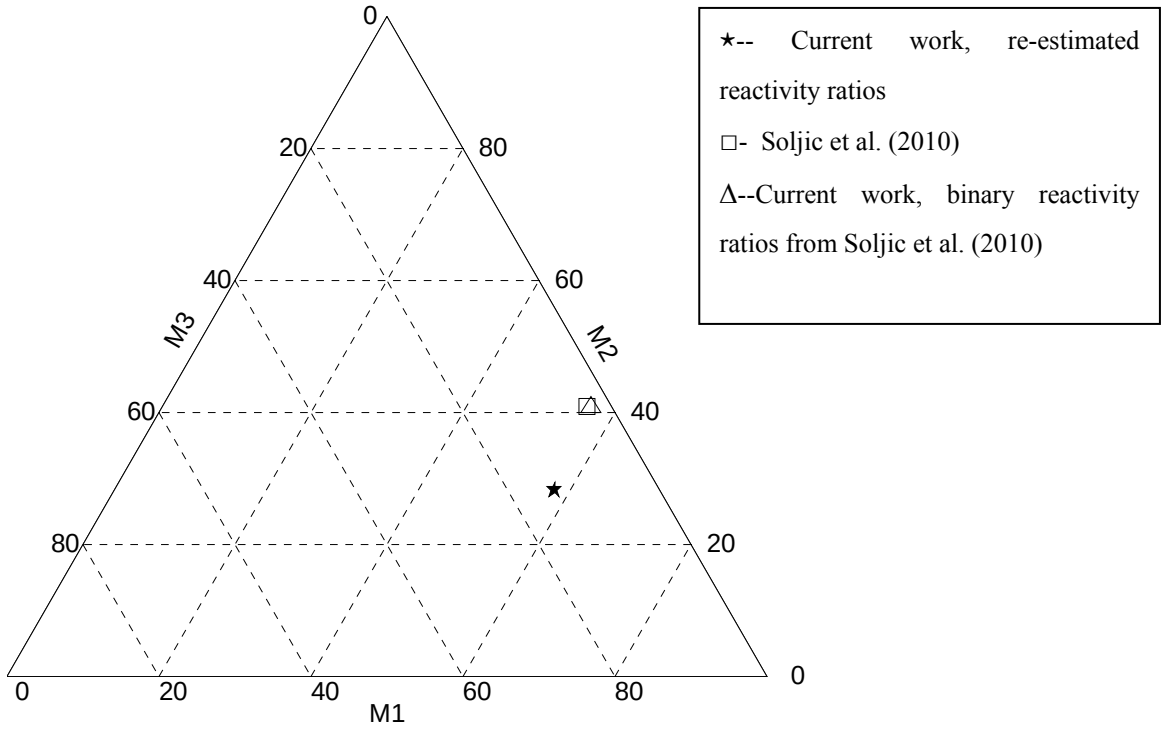

Figure 6-12. Azeotropic composition for the terpolymerization of DMAEMA(M_1)/ DMA(M_2)/MMA(M_3)

Another distinguishable difference between the azeotropic points obtained from binary reactivity ratios and ternary reactivity ratios is the feasibility of measuring these compositions in real experiments. The azeotropic compositions based on binary reactivity ratios, in the first two rows of Table 6.5, have values of 0.03 and 0.026 for the mole fraction of (MMA)M_3. Producing such a mole fraction in a real experiment can be very difficult, not to mention that based on actual amounts of the materials used for such an experimental run, this small amount of (MMA)M_3 can even be translated into experimental error. On the other hand, the azeotropic composition based on ternary reactivity ratios, in the third row of Table 6.5, contains sensible portions of each monomer.

Similar to the analysis for the previous case studies, the magnitude of the compositional drift for the azeotropic compositions shown in Table 6.5 was calculated based on eq. (6.31). The compositional drift was 0.7% for Soljic et al. (2010) versus 0.0% for our calculated

azeotropes with both binary and ternary reactivity ratios. The difference between Soljic et al. (2010) and our calculated azeotropic composition can be attributed to employing different reactivity ratio values in our calculations. This is to be expected due to the sensitivity of the composition of the azeotropic point to the values of the reactivity ratios that are employed in the corresponding calculations. Since both calculated azeotropic compositions by our approach show no compositional drift, it can be suggested that these compositions are both contained within a "pseudo-azeotropic" region (recalling from section 6.3.2.3 that a "pseudo-azeotropic" region is a domain containing low compositional drift points).

For the azeotropic composition obtained by the re-estimated reactivity ratios, the cumulative terpolymer composition over the full conversion is illustrated in Figure 6.13. It is evident in this figure that the azeotropic condition is satisfied for this composition.

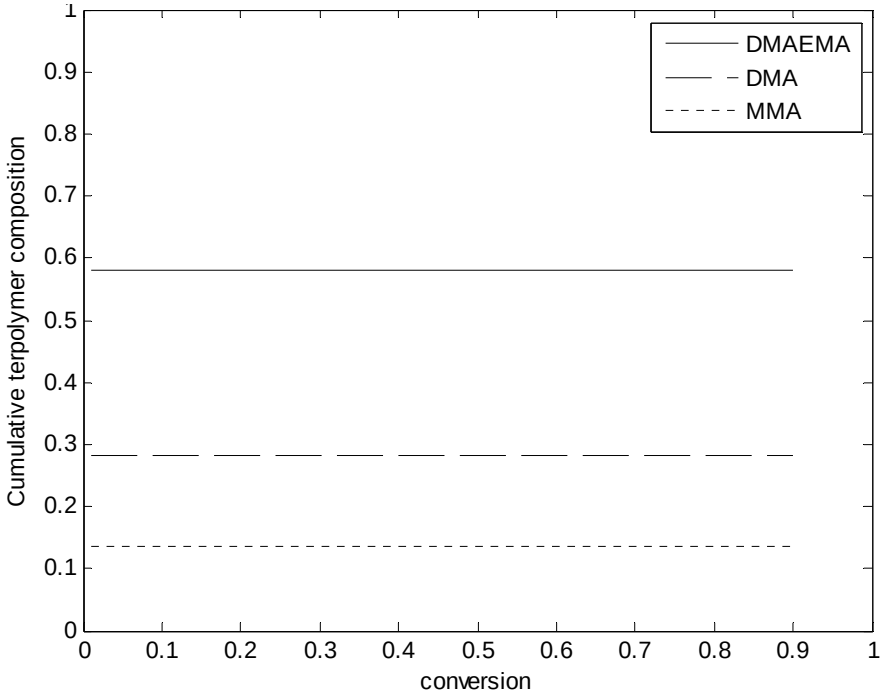

Figure 6-13. Compositional drift in terpolymerization of DMAEMA(M_1)/ DMA(M_2)/MMA(M_3)

6.6.3.1 Sensitivity of azeotropic composition vs. reactivity ratio values

In a way similar to the analysis of subsection 6.6.2.1, and using the re-estimated reactivity ratio values based directly on the terpolymerization experimental data, Figure 6.14 illustrates three joint confidence regions for the three pairs of reactivity ratios. Open circles are the point estimates of the reactivity ratios used to calculate the azeotropic composition. Stars on and within the joint confidence regions represent selected sets of reactivity ratios. Subsequently, the corresponding azeotropic compositions are calculated for each set and the results are shown in Figure 6.15. In this figure, black dots correspond to a region of possible azeotropic points. Basically, these points can define the "pseudo-azeotropic" domain. It can be seen that these pseudo-azeotropic points are aligned with the triangle's side which denotes the mole fraction of M_2(DMA). Also, it is evident from this figure that the "pseudo-azeotropic" domain does contain the values based on binary reactivity ratios (see Δ and □ on Figure 6.15) but not the calculated azeotropic point (*) based on the re-estimated reactivity ratios. The behavior of Figure 6.15 is notably different from that of Figure 6.11 (case study 2), confirming again that one may easily be led to numerical artifacts, with respect to a single azeotropic point, due to the sensitivity of the location of the true azeotropic point to the employed reactivity ratio values.

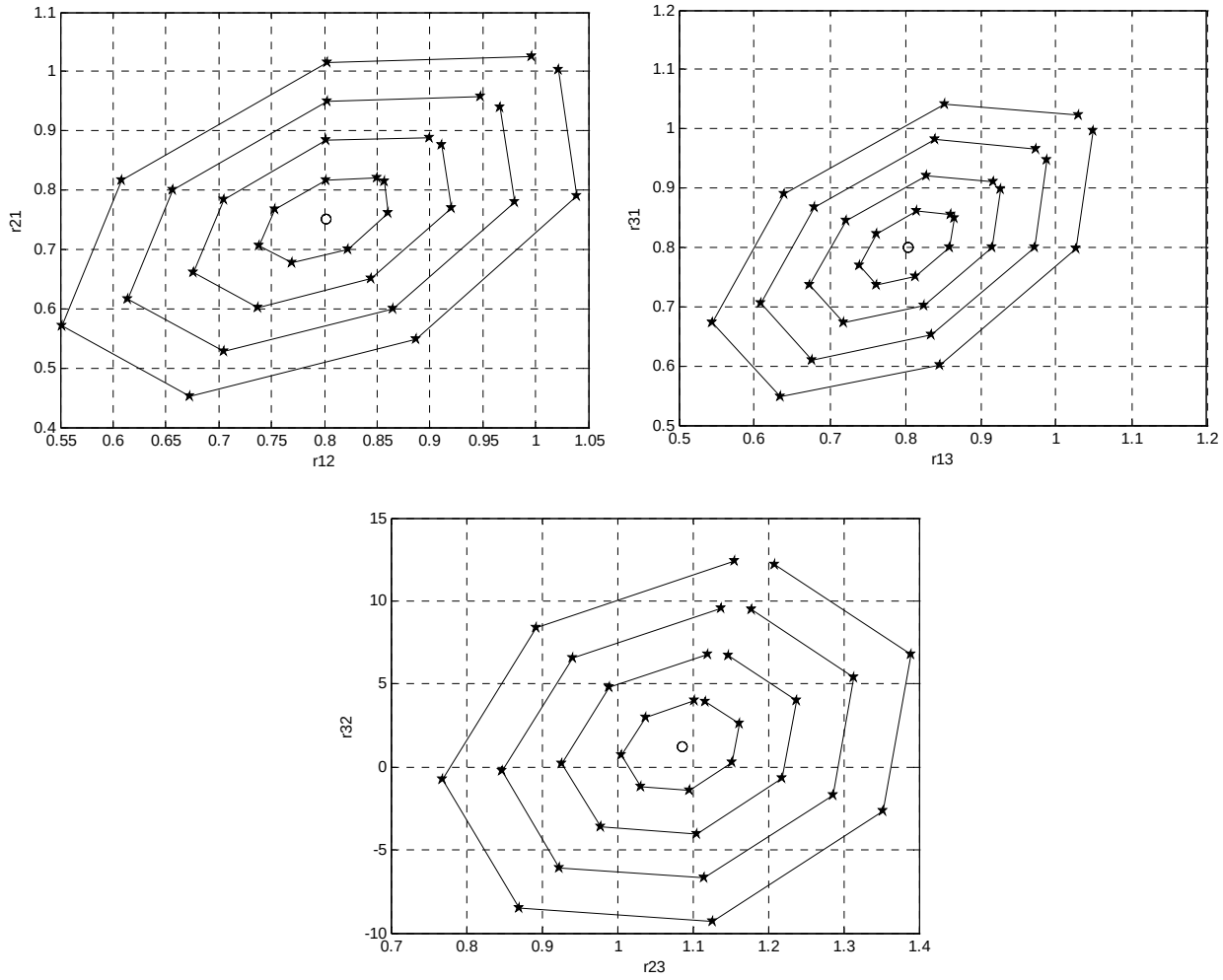

Figure 6-14. The three joint confidence regions for terpolymerization of DMAEMA(M_1)/ DMA(M_2)/MMA(M_3)

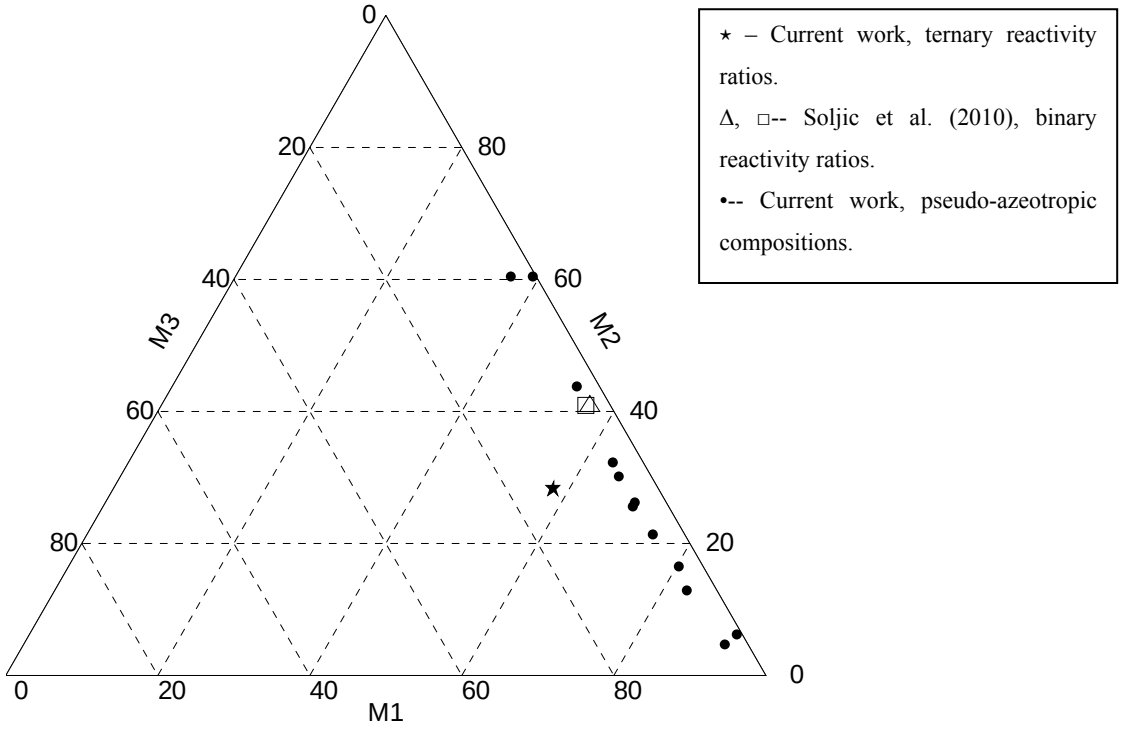

Figure 6-15. "Pseudo-azeotropic" domain in terpolymerization of DMAEMA(M_1)/DMA(M_2)/MMA(M_3)

The results obtained in case study 3 with respect to the pseudo-azeotropic points are not what has been observed in previous case studies. One important point to consider is mentioned by Soljic et al. (2010). In this methacrylate system, all the determined reactivity ratios showed that the addition tendencies of the growing radicals towards their monomers are approximately equal. As a result, the ternary azeotropic point is a natural consequence of the similar reactivity of the investigated methacrylate monomers. For this ternary system, the reactivity ratios, cited in Table 6.5, are relatively close to one. Recalling from basic multicomponent polymerization definitions, when monomer reactivity ratios are close (or equal) to unity, the composition of the feed remains constant throughout the reaction. Such a polymerization system is called an ideal system and for such a system the compositional drift is very small (zero, ideally). Hence, for the almost ideal terpolymer system of case study 3, it must be noted that, based on the fact that almost any feed composition will yield very low (or almost zero) compositional drift, then the entire triangular plot represents a pseudo-

azeotropic domain. In order to investigate the special nature of this terpolymerization system, terpolymer compositions were calculated (using the AG equations and re-estimated ternary reactivity ratios) for all experimental feed compositions reported in Soljict et al. (2010). Figure 6.16 shows these corresponding composition pairs (feed and terpolymer). Open circles are the feed compositions and inverted triangles are the corresponding terpolymer compositions. Also, the azeotropic compositions, presented in Figure 6.15, are shown in this figure. It can clearly be seen from Figure 6.16 that the magnitude of the compositional drifts are either very small or completely negligible, thus confirming that the entire triangle represents a pseudo-azeotropic domain.

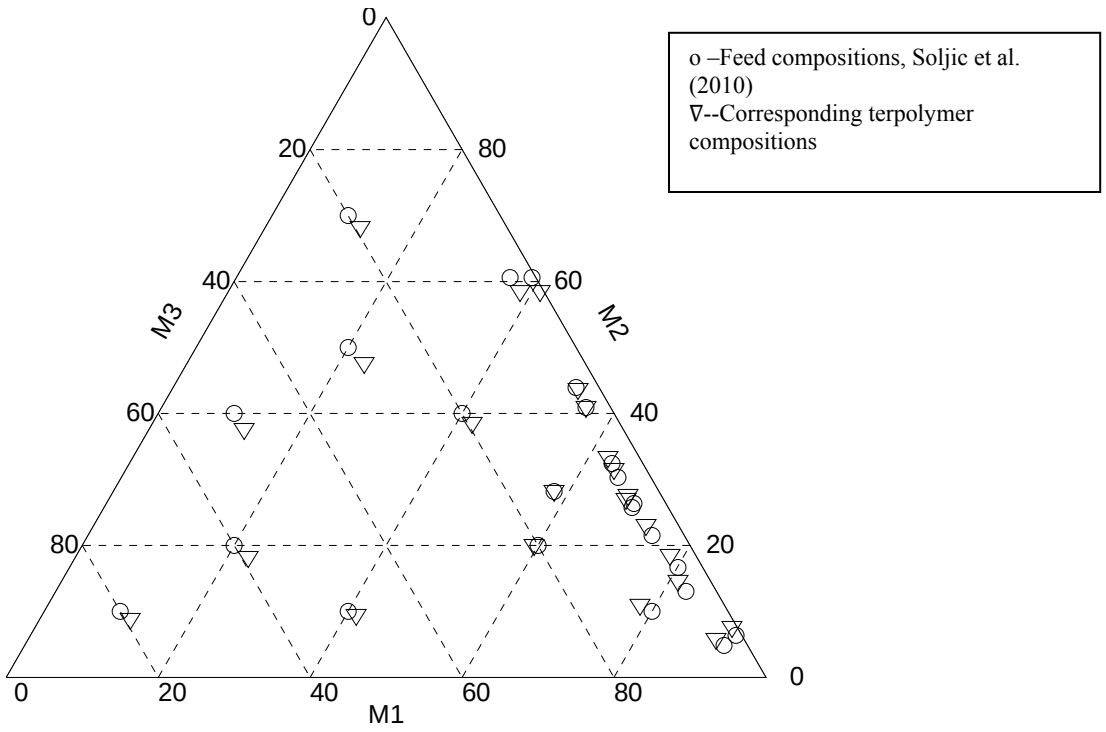

Figure 6-16. Feed and terpolymer compositions in the terpolymerization of DMAEMA(M_1)/ DMA(M_2)/MMA(M_3)

6.6.4 Case 4: N-antipyryl acrylamide/Acrylonitrile with Methyl acrylate, Ethyl acrylate, Buthyl acrylate, and styrene

Four terpolymerization systems of N-antipyryl acrylamide (NAA, M_1)/acrylonitrile (AN, M_2) with different alkylacrylates- methyl acrylate (MA), ethyl acrylate (EA), buthyl acrylate (BA)- or styrene (Sty) in solution at 65℃ were studied by El-Hamouly and Azab (1994). The reported values of reactivity ratios were obtained from corresponding binary systems from the literature. These reactivity ratios for all four ternary systems are shown in Tables 6.6- 6.9. Also, El-Hamouly and Azab (1994) stated that the experimental data agreed well with calculations based on the AG equations. Their primary intention was to determine unitary, binary, and ternary azeotropes of the terpolymerizations in question. As mentioned earlier, unitary and binary azeotropic curves are categorized as "partial azeotropy" for a system. The intersection of unitary or binary curves can give a graphical solution for the ternary azeotropic point. The reported ternary azeotropic compositions of these ternary systems are shown in Tables 6.6-6.9 as well. Our goal is (1) to calculate the azeotropic composition using our numerical technique in order to compare the results with the reported azeotropic point in the reference paper, and (2) to confirm the existence of the partial azeotropy curves for each case and check whether their intersection results in the same calculated ternary azeotropic point or not.

For the first part, the reported reactivity ratios in the reference paper were used. Our calculated azeotropic compositions are also shown in Tables 6.6-6.9. Figures 6.17 a-d show the reported azeotropic compositions and our calculated ones for the four ternary systems shown in Tables 6.6-6.9. The star and the circle in each triangular plot represent the azeotropic points from the current work and from El-Hamouly and Azab (1994), respectively. According to these results, it can be seen that using our approach has resulted in slightly different azeotropic points from what was calculated by El-Hamouly and Azab (1994). For the NAA/MA/AN and NAA/BA/AN terpolymerizations, the differences are more pronounced than in the other two systems.

Table 6-6. Reactivity ratios and azeotropic composition for NAA (M_1)/MA (M_2)/AN (M_3)

Reactivity ratios			M_1	M_2	M_3
r_{12}	0.64	Azeotropic composition, El-Hamouly and Azab (1994)	0.31	0.10	0.59
r_{21}	0.18				
r_{13}	0.80				
r_{31}	1.10	Azeotropic composition, current work	0.438	0.108	0.458
r_{23}	0.67				
r_{32}	1.26				

Table 6-7. Reactivity ratios and azeotropic composition for NAA (M_1)/EA (M_2)/AN (M_3)

Reactivity ratios			M_1	M_2	M_3
r_{12}	0.70	Azeotropic composition, El-Hamouly and Azab (1994)	0.37	0.09	0.54
r_{21}	0.18				
r_{13}	0.80				
r_{31}	1.10	Azeotropic composition, current work	0.395	0.087	0.518
r_{23}	0.93				
r_{32}	1.12				

Table 6-8. Reactivity ratios and azeotropic composition for NAA (M_1)/BA (M_2)/AN (M_3)

Reactivity ratios			M_1	M_2	M_3
r_{12}	0.57	Azeotropic composition, El-Hamouly and Azab (1994)	0.23	0.10	0.67
r_{21}	0.32				
r_{13}	0.80				
r_{31}	1.10	Azeotropic composition, current work	0.281	0.097	0.629
r_{23}	0.89				
r_{32}	1.20				

Table 6-9. Reactivity ratios and azeotropic composition for NAA (M1)/Sty (M2)/AN (M3)

Reactivity ratios			M_1	M_2	M_3
r_{12}	0.71	Azeotropic composition, El-Hamouly and Azab (1994).	0.665	0.305	0.03
r_{21}	0.25				
r_{13}	0.80				
r_{31}	1.10	Azeotropic composition, current work	0.685	0.300	0.015
r_{23}	0.41				
r_{32}	0.04				

In relation to partial azeotropy, the presentation of the intersection of binary azeotropic curves was chosen in this case study as the most indicative. As mentioned earlier, the calculated azeotropic point by our numerical technique can be viewed as the intersections of three binary azeotropic curves. For the four terpolymerizations in Tables 6.6-6.9, binary azeotropic curves are presented in Figures 6.17 a-d for the M_1/M_2, M_1/M_3, and M_2/M_3 pairs. In each triangular plot, the star is the calculated azeotropic point using our approach; the binary azeotropic curves have a unique intersection, which is exactly the same as the location of the star. The open circle is the reported azeotropic point in the reference paper. It can be seen that for all four ternary systems, El-Hamouly and Azab (1994) reported azeotropic points that are not located at the intersection of the binary azeotropic curves. One potential explanation could be incorrect calculations in obtaining the partial azeotropy curves in the reference paper that resulted in incorrect intersections. This is again due to the graphical approach that has often resulted in flawed visual determinations of azeotropic compositions.

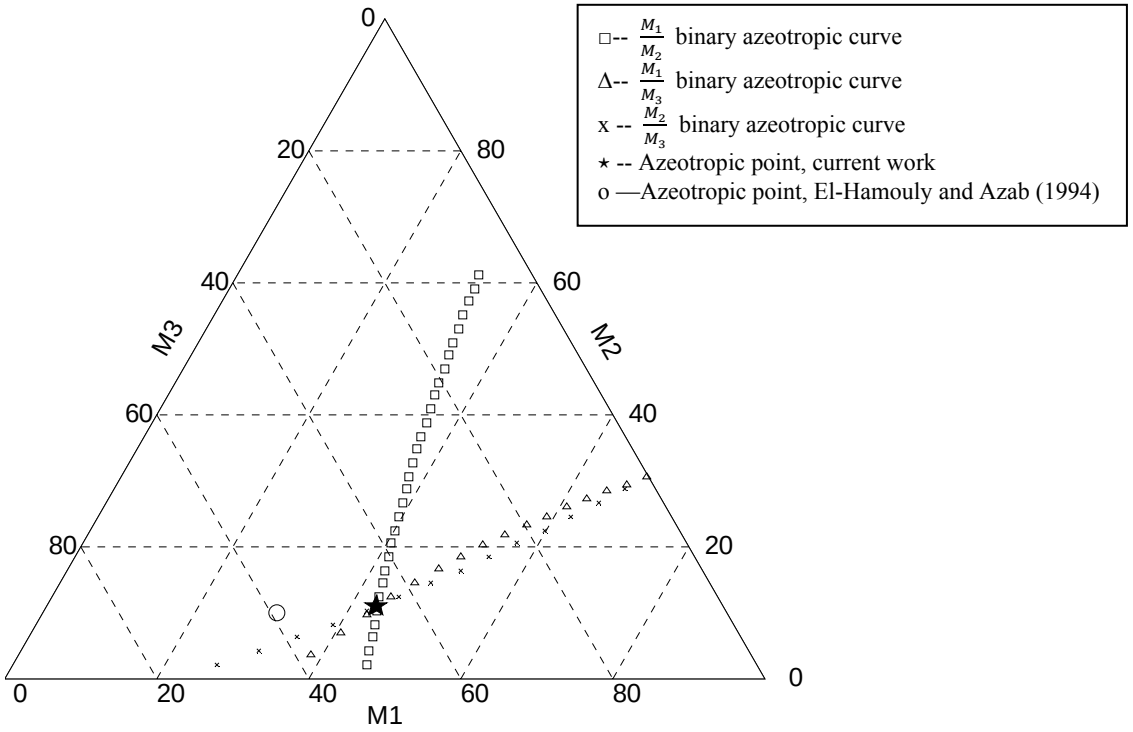

Figure 6-17 a. Ternary azeotropic points and binary azeotropic curves for NAA(M_1)/MA(M_2)/AN(M_3)

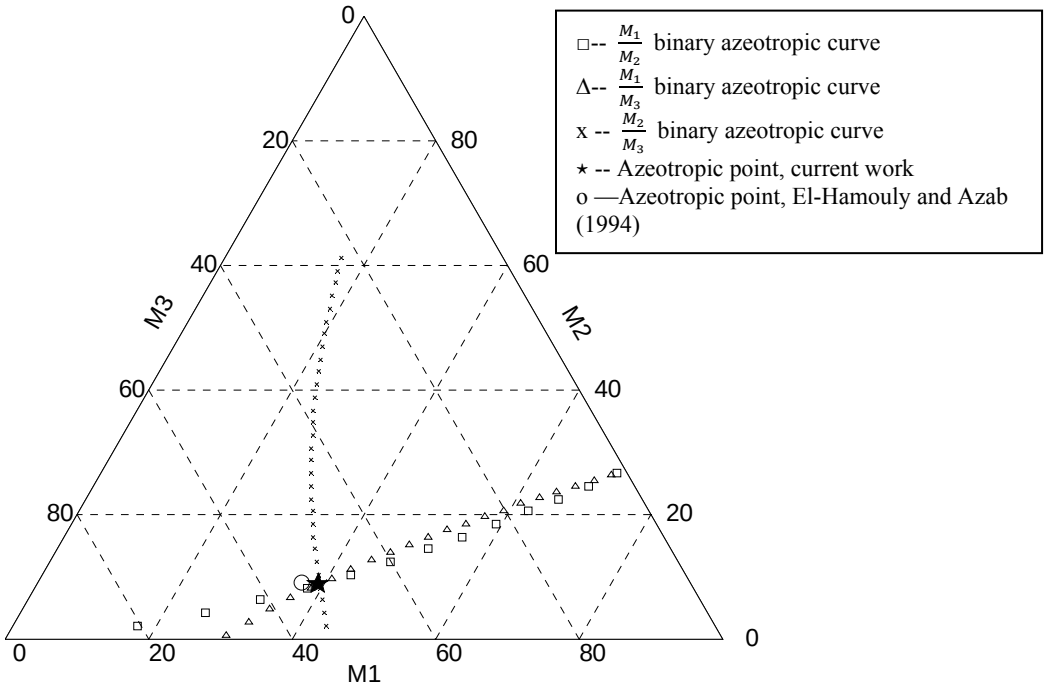

Figure 6-17 b. Ternary azeotropic points and binary azeotropic curves for NAA(M_1)/EA(M_2)/AN(M_3)

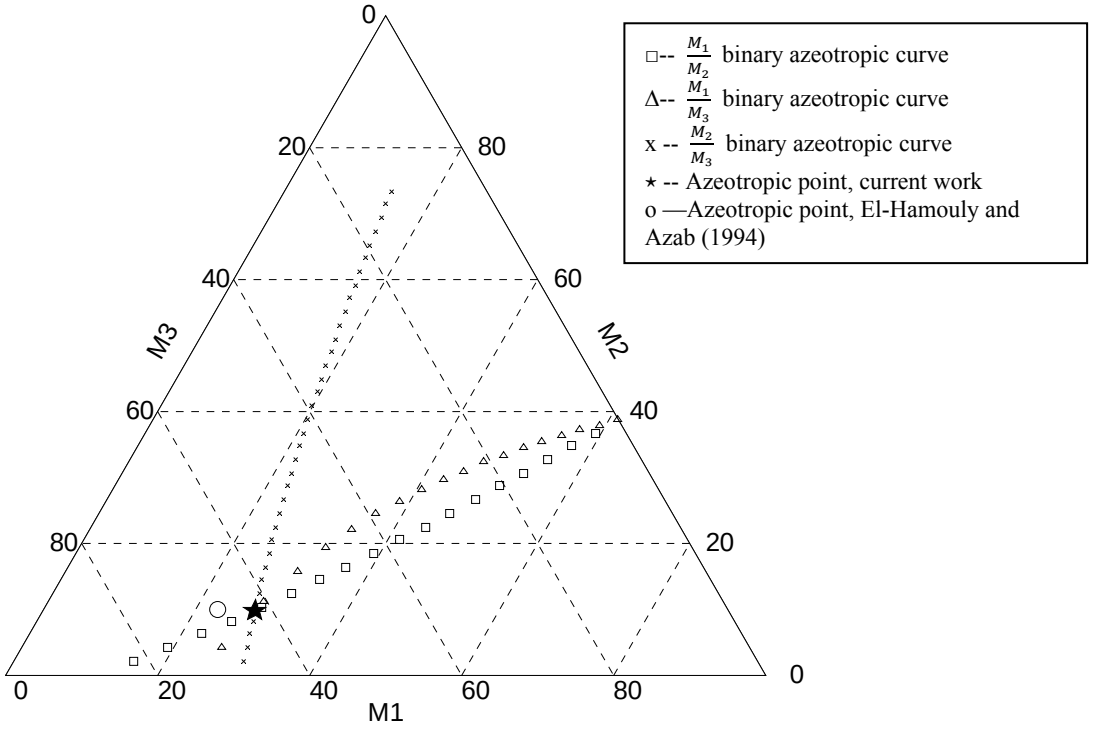

Figure 6-17 c. Ternary azeotropic points and binary azeotropic curves for NAA(M_1)/BA(M_2)/AN(M_3)

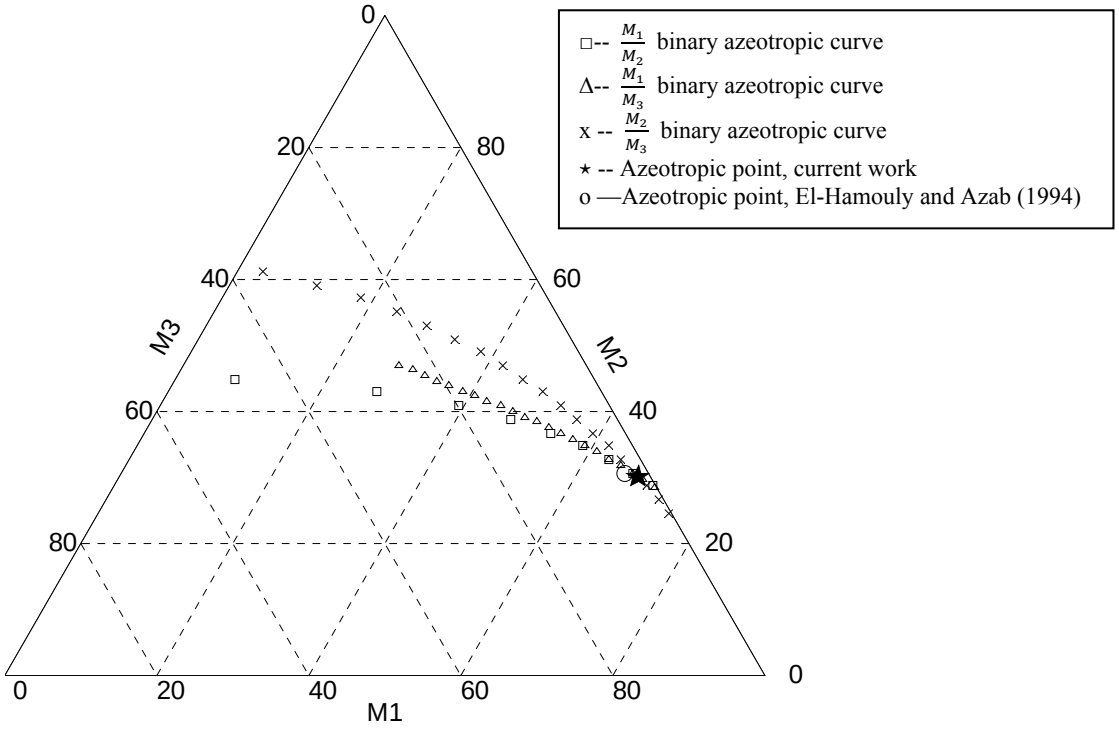

Figure 6-17 d. Ternary azeotropic points and binary azeotropic curves for NAA(M_1)/Sty(M_2)/AN(M_3)

Next, following the same type of analysis as in previous case studies, the cumulative compositions of the terpolymerization systems versus conversion were studied in order to check whether our calculated azeotropic points maintain a constant terpolymer composition during the polymerization, especially at higher conversion levels. Figure 6.18 shows the pictures for these four ternary systems. It is evident that the azeotropic condition is satisfied in each case. Moreover, for each system, the value of the compositional drift criterion based on eq. (6.31) and was found to be zero.

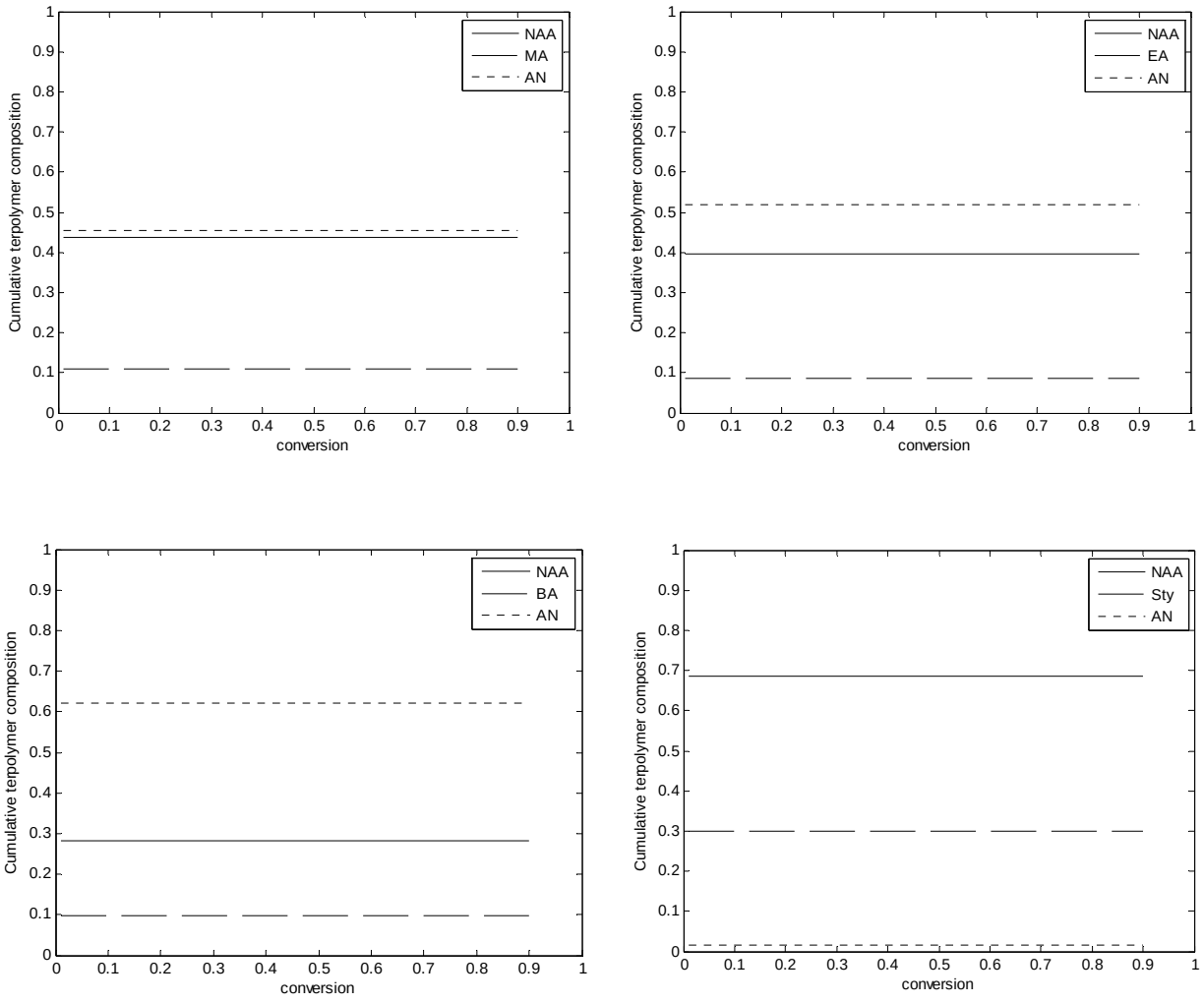

Figure 6-18. Cumulative terpolymer composition versus conversion, case 4

6.7 Summary of Main Results

The main objective of this chapter was to present a general, direct and reliable approach to locate azeotropic points in multicomponent polymerizations. The central focus has been on ternary systems. Typically, for terpolymerization systems, azeotropic compositions have traditionally been calculated through graphical approaches, which were only approximate.

Our question at the outset was whether the numerically calculated azeotrope compositions by our approach were in agreement with those obtained from prior graphical or other approaches.

Table 6.10 was thus created to summarize the analysis of the case studies so as to be able to easily identify the pertinent results from each study. As it is necessary to take into account the error associated with each calculated composition, an error limit of ±5% has been used as an indicator of the level of agreement between our results and the literature reported numbers.

The approaches used by the literature papers listed in Table 6.10 are the one by Tarasov et al. (1960), or solving a 4^{th} order polynomial, or using partial azeotropy concepts, which have all been discussed within the case studies of section 6.6. Also, in cases where no azeotropic composition was found for a certain system, then the corresponding azeotropic composition column entry shows NSF as "no solution found", which indicates a major disagreement between our results and the published values. In addition, it should also be mentioned that Table 6.10 contains several other ternary systems studied by Wittmer et al. (1967), Rios and Guillot (1987) and Azab (2004), which have not been presented as separate case studies, but only the final results are included in the table, for the sake of brevity.

A few general remarks from the case studies of Table 6.10 follow:

- ✓ Our general numerical approach is capable of locating the correct azeotropic composition for any ternary system, if such a point exists.

- ✓ Compared to all prior approaches for azeotropic composition calculation in the literature, our numerical approach can be considered as general, direct, reliable, and more straightforward.

- ✓ Using binary reactivity ratios in the calculation of a ternary azeotrope may result in an inaccurate azeotropic point due to the effect of errors associated with binary reactivity ratio estimates.

✓ Slight changes in the values of reactivity ratios have a strong influence on the position of the ternary azeotrope. The location of the azeotropic point is sensitive to error propagation from reactivity ratio estimation.

✓ Very few (if any) publications exist in the literature that give complete confirmations of the azeotrope existence, both theoretically and experimentally.

Table 6.10. Summary of important results from case studies

Reference	Components			Azeotropic Composition			Approach used	Results
	M_1	M_2	M_3	M_1	M_2	M_3		
Wittmer et al. (1967)	acrylonitrile	ethyl vinyl ether	methyl methacrylate	0.590	0.087	0.321	Tarasov et al. (1960)	√
Saric et al. (1983)	acrylonitrile	styrene	2,3 dibromopropylacrylate	0.232	0.575	0.193	Partial azeotropy	√
Soljic et al. (2010)	N,N-dimethylaminoethyl methacrylate	dodecyl methacrylate	methyl methacrylate	0.582	0.281	0.137	Partial azeotropy	√
El-Hamouly and Azab (1994)	N-antipyryl acrylamide	methyl acrylate	acrylonitrile	0.438	0.108	0.458	Partial azeotropy	X
El-Hamouly and Azab (1994)	N-antipyryl acrylamide	ethyl acrylate	acrylonitrile	0.395	0.087	0.518	Partial azeotropy	√
El-Hamouly and Azab (1994)	N-antipyryl acrylamide	butyl acrylate	acrylonitrile	0.281	0.097	0.062	Partial azeotropy	X
El-Hamouly and Azab (1994)	N-antipyryl acrylamide	styrene	acrylonitrile	0.685	0.300	0.015	Partial azeotropy	√
Azab (2004)	tri-n-butyltin acrylate	Methacryloyloxytetrahydro phthalimide	styrene	0.374	0.231	0.394	Partial azeotropy	X
Azab (2004)	tri-n-butyltin acrylate	Methacryloyloxytetrahydro phthalimide	acrylonitrile	0.681	0.111	0.208	Partial azeotropy	X
Wittmer et al. (1967)	1,3-butadiene	styrene	diethyl fumarate	0.291	0.446	0.263	Tarasov et al. (1960)	√
Wittmer et al. (1967)	2-chloroallylacetate	maleic anhydride	vinylchloride	NSF			Tarasov et al. (1960)	X
Rios and Guillot (1987)	acrylonitrile	styrene	4-vinylpyridine	0.36	0.58	0.06	4th-order polynomial	√
Rios and Guillot (1987)	methyl methacrylate	styrene	4-vinylpyridine	0.239	0.365	0.396	4th-order polynomial	√

NOTE: √ = Agree, X = Disagree
NSF= no solution found

Chapter 7. On-line Reactivity Ratio Estimation

7.1 On-line Reactivity Ratio Estimation

Real-time monitoring of polymerization reactions can be utilized for following polymerization kinetics requiring continuous or periodic measurements on the reaction solution. A detailed overview of on-line and in-line techniques for the monitoring of polymerization reactors has recently been given by Fonseca et al. (2009). Among these techniques, real-time infrared (IR) spectroscopy is a very popular technique for monitoring such polymerizations and associated reactions. Most of the investigations have concentrated on homopolymerization, although reports on *in situ* Fourier transformation infrared (FTIR) monitoring of copolymerization have also appeared (e.g., Giz et al. (2000), Hua and Dube (2002), and Shaikh et al. (2004)).

As one can see from the literature on reactivity ratio estimation, typical practice is to use at best 8-15 copolymer composition data points, usually at low conversions, collected off-line in the batch mode. If data points are used at higher conversions, again 20-30 (at best) off-line copolymer compositions may be used over several feed mole fractions. . On the other hand, on-line techniques, which would in principle allow hundreds of copolymer composition or residual (unreacted) monomer concentration data to be collected, could enable much more information to be extracted from each experiment and thus assist in the calculation of more precise and reliable reactivity ratios.

In this chapter, we are revisiting a paper by Shaikh et al. (2004), which used data from a single copolymerization experiment monitored *in situ* by FTIR. The authors showed that their method is capable of generating a lot of data points very quickly. A large number of data points is indeed advantageous from a statistical analysis viewpoint, because in principle it can increase the information content obtained from the experiment. Subsequently, it depends on the application of the most appropriate parameter estimation technique to

exploit/make use of this enhanced information content. This is exactly the point of this chapter, where again, after we employ the EVM methodology, we show that our technique is superior to what has been used in the literature.

7.2 Case Study: Isoprene (IP)/Isobutylene (IB) Copolymerization

The IP/IB copolymerization system was studied in Shaikh et al. (2004), using on-line FTIR data for the monitoring of the reaction and the subsequent estimation of reactivity ratios. Shaikh et al. (2004) stated that the measurement of reactivity ratios in systems with high IP content is difficult due to the tendency of IP to cyclize, branch, and crosslink, leading to insoluble products. Due to the potential side reactions that might occur, in the IB/IP copolymerization studies, the composition ranges were severely constrained to low IP content. It has been observed in the literature that the reactivity ratio values calculated for IP have in some cases been greater than IB and in others less than IB. Thus, as is usually the case with many copolymerization systems, literature data collected from badly designed experiments and using unreliable parameter estimation techniques cannot be trusted, as it cannot be decided which one of these monomers is more reactive than the other and the results are fairly contradictory.

Shaikh et al. (2004) performed IP/IB copolymerizations with initial feed compositions varying from 10 to 50 mol% of IP (see Figure 7.1 for a schematic of the experimental set-up used; attenuated total reflectance (ATR) and transmission (TR) FTIR modes/probes were used). In this approach, the disappearance of monomers was monitored simultaneously in time, so a single experiment would be composed of a large number of data with varying feed compositions. Shaikh et al. (2004) provided residual monomer concentration data for IB and IP from four different runs (two with the ATR probe and the other two with the TR probe), and the authors pointed out that based on the results, the TR probe seemed more sensitive and in general provided less scattered (and hence, more reliable) concentration values than the ATR probe.

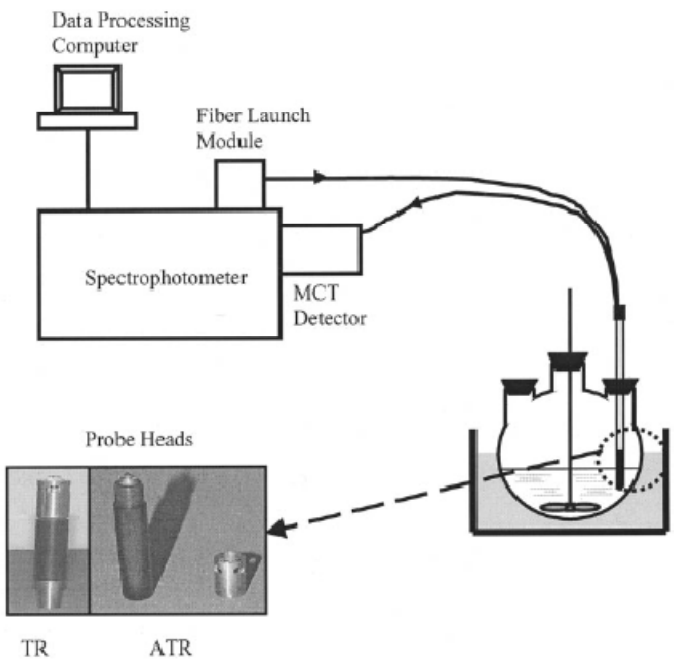

Figure 7-1. Real-time FTIR polymerization monitoring using a fiber-optic probe, Shaikh et al. (2004)

7.2.1 Data Evaluation

Shaikh et al. (2004) translated FTIR spectra to individual monomer concentrations as a function of time (in what follows, monomer 1 refers to IP and monomer 2 is IB). Eventually, they gave plots of $\ln\left(\frac{[M_i]_0}{[M_i]_t}\right)$ versus time per run, where $[M_i]_0$ is the initial monomer concentration and $[M_i]_t$ is the unreacted (unbound, residual) monomer concentration at any time *t*. For runs 1, 3, and 4, the plots of $\ln\left(\frac{[M_i]_0}{[M_i]_t}\right)$ versus time were included in the reference paper, and are shown in Figure 7.2.

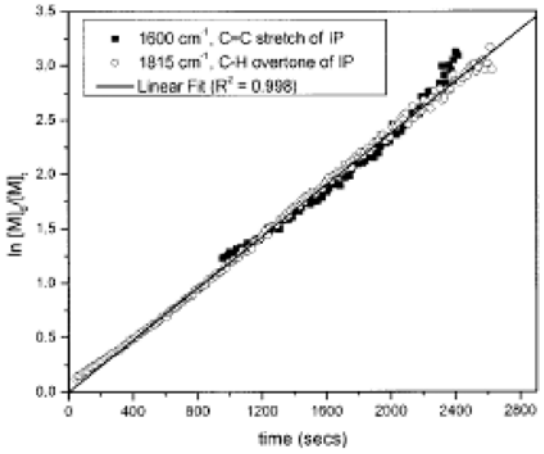

(a) ln $(\frac{[M]_0}{[M]_t})$ versus time plots, monitored with the TR probe (run 1)

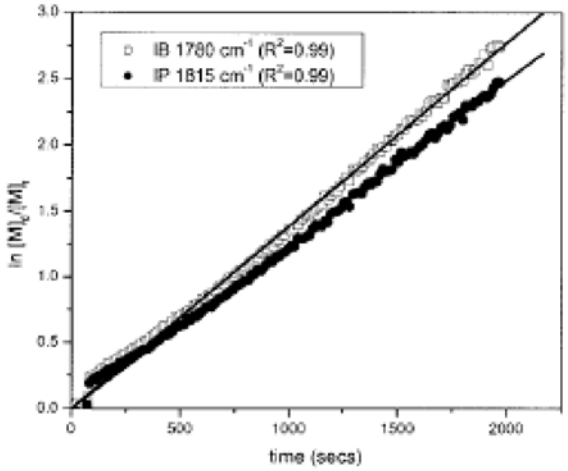

(b) ln $(\frac{[M]_0}{[M]_t})$ versus time plots, monitored with the TR probe (run 3)

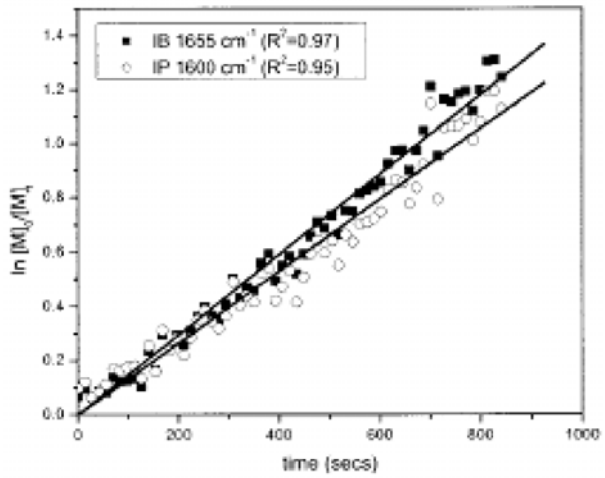

(c) ln $(\frac{[M]_0}{[M]_t})$ versus time plots, monitored with the ATR probe (run 4)

Figure 7-2. ln $(\frac{[M]_0}{[M]_t})$ versus time plots for three runs presented in Shaikh et al. (2004)

According to Shaikh et al. (2004), when working with FTIR monitoring, instantaneous differential monomer consumption was assumed to be equal to the instantaneous copolymer composition. The time interval (δt) between two consecutive data points (measurements) was 14s. Therefore, the instantaneous copolymer compositions, $d[M_i]_t$, were calculated as shown below:

$$d[M_1]_t = [M_1]_{t+\delta t} - [M_1]_t \tag{7.1}$$

$$d[M_2]_t = [M_2]_{t+\delta t} - [M_2]_t \tag{7.2}$$

The mole fractions of unreacted monomer 1 and 2 in the polymerizing mixture were defined as eqs. (7.3) and (7.4):

$$[f_1]_t = \frac{[M_1]_t}{[M_1]_t + [M_2]_t} \tag{7.3}$$

$$[f_2]_t = \frac{[M_2]_t}{[M_1]_t + [M_2]_t} \tag{7.4}$$

The instantaneous mole fraction of monomer 1 in the copolymer ($[F_1{}^{exp}]_t$) was determined by eq. (7.5).

$$[F_1{}^{exp}]_t = \frac{d[M_1]_t}{d[M_1]_t + d[M_2]_t} \tag{7.5}$$

For reactivity ratio estimation, the theoretical mole fraction of monomer 1 was also required and was calculated by the Mayo-Lewis model as in eq. (7.6).

$$[F_1{}^{th}]_t = \frac{r_1[f_1]_t^2 + [f_1]_t[f_2]_t}{r_1[f_1]_t^2 + 2[f_1]_t[f_2]_t + r_2[f_2]_t^2} \tag{7.6}$$

Shaikh et al. (2004) estimated reactivity ratios using nonlinear least squares (NLLS) and their results are presented in Table 7.1 for runs 1, 3, and 4. It can be seen in this table that the

point estimates from runs 1 and 3 are in good agreement, whereas for run 4, no reactivity ratios were reported in the reference paper and it was mentioned by the authors that the NLLS method did not yield any point estimates.

Table 7-1. Reactivity ratios for IP(M_1)/IB(M_2) copolymerization, estimated by the NLLS method in Shaikh et al. (2004)

Run No.	IP mol% in feed	Probe	r_1	r_2
1	10.00	TR	0.97	1.18
3	27.50	TR	0.86	1.16
4	49.80	ATR	No convergence	

7.2.2 Our Approach to Parameter Estimation

Our objective is to implement the EVM method on the data sets obtained by Shaikh et al. (2004), re-estimate the related reactivity ratios and compare these values with the reported point estimates of Table 7.1. The data plots from Shaikh et al. (2004) were digitized (using the piece of software ENGAUGE) and typical results are shown in Figures 7.3 and 7.4 (digitized data for ln $(\frac{[M_i]_0}{[M_i]_t})$ versus time for IP and IB, respectively). For each figure, a trend line has been fitted to the concentration points and its equation has also been displayed on the plot.

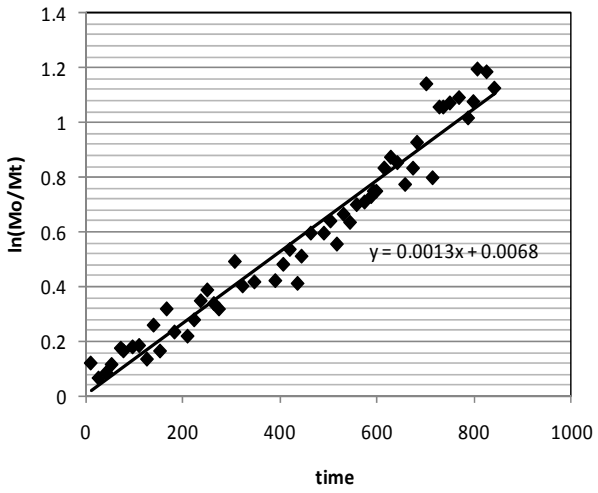

Figure 7-3. Digitized plot for IP (M_1) concentration in run 4

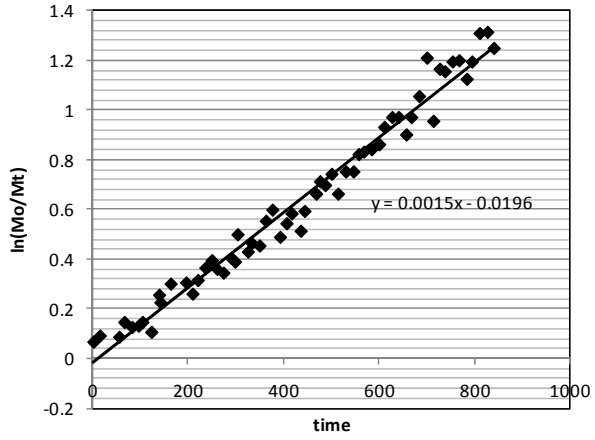

Figure 7-4. Digitized plot for IB (M_2) concentration in run 4

The next step was to calculate the mole fractions of IP and IB as *(f_i, F_i)* pairs based on the values of ln $(\frac{[M_i]_0}{[M_i]_t})$ versus time and using eqs. (7.1) - (7.5). To make sure that the time intervals, δt, of our digitized concentration ratios, are exactly 14 sec for all data points, the trend line equation was used to calculate the value of ln $(\frac{[M_i]_0}{[M_i]_t})$ at 14 s intervals. Eventually, the obtained values of the mole fraction data points *(f_i, F_i)* for IP are presented in Table 7.2.

Table 7-2. Experimental feed and copolymer composition for IP(M_1)/IB(M_2) copolymerization

f_1	F_1^{exp}	f_1	F_1^{exp}	f_1	F_1^{exp}	f_1	F_1^{exp}	f_1	F_1^{exp}	f_1	F_1^{exp}	f_1	F_1^{exp}
0.49	0.46	0.58	0.55	0.66	0.63	0.73	0.71	0.80	0.78	0.85	0.83	0.89	0.87
0.50	0.47	0.59	0.56	0.67	0.64	0.74	0.72	0.80	0.78	0.85	0.84	0.89	0.88
0.51	0.48	0.60	0.57	0.68	0.65	0.75	0.73	0.81	0.79	0.86	0.84	0.89	0.88
0.52	0.49	0.61	0.58	0.69	0.66	0.76	0.73	0.81	0.8	0.86	0.85	0.90	0.89
0.53	0.50	0.62	0.59	0.69	0.67	0.76	0.74	0.82	0.80	0.87	0.85	0.90	0.89
0.54	0.51	0.62	0.6	0.70	0.68	0.77	0.75	0.83	0.81	0.87	0.86	0.90	0.89
0.55	0.52	0.63	0.60	0.71	0.68	0.78	0.75	0.83	0.81	0.87	0.86		
0.56	0.53	0.64	0.61	0.72	0.69	0.78	0.76	0.84	0.82	0.88	0.86		
0.57	0.54	0.65	0.62	0.73	0.70	0.79	0.77	0.84	0.82	0.88	0.87		

The implementation of the EVM method on the copolymer composition data of Table 7.2 using the instantaneous model was done as described in Chapter 3. The error levels were assumed to be, as usual, ±1% for feed composition and ±5% for copolymer composition. However, since in this case the authors did not provide information about the error level in their data sets, the additional error levels of ±10% and ±15% for copolymer compositions were also tried.

7.2.3 Results and Discussion

The EVM point estimates are shown in Table 7.3. Since for run 4, Shaikh et al. (2004) did not calculate any point estimates due to the non-convergence of their NLLS method, they reported reactivity ratio estimates obtained from processing all the runs together. These values are also presented in Table 7.3.

Table 7-3. Reactivity ratio estimates for IP(M_1)/IB(M_2) copolymerization

Reference	Parameter estimation method	Data source	r_1	r_2
Current work	EVM	Run 4	0.8842	1.1314
Shaikh et al. (2004)	NLLS	Runs 1,2,3,and 4	0.99	1.17

The 95% joint confidence regions (JCR) obtained from the EVM method at three different error levels are presented in Figure 7.5. The open circle represents point estimates obtained in the current work (shown in Table 7.3 as well), and the star represents the point estimates reported in Shaikh et al. (2004).

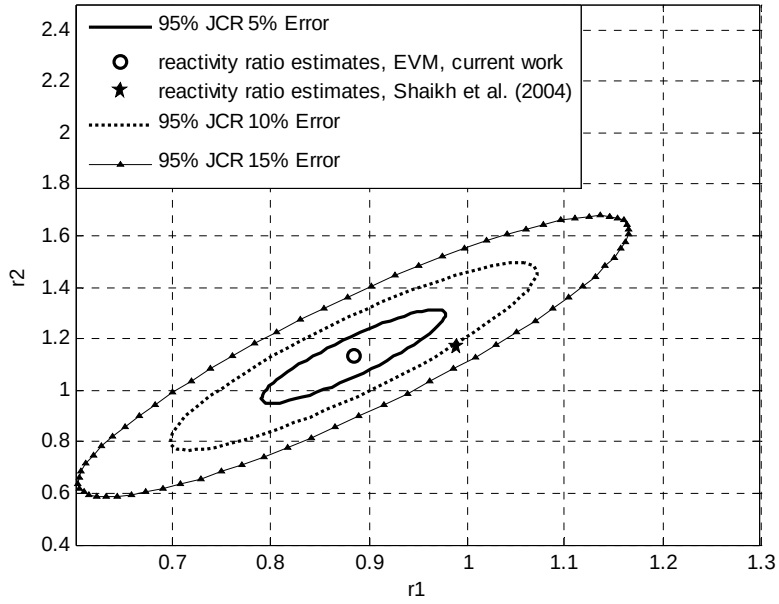

Figure 7-5. JCR for reactivity ratio estimation in IP(M_1)/IB(M_2) copolymerization

It can be seen in this figure that the point estimates from the reference paper fall outside of the ±5% error level JCR and even for the ±10% error, these reactivity ratios are hardly contained within the corresponding JCR. Only the ±15% error level JCR includes these point estimates. These results indicate that the amount of error associated with the experimental data is larger than what is normally expected. A few remarks can now be made considering the estimation results of Table 7.3 and Figure 7.5: (1) In Shaikh et al. (2004), the NLLS method could not converge with the data from run 4. This could be a result of the fact that the independent variable (f_1) is not exactly error-free. On the other hand, EVM had no problem with the data of run 4. (2) It seems that the error in the measurement data of Shaikh et al. (2004) is about 10-15% (as discussed above with respect to Figure 7.5). This is an often

hidden benefit of using the EVM procedure, namely back-calculating the error level of the data set used, even if such error is not reported.

In summary, by re-visiting this paper, it has been demonstrated that reactivity ratios can be determined from a single run using an on-line monitoring approach, provided it has a sufficiently large number of data points. This approach does yield reliable results and the values are not significantly different from previous estimates in the literature for this system. In addition, this case study is a great example of the potential uses of EVM on-line!

Chapter 8. Concluding Remarks and Recommended Future Steps

8.1 Concluding Remarks

The work conducted in this thesis built on previous work in the thesis by Hauch (2005) and was motivated by still unanswered questions with respect to existing techniques and approaches for reactivity ratio estimation in multicomponent polymerizations. Reactivity ratio estimation is well studied for copolymerization reactions with instantaneous composition models and low conversion data. However, the effect of using cumulative copolymer composition models (with low, medium and high conversion data) still requires further investigations, and this is what triggered the work and the different chapters in this thesis. The work in this thesis used the error-in-variables-model (EVM) parameter estimation technique, since this technique is one of the most general, advanced and reliable ones, as it takes into account error in all variables involved (i.e., it does not distinguish between dependent and independent variables).

In Chapter 4, we pointed out practical (experimental) and theoretical (numerical) difficulties arising when working with the analytical integration (over conversion) of the instantaneous copolymer composition equation, also known as Meyer-Lowry model. A more general approach, based on the direct numerical integration of the copolymerization composition ordinary differential equations, was subsequently adopted and compared with the Meyer-Lowry analytical solution. The case studies included in Chapter 4 led to the following two main categories of conclusions:

- At low conversion, reactivity ratio estimation results using the cumulative models are in excellent agreement with the estimation results obtained from the instantaneous Mayo-Lewis model. In addition, provided that low conversion experimental data are sufficiently extensive and spanning the conversion range from 1-5 % (i.e., when not all data points are at the same conversion level for all practical

purposes), the cumulative models are able to provide higher precision reactivity ratios compared to the instantaneous model, as shown from the corresponding joint confidence regions (JCRs) of a smaller area. This is related to the higher information content involved in the parameter estimation technique in this case, since the cumulative models use both copolymer composition and conversion information, versus only composition for the instantaneous model. As a result, the parameter estimates with the cumulative models are of higher quality (i.e., more reliable).

- At high conversion levels, our results are in acceptable agreement with the very few reported values in the literature, thus confirming the capability of our parameter estimation technique when implemented on high conversion range data as well. Although the Meyer-Lowry model and direct numerical integration provide similar results (when used up to moderate (mid-range) conversion levels, i.e., up to 30-50 % conversion), working with the direct numerical integration has the benefit of avoiding experimental and numerical difficulties associated with the use of the Meyer-Lowry model, thus making the direct numerical integration (and the related cumulative model) the preferred approach. The direct numerical integration model can be used for parameter estimation over the full conversion range, whereas the same does not hold for the Meyer-Lowry model, as some of its assumptions are usually violated when conversion levels exceed 40-50 %.

The investigation on reactivity ratio estimation was extended from copolymerization systems to terpolymerization systems in Chapter 5. The typical approach in the literature regarding monomer reactivity ratios in ternary systems is to borrow the information available from the copolymerization monomer pairs instead of studying the terpolymerization experimental data directly. Our research started by implementing the EVM method on the classic instantaneous terpolymerization model (Alfrey-Goldfinger model), in order to determine reactivity ratios based directly on terpolymerization experimental data. The main contributions from this chapter are as follows:

- Our case studies confirmed that implementing EVM directly on terpolymerization data has a great potential to improve the results, in that the use of

binary reactivity ratios seems to be an oversimplification, not only with respect to the values themselves, but also with respect to not including measures (and hence effect) of their uncertainty.

- Since the success of analysis is strongly dependent on the information contained in the data, data accuracy and experimental design are extremely important for parameter estimation and thus they can affect the conclusions drawn. Therefore, terpolymerization experiments with replicates and good experimental designs are preferable for parameter estimation.

With respect to azeotropy in multicomponent polymerization, our research focused on ternary systems in Chapter 6. The main objective of this chapter was to present a general, direct and reliable approach to locate azeotropic points in multicomponent polymerizations. Typically, for azeotropic systems, the literature has been dominated by graphical solutions, which are only approximate. Our approach consisted of solving the Alfrey-Goldfinger equations (set of nonlinear algebraic equations) in order to arrive at a general, direct numerical solution of the terpolymerization azeotropic composition. The main remarks from this chapter are the following:

- Our general numerical approach is capable of locating the correct azeotropic composition for any ternary (or multicomponent) system, if such a point exists. Compared to all prior approaches for azeotropic composition calculation in the literature, our numerical approach is general, direct, reliable, and more straightforward.
- The location of an azeotropic point is highly dependent on the values of the reactivity ratios and even slight changes in the values of reactivity ratios can result in the position of the azeotropic point to be shifted (in some cases, the changes in these values can turn an azeotropic terpolymerization to a seemingly non-azeotropic one).
- Binary reactivity ratios that are readily used by researchers when working with ternary systems may result in an inaccurate azeotropic point because of the effect of related errors of the binary reactivity ratios.

Finally, Chapter 7 presented a special case study, still using EVM, for determining reactivity ratios on-line.

8.2 Future Recommendations

The following points are suggested for future steps, divided into immediate and long-term steps.

8.2.1 Immediate Steps

- The performance of the cumulative models at different conversion levels (approximately 10%-50% or low to moderate, 50%-70% or moderately high, and more than 70% or full conversion range) could be tested further with real data from different copolymerization systems. Examples of available data sources for cumulative copolymer compositions are Dube et al. (1990) for Sty/BA, and Dube et al. (1995) for MMA/VAc and BA/VAc.
- In working with the Meyer-Lowry model, it has been observed that full conversion data or certain values of reactivity ratios forced the execution of the parameter estimation method to abort and therefore no results were obtained. It is thus recommended to monitor the numerical execution process step by step, and find out reasons/point(s) that are causing these sorts of problems.
- The methodology, explained in Chapter 4 for copolymerizations, could become the basis for applying cumulative composition models to high conversion terpolymerization data. Subsequently, terpolymerization reactivity ratios can be estimated based on high conversion ternary experimental data, which is expected to increase the precision of the results similar to binary systems. This can also suggest an experimental prescriptive procedure (with the minimum number of experiments or

with one experiment only as a last resort) that can be used to show that a certain terpolymer system has an azeotropic point (i.e., proof of existence of azeotropy in multicomponent systems). The extended Walling- Briggs model, mentioned in Chapter 2 related to multicomponent systems, will be a good starting point, once reliable reactivity ratios are available.

8.2.2 Long-term Steps

- To increase the reliability of the parameter estimation results based on cumulative copolymer composition models, one might consider time as an independent variable in the parameter estimation procedure and make use of a fully mechanistic model (set of differential and algebraic equations) for co- or ter-polymerization. However, it must be noted that the use of time as independent variable can become a complex issue, highly constrained by other kinetic parameters of the fully mechanistic model.
- For the goal of parameter estimation, there is a minimum required number of data points, at least equal to the number of parameters to be estimated, and for this reason, many of the existing data sets in the literature are not sufficient. Therefore, a well-designed terpolymerization experiment should be performed with the appropriate replication so as to be able to accurately test the current EVM procedure. For copolymerization cases, Burke et al. (1993) investigated the experimental design problem extensively. For terpolymerizations, however, the problem is still open. The aim of this type of investigations would be to determine the following points: (1) optimal feed points for estimation of reactivity ratios, (2) the minimum number of required feed points for executing parameter estimation properly, and, lastly, (3) constrained designs considering restrictions for certain feed ranges.
- Further investigation is required on the effect of errors associated with the binary reactivity ratio estimates on the calculated azeotropic composition due to the

fact that slight changes in the values of reactivity ratios have a strong influence on the position of the ternary azeotrope (i.e., sensitivity of azeotropic point location to error propagation from reactivity ratio estimation). Hence, increasing the reliability of the reactivity ratio point estimates can directly increase the accuracy of the location of the corresponding azeotropic point.

- In our study as well as in the literature, it has been assumed that reactivity ratios are constant during the course of polymerization. However, at higher levels of conversion this assumption might be violated, as reactivity ratios values might change. It is therefore recommended to consider these potential changes in the procedure of calculating an azeotropic composition (i.e., the location of the azeotropic point may shift during polymerization, thus generating a "root locus" (or "branches") of possible azeotropic points).
- The ultimate diagnostic check would be to design and run lab experiments to determine the terpolymer composition during the course of polymerization and the associated compositional drift (if any) at the putative azeotropic point.
- The potential of using the EVM method on-line for reactivity ratio estimation can be further explored, provided that the available on-line sensors give consistent data over the whole conversion range.
- For reactivity ratio estimation from on-line copolymerization data points, it is recommended to implement the Meyer-Lowry model or the direct numerical integration approach to estimate reactivity ratios on-line. As the corresponding on-line data sets can be fairly extensive, it is expected that utilizing high conversion data may considerably increase the precision of the point estimates.
- Finally, the question of additive vs. multiplicative error in the data during reactivity ratio estimation remains an open question.

References

1. Alfrey, T. and Goldfinger, G., *"The mechanism of copolymerization"* Journal of Chemical Physics, **12,** 205-209 (1944).

2. Alfrey, T. and Goldfinger, G.*, "Copolymerization of systems of three and more components"* Journal of Chemical Physics, **12**, 322 (1944).

3. Andrzejewska, E., Socha, E., and Andrzejewski, M.*, "Cross-linking photocopolymerization of dodecyl methacrylate with oxyethylene glycol dimethacrylates: Kinetics and reactivity ratios"* Polymer, **47**, 6513-6523 (2006).

4. Azab, M. M.*, "Azeotropy in terpolymerizations"* Polymer Institute, **53**, 1007-1012 (2004).

5. Bard, Y.*, "Nonlinear Parameter Estimation"* Academic Press, New York (1988).

6. Bates, D. M. and Watts, D. G., *"Nonlinear Regression Analysis and its Applications"* Wiley, New York (1988).

7. Box, G. E. P. and Draper, N. R., *"Bayesian estimation of common parameters from several responses"* Biometrika, **52**, 355-365 (1965).

8. Bourdais, J., *"Reactivity of acrylic acid in copolymerization"* Bulletin De La Societe Chimique De France, 485-489 (1955).

9. Brar, A. S., Thiyagarajan, M. and Dutta, K., *"Microstructure determination of poly (trans-4-acryloyloxyazobenzene) by NMR spectroscopy"* Polymer, **39**, 5507-5513 (1998).

10. Brar, A. S., Dutta, K. and Hekmatyar, S. K, *"Stereochemical and compositional assignment of acrylonitrile/methyl methacrylate copolymers by DEPT and inverse HECTOR NMR spectroscopy"* Journal of Polymer Science Part A: Polymer Chemistry, **36**, 1585-1597 (1998).

11. Brar, A. and Hekmatyar S., *"Microstructure determination of the acrylonitrile-styrene-methyl methacrylate terpolymers by NMR spectroscopy"* Journal of Applied Polymer Science, **74**, 3026–3032 (1999).

12. Braun, D., Brendlein, W., Disselhoff, G. and Quella, F., *"Computer-program for calculation of ternary azeotropes"* Journal of Macromolecular Science-Chemistry, **A9**, 1457-1462 (1975).

13. Burke, A. L., Duever, T. A., and Penlidis, A., *" Revisiting the design of experi- ments for copolymer reactivity estimation"* Journal of Polymer Science Part A: Polymer Chemistry, **31**, 3065-3072 (1993).

14. Chen. W. C., Chaung, Y., and Chiu, W. Y., *" Kinetics study of an acrylic tetrapolymer: Poly (IBMA-MMA-MMA-TBMA)"* Journal of Polymer Science Part A: Polymer Chemistry, **79**, 853-863 (2001).

15. Dalvi, A., Personal communication (2004).

16. Draper, N. R. and Smith, H., *"Applied Regression Analysis" Wiley*, New York (1998).

17. O' Driscoll, K. F., Kale, L. T., Garcia-Rubio, L. H. and Reilly, P. M., *"Applicability of the Mayo-Lewis equation to high-conversion copolymerization of styrene and methylmethacrylate"* Journal of Polymer Science. Part A-1: Polymer Chemistry, **22**, 2777-2788 (1984).

18. Dube, M., Sanayei, R. A., Penlidis, A., O' Driscoll, K. F. and Reilly, P. M., *"A microcomputer program for estimation of copolymerization reactivity ratios"* Journal of Polymer Science Part A: Polymer Chemistry, **29**, 703-708 (1991).

19. Dube, M. A. and Penlidis, A., *"A Systematic approach to the study of multicomponent polymerization kinetics: The butyl acrylate/methyl methacrylate/vinyl acetate example 3. Emulsion homo- and copolymerization in a pilot plant reactor"* Polymer International, **37**, 235-248 (1995).

20. Duever, T. A., O' Driscoll, K. F. and Reilly, P. M., *"The use of the error-in-variables-model in terpolymerization"* Journal of Polymer Science Part A-Polymer Chemistry, **21**, 2003-2010 (1983).

21. Fernandez-Garcia, M., Canamero, P. F. and Fuente, J. L., *"Synthesis and characterization of functional gradient copolymers of glycidyl methacrylate and butyl acrylate"* Reactive & Functional Polymers, **68, 1**384–1391 (2008).

22. Finemann, M. and Ross, S., *"Linear method for determining monomer reactivity ratios in copolymerization"* Journal of Polymer Science, **5**, 259-262 (1950).

23. Fonseca, G. E., Dube, M. A., Penlidis, A., *"A Critical overview of sensors for monitoring polymerizations"* Macromolecular Reaction Engineering, **3**, 327-373 (2009).

24. Fuente, J. L., Canamero, P. F., and Fernandez-Garcia, M., *"Synthesis and characterization of glycidyl methacrylate/butyl acrylate copolymers obtained at a low temperature by atom transfer radical polymerization"* Journal of Polymer Science Part A: Polymer Chemistry, **44**, 1807–1816 (2006).

25. German, A. L. and Heikens, D., *"Copolymerization of ethylene and vinyl acetate at low pressure: Determination of the kinetics by sequential sampling"* Journal of Polymer Science Part A: Polymer Chemistry, **9**, 2225-2232 (1971).

26. Giz, A., Catalgil-Giz, H. C., Alb, A. Brousseau, J., Reed, W. F., *"Kinetics and mechanisms of acrylamide polymerization from absolute online monitoring of polymerization reaction"* Macromolecules, **34**, 1180-1191 (2001).

27. Hagiopol, C., *"Copolymerization: Toward a Systematic Approach"* Kluwer Academic/Plenum Publishers, New York (1999).

28. Ham, G. E., *"General relationships among monomers in copolymerization"* Journal of Polymer Science, Part A, **2**, 2735-2748 (1964).

29. Ham, G. E., *"Proof of validity of expanded copolymerization equations"* Journal of Polymer Science, Part A, **2**, 3633-3638 (1964).

30. Ham, G. E., *"Calculation of copolymerization reactivity parameters from product probabilities"* Journal of Polymer Science, Part A, **2**, 4181-4189 (1964).

31. Ham, G. E., *"Multicomponent polymerizations"* Journal of Macromolecular Science-Chemistry, 403-405 (1966).

32. Ham, G. E., *"Sequence distribution in terpolymers*" Journal of Macromolecular Science-Chemistry, **A19**, 699-704 (1983).

33. Ham, G. E., *"Terpolymer azeotropy*" Journal of Macromolecular Science-Chemistry, **A19**, 693-698 (1983).

34. Ham, G. E., *"Terpolymer relationships and azeotropes"* Journal of Macromolecular Science - Chemistry, **A28**, 733-742 (1991).

35. Ham, G. E., *"Triad concentrations ($P_{12}P_{23}P_{31}$ and $P_{13}P_{32}P_{21}$) as a guide to monomer reactivity in copolymers and terpolymers"* Journal of Macromolecular Science - Pure and Applied Chemistry, **A30**, 459-471 (1993).

36. El-Hamouly, S. H. and Azab, M. M., *"Azeotropy in terpolymerization of N - antipyryl acrylamide with different alkyl acrylates or styrene and acrylonitrile*" Journal of Polymer Science Part A: Polymer Chemistry, **32**, 937-947 (1994).

37. Haque, M., *"A Kinetic Study of Acrylamide/Acrylic Acid Copolymerization"* M.A.Sc. thesis, Department of Chemical Engineering, University of Waterloo (2010).

38. Hua, H. and Dube, M. A., *"In-line monitoring of emulsion homo- and copolymerizations using ATR-FTIR spectrometry"* Polymer Reaction Engineering, **10**, 21–39 (2002).

39. Hauch, E. K. D., *"Parameter Estimation in Multiresponse Problems for the Modelling of Multicomponent Polymerization Reactions"* M.A.Sc. thesis, Department of Chemical Engineering, University of Waterloo (2005).

40. Hautus, F. L. M., German, A. L. and Linssen, H. N., *"On numerical problems when reactivity ratios are computed using the integrated copolymer equation"* Journal of Polymer Science: Polymer Letters Edition, **23**, 311-315 (1985).

41. Hocking, M. B. and Klimchuk, K. A., *"A refinement of the terpolymer equation and its simple extension to two and four component systems"* Journal of Polymer Science Part A: Polymer Chemistry, **34**, 2481-2497 (1996).

42. Keeler, S. E. and Reilly, P. M., *"The error-in-variables model applied to parameter estimation when the error covariance-matrix is unknown"* Canadian Journal of Chemical Engineering, **69**, 27-34 (1991).

43. Kelen, T. and Tudos, F., *"Analysis of linear methods for determining copolymerization reactivity ratios .1. New improved linear graphic method"* Journal of Macromolecular Science-Chemistry, **A9**, 1-27 (1975).

44. Kelen, T., Turcsanyi, B. and Disselhoff, G., *"Graphical representation of terpolymerization systems"* Journal of Macromolecular Science-Chemistry, **A12**, 35-49 (1978).

45. Kinsinger, J. B., Bartlett, J. S. and Rauscher W. H., *"On the colligative nature of the specific refractive increment for statistical copolymers"* Journal of Applied Polymer Science, **6**, 529-532 (1962).

46. Koenig, J. L., *"Chemical Microstructure of Polymer Chains"* Wiley, New York; Toronto (1980).

47. Luft, G., Batarseh, B. and Cropp, R., *"High pressure polymerization of ethylene with a homogeneous metallocene catalyst"* Angewandte Makromolekulare Chemie, **212**, 131-140 (1993).

48. Madruga, E. and Fernandez-Garcia, M., *"Free-radical homopolymerization and copolymerization of di-n-butyl itaconate"* Polymer, **35**, 4437-4442 (1994).

49. Madruga, E. and Fernandez-Garcia, M., *"High conversion copolymerization of di-n-butyl itaconate with methyl methacrylate in benzene solution"* European Polymer Journal, **31**, 1103-1107 (1995).

50. Mayo, F. R. and Lewis, F. M., *"Copolymerization. I. a basis for comparing the behaviour of monomers in copolymerization; the copolymerization of styrene and methyl methacrylate*" Journal of American Chemistry Society, **66**, 1594-1601 (1944).

51. McManus, N. T. and Penlidis, A., *"A kinetic investigation of styrene/ethyl acrylate copolymerization"* Journal of Polymer Science Part A: Polymer Chemistry, **34**, 237-248 (1996).

52. Moad, G., Solomon, D. H and Spurling, T. H. *"Critical points (azeotropic compositions) in multicomponent copolymerization"* Australian Journal of Chemistry, **39**, 1877-1881, (1986).

53. Meyer, V. E. and Lowry, G. G., *"Integral and differential binary copolymerization equations"* Journal of Polymer Science, Part A, **3**, 2843-2851 (1965).

54. Odian, G. G. *"Principles of Polymerization"*, Wiley- Interscience, (2004).

55. Patino-Leal, H., Reilly, P. M. and O' Driscoll, K. F., *"On the estimation of reactivity ratios"* Journal of Polymer Science: Polymer Letters Edition, **18**, 219-227 (1980).

56. Penlidis, A., Personal Communication (2008-2010).

57. Polic, A. L., Duever, T. A. and Penlidis, A., *"Case studies and literature review on the estimation of copolymerization reactivity ratios"* Journal of Polymer Science Part A: Polymer Chemistry, **36**, 813-822 (1998).

58. Quella, F. *"Ternary and partial ternary azeotropes"* Makromolekulare Chemie, **190**, 1445-52 (1989).

59. Reilly, P. M. and Patino-Leal, H., *"Bayesian study of the error-in-variables model"* Technometrics, **23**, 221-232 (1981).

60. Ring, W. *"Ternary azeotropy in free radical copolymerization"* European Polymer Journal, **4**, 412 (1968).

61. Rios, L. and Guillot, J. *"Azeotropy in terpolymerization"* Journal of Macromolecular Science-Chemistry, **A12** (8), 1151-1174 (1987).

62. Rintoul, I. and Wandrey, C., *"Polymerization of ionic monomers in polar solvents: kinetics and mechanism of the free radical copolymerization of acrylamide/acrylic acid"* Polymer, **46**, 4525-4532 (2005).

63. Roland, M. T. and Cheng, H. N., *"Reaction probability model for four-component copolymerization"* Macromolecules, **24**, 2015-2018 (1991).

64. Rossignoli, P., *"Estimation and Design Considerations for Obtaining Reactivity Ratios"* M.A.Sc thesis, Department of Chemical Engineering, University of Waterloo (1993).

65. Rossignoli, P. J. and Duever, T. A., *"The estimation of copolymer reactivity ratios - a review and case-studies using the error-in-variables model and nonlinear least-squares"* Polymer Reaction Engineering, **3**, 361-395 (1995).

66. Rudin, A., Ableson, W. R., Chiang, S. S. M. and Bennett, G. W., *"Estimation of reactivity ratios from multicomponent copolymerizations"* Journal of Macromolecular Science – Chemistry, **A7**, 1203-1230 (1973).

67. Rudin, A., *"The Elements of Polymer Science and Engineering: An Introductory Text and Reference for Engineers and Chemists"* Academic Press, San Diego (1998).

68. Saric, K., Janovic, Z and Vogl, O., *"Copolymers of styrene with some brominated acrylates"* Journal of Macromolecular Science – Chemistry, **A19**, 837-852 (1983).

69. Slocombe, R.J., *"Multicomponent polymers. I. three-component systems"* Journal of Polymer Science, **26,** 9-22 (1957).

70. Shaikh, S., Puskas, J. E., Kaszas, G. *"A new high-throughput approach to measure copolymerization reactivity ratios using real-time FTIR monitoring"* Journal of Polymer Science, Part A: Polymer Chemistry, **42**, 4084–4100 (2004).

71. Shawki, S. and Hamielec, A., *"Estimation of the reactivity ratios in the co-polymerization of acrylic-acid and acrylamide from composition-conversion measurements by an improved non-linear least-squares method"* Journal of Applied Polymer Science, **23**, 3155-3166 (1979).

72. Shukla, A. and Srivastava, A., *"Terpolymerization of linalool, styrene, and methyl methacrylate: Synthesis, characterization, and a kinetic study"* Polymers for Advance Technologies, **15,** 445-452 (1994).

73. Soljic, I., Jukic, A. and Janovic, Z., *"Terpolymerization kinetics of N,N-dimethylaminoethyl methacrylate/alkyl methacrylate/styrene systems"* Polymer Engineering Science, **50**, 577-584 (2010).

74. Soljic, I., Jukic, A. and Janovic, Z., *"Free radical copolymerization of N,N-dimethylaminoethyl methacrylate with styrene and methyl methacrylate: monomer reactivity ratios and glass transition temperatures"* Polymer International, **58**, 1014-1022 (2009).

75. Tarasov, A. I., Tskhai, V. A. and Spasskii, S. S., *"Composition equations of three-component copolymers"* Vysokomolekulyarnye Soedineniya, **2**, 1601-1607 (1960).

76. Tidwell, P. W. and Mortimer, G. A., *"An improved method of calculating copolymerization reactivity ratios"* Journal of Polymer Science, Part A, **3**, 369-387 (1965).

77. Tomescu, M., *"Azeotropy of multicomponent copolymerization"* Materiale Plastics (Bucharest, Romania), **16**, 205-206 (1979).

78. Walling, C. and Briggs, E., *"Copolymerization .3. systems containing more than 2 monomers"* Journal of the American Chemical Society, **67**, 1774-1778 (1945).

79. Wamsley, A., Jasti, B., Phiasivongsa P., and X. Li, *"Synthesis of random terpolymers and determination of reactivity ratios of N-carboxyanhydrides of leucine,beta-benzyl aspartate, and valine"* Journal of Polymer Science, Part A: Polymer Chemistry, **42**, 317–325 (2004).

80. Wittmer, P., Hafner, F., and Gerrens, H. *"Occurrence of azeotropes in copolymerization with more than two comonomers"* Makromolekulare Chemie, **104**, 101-119 (1967).

81. Van der Meer, R., Linssen, H. N. and German, A. L., *"Improved methods of estimating monomer reactivity ratios in copolymerization by considering experimental errors in both variables"* Journal of Polymer Science: Polymer Chemistry Edition, **16**, 2915-2930 (1978).

82. Zhou, X., *"Evaluation of instantaneous and cumulative models for reactivity ratio estimation with multiresponse scenarios"* M.A.Sc. thesis, Department of Chemical Engineering, University of Waterloo (2004).

Appendix A: Multicomponent Polymerization Equation

Roland and Cheng (1991) suggested an alternative way for modeling monomer mole fractions in an n-component polymerization using reaction probabilities and the Boolean function "NOT".

The reaction probability is defined as:

$$P_{ij} = \frac{k_{ij}[M_j]}{\sum_{j'=1}^{N} k_{ij'}[M_{j'}]} \tag{A.1}$$

where k_{ij} denotes the rate constant for the addition of monomer j to a propagating radical of type i, and $[M_i]$ denotes the molar concentration of monomer i.

Using material balance equations for each component and implementing the steady-state assumptions, a set of equations (containing "n" equations) results with "n" unknowns, F_i, the mole fractions of monomer i incorporated in the polymer. In addition, there is another related equation that can be used as $\sum F_i = 1$. After carrying out the remaining algebraic manipulation, back-substitutions and factoring of common terms, the final expression for the n-component composition equation is defined in terms of reaction probabilities (see Chapter 2, section 2.3.2, where an example of this type of expression is given for a four-component system, as per eq. (2.49)).

Roland and Cheng (1991) transformed the final expression for the n-component composition equation into a single equation using Boolean function "NOT". The characteristics of this function can be summarized as:

Argument function	Input to Boolean function	Results of Boolean
True	1	0
False	0	1

Using the NOT function, the n-component composition equation can be re-written as:

$$F_n \propto \sum_{i=1}^{N} P_{ai} \sum_{j=1}^{N} P_{bj} \ldots \sum_{k=1}^{N} P_{zk}\,[NOT(i=a)].[NOT(j=b)] \ldots [NOT(k=z)].$$
$$.[NOT(i.j=b.a)].[NOT(i.k=c.a)].etc.(all\ 2-term\ combinations).$$
$$[NOT(i.j.k=b.c.a)].etc.(all\ 3-term\ combinations). \quad \text{(A.2)}$$
$$etc.(up\ to\ all(N-1)-term\ combinations)$$

where a, b, c, …, z have the following values:

For *n=1: a=2, b=3, c=4, …,z=N*

n=2: a=1, b=3, c=4, …,z=N

n=N: a=2, b=3, c=4, …,z=1

Appendix B: Newton-Raphson Algorithm Validation

B1. Introduction

The Newton-Raphson method is one of many iterative root-finding procedures and is most widely used because of its combination of simplicity and stability.

B2. The Newton-Raphson Iteration

This method requires an initial guess of a solution to begin the search. If x_n is the current estimate, then the next estimate, x_{n+1}, is given by:

$$x_{n+1} = x_n - \frac{f(x_n)}{f'(x_n)} \tag{B2.1}$$

Here $f(x_n)$ represents the value of the function at x_n and $f'(x_n)$ is the derivative at x_n.

Delta-x can be defined as $|x_{n+1} - x_n|$. Theoretically, we could execute an infinite number of iterations to find a perfect root. However, since we want to speed up the process of finding the root, we can assume that the process has worked accurately when delta-x becomes less than a preselected tolerance level. The typical tolerance used in our cases is 10^{-6}, unless otherwise noted. It should also be mentioned that if the initial estimate is not close to the root, the Newton-Raphson method may not converge or may converge to the wrong root.

In our research, the objective is to calculate the azeotropic composition which consists of components' mole fractions. Therefore, the answer we are looking for is supposed to be restricted within the range of 0 to 1. Based on this fact, it is possible to check as many as

necessary initial guesses from 0 to 1 in order to make sure that a unique answer is arrived at, independently of the initial guesses.

B3. Sample Calculations/ Benchmarking

Several examples are now given of using the Newton-Raphson method to obtain solutions for the following (rather complex) nonlinear equations:

Example (a):

$$e^x - 3x = 0 \tag{B3.1}$$

Solution: $x_1 = 0.6191$ and $x_2 = 1.5121$

Note: For this example, the initial guesses are obtained by dividing the range of -2 to 2 into 10 points. The number of iterations for these 10 starting points varies from 4 to 6 depending on how close the selected initial guess is to the real solution.

Example (b):

$$3x + \sin(x) - e^x = 0 \tag{B3.2}$$

Solution: $x_1 = 0.3604$ and $x_2 = 1.89$

Note: The method of selection of the initial guesses is exactly the same as in example (a). For this example, the number of iterations for the starting points, obtained within the range of -2 to 2, varies from 4 to 7.

Example (c):

$$\begin{cases} 4 - x^2 - y^2 = 0 \\ 1 - e^x - y = 0 \end{cases} \tag{B3.3}$$

Solution: $x = -1.82$ and $y = 0.83$

Note: Similarly, the initial guesses are selected as 10 (x,y) pairs within the range of -2 to 2. The number of iterations for the starting points varies from 2 to 9.